Fluorogenic Sydnone Dyes for Labeling DNA and Diarylsydnone-Modified Nucleosides as Photoactivatable Nucleosides

Zur Erlangung des akademischen Grades einer
DOKTORIN DER NATURWISSENSCHAFTEN
(Dr. rer. nat.)

von der KIT-Fakultät für Chemie und Biowissenschaften
des Karlsruher Instituts für Technologie (KIT)

genehmigte

Dissertation

von
M. Sc. Kerstin Müller
aus Bad Rappenau

Karlsruhe, 2025

Dekan:	Prof. Dr. Martin Bastmeyer
Referent:	Prof. Dr. Hans-Achim Wagenknecht
Korreferentin:	Prof. Dr. Ute Schepers

Tag der mündlichen Prüfung: 10.02.2025

Meinen Eltern

„Phantasie ist wichtiger als Wissen, denn Wissen ist begrenzt“

Albert Einstein

Danksagung

Die vorliegende Arbeit wurde im Zeitraum vom August 2021 bis Dezember 2024 am Institut für Organische Chemie des Karlsruher Instituts für Technologie (KIT) im Arbeitskreis und unter der Leitung von Prof. Dr. Hans-Achim Wagenknecht angefertigt.

Mein besonderer Dank gilt meinem Doktorvater Prof. Dr. Hans-Achim Wagenknecht für die hervorragende Betreuung, die interessante Themenstellung sowie die wissenschaftlichen Freiheiten, welche es mir ermöglicht haben, meine eigenen Ideen zu entwickeln und umzusetzen und mich auf diese Weise als Wissenschaftlerin weiterzuentwickeln. Vielen Dank für die sehr gute Arbeitsatmosphäre und die stets offene Tür bei beruflichen Dingen als auch privaten.

Danke auch an Prof. Ute Schepers für die Übernahme der Zweitkorrektur dieser Arbeit.

Des Weiteren möchte ich mich bei dem Graduiertenkolleg 2039 für den wertvollen interdisziplinären wissenschaftlichen Austausch, die zahlreichen Weiterbildungsmöglichkeiten und die finanzielle Unterstützung bedanken.

Danke außerdem an Prof. Dr. Frederic Friscourt für die Möglichkeit eines Forschungsaufenthalts in deiner Arbeitsgruppe an der University Bordeaux und deine Unterstützung von fachlicher Seite, aber auch darüber hinaus. Mein Dank gilt dem ganzen Arbeitskreis, der mich freundlich aufgenommen hat und die schönen Events mit euch zusammen während dieser drei Monate in Bordeaux. Danke für die schöne Zeit!

Dem KHYS danke ich für die Förderung des Auslandsaufenthaltes und für die Unterstützung bei Weiterbildungskursen.

Ein Dank geht auch an meine aktuellen und ehemaligen Kollegen für die angenehme Arbeitsatmosphäre und Zusammenarbeit. Es war toll, ein Teil dieser Gruppe zu sein und ich werde immer positiv auf diese Jahre zurückblicken.

Im Speziellen möchte ich mich bedanken bei:

Claudia Sommer und Ariane Baumgart für die Unterstützung in organisatorischen Dingen jeglicher Art sowie Anette Hochgesandt und Lara Hirsch für das Messen zahlreicher Masse-Proben. Ariane danke, dass deine Tür für mich immer offen stand und für deine Unterstützung!

Meiner Bachelorstudentin Christin Papke und meiner Vertieferstudentin Cindy Konstantin für das Interesse an und die Unterstützung bei meiner Arbeit und das begeisterte Mitarbeiten.

Elin Klauke für deine gewissenhafte Arbeit als Hiwine während deiner Zeit bei mir im Labor und für deine Freundschaft.

Ein großer Dank gilt vor allem auch meinem langjährigen Laborpartner Philipp Geng. Vielen Dank für deine Unterstützung und dein offenes Ohr. Dafür, dass du mit deinen Sprüchen und Humor mich immer aufgeheitert hast, vor allem an Tagen, an denen nichts funktionieren wollte. Mit dir habe ich alle Höhen und Tiefen erlebt, die man im Labor so haben kann. Trotzdem haben wir uns immer gegenseitig versucht zu motivieren. Ich werde unsere Zeit immer positiv in Erinnerung behalten!

Sebastian und Simon aus Labor 007. Danke für die schöne Zeit und die tollen Gespräche, ich bin immer gerne bei euch vorbeigekommen. Danke Sebastian für deine ruhige und entspannte Art die mich auch oft beruhigt hat, wenn ich mir selbst zu viel Stress gemacht hab. Simon danke das du immer gute Stimmung verbreitest und dir immer Zeit genommen hast, wenn ich euer Labor besucht habe.

Basti, Rita und Lisa dafür, dass bei euch immer gute Stimmung im Labor herrschte und eure positive Art. An dieser Stelle möchte ich mich besonders bei Basti bedanken. Danke für deine unkomplizierte Art und die langen und netten Unterhaltungen zu allen Angelegenheiten.

Eileen danke für deine liebe Art und deine Hilfsbereitschaft! Ohne dich hätte ich das mit den Zellexperimenten in so kurzer Zeit nicht geschafft! Danke das du dir so viel Mühe gegeben hast mich einzulernen.

Andi danke für die schönen Unterhaltungen und dein offenes Ohr!

Jan, bei dir finde ich es echt schade, dass du erst gegen Ende meiner Promotion zu mir ins Labor gekommen bist! Ich glaube, wir hätten eine coole Zeit gehabt. Vielen Dank für deine offene, positive Art und das du mich immer aufgeheitert hast, wenn die Zellexperimente mal wieder nicht funktioniert haben. Die kurze Zeit, die wir zusammen in 004 hatten, werde ich immer mit einem Lächeln in Erinnerung behalten.

Ich möchte mich auch gerne bei Dennis Lamade bedanken. Unsere gemeinsame Zeit im Arbeitskreis Wagenknecht werde ich nie vergessen. Du hast mich durch deine Betreuung im Vertiefer damals sehr in meiner Selbstständigkeit und Entwicklung als Forscherin gefördert, dadurch das du mir sehr viel wissenschaftliche Freiheiten gegeben hast. Du bist nicht nur ein Arbeitskollege, sondern auch ein richtiger Freund geworden!

Cedric, Kai-Ching und Ramona danke, dass ihr euch die Zeit genommen habt, meine Arbeit Korrektur zu lesen.

Ein besonderer Dank geht auch an meine Schwester Ramona. Du warst immer für mich da und bist die beste Schwester die man sich wünschen kann! Bitte bleib so wie du bist! Danke sagen möchte ich auch meinen Eltern. Ihr habt mich immer unterstützt und gefördert und mich zu dem Menschen gemacht, der ich heute bin. Danke für eure bedingungslose Unterstützung! Vielen Dank auch an meine Tanten Marianne und Angela ihr wart immer für mich da, wenn ich Sorgen und Probleme hatte.

Lara und Kristin ihr seid meine besten Freundinnen, ohne euch wäre die bisherige Zeit nur halb so schön gewesen. Danke, dass ihr seit der Schulzeit mit mir durch Dick und Dünn geht und dass ihr immer für mich da seid und es schafft mich in stressigen Phasen auch mal abzulenken.

Zu guter Letzt möchte ich meinen Freund Felix danken. Danke, dass du mich immer bedingungslos unterstützt und mich immer wieder aufbaust durch deine optimistische entspannte Art. Auf dich kann ich immer zählen. Ohne dich hätte ich diesen Weg zur Promotion nicht geschafft!

Zusammenfassung

Die Visualisierung von Zellprozessen ist für das Verstehen von biochemischen Vorgängen unerlässlich. Eine der wichtigsten Methoden für die Visualisierung ist die bioorthogonale Chemie. Diese wurde 2003 von *Bertozzi* eingeführt und mit einem Nobelpreis 2022 geehrt. Die Coronapandemie zeigte das Potential von Impfstoffen auf mRNA-Basis, was in einem verstärkten Forschungsinteresse an Therapeutika auf Nucleinsäuren-Basis resultierte.

Die vorliegende Doktorarbeit ist in zwei Hauptteile gegliedert. Im ersten Projekt wurden fünf verschiedene Sydnonfarbstoffe synthetisiert und anschließend charakterisiert. Der verwendete Cyanin-Styryl-Farbstoff weist eine sehr hohe Photostabilität und eine hohe Stokes-Verschiebung von bis zu 0.52 eV auf. Die Farbstoffe wurden mit zwei Bicyclo[6.1.0]non-4-in-Nucleisiden auf deren Kinetik und Fluoreszenzsteigerung untersucht. Die drei Sydnonfarbstoffe mit der größten Fluoreszenzsteigerung wurden mit Bicyclo[6.1.0]non-4-in-modifizierter DNA umgesetzt, dabei wurde ein starker Anstieg der Kinetik und Fluoreszenzsteigerung im Vergleich zur Reaktion mit den Nukleosiden beobachtet. Im Vergleich zum Nucleosid war der Fluoreszenzanstieg ein bis zu 8-facher Anstieg und die Kinetik vertausendfachte sich nahezu. Des Weiteren zeigte einer der Sydnonfarbstoffe eine Verschiebung des Fluoreszenzmaximums um 123 nm bei Reaktion mit Bicyclo[6.1.0]non-4-in-modifizierter DNA im Vergleich zur Fluoreszenz mit einem Bicyclo[6.1.0]non-4-in-Nukleosid. Anschließend wurden die Ergebnisse der ringspannungsgetriebenen Sydnon-Alkin-Cycloaddition der drei vielversprechendsten Sydnonfarbstoffe auf fixierte *HeLa* Zellen übertragen.

Im zweiten Teil der Arbeit wurden zwei diarylsydnonmodifizierte Nukleoside hergestellt. Die beiden Nukleoside wurden jeweils mit N-Methylmaleimid durch Belichtung mit in einer Photoclickreaktion umgesetzt. Dabei konnten diese in hoher Geschwindigkeit in ein Pyrazolin überführt werden. Mit N-Methylmaleimid wurde bei der Photoclickreaktion auch ein starker Fluoreszenzanstieg beobachtet. Des Weiteren wurden die beiden Nukleoside in einer ringspannungsgetriebenen Sydnon-Alkin-Cycloaddition mit Bicyclo[6.1.0]non-4-in als Alkoholkonjugat umgesetzt. Dabei zeigte sich, dass diarylsydnonmodifizierte Nukleoside deutlich langsamer reagieren und ihre Reaktionszeit über 12 Stunden länger ist als die von

sydnonmodifizierten Nukleosiden. Zudem wurden diarylsydnonmodifizierte DNA-Stränge durch postsynthetische Modifikation synthetisiert.

Table of Contents

Abbreviations

ACN	acetonitrile
BARAC	biarylazacyclooctyne
BCN	bicyclononyne
Bz	benzoyl
COMBO	carboxymethylmonobenzocyclooctyne
CuAAC	copper-catalyzed azide-alkyne cycloaddition
d	doublet
dd	doublet of doublet
dt	doublet of triplet
DCM	dichloromethane
DIBAC	dibenzoazacyclooctyne
DIBO	dibenzocyclooctyne
DIFBO	difluorobenzocyclooctyne
DIFO	difluorocyclooctyne
DIPEA	*N,N*-diisopropylethylamine
DMF	*N,N*-dimethylformamide
DMSO	dimethylsulfoxide
DNA	deoxyribonucleic acid
DMTr	4,4'-dimethoxytrityl
Em.	emission
ESI	electron-spray ionization
Exc.	excitation
FRET	Förster resonance energy transfer
HeLa	human cervical cancer cells
HOMO	highest occupied molecular orbital
HPLC	high performance liquid chromatography
HRMS	high resolution mass spectrometry
I	intensity
iEDDA	inverse electron-demand Diels-Alder cycloaddition

LUMO	lowest unoccupied molecular orbital
m	multiplet
MALDI	matrix-assisted laser desorption ionization
MeOH	methanol
mRNA	messenger ribonucleic acid
NHS	N-hydrocysuccinimide
NMM	N-methylmaleimide
OCT	cyclooctyne
PBS	phosphate buffered saline
q	quartet
Quant.	quantitative
r.t.	room temperature
RNA	ribonucleic acid
ROS	reactive oxygen species
s	singlet
SPAAC	strain-promoted azide-alkyne cycloaddition
SPSAC	strain-promoted sydnone-alkyne cycloaddition
t	triplet
TBDMS	*tert*-butyldimethylsilyl
TBTA	tris((1-benzyl-1H-1,2,3-triazol-4-yl)methyl)amine
TCO	trans cyclooctene
THF	tetrahydrofuran
THPTA	tris(hydroxypropyltrazolyl)-methylamine
TLC	thin-layer chromatography
TOF	time of flight
UV	ultraviolet (light)
Vis	visible (light)

1. Introduction

All cells in the human body contain the same chromosomes and thus the same set and number of genes. Despite this, different cell types, such as muscle and nerve cells, exhibit distinct characteristics and functions. This differentiation is achieved through gene regulation, a process that ensures only specific genes are expressed in a given cell type. There are different pathways of gene regulation, one is that only specific genes are expressed based on epigenetic modifications to the DNA, the other path is the regulation by microRNA.[1,2] MicroRNA are short non-coding RNA strands, which have the ability to regulate the gene expression very precisely on the post-transcriptional level. As microRNAs play an essential role in modulating protein production, they influence nearly all biological processes.[3] A misregulation of microRNA can play a role in several illnesses, like cancer and diabetes, highlighting microRNA's potential as therapeutic targets. Advances in microRNA research have opened the door to innovative treatment strategies.[2] *Victor Ambros* and *Gary Ruvkun* were honored with the 2024 Nobel Prize in medicine for their significant insights into gene regulation via microRNA.[1] This emphasizes the importance of understanding gene regulation in cells and cell processes in general. To follow those processes in their natural enviroment, the bioorthogonal chemistry is nowadays a crucial tool.[4] The method is based on adapting chemical reactions so that they can take place in a living organism without negatively affecting or disturbing them. Despite the complexity of biological systems, a series of chemical reactions have been developed since the introduction of bioorthogonal chemistry in 2003 that are suitable for use in living cells.[5,6] Especially fluorescent probes have proven to be useful for elucidating such processes. Despite the progress made so far, fluorescent probes often have a large signal-to-noise ratio and low photostability.[6–8] Often the fluorophores need to be used in excess to ensure an efficient conversion of the reaction with the target molecule in the cell. The excess of unreacted dye results in a strong background fluorescence which makes the visualization via fluorescence microscopy difficult. It is a common practice to wash the excess dye away several times to reduce background fluorescence. However, this is very difficult to implement in small cell samples and impossible in vivo.[9] Fluorogenic probes are a new approach to solve this problem. These probes are dyes which have a functional group attached on the dye core that quenches their fluorescence. After a bioorthogonal reaction

with a target molecule, the structure of the quenching moiety changes, and the fluorescence of the dye is restored.[10] A prominent example of fluorescent probes are tetrazine-modified dyes.[11,12] They are widely used because of their fast click reactions with a lot of different chemical reporters. Less prominent examples are fluorogenic sydnone dyes.[13] Those sydnone dyes are used only for the labeling of proteins, but like tetrazine dyes they also have beneficial properties like high stability and fast reaction rates.[13] Another tool to investigate cell processes is the photoclick reaction which enables high spatiotemporal control of the reaction, for which fluorescent tetrazole dyes, but also recently diarylsydnones are often used.[14,15] All the above-mentioned bioorthogonal labelling tools are mostly developed for the labeling of proteins. The labeling of other biomolecules like DNA and RNA has been investigated much less than that of proteins.[6] The number of publications on nucleic acids corresponds to only about one fifth of the publications on proteins. Nevertheless, nucleotides play a key role in all organisms, and recent developments, like the mRNA vaccine against Covid-19 or the development of Spiranza™, an antisense oligonucleotide for treating spinal muscle atrophies, show the high potential of nucleic acids in medicines and the need for further investigation.

The present work deals with the development of fluorogenic sydnone dyes for selective visualization of nucleic acids in biological systems and the development of diarylsydnones as chemical reporters for postsynthetic labeling methods of nucleic acids.

2. Aim of the work

This work is divided into two chapters. The first chapter focuses on the development of fluorogenic sydnone dyes. The dye moieties are based on cyanine-styryle dyes which are already established in the *Wagenknecht* group. The fluorescence quenching sydnone moiety is attached to the dyes via a vinyl bridge to ensure effective fluorescence quenching via conjugation (**figure 1**). The sydnone dyes are first analyzed for their spectroscopic properties and for their stability in aqueous solutions. In a next step, the sydnone dyes are examined in regard to their reactivity with BCN-modified nucleosides and compared with each other in terms of kinetics and fluorescence enhancement (turn-on). The three most promising sydnone dyes are chosen to react with BCN-modified DNA and their ability to label BCN-modified DNA in HeLa cells.

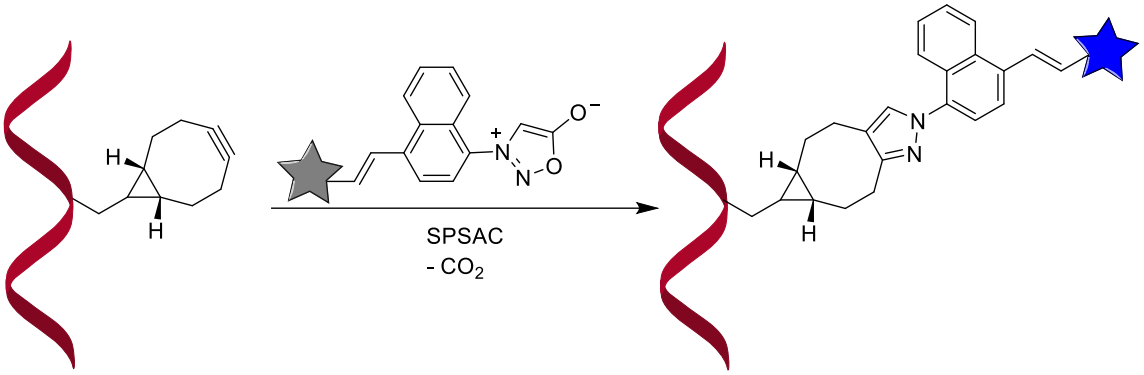

Figure 1: Schematic representation of the strain-promoted sydnone-alkyne cycloaddition (SPSAC) with fluorogenic sydnone dyes on oligonucleotides.

The focus of the second chapter is the synthesis of diarylsydnones for bioorthogonal labeling. The two synthesized diarylsydnones are used to prepare diarylsydnone-modified nucleosides (**figure 2**). In a next step, they are employed in either a photoclick reaction or a strain-promoted sydnone alkyne cycloaddition. The reactions were monitored via absorption and fluorescence spectroscopy. Additionally, diarlysydnone-modified DNA is prepared, followed by utilizing them in a photoclick reaction.

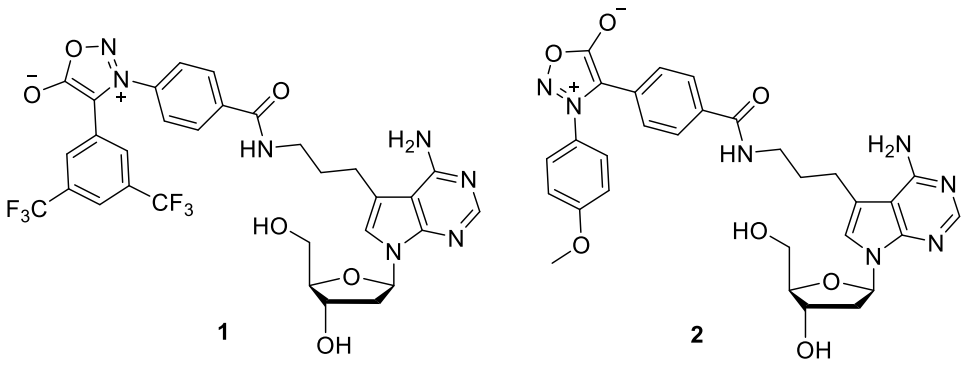

Figure 2: Structure of the diarylsydnone-modified nucleosides **1** and **2**.

3. Theoretical Background

3.1. Bioorthogonality

Bioorthogonal chemistry has revolutionized biological research by enabling to mark and track molecules such as proteins, nucleic acids, and glycans within living cells and even in living organisms.[16] This has led to a better understanding of complex biological systems, pathogenic mechanisms and to the development of targeted therapeutics. Bioorthogonality refers to chemical reactions that can take place within living cells or organisms without disrupting natural biochemical processes.[16,17]

The strategy of biorthogonal labeling consists of two steps (**figure 3**): In the first step a monomer of the biopolymer of interest is equipped with a chemical moiety that does not naturally occur in biological systems. Methods such as metabolic incorporation are used to introduce the monomer into the biopolymer. In the second step, the modified biopolymer is reacted with a suitable reaction partner, that selectively reacts with it. This probe usually contains a fluorescent tag or another functional group allowing the visualization of the labeled biomolecule.[16,18]

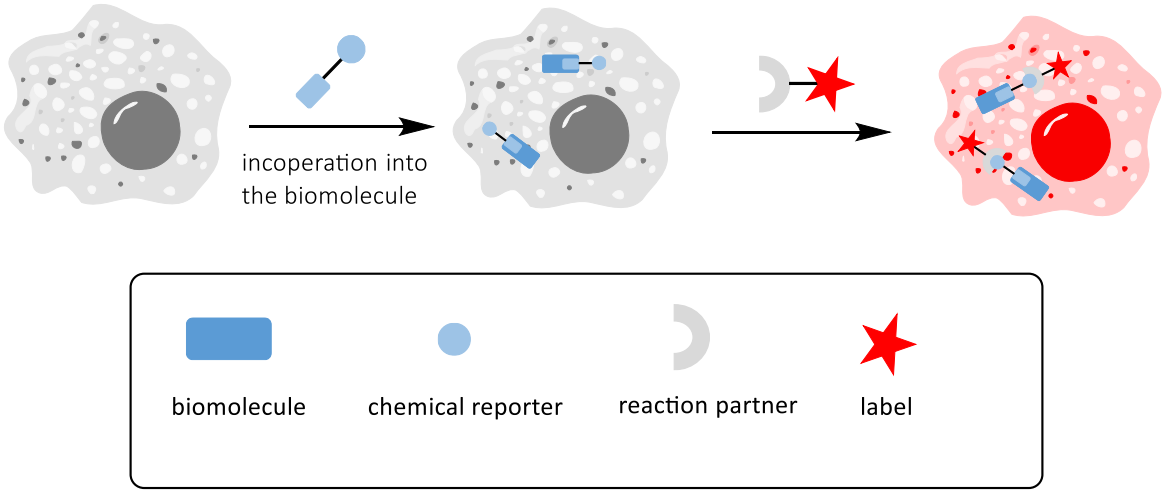

Figure 3: Schematic representation of the concept of bioorthogonal labeling. First, a chemical reporter modified monomer is integrated into the biomolecule via metabolic or enzymatic incorporation. The next step is selective labeling with a reaction partner that carries a label (e.g. a fluorescent dye).

Important for the first step is that the introduced chemical reporter does not alter the function of the biomolecule or interacts or reacts with other chemical groups of biomolecules of the biological system. Another important requirement is that the modified monomer is accepted by the enzymes which carry out the metabolic incorporation.[19] *Wagenknecht et al.* showed how the size of the chemical moiety influences the incorporation efficiency of the modified 2'-deoxynucleosides into cellular DNA (**figure 4**).[20]

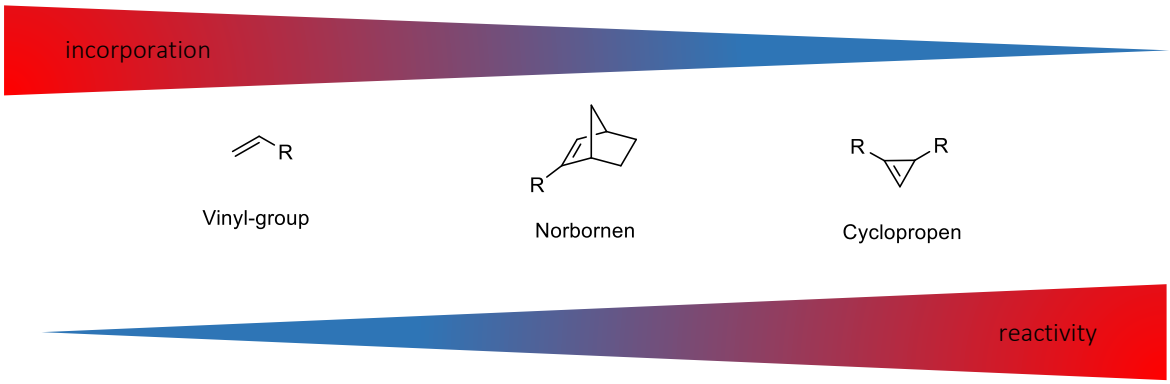

Figure 4: Overview over important dienophiles for bioorthogonal labeling and their correlation of efficient metabolic incorporation into DNA and their reactivity in iEDDA reactions.[19]

Furthermore, there are the following criteria which must be fulfilled to call a labeling reaction bioorthogonal: The labeling reaction must be biocompatible, which means that the reaction must proceed under physiological conditions such as a water milieu, neutral pH, physiological temperature, normal pressure and O_2 atmosphere.[4,16,21] Both the chemical moiety and the probe must be stable in the biological environment, resisting degradation, hydrolysis, or other side reactions that could compromise their reactivity. The formed product should be stable to enable multiple analyses and long-term studies.[21] The chemoselectivity of the reaction is critical: The used functional groups should only react with each other and not form any side products or react with naturally occurring nucleophiles in cells to avoid unspecific labeling. Additionally, the used functional group and the resulting product should also show no cell toxicity.[21] Another important criteria is the rate constant of the used reaction.[5,22] Typically, biological labeling reactions follow second-order kinetics, so they depend on both the reaction rate constant and the concentration of both reactants. High rate constants enable the efficient labeling of biological processes that occur on very short timescales, down to the microsecond range

and also allow the use of low concentrations of the reaction partners.[23] This helps to minimize problems like cell toxicity or solubility problems of the reaction partners.[4,24,25] In recent years, new reactions have emerged, which meet many of the outlined criteria.[6] The following chapter will present a selection of these ''Click'' reactions

3.2 Bioorthogonal labeling reactions

Bioorthogonal reactions are often classified under the concept of ''click chemistry'', a term introduced by *Sharpless*.[26] This concept comprises reactions characterized by high yields, mild reaction conditions, broad applicability, and high specificity. The most well-known example of a ''click'' reaction is the copper-catalyzed azide-alkyne cycloaddition (CuAAC). The CuAAC was developed by *Sharpless* and *Meldal* in the early 2000s and is a 1,3-dipolar cycloaddition for the formation of 1,2,3-triazoles starting from azides and terminal alkynes (figure 5).[26,27]

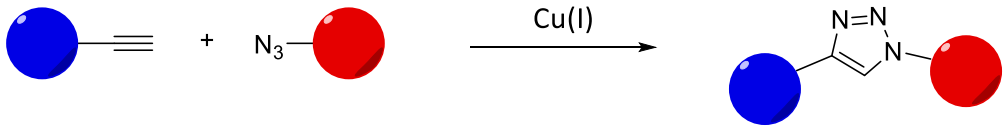

Figure 5: Schematic representation of the copper(I)-catalyzed azide-alkyne cycloaddition. The terminal alkyne reacts with an azide to form a 1,2,3-triazole.

The CuAAC shows high stereoselectivity and regioselectivity and is easily performed. Furthermore, it has a high efficiency and a high tolerance towards functional groups. Based on the previously presented properties, it becomes apparent that this reaction completely fulfills the criteria of click chemistry established by Sharpless. A big advantage of using azides in bioorthogonal reactions is that they are absent in living systems and are non-toxic to cells. Additionally, the reaction can be performed under mild conditions like room temperature and shows high conversions of various azides and alkynes to the resulting triazoles. Also, it is one of the fastest methods for bioorthogonal labeling with up to k_2 = 200 $M^{-1}s^{-1}$. Furthermore, the reaction generates only 1,4-disubstituted triazoles.[26,27] However, the use of Cu(I) salts, which are needed to carry out the reaction under mild conditions, is a big disadvantage for in vivo experiments. Copper (I) promotes the formation

of reactive oxygen species (ROS) through redox reactions, which in turn leads to oxidative damage withing the cells and is therefore considered cell toxic.[28–30] However, Cu(I) can form a complex with water-soluble ligands such as tris(benzyltriazolylmethyl)amine (**TBTA**), tris(3-hydroxypropyltriazolmethyl)amine (**THPTA**) or 2-[4-((Bis[1-tert-butyl-1H-1,2,3-triazol-4-yl)methyl]-amino)-methyl)-1H-1,2,3-triazol-1-yl]ethylhydrogensulfate (**BTTES**).[31–33] **TBTA** and **THPTA** increase the electron density of the Cu(I) and thus additionally accelerate the reaction. Nevertheless, in the case of **TBTA** the ligand complexes showed a higher toxicity towards cells compared to free copper. When **BTTES** was used for the CuAAC, *Wu et al.* were able to create images of glycan biosynthesis during early zebrafish development.[34] In the past years, various methods have been established in the field of copper-free ''click chemistry''. The most common of these include the strain-promoted azide-alkyne Cycloaddition (SPAAC)[35], the strain-promoted sydnone-alkyne Cycloaddition (SPSAC)[36], the Diels-Alder reaction with inverse electron demand reaction (iEDDA)[37] and the photoclick reaction.[38,39]

3.3. Copper-free labeling methods

3.3.1 Strain-promoted azide-alkyne cycloaddition (SPAAC)

The strain-promoted azide-alkyne cycloaddition (SPAAC) is a copper-free variant of the CuAAC, developed by the nobel laureate *Bertozzi* to overcome the limitations of the CuAAC in living systems.[40] The reaction is like the CuAAC a [3+2]-dipolar cycloaddition of an azide and a strained alkyne, for example a cyclooctyne (COT), under formation of triazoles. However, the activating barrier is lowered by the ring tension of the used alkyne eliminating the need for additional catalysts. *Bertozzi* used a biotinylated cyclooctyne derivate by reaction with an azido-modified sugar for glycan labeling. Furthermore, the rate constant of the SPAAC compared to the CuAAC is lower. The rate constant depending on the used azide was between $k_2 = 1.1 \cdot 10^{-3}\ M^{-1}\ s^{-1} – 2.4 \cdot 10^{-3}\ M^{-1}s^{-1}$, which is significantly lower than the rate constants of the CuAAC.[5,41] Although this circumstance can be partly compensated, for example by adjusting the alkyne concentration, there are more efficient possibilities through corresponding modifications of the COT core. Also, the reaction rate is strongly influenced by the solvent utilized for the reaction, as water was reported to

speed up 1,3-dipolar cycloadditions, compared to acetonitrile or methanol used as a solvent, which makes it hard to compare reaction rates of different strain alkynes with each other.[42] The COT's reactivity can be increased by modifying the cyclooctyne (COT) with electron-withdrawing substituents such as geminal difluoro groups in the case of Difluorocyclooctyne (DIFO, $k_2 = 7.6 \cdot 10^{-2}$ $M^{-1}s^{-1}$)[43,44] and Difluorobenzocyclooctyne (DIFBO, $k_2 = 2.2 \cdot 10^{-1}$ $M^{-1}s^{-1}$).[45] Also, through benzylanellation like in the case of carboxymethylbenzocyclooctyne (COMBO, $k_2 = 0.24 \cdot 10^{0}$ $M^{-1}s^{-1}$)[46], dibenzocyclooctyne-1,4-dione (DIBO, $k_2 = 1.7 \cdot 10^{-1}$ $M^{-1}s^{-1}$)[47], azadibenzocyclooctyne (DIBAC, $k_2 = 3.1 \cdot 10^{-1}$ $M^{-1}s^{-1}$)[48] and biarlyazacyclooctyne (BARAC, $k_2 = 9.6 \cdot 10^{-1}$ $M^{-1}s^{-1}$)[49] an increase of the rate constant could be achieved through additional ring strain (figure 6).

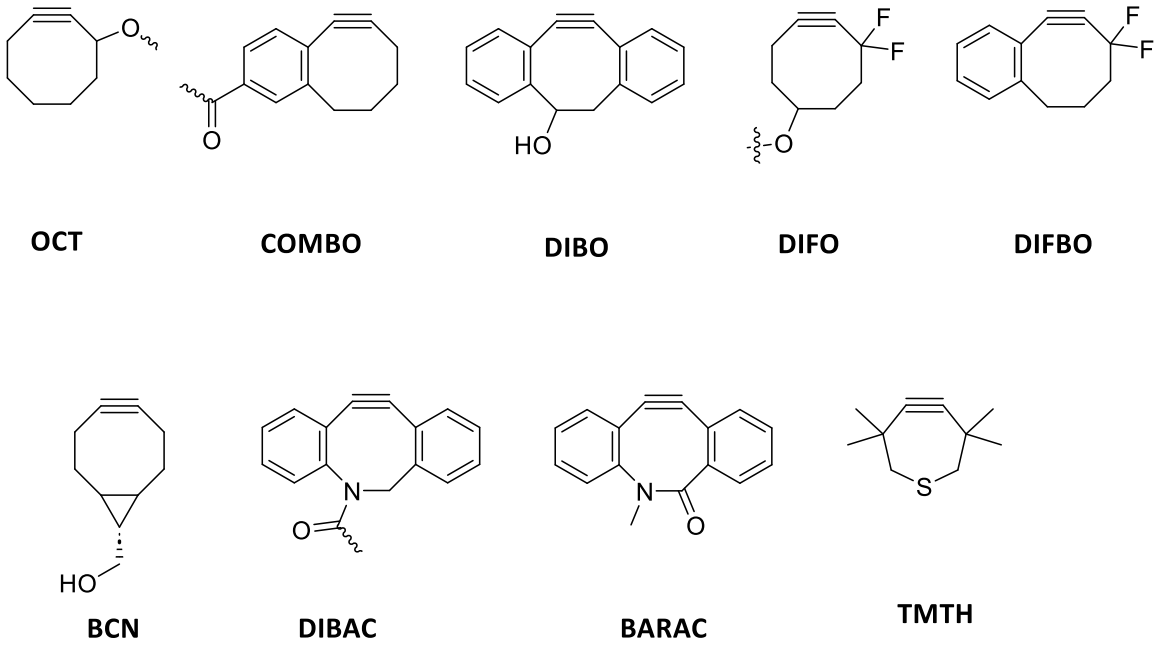

Figure 6: Structures of various cyclooctynes as reaction partner for the strain-promoted azide-alkyne-cycloaddition (SPAAC). Cyclooctyne (**OCT**), Carboxymethylbenzocyclooctyne (**COMBO**), Dibenzocyclooctynol (**DIBO**), Difluorocyclooctyne (**DIFO**), Difluorobenzocyclooctyne (**DIFBO**), Bicyclo[6.1.0]nonin (**BCN**), Azadibenzocyclooctyne (**DIBAC**), Biarylazacyclooctyne (**BARAC**), Tetramethylthiacycloheptyne (**TMTH**).

The reactivity can be further enhanced by additionally introducing heteroatoms like nitrogen (N) into the cyclooctyne ring, as in BARAC and DIBAC, which is reflected in the reaction kinetics compared to DIBO.[50] The disadvantage of this concept is that the steric hindrance is higher, and the water solubility decreases which makes the reaction in

aqueous, living systems difficult.[51] The reactivity is also influenced by the ring size, that is why cyclononynes are usually too unreactive whereas cycloheptynes are highly reactive but correspondingly unstable. *Bertozzi et al.* could achieve the highest reaction rates by synthesizing a cycloheptyne in which one carbon atom is substituted by a sulfur atom to slightly reduce the ring tension. This enabled them to develop a tetramethylthiacycloheptyne (TMTH) that is stable but still exhibits a high reaction rate ($k_2 = 4.0 \cdot 10^0$ $M^{-1}s^{-1}$).[50] Nevertheless, the stability of TMTH is insufficient to make it suitable for the bioorthogonal labeling of biomolecules. A compromise must be found between reactivity and size. This compromise is realized in bicyclo[6.1.0]nonyne (BCN, $k_2 = 0.14 \cdot 10^0$ $M^{-1}s^{-1}$) by obtaining the necessary reactivity from the fused cyclopropyl ring, although bulky aromatic ring systems are avoided.[46,52]

The principle of bioorthogonal labeling of modified DNA and RNA via SPAAC is based on markers that have a complementary functionalization. For this purpose, both the azide and the cyclooctyne moiety can be inserted into the nucleic acids. *Heaney et al.* reported a conjugation method for the postsynthetic modification of DNA at the 5' -end of oligonucleotides using a non-fluorinated cyclooctyne **I** (**figure 7**). **I** reacted successfully with a variety of azides, each with different steric and electronic properties.[53] Moreover, it was discovered that cyclooctynes are reactive towards other dipoles, such as nitrile oxides. *Madder et al.* showed that nitrile oxides can react fast with cyclooctyne under mild and aqueous conditions, achieving full conversion in 10 min.[54] Building on this, *Filippov et al.* extended this approach by using a phosphoramidite building block **II** (**figure 8**) to incorporate a more reactive cyclooctyne: DIBAC, at the 5'-end of single stranded RNA. **II** enabled a rapid and quantitative reaction with various reaction partners such as fluorescent dyes and showed an even higher reaction rate compared to **I**, achieving complete conversion in just one minute.[55]

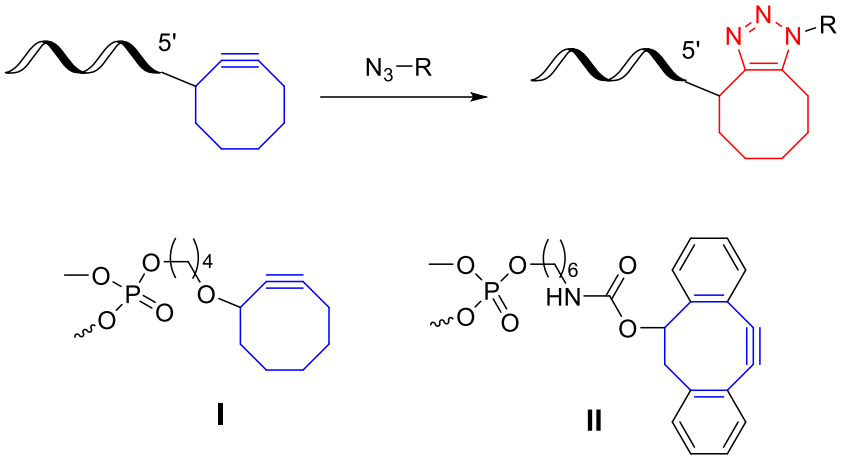

Figure 7: Example cyclooctyne building blocks **I** and **II** for the postsynthetic conjugation of DNA and RNA using strain-promoted-azide-alkyne cycloaddition (SPAAC).

Fluorogenic probes have been developed for SPAAC to enhance their potential for biological applications. In particular *Boons et al*. synthesized a novel dibenzocyclooctyne derivate with a cyclopropenone group (FI-DIBO).[56] Upon reacting with suitable dipolarophiles, FI-DIBO undergoes a significant enhancement in fluorescence properties, exhibiting up to a 160-fold increase in quantum yield and a remarkable 13000-fold boost in fluorescence intensity (**figure 8**). Like other cyclooctynes, FI-DIBO can react not only with azides but also with mono- or disubstituted diazo compounds, nitrons and nitriloxides. Among these, reactions with monosubstituted diazo compounds proved especially promising, leading to the formation of aromatic pyrazoles via tautomerization. Although these reactions proceeded more slowly compared to those with azides, they offered distinct advantages due to their physical properties.[57] Additionally, cycloalkynes can engage in various cycloaddition reactions with different functional groups, such as [1+2] cycloadditions with carbenes, [2+2+2] cycloadditions with nitriles, [2+2] cycloadditions with ketenes, and [4+2] cycloadditions with tetrazines.[51]

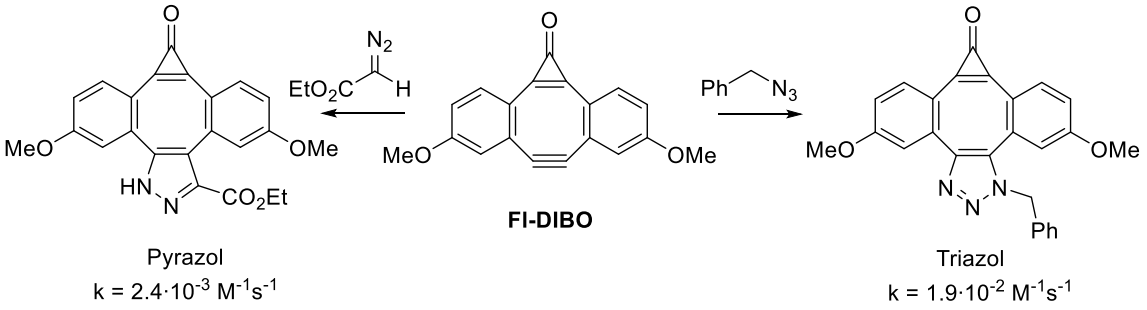

Figure 8: Dibenzocyclooctyne derivate with cyclopropenone group (FI-DIBO) for use as a fluorogenic probe for SPAAC with diazocompounds and azides.[56,57]

Brown et al. took a different approach by employing DIBO for the functionalization of nucleosides instead of a dye modification (**figure 9**). They developed derivates modified with DIBO or BCN that could be attached to either the 5-position of the nucleobase or to the 2'-position of the ribose. The 5-position modifications were incorporated into oligonucleotides as phosphoramidite or triphosphate and were used to label the major groove of DNA.[58] On the other hand, modifications at the 2'-position were designed for selective labeling in the minor groove, those building blocks could only be incorporated chemically via solid-phase synthesis.[59]

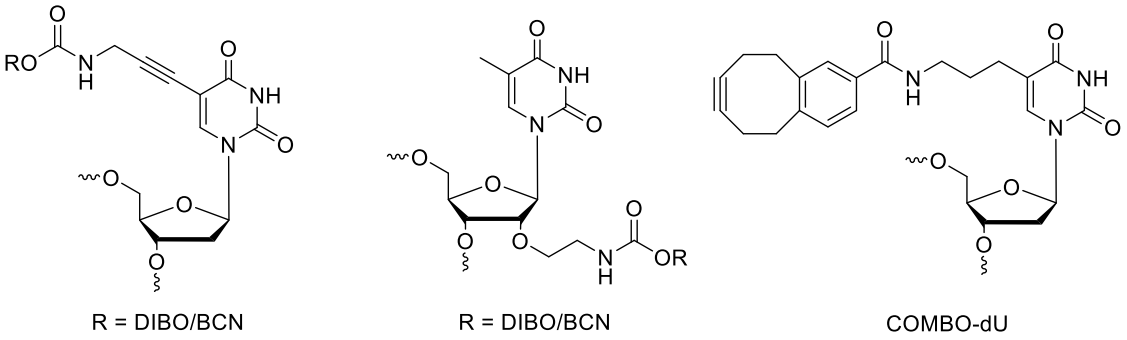

Figure 9: Selected example of cyclooctyne-modified nucleic acids.[58–60]

Wagenknecht et al. successfully incorporated a COMBO-modified nucleoside (COMBO-dU) as phosphoramidite into oligonucleotides via solid phase synthesis. The COMBO-dU shown in **figure 9** is linked via a flexible alkyl linker to the nucleoside. The flexible linker showed superior optical properties compared to one with a rigid alkyne linker, which underscored the significance of how a chemical reporter is linked to a building block.[60] Furthermore, the modified oligonucleotides shown in **figure 9** were transported into cells and labeled

with fluorescent dyes in vivo. As the above-mentioned examples show, researchers have made significant progress in using DIBO to modify nucleic acids. Furthermore, *Taton et al.* showed that DIBO-modified groups can endure both the rough conditions of solid phase synthesis and the high temperatures required for PCR.[61] Overall, these studies highlight that cyclooctynes are reliable and stable for bioorthogonal labeling of nucleic acids with SPAAC, and in most cases, polymerases will tolerate these modifications. However, challenges can arise dealing with bulkier, more lipophilic compounds such as benzyl-fused cyclooctynes.[62] Furthermore, nucleic acids can be modified with azide groups, expanding the scope of bioorthogonal applications.

Several azide-modified building blocks have been successfully used to label oligonucleotides via SPAAC with various cyclooctynes, although some challenges had to be overcome.[59,63–66] The main problem being the reactivity of azides with phosphorus(III), which is crucial in phosphoramidite synthesis. During the phosphoramidite synthesis the azides undergo a Staudinger-like reaction with the phosphorus (III) which prevent the building blocks from being incorporated into nucleic acids.[65,67–71] *Rentmeister et al.*, who developed a method for labeling RNA, found a promising solution to this problem.[72] They synthesized several different azide-modified guanosine building blocks and transferred their azide groups chemoenzymatically onto the 5’ cap of eukaryotic mRNAs using methyltransferases. In the next step, the modified mRNA was labeled with DIBO-modified dyes.[72–74] This method was also used to transfer the azide group to the poly(A) tail of mRNA for the bioorthogonal labeling in living cells.[75] A big advantage of the azide function is its small size compared to cyclooctynes groups. The small size enables a better acceptation of the modified nucleoside by for example kinases. *Luedtke et al.* were able to integrate an azide-modified 2’-deoxyuridine metabolically into cellular DNA and then label it in vivo using BCN-modified AlexaFluor488 dyes.[76]

3.3.2 Strain-promoted sydnone-alkyne cycloaddition (SPSAC)

Another copper-free labeling method is the strain-promoted sydnone-alkyne cycloadditon (SPSAC). Sydnones were discovered by *Early* and *Mackney* in 1935 and got in focus for bioorthogonal labeling due to their high stability under physiological conditions. Sydnones are mesoionic compounds. Mesoionic structures are heterocycles that have a dipolar

character in which the charge is delocalized. The most frequently used resonance structure in the literature has a negative charge on the exocyclic oxygen atom, and a positive charge on the 3- nitrogen atom (**figure 10**).[77]

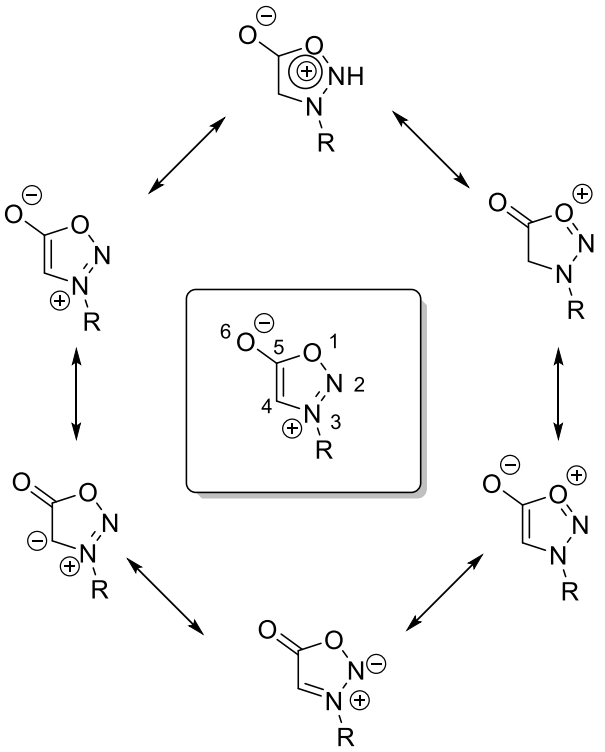

Figure 10: Resonance structures of sydnones.[78]

Sydnones react in SPSAC with various cycloocytynes and also with terminal alkynes in CuAAC reactions under extrusion of CO_2 (**figure 11**).[79,80] *Taran et al.* investigated how different substitutions on the sydnone core influence the rate constants of the SPSAC (**table 1**). Substitutions at the 4-position had varying effects, halogens increased the reaction rate, while electron withdrawing groups like CF_3 groups reduced it (entries **1-3** vs. **4**). The reaction rates correlate with the electronegativity of the halogens (Cl>Br>I). Modification on the 3-N position with electron-donating groups compared to an unmodified phenyl sydnone (entry **5** vs **6**) slowed down the reaction. In contrast, electron-withdrawing groups such as trifluoromethyl, nitro and carboxyl groups significantly increased the reaction rates by 2- to 10-fold (entries **7** - **9**). By combining those beneficial properties, a 10-fold faster reaction rate was observed with SPSAC, compared to azides.[36]

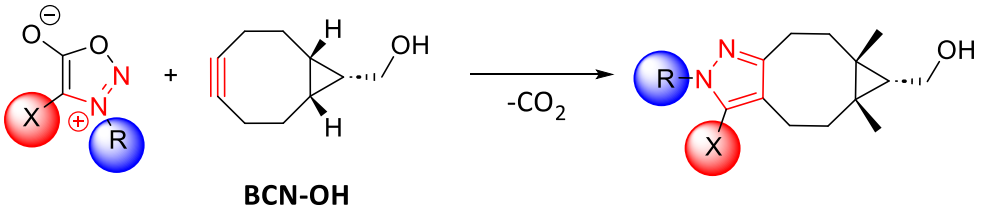

Figure 11: Strain-promoted sydnone alkyne cycloaddition (SPSAC). Reaction of a sydnone and BCN-OH.

Table 1: Influence of different substituents on the reaction rate constants of SPSAC with BCN-OH. Reaction conditions: [Sydnone] = 100 µM, [BCN-OH] = 150 µM, 0.10 M (pH 7.4) PBS with 10 % DMSO, 25 °C.[36,81]

Experiment number	R	X	k_2 [$M^{-1}s^{-1}$]
1	C_6H_5	Cl	0.872
2	$pCO_2HC_6H_5$	Cl	1.593
3	C_6H_5	I	0.306
4	C_6H_5	CF_3	0.008
5	$pOMeC_6H_5$	H	0.006
6	C_6H_5	H	0.027
7	$pCF_3C_6H_5$	H	0.059
8	$pCO_2C_6H_5$	H	0.199
9	$pNO_2C_6H_5$	H	0.289

Houk and *Murphy* investigated sydnone-alkyne cycloadditions by calculating activation free energies and confirmed their results experimentally. The most promising results were achieved by the reaction of phenyl sydnone with BARAC and DIBAC with reaction rate constants of $k_2 = 1.46 \cdot 10^0$ $M^{-1}s^{-1}$ and $k_2 = 9.02 \cdot 10^{-1}$ $M^{-1}s^{-1}$.[82] Fluorinating the sydnone instead of chlorinating it significantly accelerated the reactions, enhancing the rate constants to 42 $M^{-1}s^{-1}$ with BCN, 900 $M^{-1}s^{-1}$ with DIBAC, and 1500 $M^{-1}s^{-1}$ with TMTH.[83] The results of the fluorination show the changeability of the reactivity of the sydnones through substitution at the sydnone ring and demonstrate the potential of the sydnones as chemical reporters for the bioorthogonal labeling of biomolecules. In the past few years, great progress has been made in terms of fluorogenic labeling with sydnones. *Friscourt et al.* investigated the quenching behavior of sydnones and observed a strong quenching effect on the dye coumarin.[84] Coumarin is known in literature to be quenched by several

functionalities, such as alkynes and azides.[85–87] The quantum yield of coumarin compared to coumarin-sydnone is six times higher, which shows the quenching effect of the sydnone (Φ_F (Coumarinsydnone) = 0.005, Φ_F (Coumarin) = 0.03). In the case of a reaction with the opposite functionality, like BCN, the quenching was reversed and leads in the case of BCN as a reaction partner to a 132-fold fluorescence enhancement.[84] Another approach investigated 3,4-disubstituted sydnones for highly fluorescent turn-on SPSAC reactions with the already mentioned fluorogenic dibenzocyclooctyne FI-DIBO (**figure 12**).[56] The resulting pyrazole cycloadducts were found to be highly fluorescent with good photophysical properties including excellent fluorescence enhancement (up to 240-fold), quantum yields over 45% and large Stokes shifts. Additionally, their high stability makes them excellent chemical reporters for the detection of proteins in cellular extract. Therefore, they modified the proteins of interest with a sydnone via an NHS-ester coupling and incubated the modified proteins with FI-DIBO. The labeled protein could be easily detected through in gel visualization due to the high turn-on.[79] *Taran et al.* also showed that sydnones can be used as fluorogenic probes for no-wash protein labeling and in-cell imaging. Consequently, a sydnone profluorophore was synthesized that after the bioorthogonal reaction has taken place, is unquenched leading to a high fluorescence enhancement and enabled the labeling of DIBAC-modified myoprotein.[13]

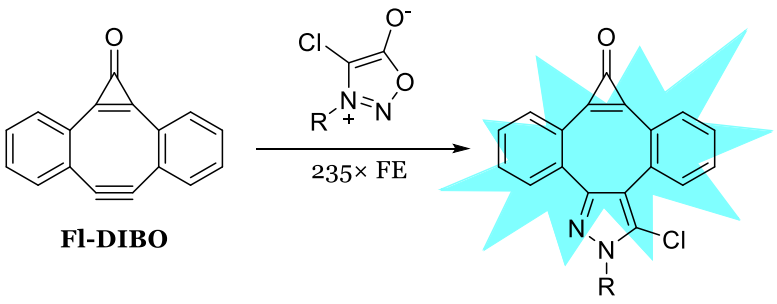

Figure 12: Reaction between a chlorinated sydnone and FI-DIBO.[79]

Wagenknecht et al. were the first group that successfully modified DNA and nucleosides with a sydnone moiety in 2021.[88] The postsynthetic sydnone-modified DNA was used for bioorthogonal labeling with cyclooctynes in vitro and in vivo. For the first time, two different sydnones were modified with 2'-deoxyuridine and 7-deaza-2'-deoxyadenosine

(figure 13). The difference between the two sydnones is that one is bearing a chlorine atom on the sydnone-core. As *Taran et al.* earlier reported chloro-modified sydnones show a higher reaction rate than unsubstituted sydnones, those results are in line with the observed reaction rates of the sydnone-modified nucleosides: The non-halogenated sydnone-modified nucleosides (k_2 = 7.0 · 10^{-2} $M^{-1}s^{-1}$) were significantly slower than the chlorosydnone-modified nucleosides (k_2 = 4.4 · 10^{0} $M^{-1}s^{-1}$). To modify DNA with the two sydnones, solid-phase synthesized DNA was postsynthetically modified with the corresponding NHS-sydnone ester. Labeling the chlorosydnone-modified DNA with five equivalents of DIBAC-modified Cy3 could be achieved in two minutes. Subsequently, in vivo experiments with fixed HeLa cells showed distinct fluorescence of the cells through SPSAC.[81,88]

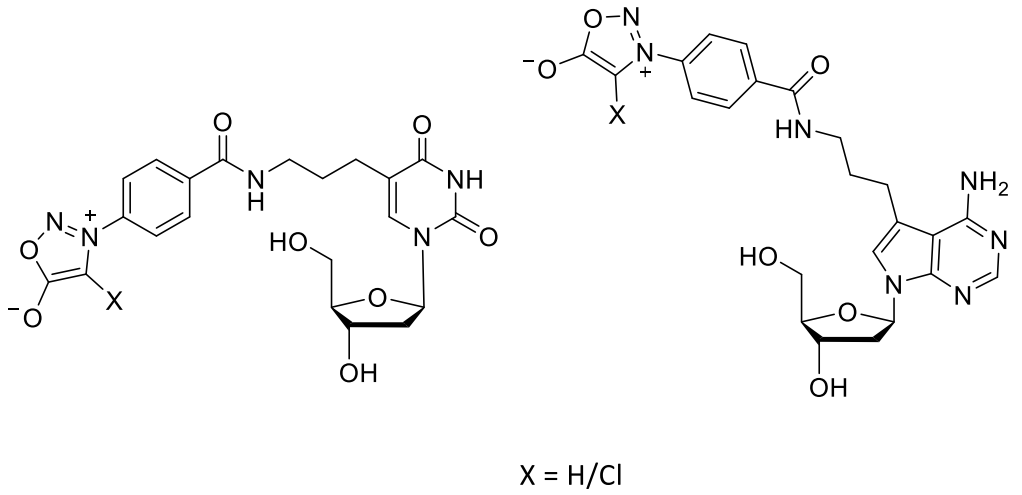

Figure 13: Structures of the sydnone-modified nucleosides.[88]

3.3.3 Photoinduced labeling methods

In nature, many organisms harness light energy for the biosynthesis of complex biomolecules. The most prominent example in nature is photosynthesis where plants convert carbon dioxide and water into carbohydrates. The light-absorbing chlorophyll plays a crucial role in this process by acting as a photosynthesizer and by capturing light.[89] A big advantage of photoactivated reactions is that no additional substances like transition metals, acids or bases are needed, which makes these types of reactions interesting for

applications in organic synthesis. By combining photoactivation with the principles of click chemistry, the new class of the so called ''photoclick'' reactions has emerged.[90,91] A big advantage compared to the previously mentioned methods is that the photoclick reaction enables a high spatiotemporal control of the reaction, which means that this type of reaction allows the determination of the exact time and place at which the reaction is to be started. Another advantage is that the modified monomers can be introduced into the targeted system, for example the cell, and are unreactive until the reaction is triggered by irradiation with light of a suitable wavelength.[92] An overview of selected photoactivatable labeling methods is shown in figure 14.

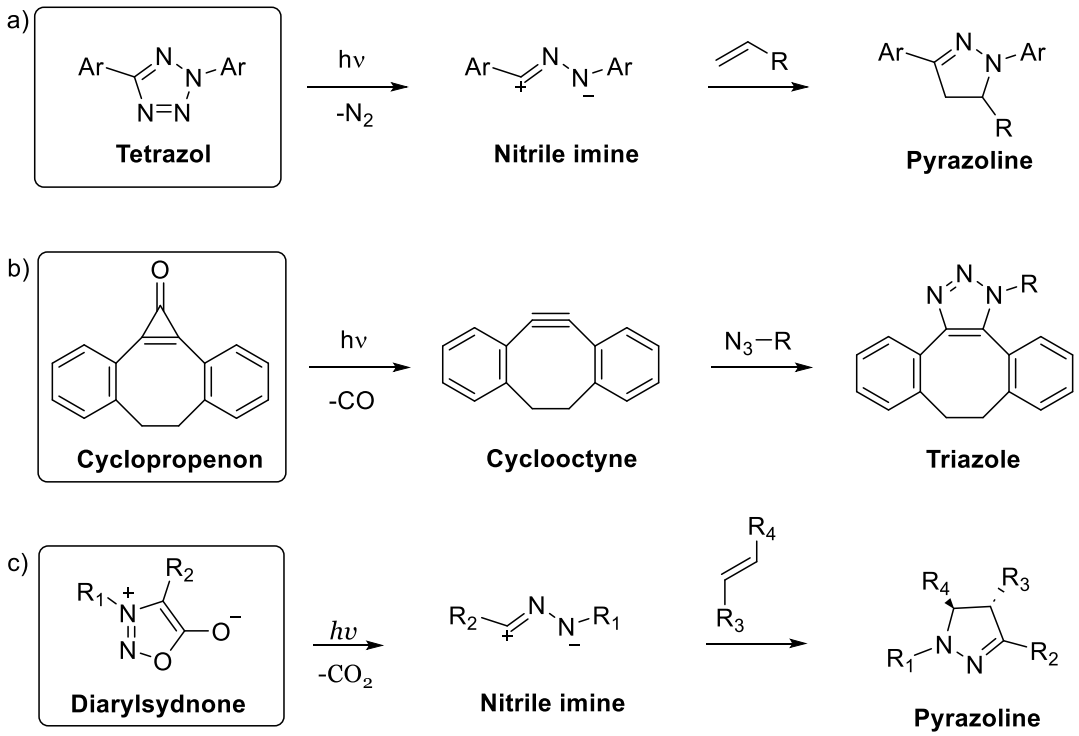

Figure 14: Overview of various photoactivatable reactions: a) photoclick reactions with tetrazoles, b) photoactivatable reactions SPAAC with cyclopropenones, c) photoclick reactions with diarylsydnones (R_1, R_2 = Ph).

The most prominent example of photoactivable reactions is the 1,3-dipolar cycloaddition between photoactivated tetrazoles and alkenes. *Huisgen et al.* reported first that exposing 2,5-diphenyltetrazole to mercury lamp irradiation in the presence of various alkenes results in the formation of pyrazolines.[39,93,94] The mechanism of this reaction was described as a two-step mechanism. In the first step, a photoinduced cycloreversion of the tetrazole

under extrusion of nitrogen takes place forming a nitrile imine. The in situ generated nitrile imine immediately undergoes a 1,3-dipolar cycloadditon with dipolarophiles (e. g. alkenes) leading to pyrazoline photoclick products (**figure 15**).[95,96] The described reaction is known for high reaction rates (k_2 = 58 $M^{-1}s^{-1}$).[97] *Holm et al.* examined the formation of the nitrile imine spectroscopically.[98] The results of their experiments showed that ring opening of the 2,5-diaryltetrazoles only occurred when exposed to light at an excitation wavelength of approximately λ = 290 nm, with the electronic properties of the substituents appearing to have only minimal influence. Further studies of *Liu et al.* showed that the rate-determining step in the photoinduced 1,3-dipolar cycloaddition is the formation of the nitrile imine.[99]

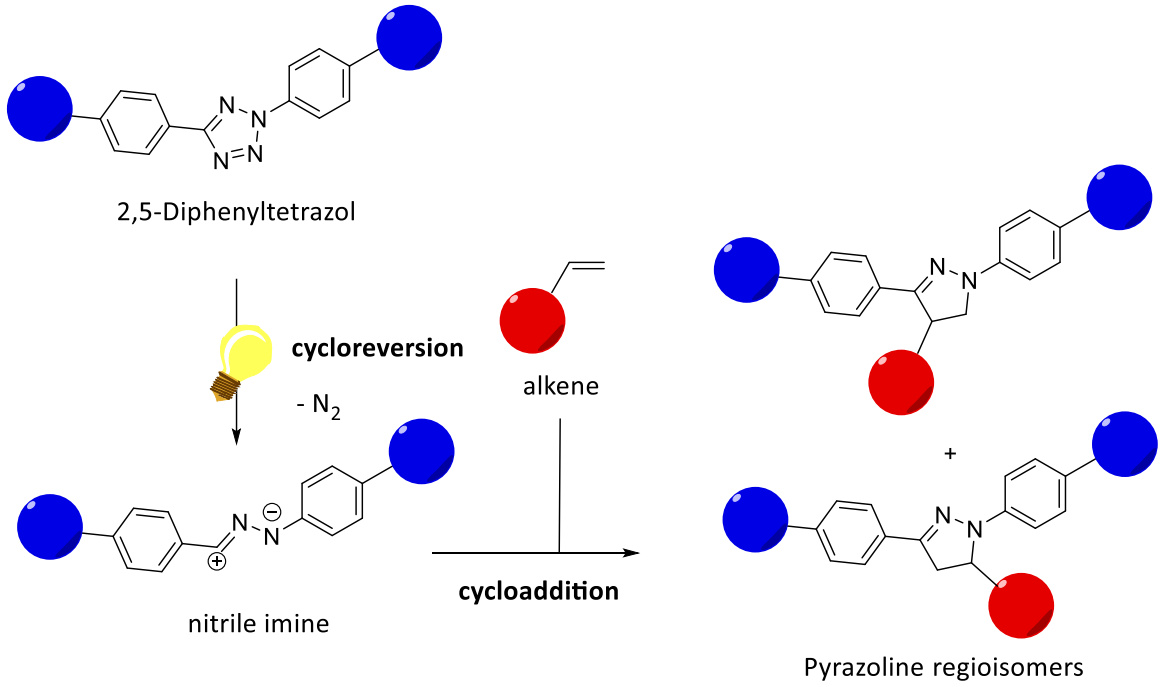

Figure 15: Schematic representation of the photoclick reaction. As a result of photoinduced cycloreversion, the corresponding nitrile imine is formed with elimination of elemental nitrogen. In a 1,3-dipolar cycloaddition, the nitrile imine reacts with a dipolarophil (e.g. alkene) to form the pyrazoline.

A limiting factor is the chemoselectivity of the reactants. The nitrile imine is highly reactive and shows cross reactivity with different moieties that are present in cellular environments, like water, amines[100], thiols[101] and carboxylic acids[102,103] (**figure 16**). One approach to prevent undesired nucleophilic addition reactions is to use sterically hindered nitrile imines favoring the 1,3-cycloaddition.[104] Another approach used by *Yu et al.* is to protect the nitrile imine from a nucleophilic attack through static and electrostatic effects by

introducing two negative partial charged trifluoromethyl groups.[105] Furthermore, *Lin et al.* were able to show that a regioselective reaction in a protic solvent (EtOH/H_2O 1:1) is possible with high yields.[106]

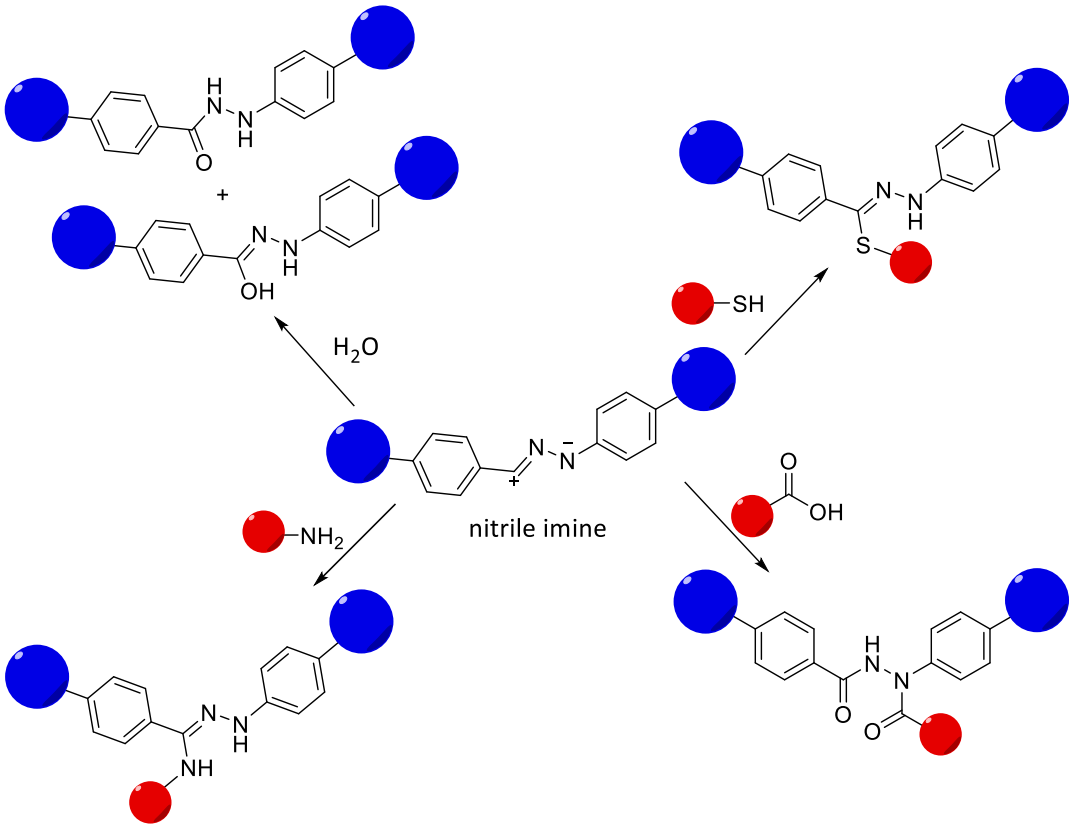

Figure 16: Overview of possible side reactions of nitrile imine with certain nucleophiles. Nitrile imines can react with nucleophiles present in biological systems, such as water, thiols, carboxylic acids and amines.

Optimizing the activation wavelength is in addition to selectivity a major focus of current research in photoclick chemistry.[107,108] The first described tetrazoles can only be activated by irradiation in the UV range; for activation in in vivo applications, visible light or near infrared light is favored more because longer wavelengths can better penetrate tissue layers and skin.[37,108,109] A bathochromic shift of the excitation wavelength can be achieved by embedding the tetrazole scaffold in larger aromatic systems. For instance, *Lin et al.* synthesized naphthalene-substituted tetrazoles with an excitation wavelength of 365 nm.[110,111] Another example for visible light activation is a tetrazole with two naphthyl substituents which can be activated by a two-photon femtosecond laser system at 700 nm. This tetrazole was used to stain microtubuli in living cells.[112] Furthermore, *Barner-Kowollik* synthesized an N,N-dimethylaminopyrenylated tetrazole which can be activated by green

light (λ = 515 nm) The advantage of this tetrazole is that no laser is needed, which would be much more expensive than the use of LEDs. Drawbacks for the pyrenyltetrazole is its poor water solubility, which makes it unusable in living systems.[113,114]

Aside from protein modification, tetrazoles have also been used for oligonucleotide labeling. *Wagenknecht et al.* were the first to explore this application by synthesizing several different tetrazole-modified 2'-deoxyuridine building blocks and successfully incorporate them into DNA and RNA using phosphoramidite synthesis, enzymatic methods or postsynthetic modification. The tetrazole-modified DNA strand was subsequently labeled via a photoclick reaction using irradiation between $\lambda_{exc.}$ = 300 - 405 nm, followed by reaction with sulfo-Cy3 maleimide.[115,116] This allowed for the determination of rate constants ranging from k_2 = 23 $M^{-1}s^{-1}$ to k_2 = 89 $M^{-1}s^{-1}$.[115] In a reverse approach, *Zhang et al.* were able to successfully incorporate a vinyl-modified 2'-deoxyuridine metabolically into DNA and label it with a water-soluble coumarin- fused tetrazole at an excitation wavelength of $\lambda_{exc.}$ = 350 nm, leading to a high fluorescence both in living cells and zebrafish.[117] The first example of RNA labeling by photoclick reaction was investigated by *Rentmeister et al.* by incorporating a guanosine modified with a vinyl group into an oligonucleotide as a 5'-mRNA cap and subsequently performed a photoclick reaction with a diaryltetrazole.[118] In 2023, *Wagenknecht et al.* developed an N,N-dimethylaminopyrene-modified tetrazole that could be used to label cellular DNA and was excited in the visible range at 450 nm.[14]

Another photoactivatable labeling reaction can be performed with cyclopropenones. Cyclopropenones are cyclopropene-masked dibenzyl-substituted cyclooctynes, which can react after elimination of carbon monoxide through irradiation in a strain-promoted azide alkyne reaction with azides. In 2003, *Popik et al.* investigated the behavior of different cyclopropenone derivatives under UV irradiation, discovering that they quantitatively convert to their corresponding alkynes with the elimination of carbon monoxide.[119] For some of the diphenylcyclopropenones, quantum yields of over 70 % were achieved due to photoinduced decarbonylation.[120] This approach to bioorthogonal labeling is essentially a photoinduced variant of SPAAC. The cyclopropene modification acts as a protecting group to mask the reactive alkyne. Unlike previously described labeling methods, this labeling

method enables a spatiotemporal control of the reaction because only through exposure to specific wavelengths a reactive species is build (**figure 17**).

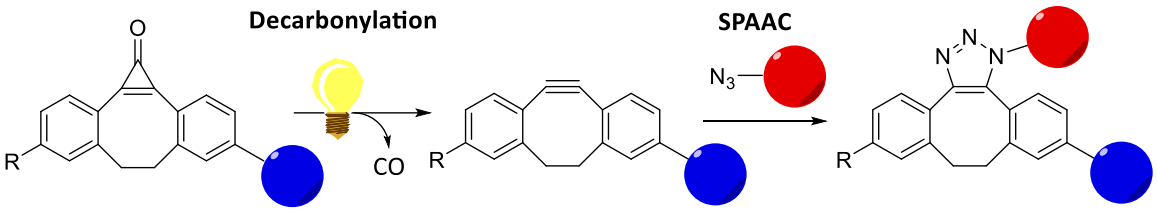

Figure 17: Schematic representation of photoinduced SPAAC: The first step is the decarbonylation through exposure of light to form the corresponding cyclooctyne. The formed cyclooctyne can react in a second step with an azide in a SPAAC to form a triazole.

Substituents at the cyclopropenones significantly influence their spectroscopic properties and also their stability.[121] Nevertheless, the reaction rates of the SPAAC are mainly determined by the specific SPAAC reaction. *Popik et al.* reported reaction rate constants of up to $k_2 = 7.6 \cdot 10^{-2}$ $M^{-1}s^{-1}$ for the reaction between cyclopropene-masked dibenzyl-substituted cyclooctynes (photo-DIBO) and benzyl azide, with further improvements achieved by incorporating heteroatoms into the cyclooctyne ring (see **figure 18**, photo-ODIBO).[120] A special case is the photo-DIBOD, a dual cyclopropenone: In a first step, a selective decarbonylation could be achieved, this selectivity is made possible by significantly lower quantum yield for the double decarbonylation compared to the single decarbonylation. After the reaction with an azide, the second decarbonylation can be carried out. The resulting cyclooctyne has an additional ring strain cause by the triazole. The second cycloaddition proceeds with a substantially faster reaction rate of $k_2 = 34$ $M^{-1}s^{-1}$ compared to the reaction rate of the first cycloaddition $k_2 = 1.66 \cdot 10^{-2}$ $M^{-1}s^{-1}$.[122,123] There are also cyclopropenone structures which are based on cycloheptynes. For example, *Bertozzi et al.* synthesized a selenium cycloheptyne, which is unfortunately unsuitable for bioorthogonal reactions due to the instability of the alkyne formed by decarbonylation.[124] The dibenzosilacyclohept-4-yne investigated by *Klàn et al.* showed high reactivity towards azides and showed good quantum yields.[125] *Popik* and *Boons* showed that a cyclopropenone-masked dibenzocyclooctyne biotin conjugate can be used for the labeling of glycoproteins in vivo. Through photodecarbonylation, a ring strained alkyne is received and reacts in a next step with an azide-modified glycoprotein.

This is followed by the detection of the product with an avidin-modified Alexa Fluor 488 dye.[120] Furthermore, *Spitale et al.* used cyclopropenones to label azide-modified RNA in cellular environment.[126] Moreover, there are no further applications in the field of nucleic acid labeling. Nevertheless, due to their high stability and biocompatibility, these offer great potential for biological application.

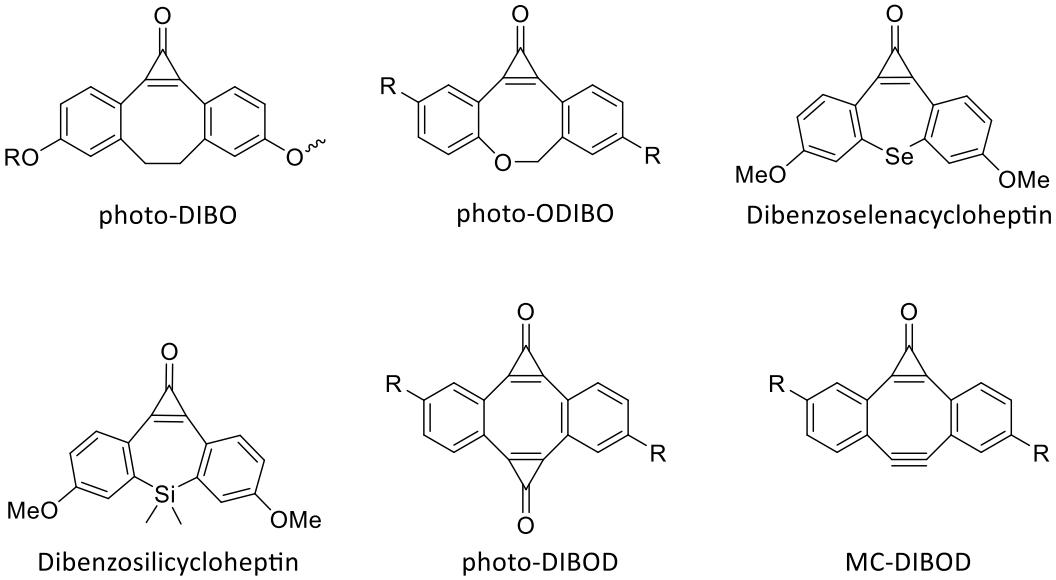

Figure 18: Structures of selected cyclopropenones for photo-induced SPAAC.

Another class of molecules for photoactivatable labeling are diarylsydnones. By irradiation of the sydnone with light, a nitrile imine is generated through extrusion of carbon dioxide. The in situ generated nitrile imine immediately undergoes a 1,3-dipolar cycloaddition with dipolarophiles (e.g. alkenes) leading to a pyrazoline photoclick product.[127–129] Compared to the strain promoted-sydnone-alkyne cycloaddition (SPSAC) the photoclick reaction of sydnones lead to an increase in the rate constants of up to five times. As shown in **figure 19**, it should be noted that in the SPSAC, a 1,5-substituted pyrazole is generated, whereas in the photoclick reaction a 1,3-substituted pyrazoline is generated.

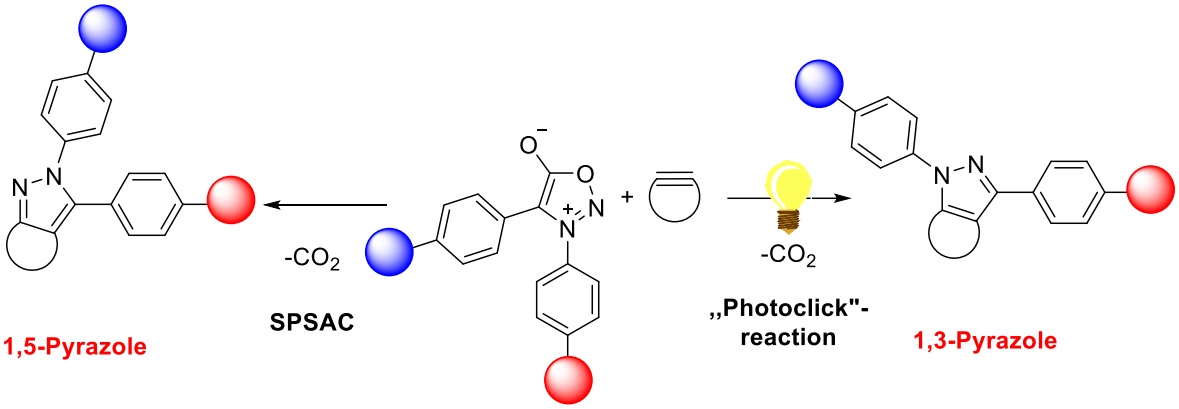

Figure 19: Formation of differently substituted pyrazole products depending on the used reaction conditions. In the SPSAC reaction the 1,5-pyrazole is generated and in the photoclick reaction the 1,3-pyrazoline is build.

In 2018, *Yu et al.* developed a small library of diarylsydnones based on aryl-pairing combinations and investigated the photoclick reaction with alkenes. Furthermore, they used a diarylsydnone for highly fluorescent turn-on ligation of TCO-modified proteins.[15] Another approach from *Yu et al.* in 2019 showed that the reaction of diarylsydnones with strained alkynes under photoclick conditions can also be used for the labeling of Cetu-BCN on the cell surface.[130]

3.4 Dual bioorthogonal labeling

Biological processes are often based on complex interactions between different biomolecules. The visualization of those interactions makes it necessary to visualize two or more components simultaneously. With the help of several probes in a single biomolecule it is also possible to follow conformational changes or molecular dynamics. Also, in medical drug development, there are approaches that simultaneously have diagnostic and therapeutic functions.[131,132] To track interactions between for example proteins and oligonucleotides it is feasible to use more than one bioorthogonal reaction within the same system. Therefore, the chosen reactions must not only be bioorthogonal to the cellular environment, but also orthogonal to each other. Many known bioorthogonal reactions are not compatible with each other and a wide range of possible side reactions can occur. Several approaches currently exist to identify orthogonal bioorthogonal reactions or to modify the reactants of the respective reactions to create orthogonality.[133–135] One

approach is to combine two bioorthogonal reactions with different mechanisms of bioorthogonality. *Burley et al.* found that the combination of SPAAC and CuAAC is possible due to the controlled modulation of the copper-glutathione ratio. The glutathione concentration acts as an activator for the CuAAC as it regulates the oxidation state of the copper.[136] Another approach on dual labeling is from *Jäschke et al.*, who used the CuAAC and the inverse electron demand Diels-Alder reaction (IEDDA) for the dual labeling of alkyne-modified DNA in vivo. Nevertheless, both reactions are based on the same cycloaddition mechanism. Both react orthogonally with different alkynes. For the CuAAC, alkynes with HOMOs of lower energy are used, whereas for the IEDDA reaction, alkynes with HOMOs of high energy are utilized. Another possibility to modulate reaction specificity is to utilize sterically hindered groups.[137] *Hildebrand et al.* combined SPAAC and IEDDA as orthogonal reactions by using a sterically hindered cyclooctyne. Due to the steric hinderance the side reaction between the cyclooctyne and tetrazine was slowed down successfully, so that a dual orthogonal labeling was possible even in vivo in mice and enabled fluorescence-guided tumor resection.[132,138]

In 2024, *Wagenknecht et al.* developed a dual bioorthogonal labeling strategy using photoclick and IEDDA for the metabolic labeling of DNA. In this approach, a 1-methylcyclopropene nucleoside (1-MCP) and a 3-methylcyclopropene nucleoside (3-MCP) were incorporated into cellular DNA in vitro or in cells using metabolic labeling in combination with an SNT-transporter.[139,140] In a second step, the 3-MCP was labeled with a tetrazole via photoclick reaction and 1-MCP was labeled with a tetrazine dye via IEDDA reaction. The orthogonality is given due to the 3-methyl group of the cyclopropene which introduces steric hinderance in the transition state and effectively impedes the IEDDA reaction. This approach provides a versatile tool for potential applications in labeling cellular RNA.[140]

3.5 Metabolic Labeling

For the metabolic labeling of nucleic acids, chemically modified natural nucleosides are used. In a first step, the chemically modified nucleosides are put into the medium of the cells and the cellular uptake of them takes place via nucleoside transporters in the cell

membrane. In the cell within an endogenous enzyme cascade, the nucleosides are phosphorylated via three nucleotide kinases. The corresponding triphosphates are subsequently incorporated by the cellular DNA or RNA polymerases into DNA or RNA (see figure 20). The limiting process for metabolic labelling of nucleic acids is often the substrate specificity of the enzymes, especially of the nucleoside monophosphate kinase (NMP) of the phosphorylation step.[141,142]

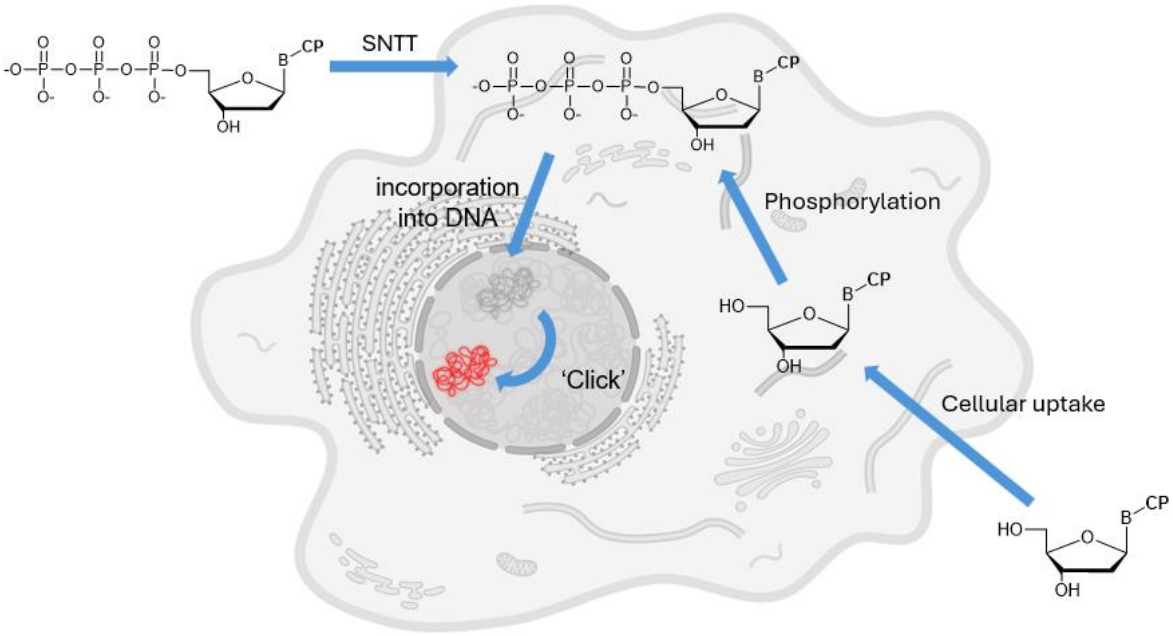

Figure 20: Schematic representation of the metabolic labelling of DNA by means of 2'-deoxynucleosides modified with a chemical reporter.

Spitale et al. investigated the crystal structure of the NMP kinase of the different nucleosides and found out that, for example, the adenosine kinase has free spaces for modification at the C2, N6 and N7 positions on the nucleobase. Nevertheless, these spaces are limited, which is why it is often not possible to use nucleosides that have already been modified with fluorescence probes due to their big size.[143] For this reason, mainly small modifications are used, which can react after incorporating into the DNA with for example a fluorescent probe, to achieve fluorescent labeling in this way.[141] Another approach to enable the incorporation of nucleoside with bigger moieties is the use of genetically modified HeLa cell lines that express a kinase of the herpes simplex virus I, which is less specific than the nucleoside monophosphate kinase of the HeLa cells.[76] However, often small modifications are used as mentioned before. For instance, *Salic* and *Mitchison*

investigated the metabolic incorporation of 5-ethynyl-2'-deoxyuridine (EdU) into DNA enabling bioorthogonal labeling through CuAAC using azide-modified fluorescent dyes.[145] Unfortunately, EdU exhibits antimetabolic and cytotoxic properties, which can negatively affect DNA stability, and the activity of enzymes involved in metabolic processes. Less toxic options can be employed by using alternative analogs such as ethynyl-modified 2'-deoxycytidine, 7-deaza-2'-deoxyadenosine, and 7-deaza-2'-deoxyguanosine.[146–150] The use of azide-modified nucleoside is also an alternative for use in metabolic labeling (figure 21).[76,151]

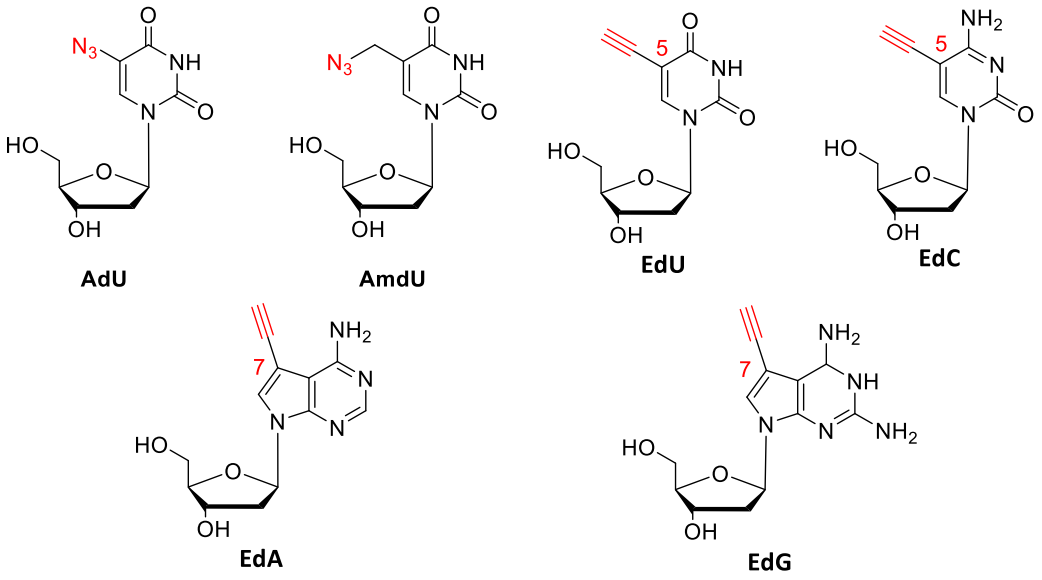

Figure 21: Overview of modified 2'-deoxynucleosides that were introduced into cellular DNA via metabolic labeling.

Also, IEDDA reactions can be used by means of metabolic labeling. To this end, vinyl-modified nucleosides e.g. 5-vinyl-2'-deoxyuridine (VdU) are incorporated metabolically and subsequently labeled by using a tetrazine-dye (figure 22).[149,152]

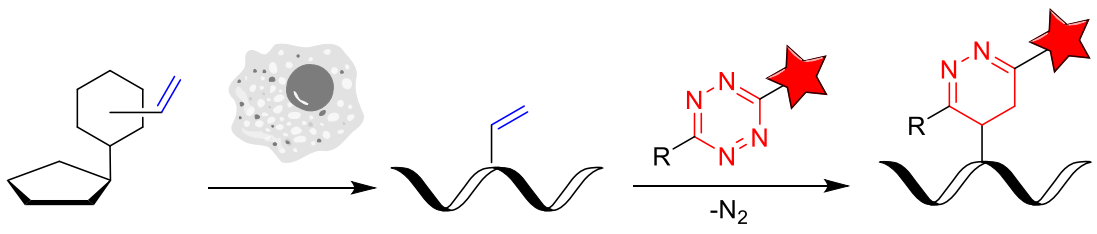

Figure 22: Vinyl-modified building blocks used for IEDDA for the metabolic labeling of nucleic acids.

Wagenknecht et al. showed that the efficiency of metabolic labeling decreases with increasing size of the chemical reporter. To enhance the metabolic incorporation, a cell medium without the addition of natural nucleosides is used. Thus, it was possible to improve the incorporation rate into the DNA by this method. However, sterically hindered chemical moiety, for example norbonene-modified nucleosides, could not be effectively labeled.[20] To bypass one or more phosphorylation steps to enable metabolic labeling with larger functional groups, one strategy is to use the triphosphates of chemically modified nucleosides. An advantage of this method is that all the phosphorylation steps, notably also the first highly selective phosphorylation step, can be bypassed. Unfortunately, the triphosphate cannot be taken up by the cell due to its highly negative charge. *Kraus et al.* developed a synthetic nucleoside triphosphate transporter (SNTT) enabling the transport of triphosphates through the cell membrane. The transporter is already commercially available and is composed of a cyclodextrin unit which can selectively include triphosphates and a long arginine-caproic acid chain as a cell penetrating agent. After crossing the cell membrane, the modified triphosphate, initially complexed with SNTT, can be replaced by natural nucleotides that are within the cell and is then incorporated into the DNA.[139]

4. Fluorogenic sydnone-dyes for bioorthogonal labeling of DNA

4.1 Synthesis of the sydnone-modified cyanine-styryle dye 3

Visualization is crucial for understanding of cellular processes bioorthogonal labeling methods are often employed for this purpose. As mentioned in chapter 3.2, most of these methods and applications have been primarily developed for proteins. Based on their successful application, the development of bioorthogonal methods for other biomolecules has increasingly become a focus of research. Of particular interest is DNA as the carrier of genetic information, along with RNA, which performs a variety of functions within cells. Visualization of transfected DNA is often realized by postsynthetic modification with a chemical reporter and subsequent reaction with a suitable reaction partner that carries a fluorescent dye. However, in cellular applications an excess of dye is typically required. This excess must be washed out after the reaction, which allows its use in fixed cells but severely limits its use in vivo. As a result, the development of fluorogenic dyes is of great interest, because they show a significant increase in fluorescence upon reacting with a chemical reporter, compared to the unreacted dye. This chapter focuses on the development of fluorogenic sydnone dyes, with the aim of synthesizing the sydnone-dye conjugate 3 shown in figure 23, and, if necessary, empirically improving its basic structure to increase its fluorogenicity.

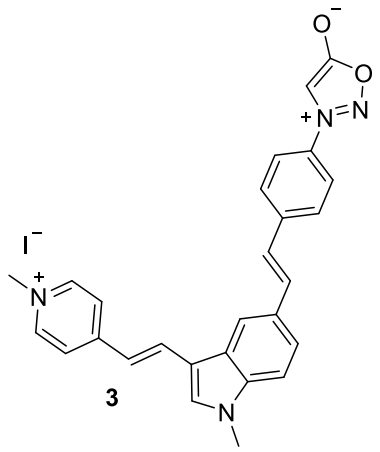

Figure 23: Structure of the sydnone dye 3.

The basic structure of the sydnone-dye conjugate was chosen based on a tetrazine-dye conjugate that had already been established in the *Wagenknecht* group. The sydnone functionality was conjugated via a vinyl bridge to the cyanine-styryl fluorophore to enable effective fluorescence quenching of the dye.[12]

Figure 24 shows a potential synthetic route for the preparation of the sydnone-dye conjugate **3**, achieved by coupling the sydnone building block **5** with the cyanine-styryl dye **4** via a Heck coupling. The cyanine-styryl dye **4** can be synthesized from a picoline and indole, while the sydnone precursor **5** can be prepared in four steps from 4-iodoaniline (**8**).

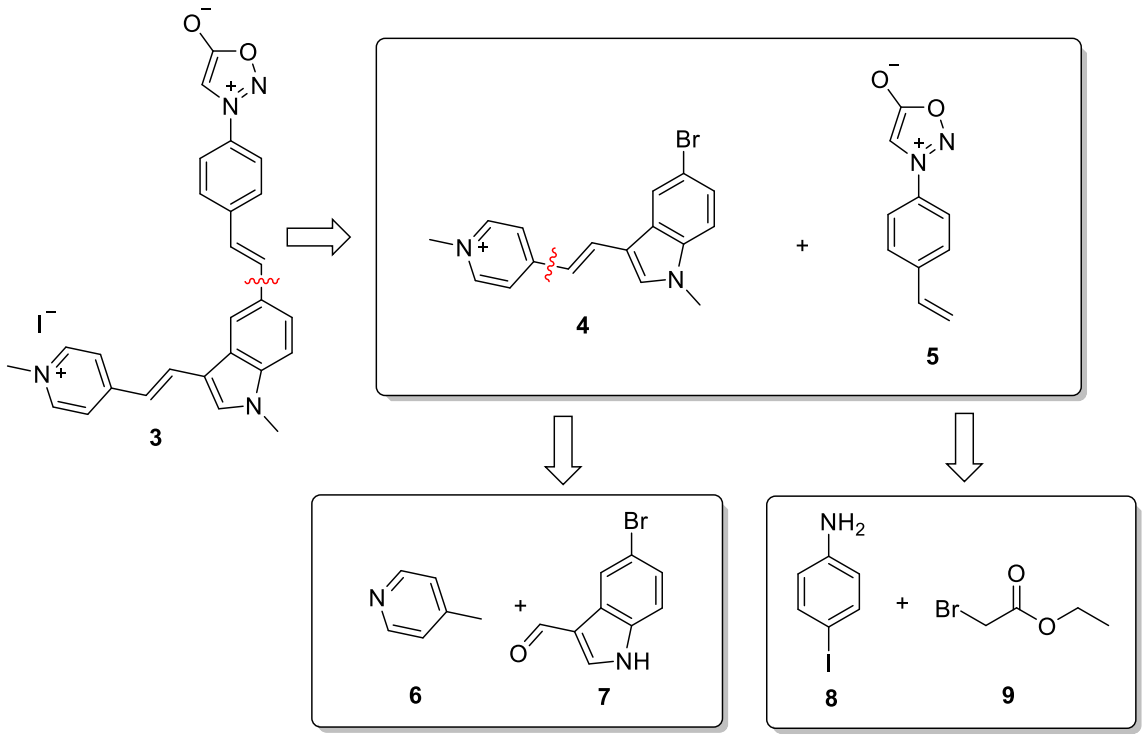

Figure 24: Retrosynthesis of the sydnone-dye conjugate **3**.

The synthesis of the cyanine-styryl dye **4** was realized in a three-step approach. The preparation of **4** started from the commercially available 4-picoline (**6**) and 5-bromo-1H-indole-3-carboxaldehyde (**7**) as shown in **figure 25**.

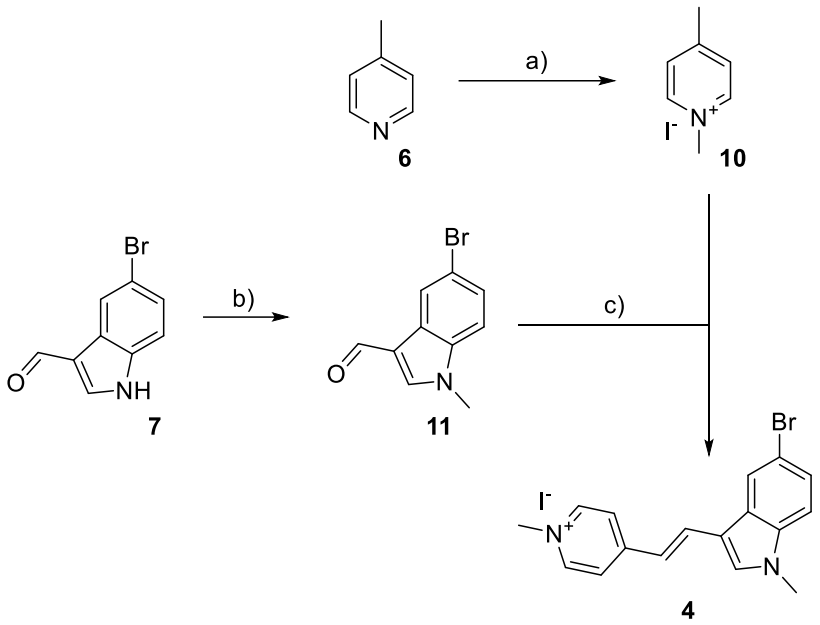

Figure 25: Synthesis strategy of the cyanine-styryl dye **4**: a) MeI, acetone, reflux, 1.5 h, 93 %; b) K_2CO_3, dimethyl carbonate, DMF, 130 °C, 18 h, 71 %; c) piperidine, EtOH, 80 °C, 18 h, 88 %.

A method established by the *Wagenknecht* group was used for the N-methylation of 4-picoline (**6**).[153,154] After 1.5 h of reaction and work-up by precipitation, **10** was isolated as a white solid in a yield of 93 %. Similarly, the commercially available 5-bromo-1H-indole-3-carboxaldehyde (**7**) was N-methylated using dimethyl carbonate as a methylation reagent to enhance the photostability of the indole **11**. The two building blocks were coupled via an aldol-like condensation using piperidine as base and ethanol as reaction to form the cyanine-styryl dye (**4**). The reaction was worked up by precipitation and washing of the dye with diethyl ether. The orange solid was obtained in a yield of 88%.

The sydnone building block **5** was prepared following the procedure published by *Taran et al.* (**figure 26**).[13]

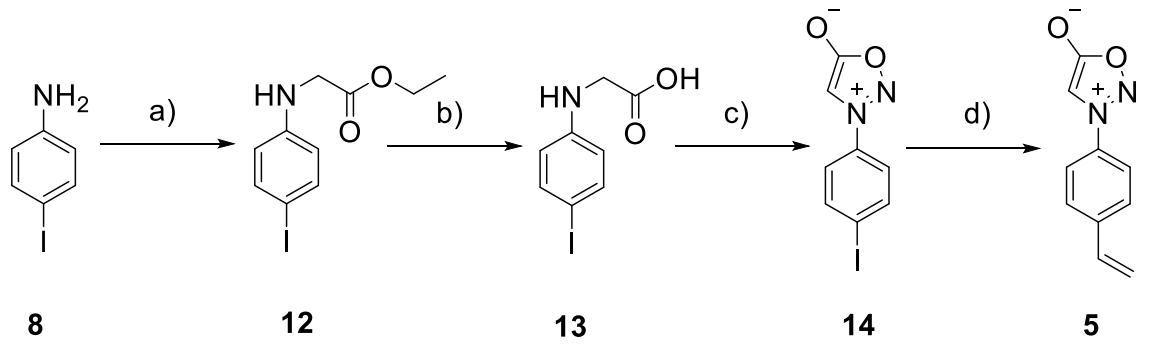

Figure 26: Synthesis strategy of the sydnone **5**: a) 1) K_2CO_3, ethyl bromoacetate (**9**), DMF, r.t., 16 h, 2) Et_2NH, DMF, r.t., 1 h, 71 %; b) LiOH, THF/water (1:1, v/v), 0 °C, 0.5 h, r.t., 1h, 79 %; c) 1) tBuONO, THF, r.t., 0.5 h, 2) TFAA, THF, r.t., 3 h, 21 %; d) $(CH_2{=}CH)_4Sn$, $Pd(PPh_3)_2Cl_2$, DMF, r.t, 16 h, 60 %.

Commercially available 4-iodoaniline (**8**) underwent N-alkylation with ethyl bromoacetate (**9**) to yield the N-4-iodophenylglycine ester **12**. The ethyl group was cleaved using LiOH, with the reaction proceeding in a THF/water mixture. The reaction was kept at 0 °C for 30 min and subsequently at room temperature for an additional 1 hour. **13** was obtained as a light brown solid with a yield of 79 %. The sydnone was synthesized starting from the N-glycine derivative **13** by a two-step reaction. The nitrogen of the N-glycine derivative was nitrosylated using tert-butyl nitrite, followed by the addition of trifluoroacetic anhydride in THF, which led to the formation of the sydnone by cyclodehydration. **14** could be obtained as a brown solid with a yield of 21 %. **14** was utilized with tetravinyltin using $Pd(PPh_3)_2Cl_2$ as a catalyst, to give **3** in a Stille coupling reaction. After reacting overnight at room temperature and purification by column chromatography, **5** was isolated as a light brown solid with a yield of 60 %.

Subsequently, the two building blocks **4** and **5** were linked to each other in a Heck coupling (**figure 27**). The reaction conditions were based on those used for the synthesis of tetrazine dyes, as reported by *Wagenknecht et al.*[12] The reaction was performed in a crimp vial using tris(dibenzylideneacetonedi)dipalladium(0) ($Pd_2(dba)_3$) as catalyst and 1,2,3,4,5-pentaphenyl-1'-(di-tert-butylphosphino)ferrocene (QPhos) as ligand, **4** and excess **5** (2.00 eq.) were added. The reactants were dissolved in DMF and triethylamine was added as base. The reaction was carried out at 80 °C overnight in a heating block. The product was precipitated by the adding diethyl ether and was washed several times with it. **3** was obtained as a reddish-brown solid with 49 % yield.

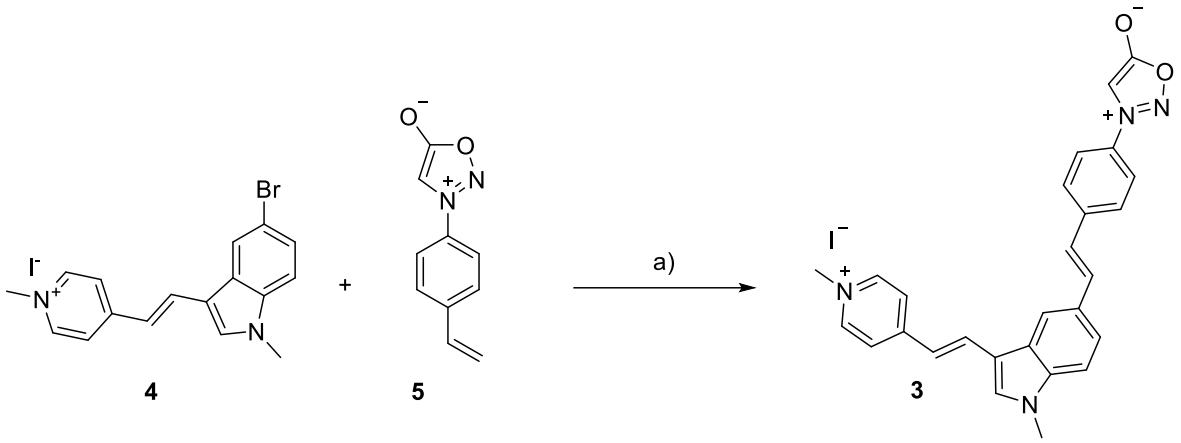

Figure 27: Synthesis of the sydnone dye **3** via Heck coupling: a) $Pd_2(dba)_3$, QPhos, Et_3N, DMF, 80 °C, 18 h, 49 %.

4.2 Synthesis of BCN-modified Nucleosides

The reactivity of the dyes, their kinetics and turn-on were investigated with the BCN-modified nucleosides **15** and **16**. BCN was selected as a reaction partner due to its high reactivity. 7-deaza-2'-deoxyadenosine and 7-deaza-adenosine were chosen as nucleosides, as previous studies demonstrated that 7-deaza-2'-deoxyadenosine has shown positive effects on turn-on efficiency and kinetics compared to deoxyuridine as nucleobase. The structure of the linker used to attach the BCN to the nucleoside has also been shown in earlier studies to significantly influence the reaction kinetics and fluorescence turn-on.[155] Based on these previous studies by *Philipp Geng*, an aminopropyl linker with a rigid propyne was selected (**figure 28**). The BCN was attached to the linker through a carbamate group.

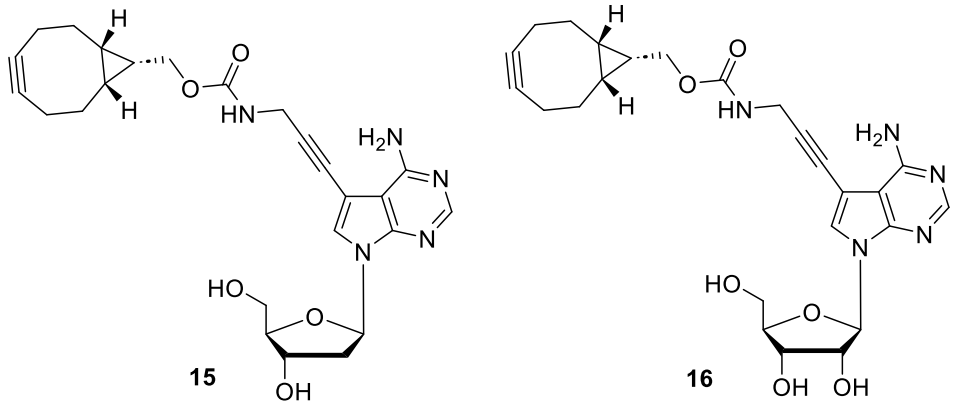

Figure 28: Structures of the synthesized BCN-nucleosides **15** and **16**.

The preparation of **15** was performed starting with the commercially available 2'-deoxyribose (**17**) and 6-chloro-7-iododeazapurine (**21**) (**figure 29**). The artificial 7-deaza-derivative can be synthesized by glycosylation with an amine component. For this purpose, the α-chlorosugar **20** was first prepared according to a synthesis described in literature.[156–158] The synthesis was performed in three steps. The anomeric center of the 2'-deoxyribose was methyl-protected by reaction with acetyl chloride in methanol. The 3'- and 5'-hydroxy group of **18** were protected with para-toluoyl protective groups. **19** was treated with 4M HCl in dioxane, leading to substitution at the anomeric center and formation of the α-chlorosugar in a yield of 86 %.

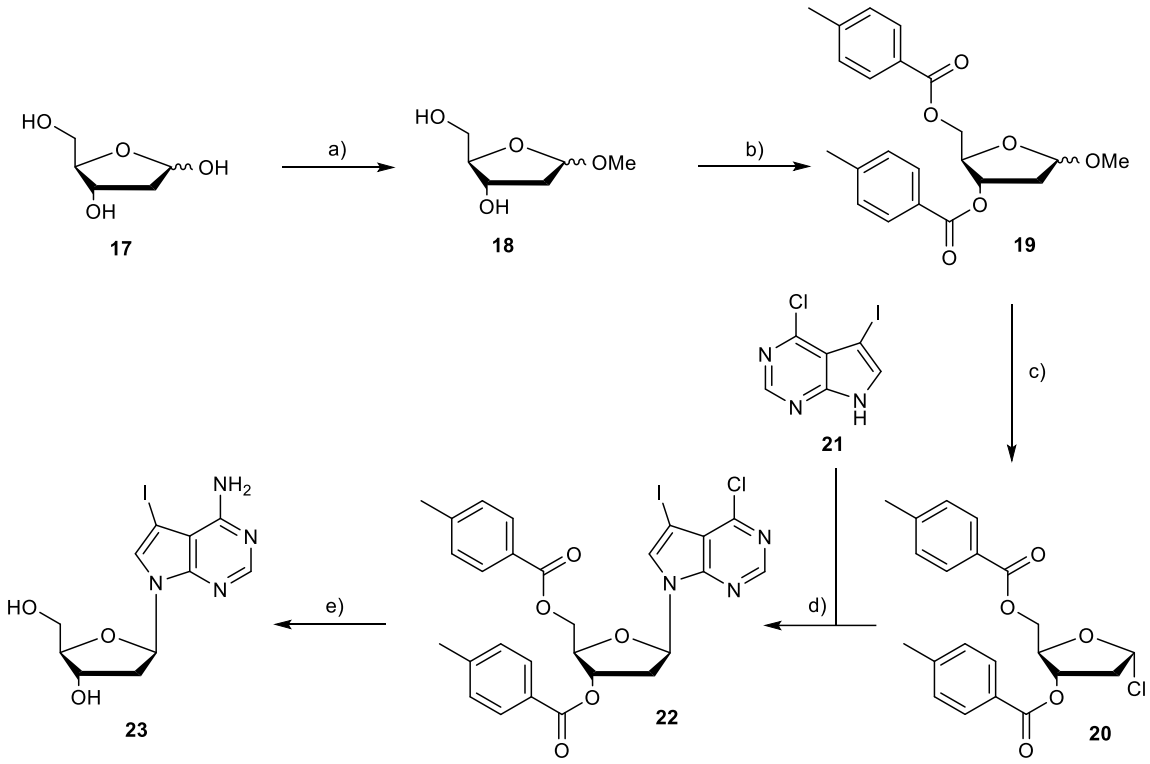

Figure 29: Synthesis of 7-iodo-7-deaza-2'-deoxyadenosine (**21**): a) Acetyl chloride, MeOH, r.t., 20 min, quant.; b) p-toluoyl chloride, Et_3N, acetone, r.t., 18 h, 42 %; c) 4M HCl/dioxane, acetic acid, 0 °C, 2 h, 86 %; d) TDA-I, KOH, MeCN, r.t., 1 h; e) 7N NH_3 in MeOH, 120 °C, 24 h, 58 % (in two steps).

The chlorosugar **20** was coupled with 6-chloro-7-iodo-7-deazapurine (**21**) using a glycosylation method established by *Seela et al.*[159,160] The reaction was catalyzed by TDA-I and resulted in the stereoselective formation of the β-nucleoside **22**. The deprotection of the p-toluoyl groups and the amination were carried out without further purification by

substitution of the chlorine atom with 7 M ammonia solution in methanol in a pressure tube at 120 °C for 24 h. In this way, **23** could be isolated as a colorless solid in a yield of 58% in two steps.[161]

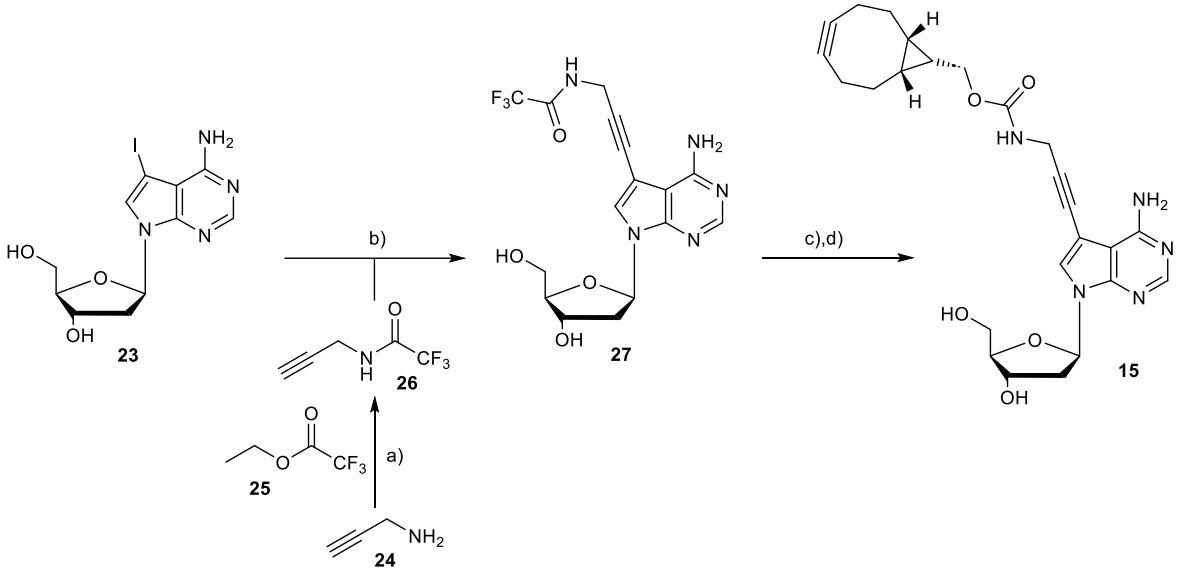

Figure 30: Synthesis of BCN-modified 7-deaza-2'-deoxyadenosine **13**: a) ethyltrifluoroacetat (**23**), MeOH, r.t., 24 h, 72 %; b) CuI, Et_3N, $Pd(PPh_3)_4$, DMF, r.t., 24 h, 95 %; c) conc. NH_4OH, r.t., 16 h; d) BCN-NHS ester, Et_3N, DMF, r.t., 16 h, 95 % (in two steps).

The synthesis of the linker **26** was performed according to a literature procedure starting from the commercially available propargylamine (**24**).[162] The amino-propargyl linker was coupled with nucleoside **23** in a Sonogashira reaction using $Pd(PPh_3)_4$ as catalyst. After 18 h reaction time and subsequent purification by column chromatography, the linker-modified nucleoside **27** was obtained with a 95 % yield (**figure 30**). The trifluoroacetyl protecting group was removed using concentrated ammonium hydroxide solution. The residue was reacted in DMF with commercially available, activated BCN-NHS ester under basic conditions. The BCN-modified 7-deaza-2'-deoxyadenosine **15** was obtained in a yield of 95 % in two steps.

To exclude the influence of the additional hydroxy groups for a future application in RNA, a BCN-modified 7-deazaadenosin was synthesized in six steps (**figure 31**). Following a procedure developed by *Spitale et al.*, the glycosylation of β-D-ribofuranose-1-acetate-2,3,4-tribenzoate (**28**) and 6-chloro-7-iododeazapurine (**21**) was carried out, and **29** was obtained as a colorless foam with a yield of 60 %.[143] The deprotection of the benzoyl

groups and the amination by substitution of the chlorine atom were carried out in a pressure tube with 7M ammonia solution in methanol at 120 °C for 24 h. The linker synthesis followed a literature procedure[162], and linker **26** was attached to the nucleoside **30** using a Sonogashira reaction. After the work-up, **31** was obtained as a light brown solid in a yield of 70 %. The propargyl linker was deprotected using a concentrated ammonium hydroxide solution and the crude product obtained was reacted without further purification with the activated BCN-NHS ester in DMF. The reaction of the free amino groups and NHS esters is pH-dependent, which is the reason why the reaction was carried out using triethylamine. The basic pH prevents amine protonation and enable the nucleophilic attack. After column chromatography, **16** was isolated as a colorless foam with a yield of 80 % in two steps.

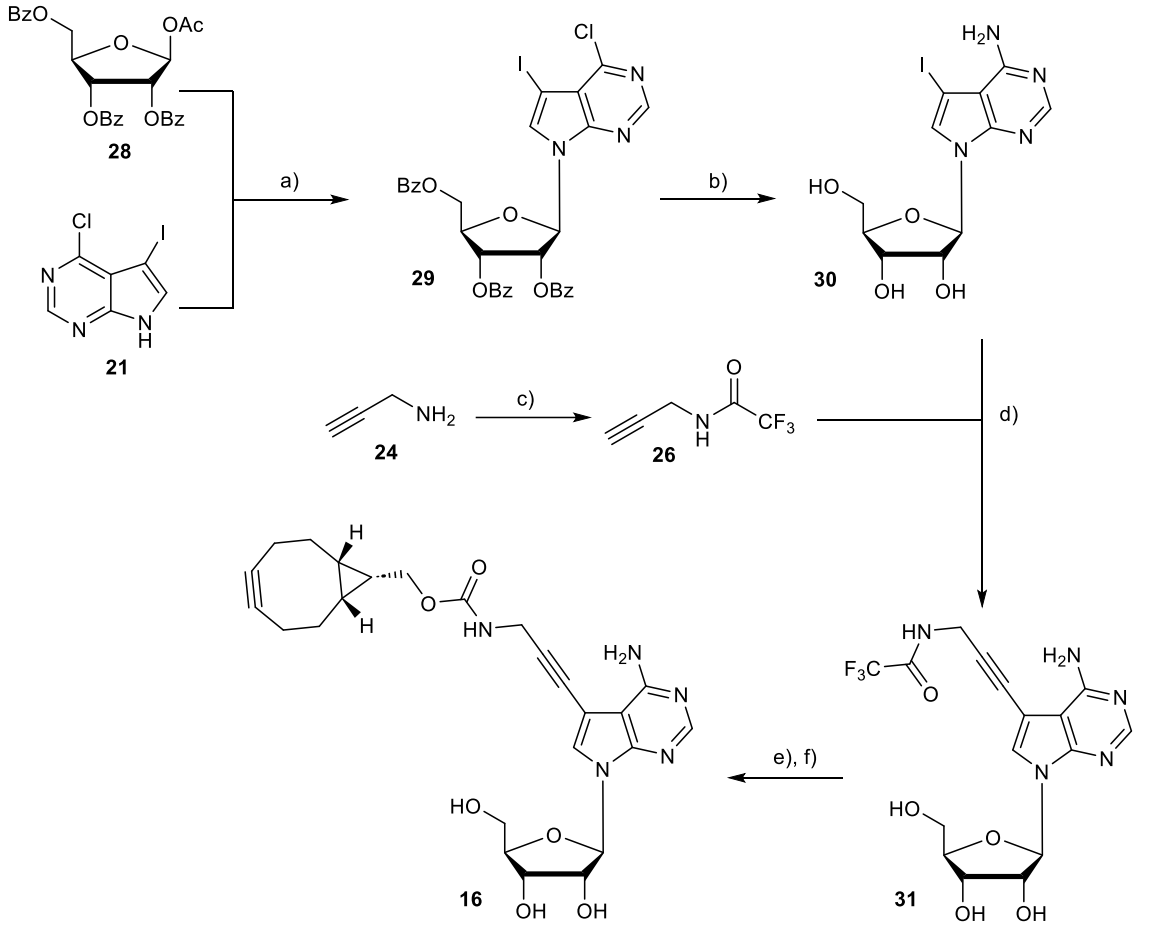

Figure 31: Synthesis of BCN-modified 7-deazaadenosine (**16**): a) 1) BSA, MeCN, r.t., 20 min, 2) **26**, TMSOTf, 80 °C, 2.5 h, 60 %; b) 7N NH_3 in MeOH, 120 °C, 24 h, 82 %; c) ethyltrifluoroacetat (**25**), MeOH, r.t., 24 h, 72 %; d) CuI, Et_3N, $Pd(PPh_3)_4$, DMF, r.t., 24 h, 70 %; e) conc. NH_4OH, r.t., 16 h; f) BCN-NHS ester, Et_3N, DMF, r.t., 16 h, 80 % (in two steps).

4.3 Bioorthogonal labeling experiments with BCN-Nucleosides

Previous studies have demonstrated that variously modified sydnones can react rapidly with BCN. The reaction can be described as a [3+2] cycloaddition, which results in the formation of pyrazoles under the release of CO_2.[36,79–82,84] In the following section, the reaction between sydnone dye **3** and the BCN-Nucleosides **15** and **16** will be investigated. The synthesized sydnone dye **3** was employed in a SPSAC to assess its potential as a fluorogenic dye for bioorthogonal DNA labeling. Various methods were used to study the reaction, such as UV-Vis-, fluorescence spectroscopy and LC-MS analysis. The reaction was characterized in terms of its reaction rate constants and fluorescence turn-on.

4.3.1 UV/Vis and fluorescence experiments

To study the reaction between the sydnone dye **3** (c = 20 µM) and the dienophiles (**15** or **16**) (c = 100 µM), a five-fold excess of the dienophile was used, ensuring complete conversion of the sydnone fluorophore. As a result, a pseudo-first-order reaction can be assumed for the evaluation due to the excess of the dienophiles rather than second-order kinetics. The reaction rate and the turn-on of the SPSAC reaction could then be determined from the measurements.

For potential application *in cellulo*, the reaction was conducted in water. Due to the limited solubility of the reactants in water, stock solutions of the reactants were first prepared in DMSO. After adding the reactants into the reaction solution, the final DMSO amount was 1 vol.%. **Figure 32** shows the reaction and the UV-Vis- and fluorescence spectra of the reaction between **3** and **15**. Additionally, a picture of the cuvettes illuminated by a UV-Lamp is shown in **figure 32**. On the left is the cuvette before the reaction started and on the right is the cuvette shown after complete conversion. The absorbance was measured at certain time intervals in order to follow the course of the reaction spectroscopically. The absorption band of the sydnone **3** decreases at 385 nm continuously, while a band at 315 nm increases at equal time intervals. This indicates the formation of the pyrazole **32**. The spectrum also showed a bathochromic shift and several isosbestic points at 297 nm, 338 nm and 441 nm, indicating the formation of only one product without any by-product in one step.

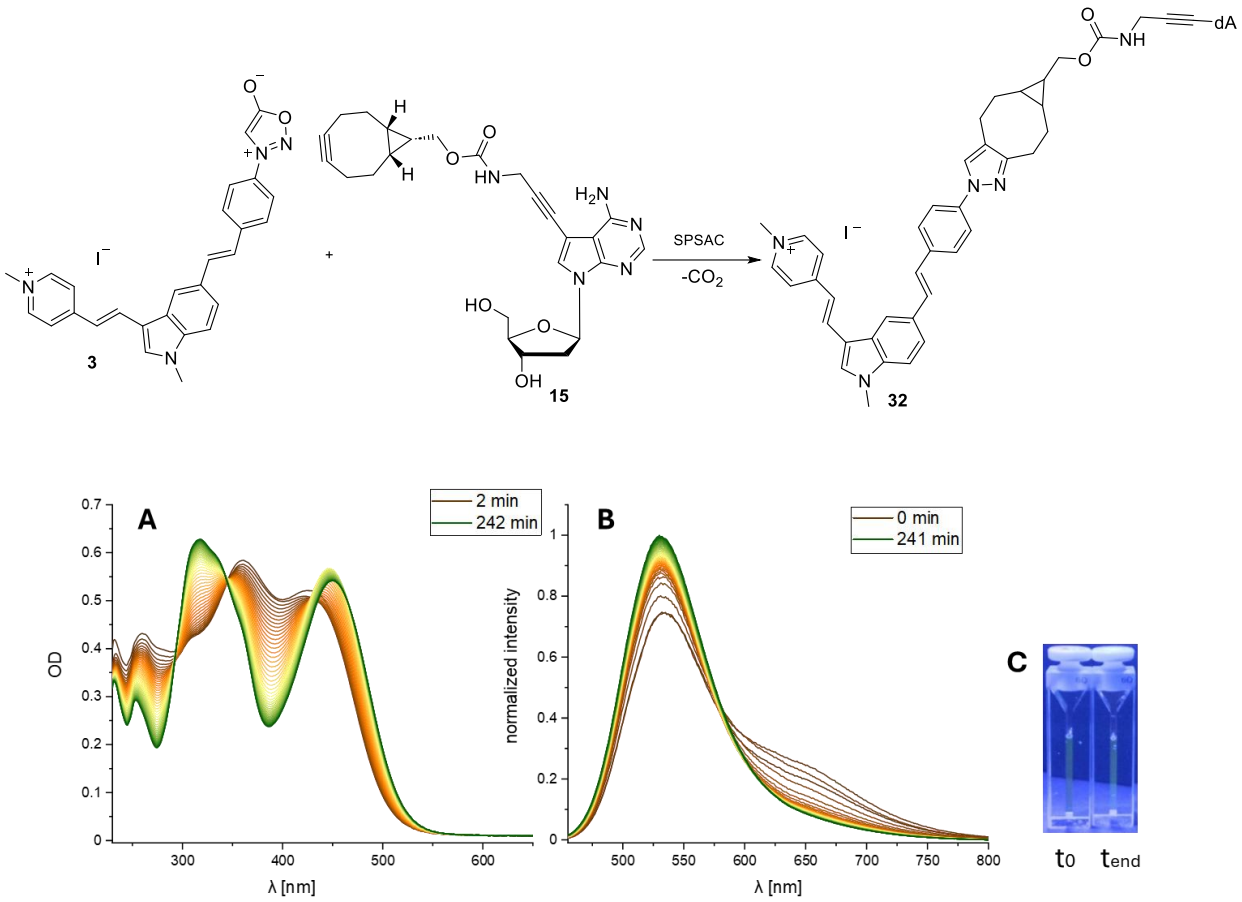

Figure 32: Example of SPSAC between **3** and **15**. **A)** changes in the absorption spectra during the SPSAC between **1** (20 µM, 1.00 eq.) and **15** (100 µM, 5.00 eq.) in H_2O/DMSO 99:1. **B)** Increase in fluorescence intensity during SPSAC **C)** visible turn-on: t_0: fluorescene of **3** at the start of the reaction, t_{end}: fluorescence after complete conversion with **15**.

The turn-on F of the reaction was determined by measuring the increase in fluorescence intensity. The absorption maximum of the dye was chosen as the excitation wavelength. The emission was measured from $\lambda_{excitation}$ + 15 nm – 800 nm. For **3**, a fluorescence maximum at λ = 546 nm was observed. First, the fluorescence spectrum of the sydnone dye **3** was recorded as a zero measurement. Subsequently, a sample was prepared with the reaction partner **15** and the SPSAC reaction was followed by fluorescence spectroscopy at defined time intervals (**figure 32**). A continuous increase in fluorescence intensity was observed over a period of 241 min. To determine the turn-on F, the integrals under the fluorescence spectra were determined. The integral of the end point I_t was set in relation to the integral of the zero measurement I_0 and calculated using the following formula (eq.**1**).

$$F = \frac{I_t}{I_0} \quad \text{(eq.1)}$$

I_t = integrated area below the obtained fluorescence spectra after time t

I_0 = integrated area below the obtained fluorescence spectra at time t = 0

By recording the increase in fluorescence at regular time intervals, the reaction rate constant k_2 can be calculated by plotting the integrated fluorescence intensities against time. The constant k_2 was then obtained from the curvature of the mono-exponential fit function (chapter 7.5). For the reaction between **3** and **15** a reaction rate constant of k_2 = 2.7 ± 0.1 $M^{-1}s^{-1}$ and a turn-on factor F = 1 could be determined. The formation of the click product **32** was also examined using LC-MS. In this case, a 1:5 ratio was again selected as the ratio of the two reaction partners. However, the reaction partners were each used in a concentration that was five times higher to enable better detection. The final concentration of the reaction partners in the reaction solution corresponded to 100 µM **3** to 500 µM **15** in water/DMSO (92.5:7.5). The HPLC chromatogram showed a high purity of all reaction partners and a clean formation of the click product **32**. The click product was further identified by ESI-MS. The kinetics of SPSAC reaction were consistent with typical reaction rates of these type of reaction. However, due to the low fluorescence turn-on, sydnone dye **3** is not suitable for use as a fluorogenic dye. Currently, there is only a limited understanding of the quenching properties of sydnones, as the number of known fluorogenic sydnone dyes is too small to establish a general theory of their quenching behavior. Therefore, in the following chapter, sydnone dye **3** was empirically further developed.

4.4 Further development of the sydnone dye 3

In order to improve quenching and thereby enhance the fluorescence turn-on, the effect of altering the steric arrangement of the sydnone dye was investigated. For this purpose, the structure was changed to bring the sydnone closer to the dye molecule. This was achieved by binding the sydnone to the 4-position of the indole moiety via a vinyl bridge (figure 33).

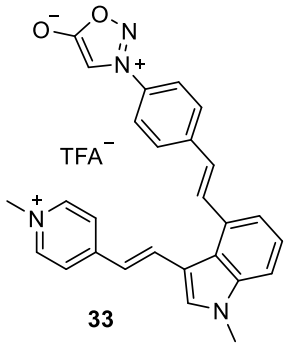

33

Figure 33: Structure of sydnone dye 33.

This modification was chosen, because it has already been shown that a rigid linker in the structures of the dienophiles, has a positive influence on turn-on and kinetics due to steric hindrance.[155] Applied to the sydnone dye, the proposed modification would provide more spatial restriction through closer proximity of the sydnone to the dye, potentially enhancing its quenching efficiency and reaction rate constants.

The synthesis was carried out in the same way as for sydnone dye 3, only the different indole building block 34 was used (figure 34).

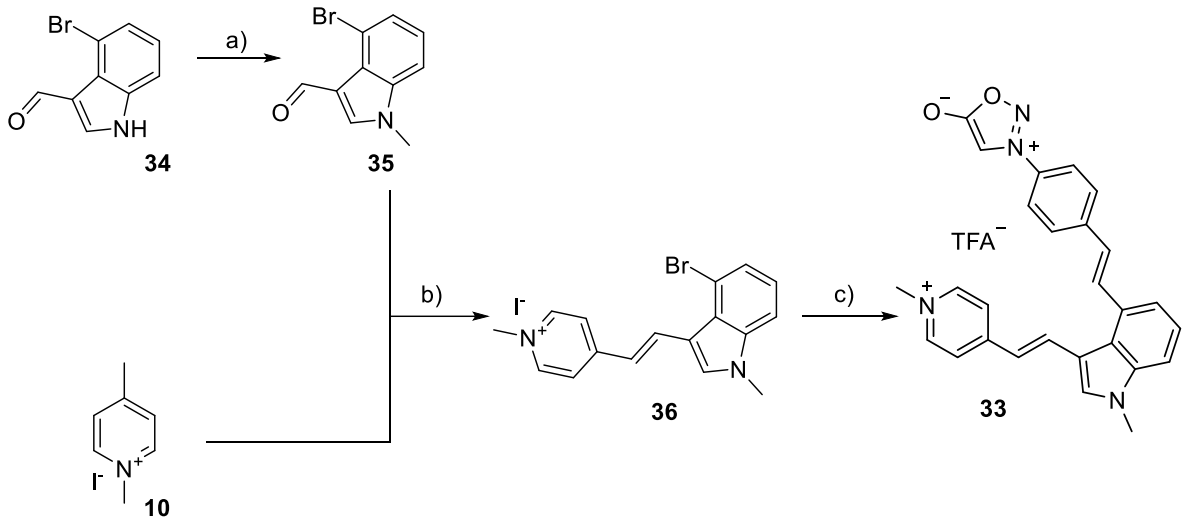

Figure 34: Synthesis of the sydnone-dye conjugate **33**: a) K_2CO_3, dimethyl carbonate, DMF, 130 °C, 18 h, 70 %; b) piperidine, EtOH, 80 °C, 18 h, 80 %; c) $Pd_2(dba)_3$, QPhos, Et_3N, DMF, 80 °C, 18 h, 45 %.

The 4-bromo-1H-indole-3-carboxaldehyde (**34**) was N-methylated using dimethyl carbonate as methylation reagent. The two building blocks **35** and **10** were combined through an aldol-like condensation reaction using piperidine as a base to form the brominated cyanine-styryl dye. The reaction was worked up by precipitation and subsequent washing of the dye with diethyl ether. The orange solid was isolated in a yield of 72 %. In the last step, the Heck reaction was carried out with **36** under the same conditions as for the synthesis of **3**. After precipitation of the product **33** through adding diethyl ether, the sydnone dye **33** was purified by preparative HPLC. During the purification, the iodide was exchanged with TFA because it was carried out in a solvent of water/acetonitrile 20 – 80 % with 0.1 % TFA as an additive. The sydnone dye **33** could be obtained with a yield of 45 %.

The absorption and fluorescence spectroscopic investigations were carried out under the same conditions as in **section 4.2**. **Figure 35** shows an example of the reaction of **33** with nucleoside **15**.

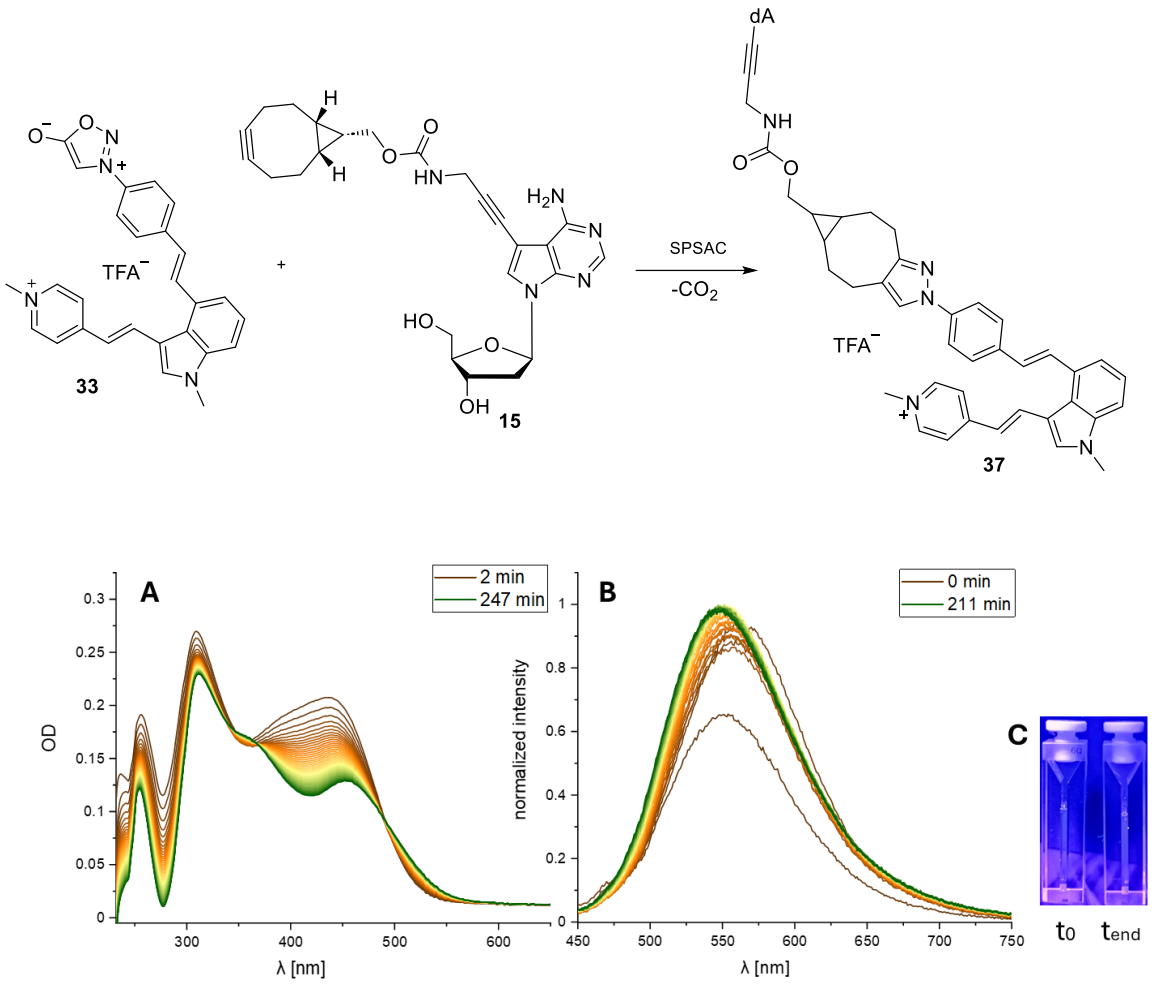

Figure 35: Example of SPSAC between **33** and **15**. **A)** changes in the absorption spectra during the SPSAC between **3** (20 µM, 1.00 eq.) and **15** (100 µM, 5.00 eq.) in H_2O/DMSO 99:1. **B)** Increase in fluorescence intensity during SPSAC **C)** visible turn-on: t_0: fluorescene of 1 at the start of the reaction, t_{end}: fluorescence after complete conversion with **15**.

The UV-Vis spectroscopic analysis showed a bathochromic shift during the reaction, and that the absorption band at 417 nm decreases continuously while a band at 355 nm, increases, indicating the formation of the pyrazole. The spectrum shows several isosbestic points at 340 nm, 364 nm and 490 nm. After 247 min no change in the absorption spectra can be observed. Fluorescence spectroscopic analysis revealed that, in comparison to sydnone dye **3**, the turn-on did not improve, and the kinetics are in the same range as for the reaction of **3** with **15**. The fluorescence maximum of the dye was at 551 nm and did not increase further after 211 min which marks the end of the reaction. As a reaction rate constant k_2 = 3.6 ± 0.8 $M^{-1}s^{-1}$ could be determined. The turn-on of **33** was 2 and is in the same range as the turn-on of **3**. The gained results showed that the increased steric

hindrance in the sydnone dye **33** does not appear to have a strong effect on the turn-on and kinetics.

Another possible way to further develop the sydnone dye is to modify the sydnone moiety itself. For this purpose, the naphthylsydnone **43** was used instead of a phenylsydnone (**figure 36**), allowing the synthesis of dyes **44** and **45**. The synthesis of these two sydnone dyes is shown in **figure 37**.

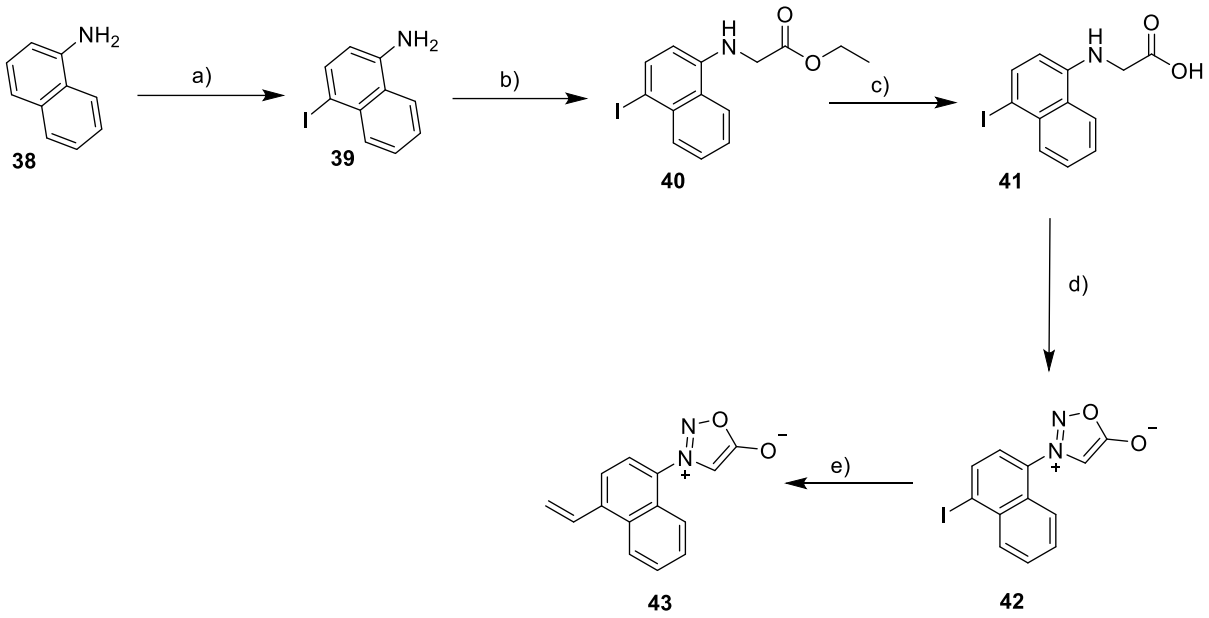

Figure 36: Synthesis of the naphthylsydnone **43**: a) NIS, DMSO, r.t., 72 h, 50 %; b) 1) K_2CO_3, ethyl bromoacetate, DMF, r.t., 16 h, 2) Et_2NH, DMF, r.t., 1 h, 20 %; c) LiOH, THF/water (1:1, v/v), 0 °C, 0.5 h, r.t., 1h, 95 %; d) 1) tBuONO, THF, r.t., 0.5 h, 2) TFAA, THF, r.t., 3 h, 90 %; e) $(CH_2{=}CH)_4Sn$, $Pd(PPh_3)_2Cl_2$, DMF, r.t, 16 h, 72 %.

Starting with commercially available 1-naphthylamine (**38**), the iodination was carried out with NIS in DMSO. After purification by column chromatography, 4-iodo-1-naphthylamine (**39**) was obtained in a yield of 50 %. **39** was N-alkylated with ethyl bromoacetate to give the N-4-iodonaphthylglycine ester **40**. The ethyl group was then cleaved with LiOH to give compound **41** as a light brown solid with a yield of 95 %. The synthesis of the sydnone was initiated from the N-glycine derivative **41** in a two-step reaction. In the first step, the nitrogen of the N-glycine derivative was nitrosylated with tert-butyl nitrite, followed by the addition of trifluoroacetic anhydride in THF, which promoted cyclodehydration and formed the sydnone ring. Compound **42** was isolated as a reddish-brown solid with a yield of 90 %. **42** undergo a Stille coupling reaction with tetravinyltin using $Pd(PPh_3)_2Cl_2$ as a catalyst.

After the reaction ran overnight at room temperature and subsequent purification by column chromatography, compound **43** was obtained as a reddish-brown solid with a yield of 72 %. The two building blocks **4/36** and **43** were then coupled using a Heck reaction (**figure 37**), following reaction conditions similar to those used for the synthesis of **3**. Upon completion of the reaction, the product was precipitated by adding diethyl ether. The crude product was further purified by preparative RP-HPLC. Compounds **44** and **45** were obtained in yields of 60 % and 45 %, respectively.

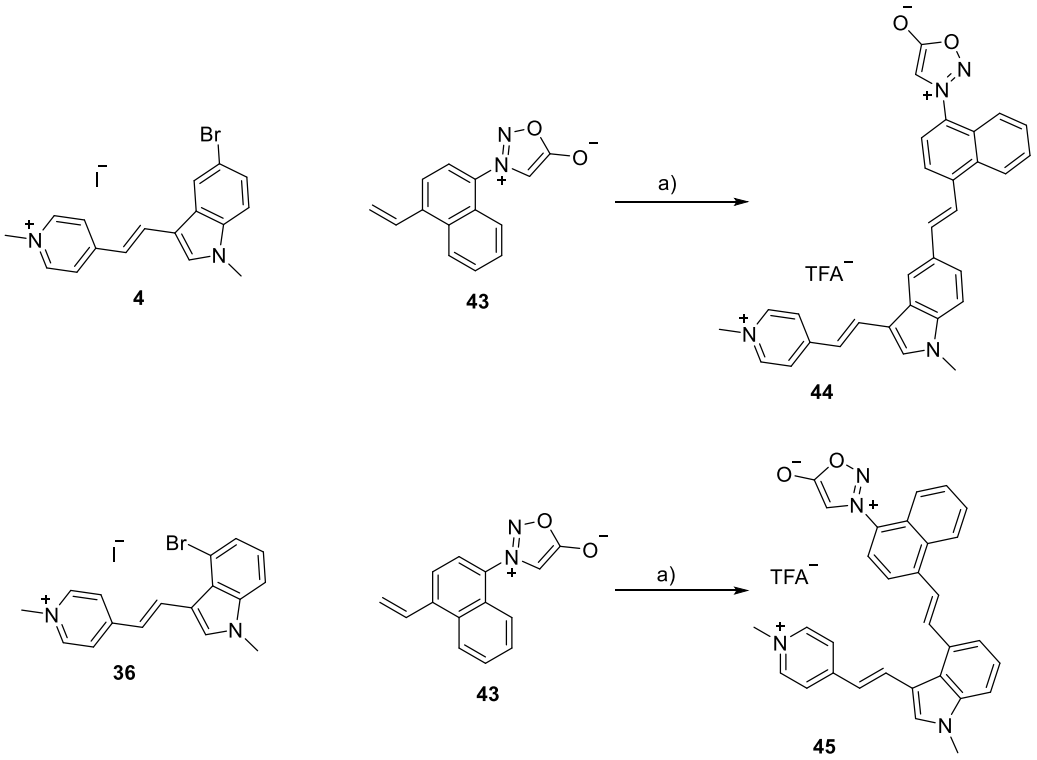

Figure 37: Synthesis of the sydnone-dyes conjugates **44** and **45** via Heck coupling: a) $Pd_2(dba)_3$, QPhos, Et_3N, DMF, 80 °C, 18 h, **44**: 60 %, **45**: 45 %.

In addition to compound **44** and **45**, another sydnone dye was synthesized, as shown in the synthetic route of **figure 38**. Sydnone building block **5** was converted to compound **46** following a procedure by *Taran et al.*[13] 4-Methylchinoline (**47**) was N-methylated using methyl iodide, yielding **48** as a yellow solid in quantitative yield. **46** and **44** undergoes an aldol-like reaction to form sydnone-dye conjugate **49**. The reaction conditions were adapted from a procedure from Taran et al.[13] The product was precipitated using diethyl ether and isolated as a dark brown solid with a yield of 50 %.

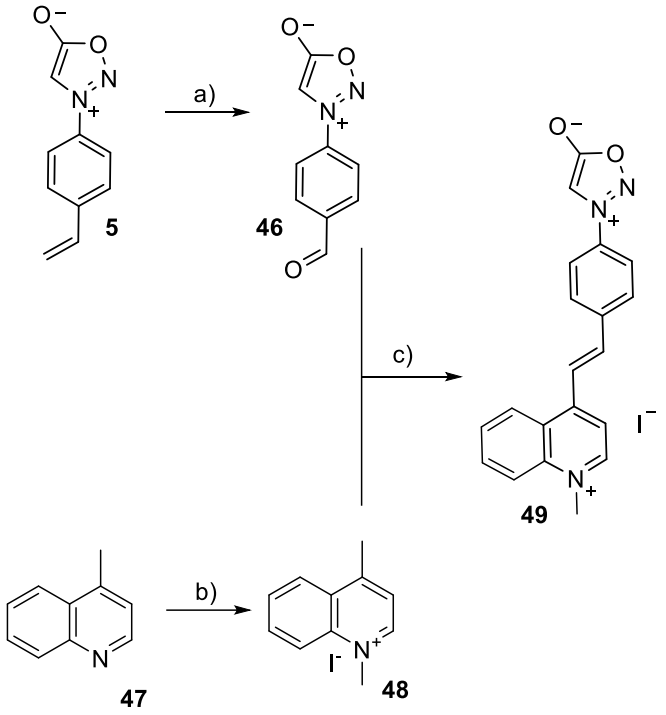

Figure 38: Synthesis of the sydnone-dye conjugate **49**: a) 1) NMO, OsO_4, acetone/water, r.t., 4 h, 2) $NaIO_4$, acetone/water, r.t., 6 h, 48 %; b) MeI, acetone, reflux, 2 h, 93 %; c) piperidine, MeOH, 75 °C, 24 h, 50 %.

The reactivity of the three synthesized sydnone dyes with nucleoside **16** was evaluated via UV-VIS and fluorescence spectroscopy. **Figure 39** shows the fluorescence spectra of the dyes. The reactions were performed under the same conditions as used for **3** and **33**. The spectra were recorded at specific time intervals to follow the progress of the reaction.

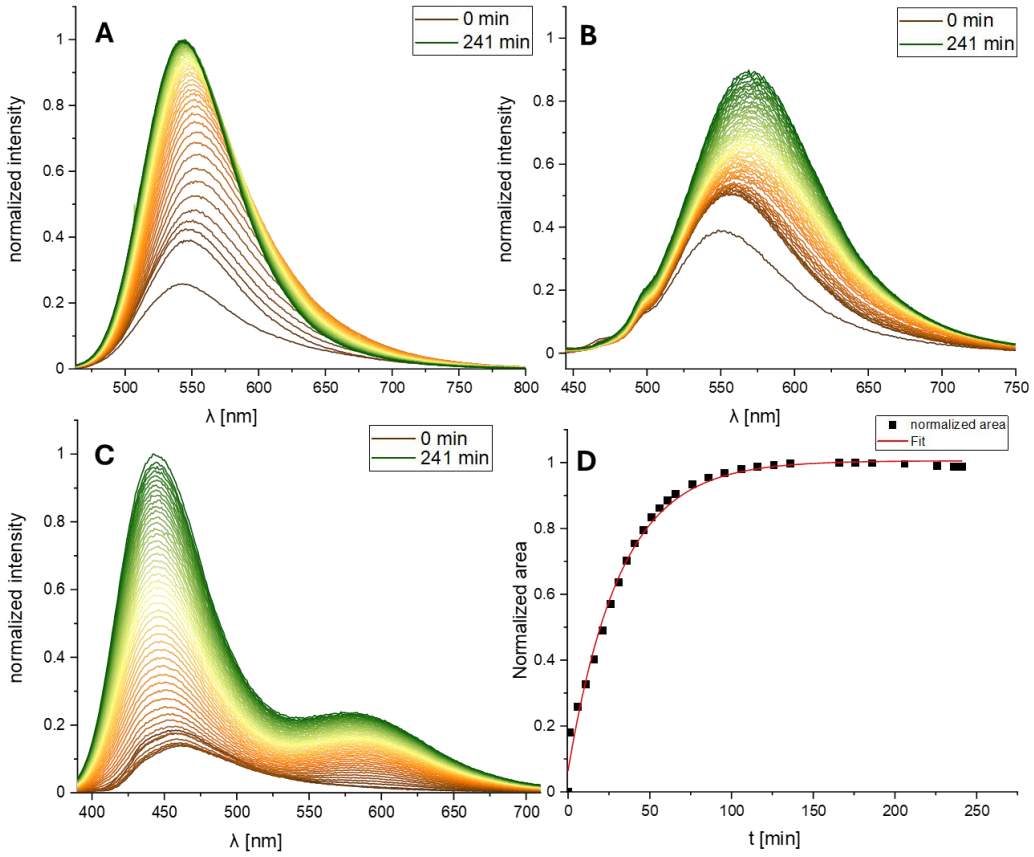

Figure 39: A) Increase in fluorescence during the SPSAC of fluorophore **44** and BCN-nucleoside (**16**) in H2O/DMSO (99:1 V/V%) at λ_{exc} = 448 nm between 463 – 800 nm. **B)** Increase in fluorescence during the SPSAC of fluorophore **45** and BCN-nucleoside (**16**) in H2O/DMSO (99:1 V/V%) at λ_{exc} = 424 nm between 439 – 750 nm. **C)** Increase in fluorescence during the SPSAC of fluorophore **49** and BCN-nucleoside (**16**) in H2O/DMSO (99:1 V/V%) at λ_{exc} = 372 nm between 387 – 710 nm. **D)** Time-resolved kinetic representation of the fluorescence intensity of the measured fluorescence of **44** with **16** with exponential fitting function: y = a + b·exp(-kx).

The fluorescence spectra showed a continuous increase in fluorescence for all dyes over the course of the reaction with nucleoside **16**. The turn-ons F of the dyes with the nucleoside could be determined using the formula shown in **chapter 4.3.1.** An 8-fold improvement in fluorescence turn-on efficiency was observed when comparing **33** to **49**. The reaction rate constants of the three dyes were also higher than for **3** and **33**. **44** showed the fastest kinetics. Nevertheless, the reaction rate constants were still in the same kinetic range of 10^0 $M^{-1}s^{-1}$. To determine these values, integrated fluorescence intensities were plotted against time and then an exponential fit was calculated. As an example, the graph of the time-resolved kinetic representation of sydnone dye **44** is shown in **figure 39**. Furthermore, the fluorescence spectrum of **49** exhibits a distinctive feature, with a local

maximum at 570 nm in addition to the global maximum at 444 nm. For better comparability, the reaction rate constants k_2 and turn-ons were summarized in table 2.

Table 2: Photophysical properties of sydnone modified fluorophores after complete conversion with BCN-modified nucleosides **15** and **16** in H_2O/DMSO (99:1 V/V%).

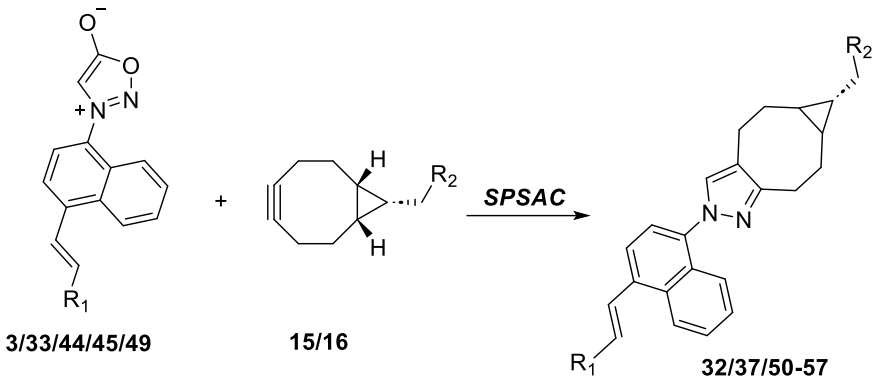

3/33/44/45/49 **15/16** **32/37/50-57**

Fluorophor	Dienophile	Product	λ_{em} [nm]	$\Delta\lambda$ [nm]	*Turn-on*	k_2 [$M^{-1}s^{-1}$]
3	**15**	**32**	547	118	1	2.7 ± 0.1
	16	**50**	547	118	1	2.2 ± 0.1
33	**15**	**37**	549	125	2	3.6 ± 0.8
	16	**51**	549	125	1	1.2 ± 0.1
44	**15**	**52**	543	95	4	7,0 ± 0.3
	16	**53**	543	95	3	5.3 ± 0.2
45	**15**	**54**	568	144	4	2.5 ± 0.2
	16	**55**	568	144	3	0.6 ± 0.03
49	**15**	**56**	444	72	8	1.3 ± 0.1
	16	**57**	444	72	7	0.4 ± 0.05

The kinetics are in the same range regardless of which nucleoside is measured with one of the dyes. Consequently, it can be concluded that the hydroxyl-group at the 2'-end has no effect on the reaction rate constants k_2 and that the kinetics will not differ in a later RNA

application compared to DNA. Also, no conclusions can be drawn about the turn-on F either as this also appears to be unaffected by the presence of the 2'OH group. Furthermore, large Stokes shifts between 72 nm and 144 nm were observed, which is very advantageous for biochemical applications, as it ensures sufficient separation between the excitation wavelength and emission band. **Figure 40** shows the optically detectable fluorescence of sydnone-modified fluorophores after complete conversion with **16** when the cuvettes are illuminated by a UV-lamp (395 nm). Comparing **3** and **33** with **44**, **45** and **49**, a significant increase in optically detectable fluorescence can be seen, although the turn-on's maximum only is 8-fold higher, compared to the least efficient dyes **3** and **33**, but the optically detectable fluorescence, i.e. the observed brightness, is not only related to the turn-on, it is also based on the product of the extinction coefficient and the fluorescence quantum yield. The fluorescence increase is thus only used to evaluate the fluorescence restored after the SPSAC and provides a value for quantifying the efficiency of the fluorophore system.

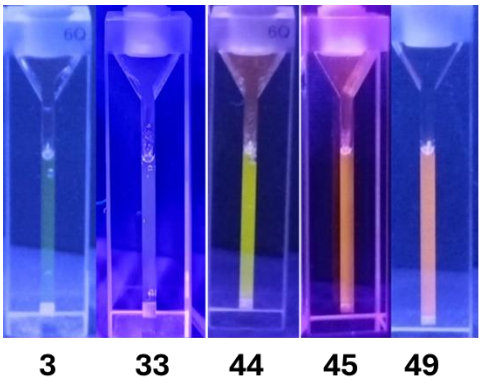

Figure 40: Visible fluorescence turn-on of **3**, **33**, **44**, **45** and **49** after complete conversion with **16**.

The three dyes with the highest visible turn-on should then be examined regard to their kinetics and their turn-on when reacting with BCN-modified DNA.

4.5 Synthesis of BCN-modified oligonucleotides

After in vitro characterization of dyes **44**, **45** and **49** with nucleosides **15** and **16**, BCN-modified DNA was synthesized to study the reaction with the dyes both in vitro and later *in cellulo*. For this purpose, 7-deaza-2'-deoxyadenosine was incorporated with a rigid linker system in a short-chain DNA of 17 base pairs using standard solid-phase synthesis. The artificial nucleoside was incorporated as a phosphoramidite. For successful solid-phase synthesis, the building blocks first had to be modified by introducing a series of protecting groups. The phosphoramidite was synthesized starting from nucleoside **27**. Initially, the free amine of the nucleoside was protected with a dimethylformamide dimethyl acetal (DMF-DMA) group, as this would interfere with the activation of the phosphoramidite during the activation step in the solid-phase synthesis. The 5'-position was protected with a dimethoxytrityl (DMT) group according to the method of Seela et al.[160] The 3'-hydroxide group was converted to the phosphoramidite by reaction with 2-cyanoethyl-N,N-diisopropylchlorophosphoramidite with DIPEA as base. **60** was obtained in quantitative yield (**figure 41**).

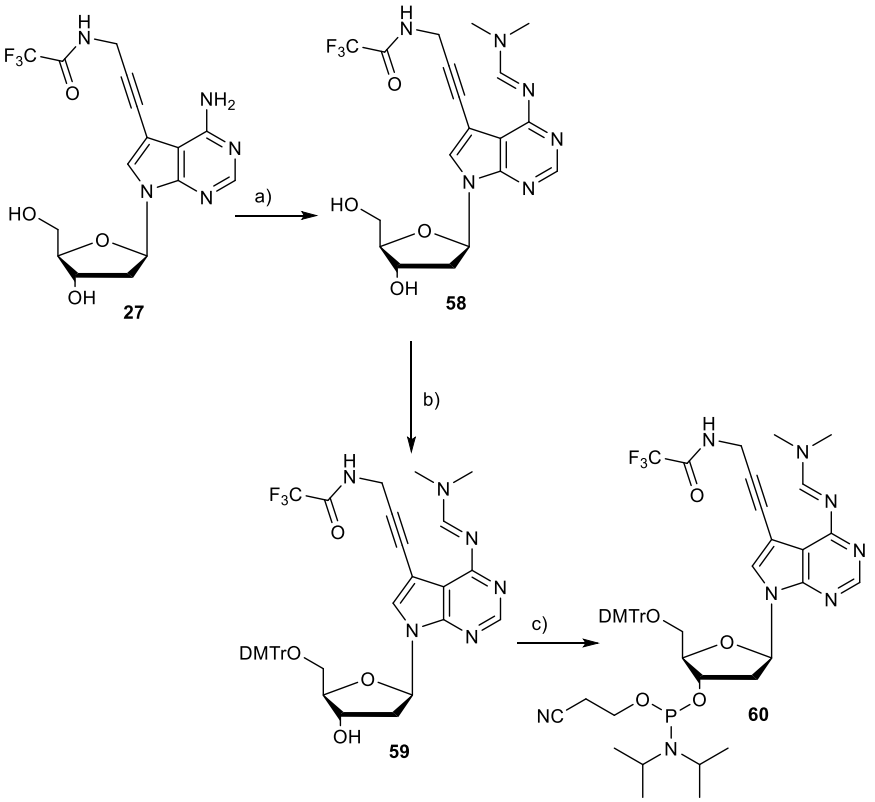

Figure 41: Synthesis of phosphoramidite **60**: a) DMF-DMA, MeOH, 40 °C, 16 h, 74 %; b) DMTr-Cl, pyridine, MeOH, r.t., 16 h, 80 %; c) 2-Cyanonethyl-N,N-diisopropylchlorophosphoramidite, DIPEA, DCM, r.t., 4 h, quant.

Subsequently, **60** was converted into **DNA1** by automated DNA synthesis (**figure 42**). The DNA sequence was taken from earlier work by the *Wagenknecht group*.[155]

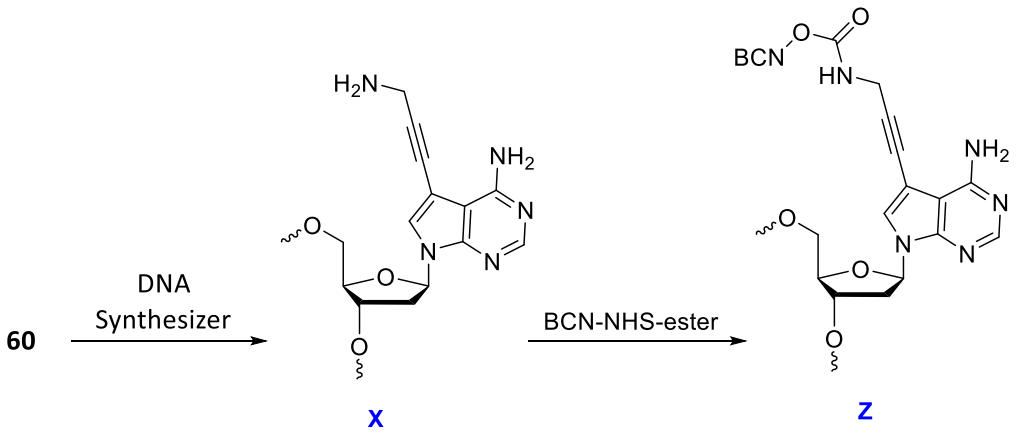

DNA1 5'-G-C-A-G-T-C-**T-T-X-T-T**-C-A-C-T-G-A-3' **DNA2** 5'-G-C-A-G-T-C-**T-T-Z-T-T**-C-A-C-T-G-A-3'

Figure 42: Synthesis of the amine-functionalized oligonucleotide (**DNA1**) after standard solid-phase synthesis with subsequent post synthesis of the amine functionalized oligonucleotide with BCN-NHS ester to give the BCN-modified oligonucleotide **DNA2**.

The synthesized oligonucleotide was cleaved from the solid support and purified using a DMT affinity column. The BCN-modified oligonucleotides were modified post-synthetically. For this, DNA1 was reacted with the BCN-NHS ester using DIPEA as a base in DMSO. The resulting BCN-oligonucleotide was purified using high-performance liquid chromatography (HPLC). The synthesized oligonucleotide DNA2 was identified using MALDI-TOF mass spectrometry (chapter 7.3, table 7). The concentration of the purified oligonucleotide was determined using UV/Vis spectroscopy and the Lambert-Beer's law.

4.6 Optical spectroscopy of BCN-modified oligonucleotides

The BCN-modified DNA prepared in chapter 4.5 was used to analyze the sydnone-modified fluorophores. A significantly smaller amount of DNA2 was available for the SPSAC experiments, which is the reason why the batch size was adjusted. The concentrations were diluted with a ratio of 1:10. To ensure comparability with the nucleoside experiments, the ratio between fluorophore and dienophile and the DMSO content of 1% were not altered. The experiments were performed and analyzed in the same way as the nucleoside experiments. The resulting fluorescence spectra are shown in figure 43.

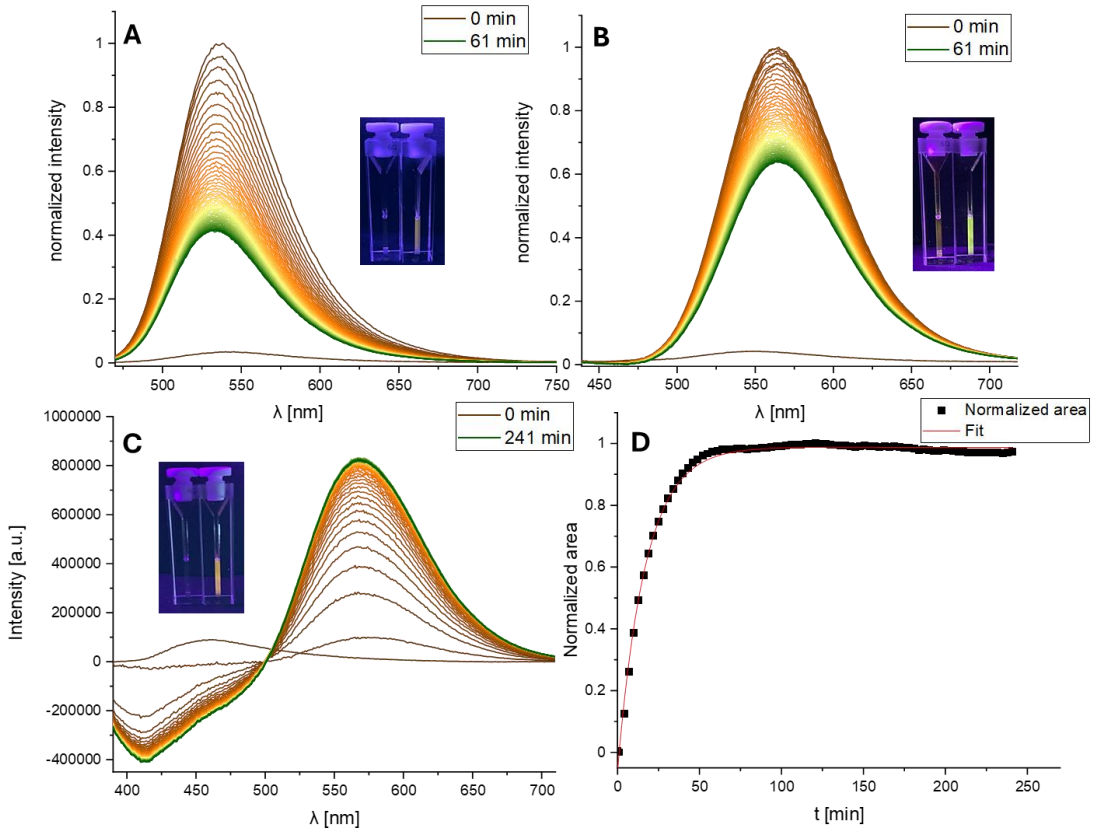

Figure 43: A) Increase in fluorescence during the SPSAC of fluorophore **44** and **DNA2** in H_2O/DMSO (99:1 V/V%) at λ_{exc} = 448 nm between 463 – 750 nm. **B)** Increase in fluorescence during the SPSAC of fluorophore **45** and **DNA2** in H_2O/DMSO (99:1 V/V%) at λ_{exc} = 424 nm between 439 – 720 nm. **C)** Increase in fluorescence during the SPSAC of fluorophore **49** and **DNA2** in H_2O/DMSO (99:1 V/V%) at λ_{exc} = 372 nm between 387 – 710 nm. **D)** Time-resolved kinetic representation of the fluorescence intensity of the measured fluorescence of **49** and **DNA2** with exponential fitting function: y = a + b·exp(-kx).

An examination of the spectra shows that the fluorescence intensities of **44** and **45** increase very rapidly and then decrease again over the course of the reaction, indicating that the dyes are interacting with the DNA as templates. The negatively charged DNA backbone allows the positively charged dyes to pre-coordinate with the DNA backbone. The template formation of dye **4** has already been investigated in an earlier work, where it was shown that template formation can be attributed to an up to tenfold increase in fluorescence.[154] This pre-coordination is reversed by the reaction with the reaction partner, causing the fluorescence to decrease again because the turn-on of the formed pyrazoline product does not exceed that of the template. Nevertheless, a turn-on of 11 (**44**) and 17 (**45**) can be observed during the formation of the click product, which is for **45** more than eight times higher than for the nucleoside. To verify this hypothesis, a reaction with BCN-modified DNA

(10 µM) and dye **44** and **45** in excess (20 µM)) was carried out. The results are shown in figure 44.

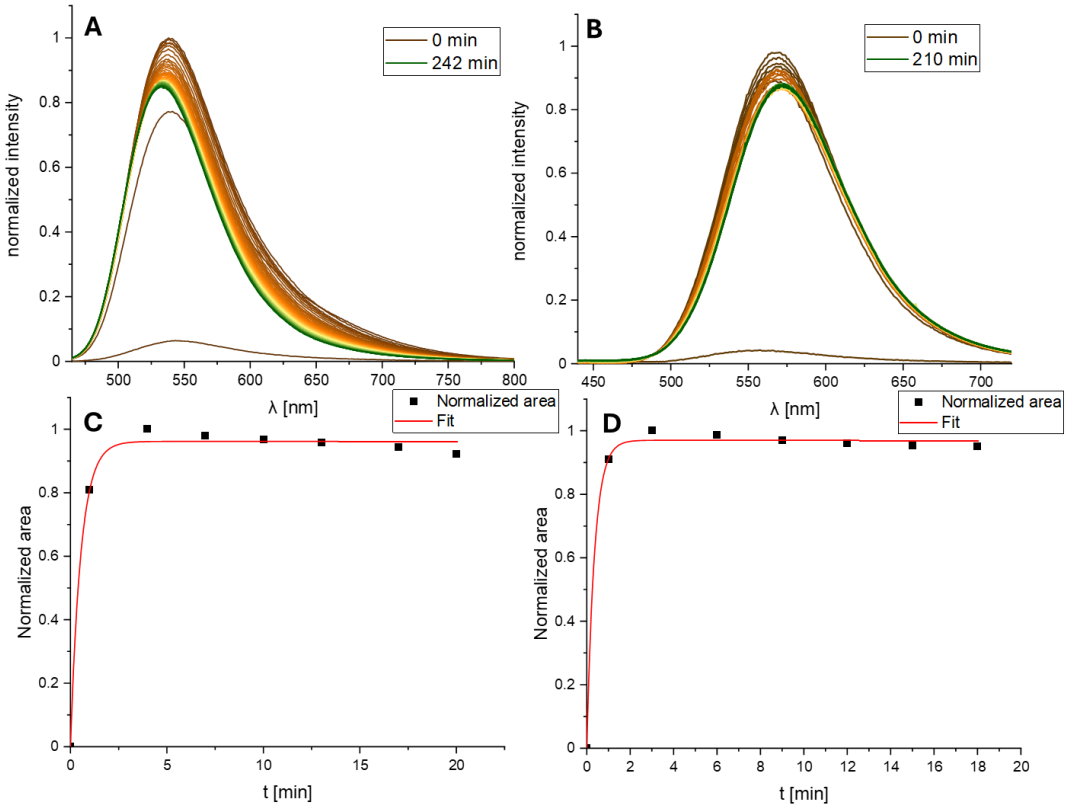

Figure 44: A) Increase in fluorescence during the SPSAC of fluorophore **44** (20 µM) and **DNA2** (10 µM) in H_2O/DMSO (99:1 V/V%) at λ_{exc} = 448 nm between 463 – 750 nm. **B)** Increase in fluorescence during the SPSAC of fluorophore **45** (20 µM) and **DNA2** (10 µM) in H_2O/DMSO (99:1 V/V%) at λ_{exc} = 424 nm between 439 – 720 nm. **C)** Time-resolved kinetic representation of the fluorescence intensity of the measured fluorescence of **44** and **DNA2** with exponential fitting function: y = a + b·exp(-kx). **D)** Time-resolved kinetic representation of the fluorescence intensity of the measured fluorescence of **45** and **DNA2** with exponential fitting function: y = a + b·exp(-kx).

A turn-on of 17 (**44**) and 21 (**45**) was observed. Due to the fact that the dye is used in excess, unreacted dye remains and continues to form DNA-templated non-covalent adducts. This confirms the assumption from an earlier study by *Philipp Geng* that template formation affects the turn-on.[155] However, the turn-on has increased compared to the reaction with nucleosides. This can be attributed to the fact that DNA further restricts the rotational freedom of the fluorophores through intercalation or binding to DNA which is different with the nucloeoside, thus further reducing vibronic relaxation from the first excited state. When **49** reacts with DNA, a turn-on of 6 is achieved, which means that there is no increase

in turn-on compared to the nucleoside. Furthermore, the turn-on of **49** is significantly lower compared to dyes **44** and **45** upon reaction with DNA. In contrast to the other two dyes, **49** is less strongly pre-coordinated due to its smaller size and greater flexibility resulting from the smaller dye unit. The turn-on does not change significantly. When looking at the kinetics of the dyes, it is apparent that the kinetics of the dyes **44** and **45** have increased 219- and 975-fold. The immense increase is also explained by the pre-coordination of the dyes with the DNA, since in the case of **49**, the dye probably had only low pre-coordination, the reaction rate constant only increased 27-fold compared to dyes **44** and **45**. **Table 3** summarizes the results of the SPSAC experiments.

Table 3: Photophysical properties of sydnone modified fluorophores after complete conversion with BCN-modified DNA in H_2O/DMSO (99:1 V/V%).

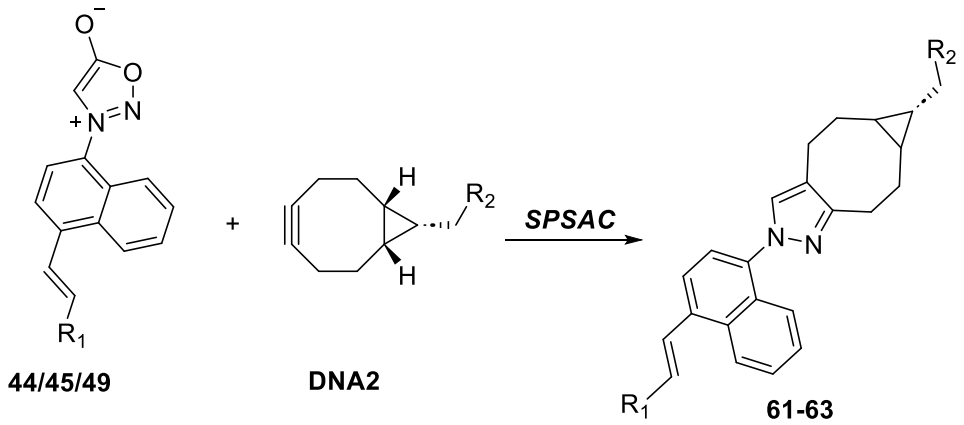

Fluorophor	Dienophile	Product	λ_{em} [nm]	$\Delta\lambda$ [nm]	*Turn-on*	$k_2 \cdot 10^3$ [$M^{-1}s^{-1}$]
44	**DNA2**	**61**	534	86	11	1.5
45	**DNA2**	**62**	564	140	17	2.3
49	**DNA2**	**63**	567	195	6	0.1

Comparing the fluorescence spectra of reaction **49** with the nucleoside and **49** with **DNA2**, it was observed that the fluorescence maximum for DNA was at 567 nm, while for the

nucleoside the fluorescence maximum was at 444 nm. The shift of the fluorescence maximum is 123 nm. Such shifts in the fluorescence maximum due to the presence of DNA have hardly been observed in the literature. In the course of the research, only two publications by *Tokar et al.*[163] and *Ustimova et al.*[164] could be found that deal with fluorescence shift studies of styryl dye-DNA complexes. Due to the limited data available, the exact mechanism of this fluorescence shift is not yet understood and requires further investigation. Nevertheless, the property of the dye is of great interest for example in the field of metabolic labeling, because the fluorescence shift could be used to distinguish whether the nucleoside supplied to the cell was accepted by the polymerases and incorporated into the DNA or is just present in the cell unincorporated.

4.7 Cell experiments

As a final step, transfection experiments were carried out to determine whether the three dyes **44**, **45** and **49** were suitable for labelling transfected BCN-modified DNA in cells. Initially, **DNA2** was transfected into HeLa cells using Lipofectamine™ 2000 and endoporter. After the transfection was complete, the cells were fixed with 4 % PFA and then incubated with the respective dye. After an incubation period of 2 h, the cells were washed twice with PBS and the cell nucleus was stained with DRAQ5. The cells were then examined under a fluorescence microscope. At the same time, a negative control was carried out with only cells to exclude autofluorescence of the cells. As a further negative control, only the dyes were incubated without **DNA2** to exclude false positive results due to the background fluorescence of the dyes. In order to have a positive control, in vitro converted **DNA2+44**, **DNA2-45** and **DNA2+49** were used for transfection. All controls were examined under the same conditions as the *in cellulo* experiments. Upon examining the cell images of the different dyes (see **figure 45-47**), it is noticeable that **45** is significantly more difficult to detect than **44** and **49**. The reason could be that excitation took place with a λ_{exc} = 488 nm laser and fluorophore **45** differs by 64 nm from the excitation wavelength of the laser with its absorption maximum and is therefore no longer effectively excited. Another reason could be that the transfection was less efficient, but this is very unlikely given the analogous procedure. However, BCN-modified oligonucleotides were successfully introduced into the

cell by transfection and successfully labelled in situ with fluorophores **44**, **45** and **49** in an SPSAC reaction.

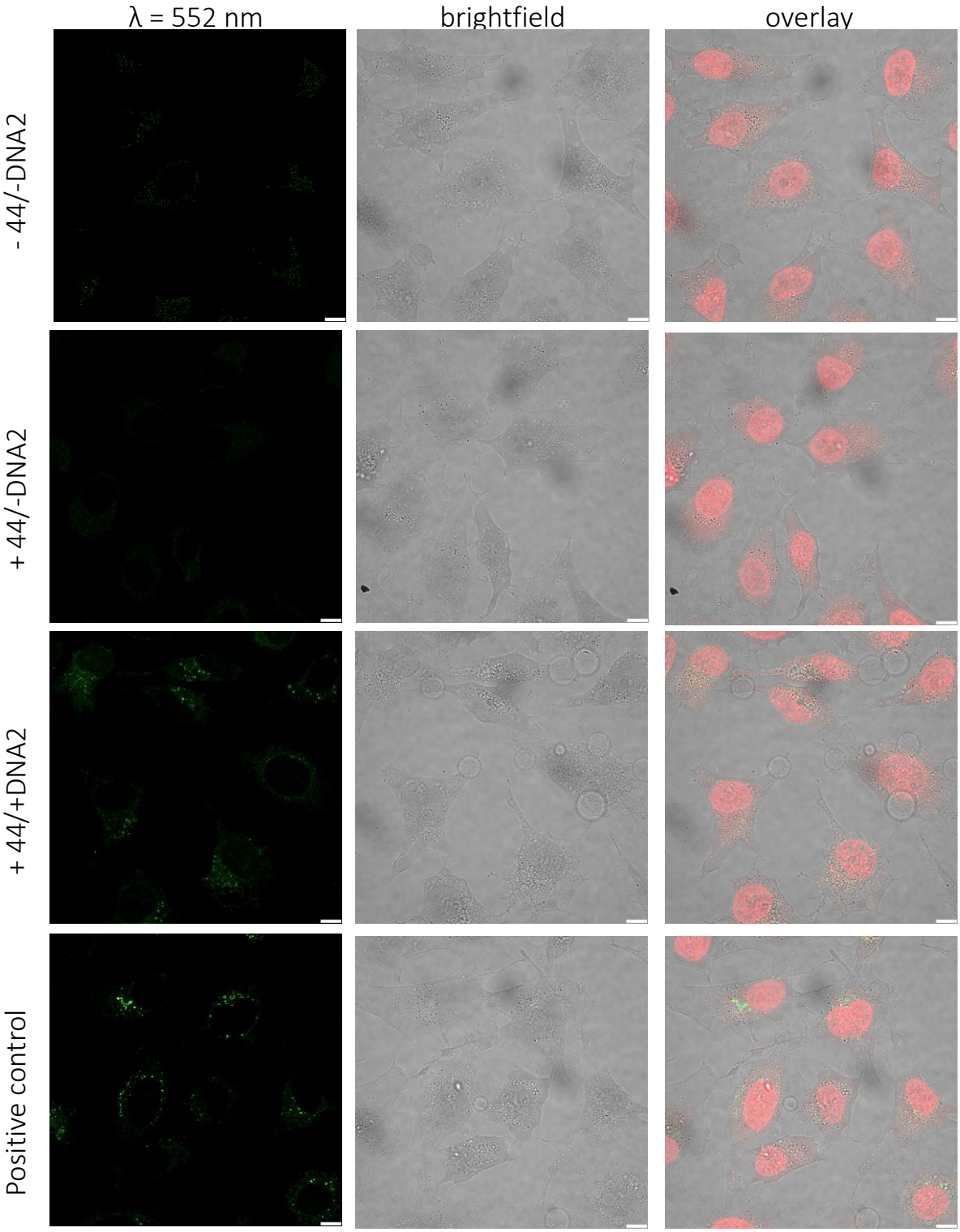

Figure 45: Fluorescence microscopic images of fixed HeLa cells treated for 2 h with fluorophore **44**. Negative control: untreated HeLa cells and fluorphore **44** without transfected DNA. λ_{exc} = 488 nm (10 % intensity), $\lambda_{em.}$ = 500-600 nm, Scale bar: 10 µm.

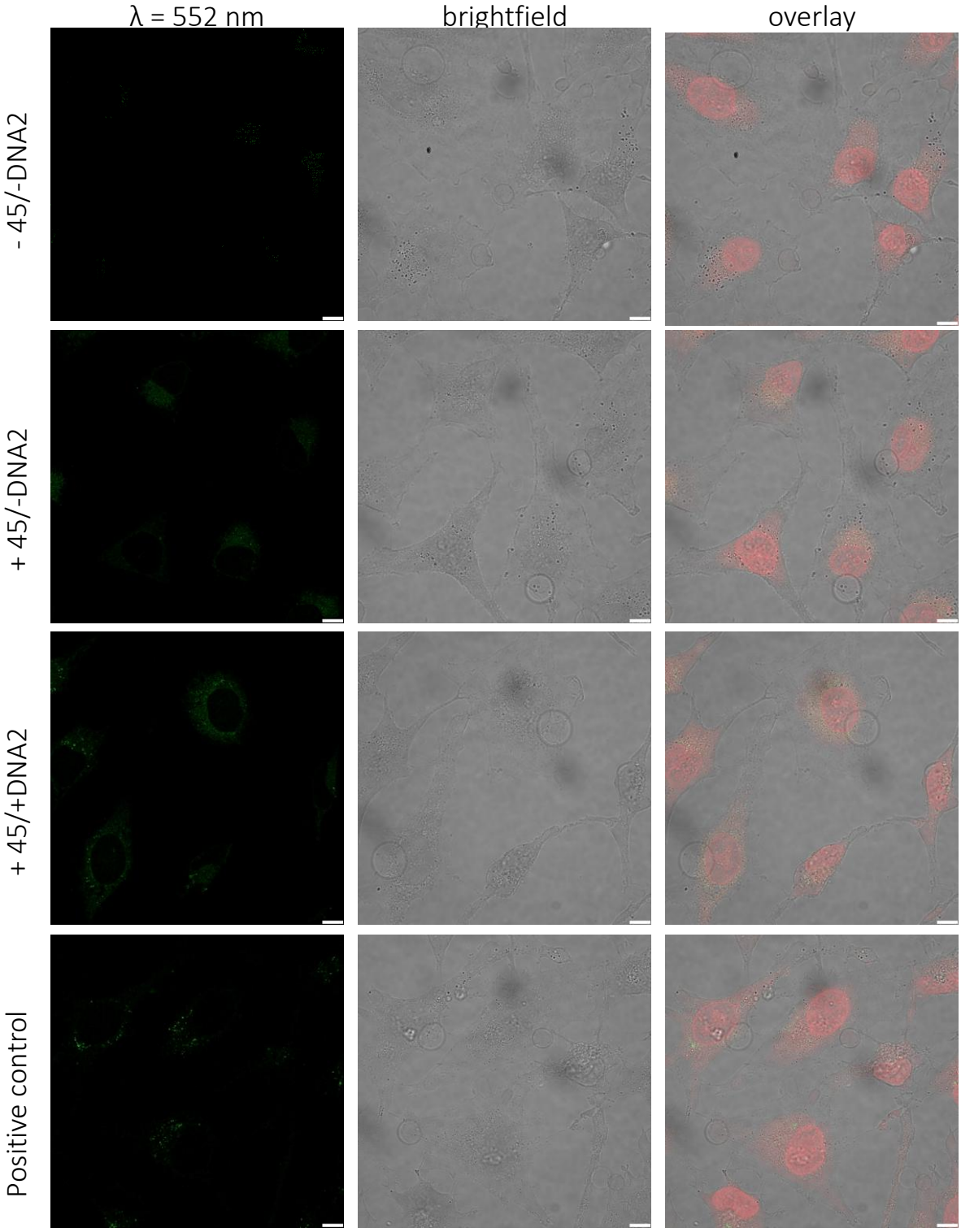

Figure 46: Fluorescence microscopic images of fixed HeLa cells treated for 2 h with fluorophore **45**. Negative control: untreated HeLa cells and fluorphore **45** without transfected DNA. λ_{exc} = 488 nm (10 % intensity), $\lambda_{em.}$ = 500-600 nm, Scale bar: 10 µm.

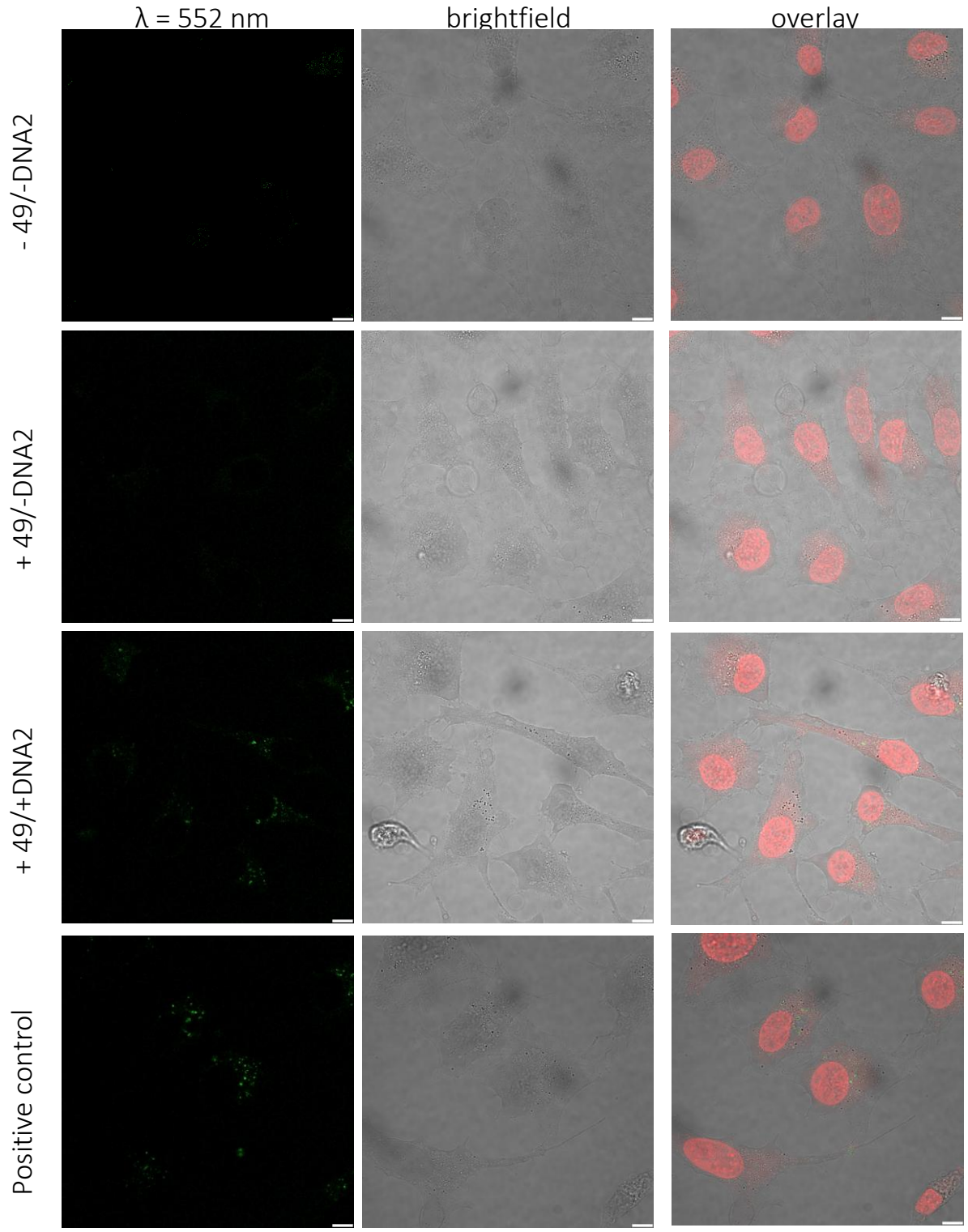

Figure 47: Fluorescence microscopic images of fixed HeLa cells treated for 2 h with fluorophore **49**. Negative control: untreated HeLa cells and fluorphore **49** without transfected DNA. λ_{exc} = 405 nm (10 % intensity), $\lambda_{em.}$ = 500-600 nm, Scale bar: 10 µm.

In summary, the sydnone-modified dyes developed in this work represent a useful addition to the range of fluorescent probes for in cellulo applications, because they show a high affinity in the bioorthogonal SPSAC reaction with modified oligonucleotides.

5. Diarylsydnone-modified oligonucleotides for bioorthogonal labeling

The second part of this work focuses on the synthesis of diarylsydnone-modified DNA. Sydnones have gained increasing interest in bioorthogonal chemistry due to their stability and their ability to react with chemical reporters via both SPSAC or photoclick reactions. By further modifying the sydnone ring with an aryl group, *Yu et al*. were able to synthesize diarylsydnones which, due to steric hindrance, only react under photoclick conditions, as the product of the SPSAC hardly forms due to steric hindrance. The use of diarylsydnones, similar to tetrazoles, allows a strong spatiotemporal control compared to conventional sydnones.[15]

5.1 Synthesis of the diarylsydnones

The synthesis of diarylsydnone **71** was carried out starting from 4-aminobenzoic acid ethyl ester (**64**). **64** was reacted with ethyl bromoacetate and DIPEA to form **65**. The ethyl group was then cleaved with 1M NaOH in ethanol at room temperature to avoid cleaving off the second ethyl group.[165] The sydnone was synthesized in two steps. First, the nitrogen was nitrosylated using tert-butyl nitrite. The sydnone ring of **67** was then formed by adding trifluoroacetic anhydride. The sydnone **67** was obtained with a yield of 75 %.[83] The sydnone was converted into the diarylsydnone by C-H activation. Therefore, **67** was reacted together with K_2CO_3 as a base and $Pd(OAc)_2$ in DMF together with **68** at 100 °C overnight.[130] After purification by column chromatography, the product could be isolated as a light brown solid with a yield of 45 %. In the next step, the ethyl group was cleaved with LiOH in water/THF mixture and then the resulting carboxylic acid was converted to the NHS ester using EDC as activating reagent. The NHS ester **71** was obtained as a light brown solid with a yield of 49 % (**figure 48**).

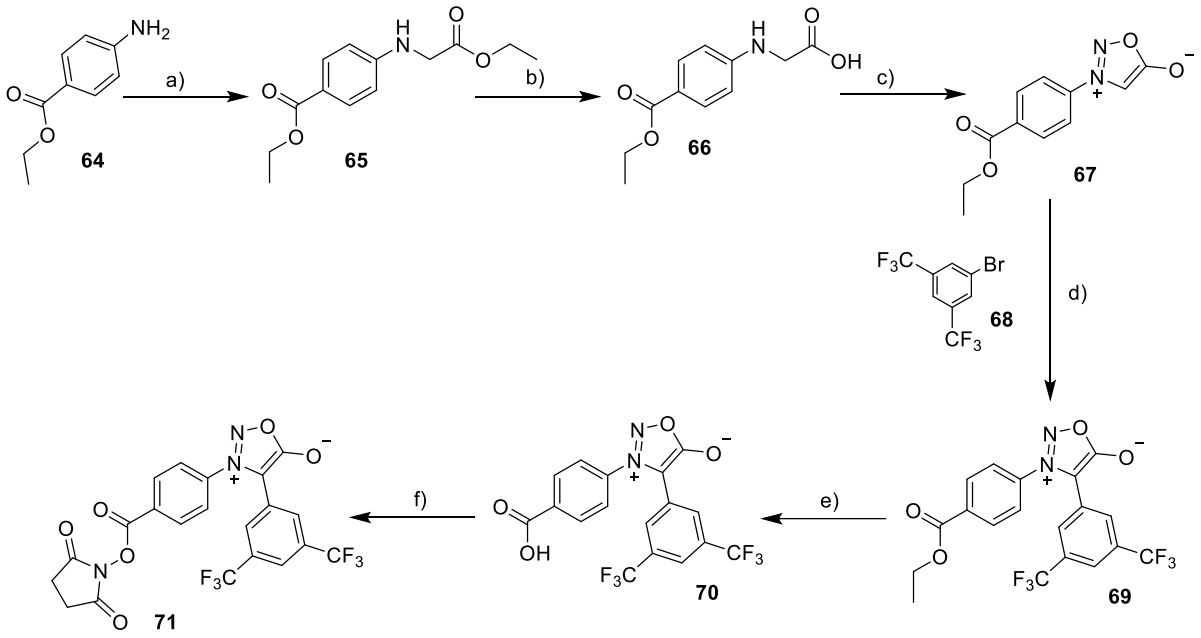

Figure 48: Synthesis of the diarylsydnone **71**: a) K_2CO_3, ethyl bromoacetate, DMF, 70 °C, 15 h, 89 %; b) 1N NaOH, ethanol, r.t., 3h, quant.; c) 1) tBuONO, THF, r.t., 1 h, 2) TFAA, THF, r.t., 3 h, 75 %; d) K_2CO_3, **68**, $Pd(OAc)_2$, DMF, 100 °C, 19 h, 45 %; e) LiOH, THF/water (1:1, v/v), r.t., 2 h; f) NHS, EDC, DMF, r.t, 16 h, 49 % (in two steps).

For the second diarylsydnone **79**, the synthesis was carried out starting from 4-methoxyaniline (**72**). It was reacted with ethyl bromoacetate and sodium acetate to afford **73**. Subsequently, the ethyl group was cleaved with NaOH in ethanol under reflux. The synthesis of the sydnone proceeded in two steps. First, the nitrogen was nitrosylated using tert-butyl nitrite. Subsequently, cyclization to the sydnone was carried out by adding trifluoroacetic anhydride. The sydnone **75** was isolated in a yield of 71 %. The synthesis to the diarylsydnone was carried out by C-H activation. For this purpose, **76** was reacted together with K_2CO_3 as a base and $Pd(OAc)_2$ in DMF together with **75** at 120 °C overnight. After purification by column chromatography, **77** was obtained as a yellow solid with a yield of 58 %.[130] The ethyl group was cleaved with LiOH and subsequently **78** was then converted to the NHS ester. The NHS ester **79** could be isolated as a yellow solid with a yield of 29 % in two steps (**figure 49**).

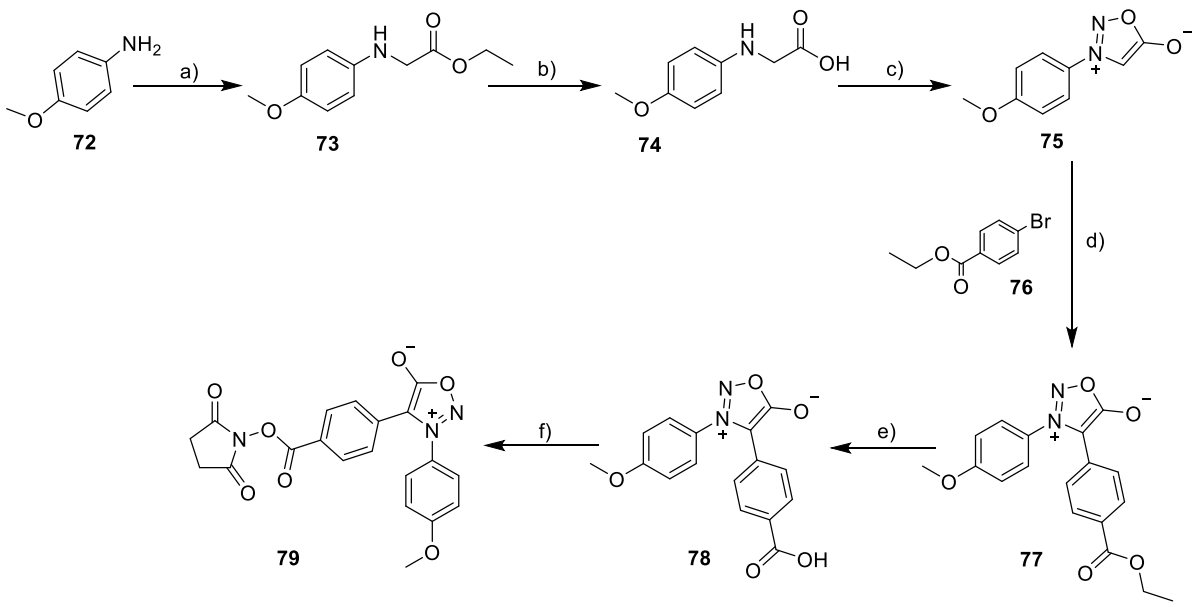

Figure 49: Synthesis strategy of the diarylsydnone **79**: a) sodium acetate, ethyl bromoacetate, ethanol, reflux, 15 h, 76 %; b) NaOH, ethanol, reflux, 1.5 h, 77 %; c) 1) tBuONO, THF, r.t., 1 h, 2) TFAA, THF, r.t., 3 h, 70 %; d) K_2CO_3, **76**, $Pd(OAc)_2$, DMF, 120 °C, 19 h, 58 %; e) LiOH, THF/water (1:1, v/v), r.t., 2 h; f)NHS, EDC, DMF, r.t, 16 h, 29 % (over two steps).

In parallel, the aminopropyl-modified nucleoside **81** and DNA building block **84** was synthesized (**figure 50**). The triple bond of **27** was hydrogenated with triethylsilane and $Pd(OH)_2/C$, followed by the removal of the trifluoroacetyl protecting group using concentrated ammonium hydroxide solution. **81** was obtained in quantitative yield. In addition, nucleoside **84** was synthesized by protecting the amine group using a DMF-DMA protecting group and further protecting the 5'-position of nucleoside **80** with 4,4'-dimethoxytrityl chloride, which resulted in **83** in a yield of 65 %. The phosphoramidite was synthesized by reaction with 2-cyanoethyl N,N-diisopropyl chlorophosphoramidite and DIPEA to yield building block **84** in 65 % yield.[166]

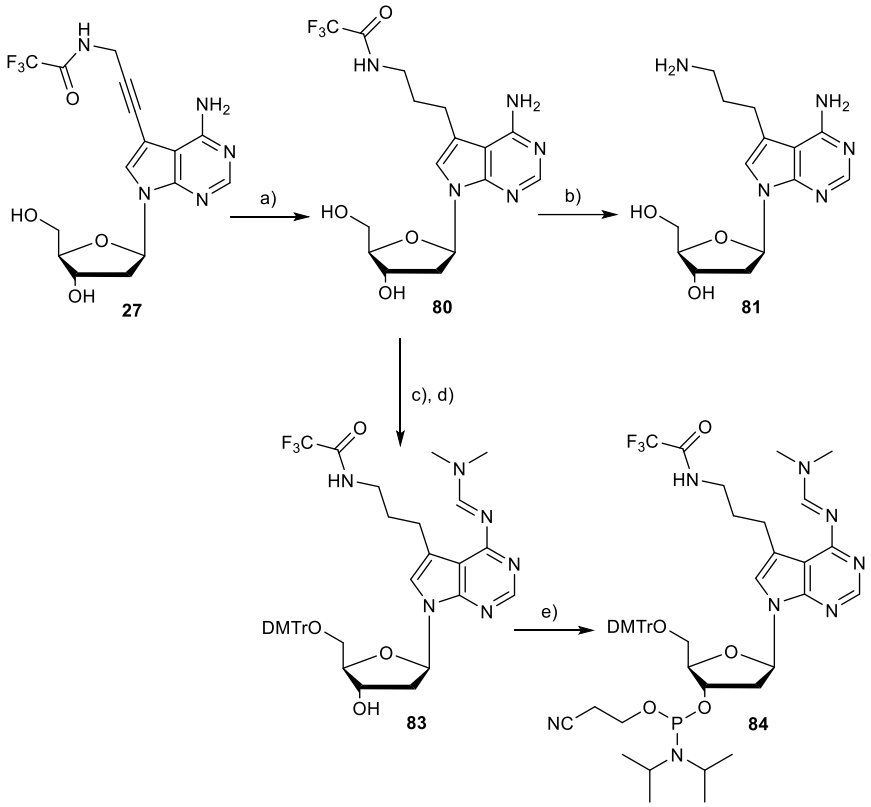

Figure 50: Synthesis of aminopropyl-modified nucleoside **81** and DNA building block **84**: a) triethylsilane, $Pd(OH)_2/C$, MeOH, r.t., 16 h, 80 %; b) conc. NH_4OH, r.t., 16 h, quant.; c) DMF-DMA, MeOH, 40 °C, 16 h, 66 %; d) DMTr-Cl, pyridine, MeOH, r.t., 16 h, 65 %; e) 2-Cyanonethyl-N,N-diisopropylchlorophosphoramidite, DIPEA, DCM, r.t., 4 h, 65 %.

The nucleoside **1** and **2** were synthesized by reaction of the NHS-esters **71** and **79** with **81** under basic conditions. The diarylsydnone-modified nucleosides were obtained in yields of 40 % (**1**) und 11 % (**2**) (**figure 51**).

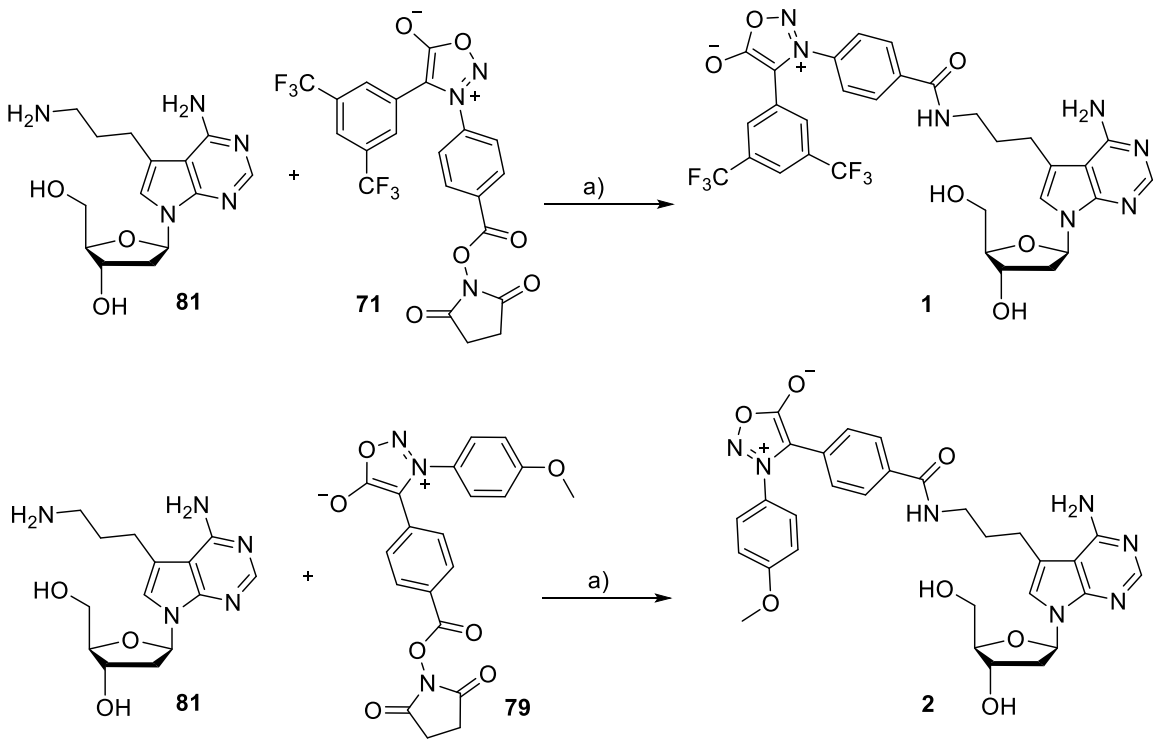

Figure 51: Synthesis of diarylsydnone-modified nucleosides **1** and **2**: a) triethylamine, DMF, r.t., 16 h, **1** 40 %, **2** 11 %.

5.2 Synthesis of diarylsydnone-modified DNA

First, the phosphoramidite building block **84** was incorporated into **DNA3** using standard solid-phase synthesis protocol (**figure 52**).

Figure 52: Synthesis of **DNA3**.

The synthesized DNA was cleaved from the solid support with ammonia and purified on a DMTr affinity column. The DNA3 was detected by Maldi-TOF mass spectroscopy. The diarylsydnones **71** and **79** were postsynthetically introduced into the DNA. For this purpose, the DNA and the respective NHS ester were dissolved in DMSO and reacted with DIPEA in a microreaction tube (**figure 53**). After purification of the modified strands via HPLC, the success of the reaction was verified by Maldi-analysis (**Chapter 7.3**, **table 7**).

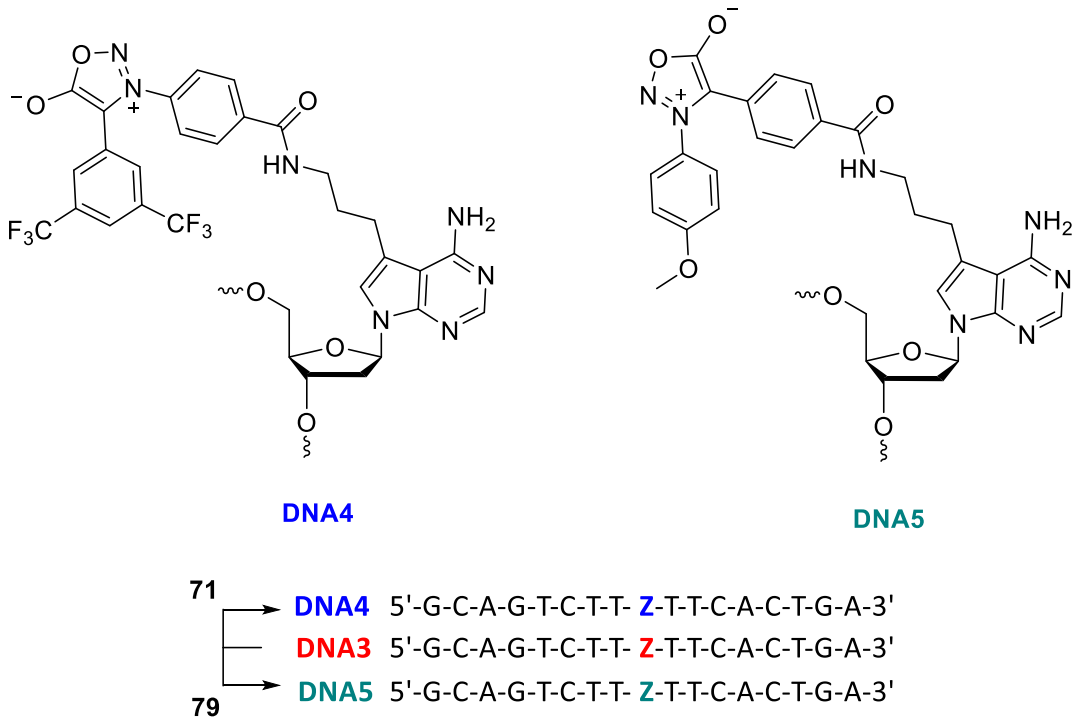

Figure 53: Sequences of **DNA4** and **DNA5**.

5.3 Bioorthogonal Labeling Experiments

5.3.1 Photoclick experiments

Photoclick labeling experiments were performed on the nucleosides **1** and **2** to gain insight into the changes in fluorescence and absorption properties for future cell applications. As a reaction partner N-methylmaleimide (NMM) was chosen. In order to perform the photoclick experiments, stock solutions of the reactants were prepared. Due to the limited solubility in water, DMSO was used as a solvent. The reaction was carried out in water/DMSO 99:1, with the final concentrations of the two reactants being **1/2** 25 µM and that of NMM 250 µM. A tenfold excess of NMM allowed the assumption of pseudo-first-order kinetics. The samples were irradiated with λ = 405 nm LEDs, and the intensity of the LED was measured before each experiment. The experiments were carried out with 25 µM **1** and 250 µM **NMM** (10.0 eq.) by irradiation with λ = 405 nm light (43.8 mW) in water/DMSO (99:1 V/V%). Absorbance and emission spectra were collected at defined times after irradiation (**figure 54**).

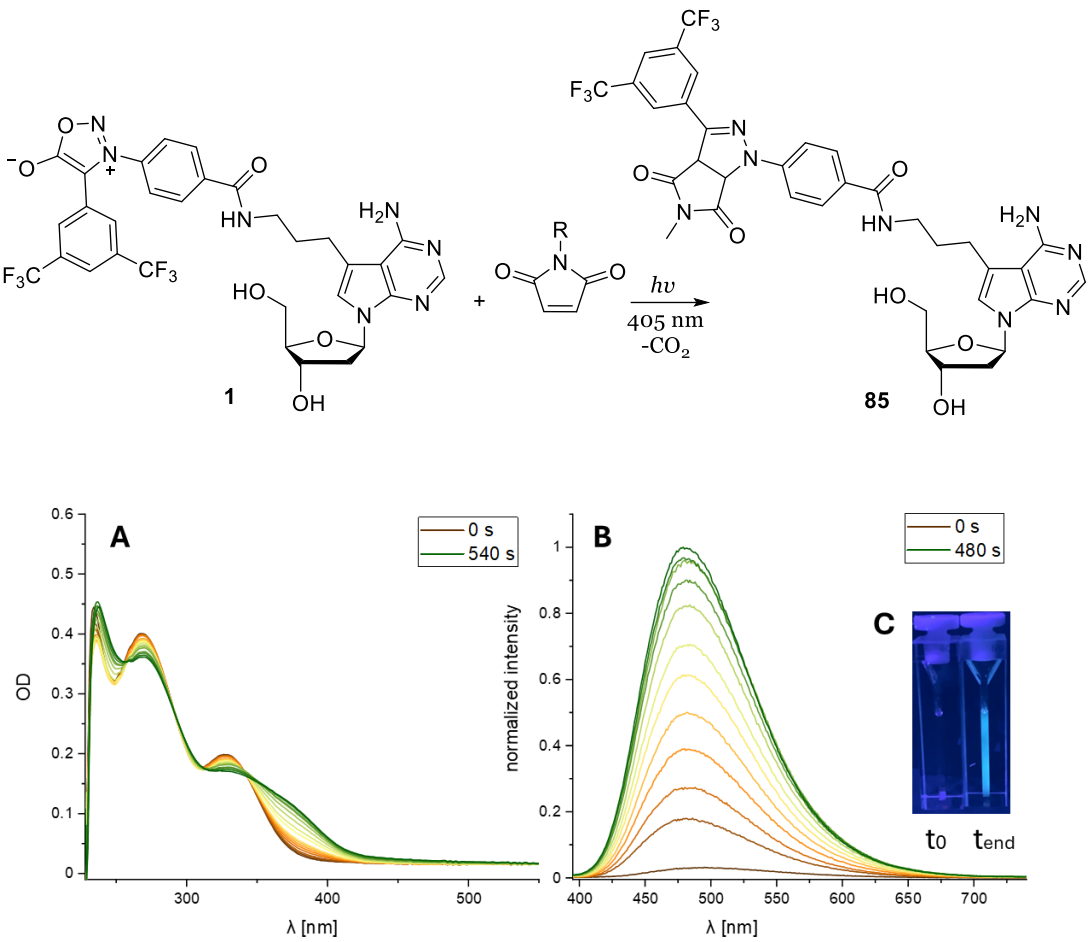

Figure 54: Photoclick reaction between **1** and **NMM** by irradiation with λ = 405 nm. **A)** changes in the absorption spectra during the photoclick reaction between **1** (25 µM, 1.00 eq.) and **NMM** (250 µM, 10.0 eq.) in H_2O/DMSO 99:1. **B)** Increase in fluorescence intensity during photoclick reaction ($\lambda_{exc.}$ = 380 nm) **C)** visible turn-on: t_0: fluorescence of **1** at the start of the reaction, t_{end}: fluorescence after complete conversion with **NMM**.

In the UV-Vis spectrum, a new band at 382 nm can be observed, which can be assigned to the formation of fluorescent pyrazoline. At the same time, a decrease in absorbance of the sydnone at 328 nm was observed. Furthermore, isosbestic points at 256 nm, 293 nm and 344 nm were observed. After 540 s, the reaction appears to be complete, as no significant change in the absorption spectrum is visible. This observation also coincides with the fluorescence spectrum, where the fluorescence hardly changes after 480 s. In the fluorescence spectrum, a strong increase in fluorescence of 25 times is observed. This increase in fluorescence is also visible when the cuvette is illuminated with a handheld UV lamp. The success of the reaction of nucleoside **1** with **NMM** was verified by ESI-MS (**chapter 7.4**, **table 13**).

The same experiment was carried out with the diarylsydnone nucleoside **2**. Compared to diarylsydnone nucleoside **1**, the fluorescence increases more strongly; a 32-fold fluorescence increase was observed. Furthermore, the fluorescence spectrum is bathochromically shifted compared to **1**. On closer inspection, an increasing shoulder at 477 nm can be seen in the fluorescence spectrum after an irradiation time of 120 s. This could indicate the formation of a by-product or the degradation of the formed click product. The reaction rate at which the pyrazoline is formed is quite similar to that of **1** (figure 55).

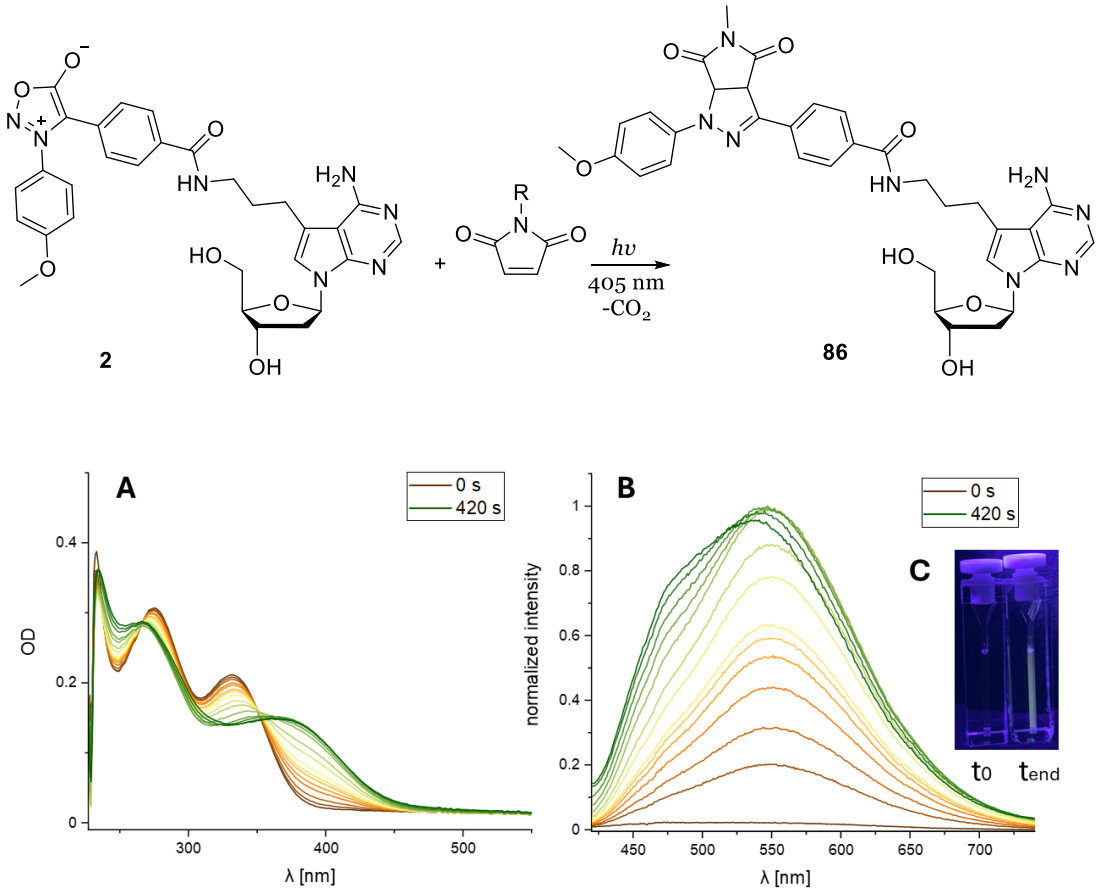

Figure 55: Photoclick reaction between **2** and **NMM** by irradiation with λ = 405 nm. **A)** changes in the absorption spectra during the Photoclick reaction between **2** (25 µM, 1.00 eq.) and **NMM** (250 µM, 10.0 eq.) in H_2O/DMSO 99:1. **B)** Increase in fluorescence intensity during Photoclick reaction ($\lambda_{exc.}$ = 400 nm) **C)** visible turn-on: t_0: fluorescene of **2** at the start of the reaction, t_{end}: fluorescence after complete conversion with **NMM**.

When examining the absorption spectrum, it is noticeable that the sydnone band is at λ = 333 nm and the pyrazoline band at λ = 403 nm. Compared to **1**, both bands are bathochromically shifted. The spectrum shows isosbestic points at 264 nm and 353 nm.

The bathochromic shift compared to **1** is also visible when the cuvette is illuminated with a handheld UV lamp. The success of the reaction of nucleoside **2** with **NMM** was verified by ESI-MS (**chapter 7.4**, **table 13**). To determine the reaction rate constants k_2 of the two photoclick reactions, the integrated fluorescence intensities were plotted against time. Based on the tenfold excess, pseudo-first-order kinetics were assumed and therefore a monoexponential fit was performed. The resulting graphs are shown in **figure 56**:

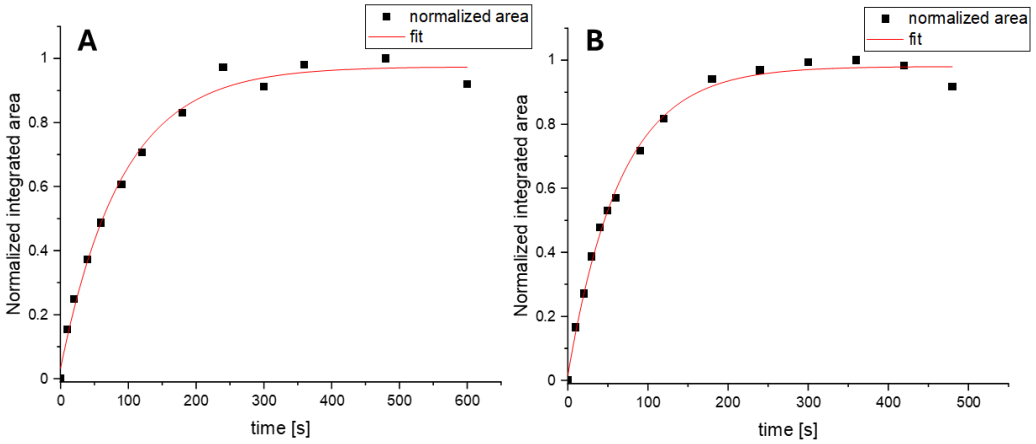

Photoclick-reaction	k_2 [$M^{-1}s^{-1}$]
1 + NMM	44 ± 4
2 +NMM	61 ± 3

Figure 56: Application of integrated areas against time. The click reactions between A) **1** + NMM and B) **2** + NMM are considered. The table shows the calculated reaction rate constants of the photoclick reaction.

The calculated reaction rate constants of the photoclick reactions under consideration are within the range characteristic of photoclick reactions ($10^1 – 10^2$ $M^{-1}s^{-1}$).

5.3.2 SPSAC experiments

It has been reported in the literature that diarylsydnone, due to steric hindrance, hardly reacts with a dienophile in an SPSAC but only by photoclick reaction.[130] To test this, **1** and **2** were reacted with BCN-OH. Every 20 minutes, a UV-Vis spectrum was recorded to check the progress of the reaction. **Figure 57** shows the obtained spectra:

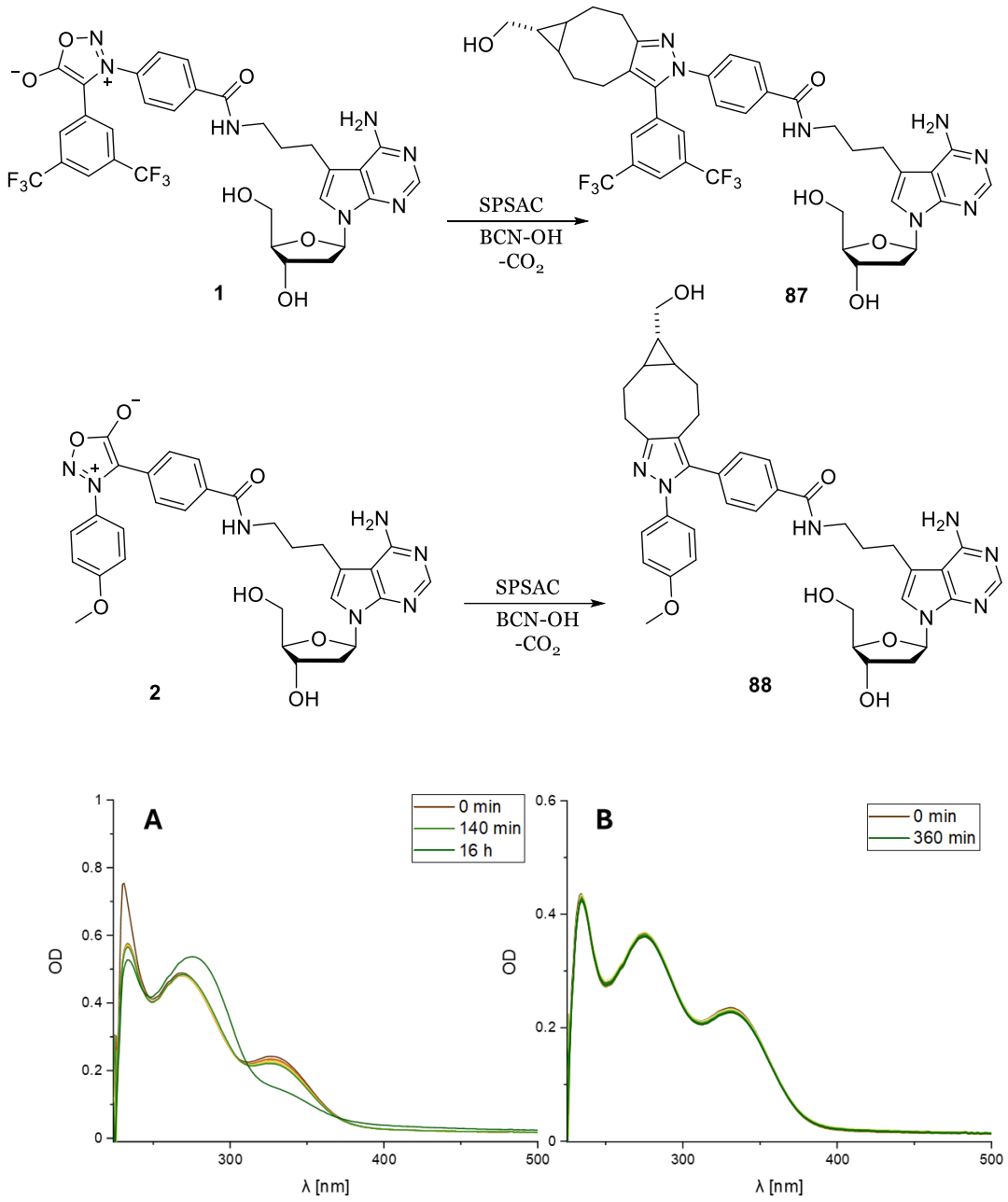

Figure 57: SPSAC reaction between **1** and BCN-OH and **2** and BCN-OH. UV-Vis spectra of the SPSAC between A) **1** + BCN-OH and B) **2** + BCN-OH.

Considering the obtained absorption spectra, there is almost no change in the absorption spectrum of **1** over a period of two hours. A significant change in the spectrum is only seen after 16 hours, which indicates the course of the SPSAC as a decrease in the sydnone band at λ = 333 nm is observed and a band at λ = 396 nm is formed, indicating the formation of the pyrazole. The absorption spectrum of **2** with BCN-OH also shows no change over a

period of 6 hours. Thus, the diarylsydnones prepared in this work also exhibit the reduced reactivity towards SPSAC described in the literature.[130]

6. Summary and Outlook

The first challenge of this work was based on the synthesis of new fluorescent sydnone dyes. The synthetic research produced five sydnone dyes through empirical development, of which three met the required criterion of a turn-on effect (figure 58). The sydnone dyes developed showed high Stokes shifts, making them well suited for biochemical applications since the excitation wavelength is separate from the emission band. SPSAC reactions were carried out with the sydnon dyes produced with the BCN-modified nucleosides **15** and **16**. On the one hand, the influence of the 2'-OH group on the kinetics of the fluorophores with the nucleosides was to be investigated, as well as the turn-on. It was found that the 2'-OH group has no significant influence on the aforementioned factors, which is why it can be assumed that similar results to those obtained with DNA labelling can be expected for labelling RNA. The strongest turn-on could be achieved with **49**. Fluorophore **44** showed the fastest kinetics. However, the kinetics all moved in a similar range, namely 10^0 $M^{-1}s^{-1}$. Furthermore, the experiments were used to preselect the empirically developed dyes based on their properties with the nucleosides in order to examine only the most successful fluorophores with BCN-modified DNA.

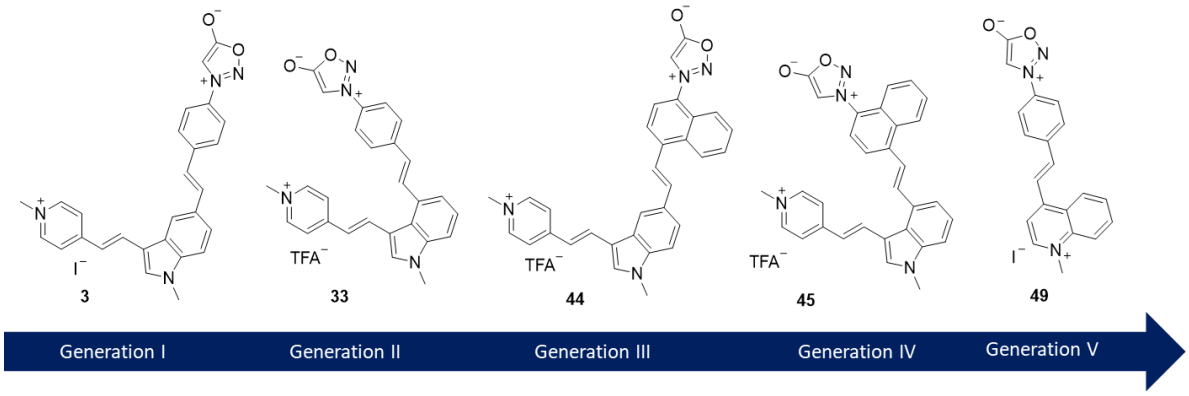

Figure 58: Overview of the developed fluorogenic sydnone dyes.

The results of the SPSAC reaction with BCN-modified DNA show a strong acceleration of the reaction rate constants, in the range of $k_2 \geq 10^3$ $M^{-1}s^{-1}$. The turn-on was also improved up to eightfold. This indicates that the increase in fluorescence intensity is not only due to the reaction with the pyrazole product, but also due to structural fluorogenicity. This can be explained by the formation of non-covalent templates with the DNA, whereby the DNA

restricts the rotational freedom of the fluorophore more strongly than the nucleoside and thus reduces the vibronic relaxation from the first excited state. Thus, the sydnone fluorophores show a strong affinity towards modified oligonucleotides and are therefore suitable for fluorescent imaging for the detection of cellular DNA in cells. In subsequent cell experiments, it was shown that previously transfected BCN-modified DNA could be detected with dyes **44**, **45** and **49** in fixed HeLa cells. The sydnone fluorophore **44** showed the best results. As a next step, the sydnone dyes could be used to detect BCN-modified DNA in living cells.

The second part of this work deals with the development of diarylsydnones as chemical reporters in nucleosides and DNA. So far, only Wagenknecht et al. have synthesized a phenyl diarylsydnone-modified nucleoside, but it has never been incorporated into DNA.[167] The diarylsydnones produced in the work could be successfully attached to the nucleoside using an NHS ester and could also be post-synthetically integrated into the DNA. The photoclick experiments with NMM showed fast reaction rate constants in the range $k_2 > 10^1$ $M^{-1}s^{-1}$. In addition, exposure was possible in the visible range at 405 nm, which is advantageous for later cell applications. In the reaction of the diarylsydnone-modified nucleosides with NMM, a 25- to 32-fold increase in fluorescence intensity was observed and the fluorescence maximum of the diarylsydnone-modified nucleosides were at 480 nm and 550 nm. Furthermore, it was observed that diarylsydnone-modified nucleosides react only very slowly compared to sydnones with BCN-OH in an SPSAC; after 6 h, almost no conversion is observed. As a next step, the prepared diarylsydnone-modified DNA should be investigated in photoclick reactions. For this purpose, for example, the DNA could be reacted with AF555-maleimide to investigate the reaction as part of a FRET system. Furthermore, diarylsydnones and sydnones could be used as chemical reporters for dual bioorthogonal labeling. Due to the low reactivity of diarylsydnones without light, it would be possible to first detect sydnone-modified DNA with a BCN- or DIBAC-modified dye and then diarylsydnone-modified DNA with a maleimide dye.

7. Experimental Section

The experimental methods used in this work are explained below.

7.1 Materials and devices

Reagents and solvents

The reagents used for synthesis were purchased from ABCR, ALFA AESAR, CARBOLUTIONS, FLUKA, MERCK, SIGMA ALDRICH, BLDpharm, TCI and VWR and used without further purification.

For syntheses, solvents were purchased from SIGMA ALDRICH, ACROS ORGANICS and FISCHER, which were at least quality level *pro analysi* (*p.A.*). Absolute solvents were also purchased and stored and used under argon. Technical solvents were used for work-up and for chromatographic purification, unless otherwise specified. Double deionised water (*Milli-Q® Direct 8/16* system from Merck *Millipore*) and high purity solvents (HPLC *grade*) were used for HPLC separations. Buffers used were filtered before.

Deuterated solvents were bought from EURISO-TOP.

Chemical Synthesis

Air- and water-sensitive reactions were carried out using Schlenk technique under an argon atmosphere (Argon 5.0, Air Liquide, 99.999 % purity). The glass equipment used was previously heated several times in a high vacuum and flushed with argon several times. Liquids were taken utilizing plastic syringes and cannulas or pipettes of the Eppendorf brand. If required, the solvents were degassed by passing in argon or by applying the *freeze-pump-thaw* method. Solids were transferred using weighing paper.

For reactions at low temperatures, the following cooling mixtures were used:

- 0 °C ice in water
- -21 °C sodium chloride in ice
- -78 °C dry ice in isopropanol

Solvents were removed under reduced pressure on a rotary evaporator at a water bath temperature of 45 °C.

NMR Spectroscopy

Nuclear magnetic resonance analyses were performed in deuterated solvents of the company EURISO-TOP. The measurements were performed on a BRUKER *Advance 400* (400 MHz 1H -NMR or 101 MHz ^{13}C-NMR) or BRUKER *Advance 500* (500 MHz ^{1}H-NMR or 126 MHz ^{13}C-NMR).

For the measurement, 5-10 mg of the sample were dissolved in approx. 0.5 ml of deuterated solvent in a measuring tube with a diameter of 5 mm. The deuterated solvents employed were [d6]-DMSO, [d1]-$CDCl_3$ and [d4]-MeOD. The measured chemical shifts (δ) were given in *parts per million* (ppm) and refer to tertramethylsilane as zero point. The spectrum was calibrated to the signals of the not fully deuterated solvent used.

[*d6*]-DMSO:	^{1}H-NMR: δ = 2.50 ppm	^{13}C-NMR: δ = 39.52 ppm
[*d1*]-$CDCl_3$:	^{1}H-NMR: δ = 7.26 ppm	^{13}C-NMR: δ = 77.16 ppm
[*d4*]- MeOD:	^{1}H-NMR: δ = 3.31 ppm	^{13}C-NMR: δ = 49.00 ppm

The measured coupling constants *J* were given in Hertz (Hz). The multiplicities of the signals were labelled with the abbreviations s (singlet), d (doublet), dd (doublet of doublet), t (triplet), q (quartet), quin (quintet) and m (multiplet) and br (broadened signal). The spectra were evaluated with the help of the software MESTRENOVA. The chemical shifts of known solvents were taken from known literature sources for example *Fulmer et al*.[168]

Thin-layer chromatography

For thin-layer chromatography, aluminum plates coated with silica gel (silica gel 60, F_{254}, layer thickness 0.250 mm) from MERCK were used. For the detection of the spot samples, UV-active samples were detected with UV light, by fluorescence quenching at λ = 254 nm or fluorescence excitation at λ = 366 nm. UV-inactive samples were stained with potassium permanganate solution (1.50 g KMnO4, 10.0 g K2CO3, 1.25 mL 10 % NaOH solution, 200 mL H2O) or Seebach solution. Saccharides were stained with a solution of sulfuric acid in

methanol (5 % H_2SO_4) and amines with a ninhydrin solution (3.00 g ninhydrin in 200 mL EtOH).

Column chromatography

Column chromatography was used to purify the crude products. Silica gel 60 (pore size 60 Å, particle size 40-63 µm) from SIGMA ALDRICH served as stationary phase. The raw products were adsorbed on *Celite S*, dry loaded or applied as a solution. Elution was carried out with overpressure generated by a hand pump.

High-performance liquid chromatography (HPLC)

Reversed-phase high-performance liquid chromatography (HPLC) of oligonucleotides was carried out on a THERMO SCIENTIFIC HPLC instrument (*Dionex UltiMate3000* autosampler, pump module, column oven, multidiode array, RS fluorescence detector, fraction collector, *Chromeleon 7* software). The separation was performed on a semi-preparative column (*VDSpehr OptiBio PUR 300* S18-SE column (250 x 10 mm, 5 µm)). The analytes were applied to the column with an injection volume of 300 µL and a flow rate of 3.50 mL/min, unless otherwise stated. The column was equilibrated with 0.05 M ammonium acetate buffer in water and eluted with various gradients of acetonitrile. The signals were measured using a UV diode array detector at wavelengths of 260 nm, 290 nm and the characteristic absorption of the respective artificial building blocks. For the monitoring of the SPSAC reactions and Photoclick-reactions between the nucleosides and their corresponding click partners via HPLC-MS an analytical column (*VDSpehr OptiBio PUR 300* S18-SE column (250 x 4.6 mm, 5 µm)) was used. A solvent gradient of acetonitrile and double-distilled water was used. The analytes were applied on the column with an injection volume of 20 µL and a flow rate of 1.00 ml/min, unless otherwise stated. For the analytical runs with the sydnone fluorophores 0.1 % TFA was additionally added to the solvents. The signals were measured using a UV diode array detector at wavelengths of 260 nm, 290 nm and the characteristic absorption of the respective artificial building blocks.

Irradiation Setup

The LEDs used in the irradiation setup were purchased from *Roithner Laser Technik GmbH* (405 nm: 5P4FCA). The irradiation setup was designed and manufactured by the University of Regensburg and the workshop of the Institute of Physical Chemistry at KIT. The setup is shown in figure 59. A *Lauda Alpha R8*-thermostat was used to cool the system (in vitro experiments, 20 °C).

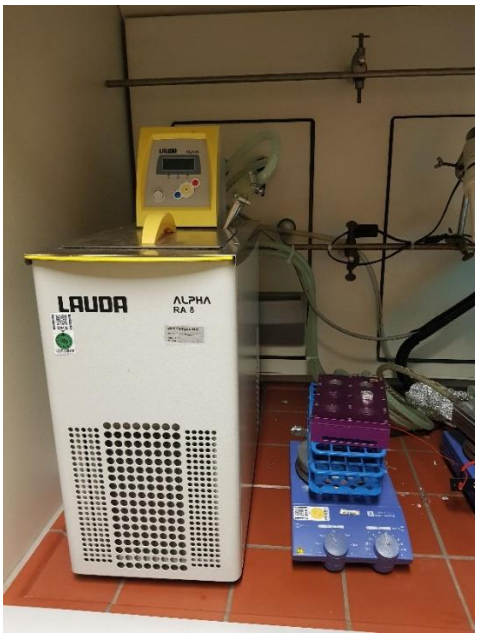

Figure 59: Irradiation setup.

Sublimation drying

Aqueous solutions were dried in a *CHRIST Alpha RVC* vacuum concentrator or after freezing in liquid nitrogen on a *CHRIST Alpha 1-2 LD Plus* lyophilization unit.

Mass Spectrometry

MALDI-TOF measurements were carried out on an *AXIMA Confidence* spectrometer from *SHIMADZU*. A standard plate made of stainless steel from the company Bruker with 386 application points was used as the target. A matrix of 3- hydroxypicolinic acid (saturated solution in acetonitrile/water=1:1) and diammonium hydrogen citrate (0.44 M in water) in a 9:1 mixture was used for DNA mass measurements. The signals were reported by their mass to charge ratio (m/z).

Small molecule masses were recorded on a Q Exactive Orbitrap and an LTQ Orbitrap XL from THERMO FISHER SCIENTIFIC using electron spray ionization (ESI). The signals were given in mass/charge ration (m/z) and the molecular ion was shown as $[M]^+$ or in protonated form as $[M+H]^+$ or $[M-H]^+$ in positive mode.

Combination of liquid chromatography and mass spectroscopy (LC-MS)

LC-MS analyses were performed using an *UltiMate 3000 Dionex* system coupled with an *LTQ Orbitrap Elite ESI* mass analyzer (*Thermo Scientific*).

Determining the concentration of oligonucleotides

For the determination of the concentration of single strand DNA, the strands were solved in aqueous solution and the concentration was examined with an ND-100 spectrophotometer from Nanodrop™. For this, the absorption was measured at 260 nm in ''Nucleic Acid'' mode. A sample volume of 1 µL was applied and the concentration was calculated using Lambert-Beer's law.

Optical spectroscopy

The examination of the synthesized substances was carried out in quartz glass cuvettes from STARNA path length 1 cm, sample volume 1 mL or 0.5 mL) at a temperature of 20 °C. All spectra were baseline-corrected using a blank.

UV/VIS spectroscopy

The absorption spectra were recorded on a Cary3500 spectrometer from AGILANT with Peltier element from AGILENT. The samples were prepared using 1 cm quartz glass cuvettes (Starna) with a volume of 1 mL at 25 °C. To determine the extinction coefficients, different concentrations were measured and applied to Lambert-Beer's law.

Fluorescence spectroscopy

Fluorescence spectra were recorded on a *Fluoromax-4* spectrofluorometer from HORIBA-SCIENTIFIC with a Peltier element from Horiba Scientific at 20 °C. The spectrometer was calibrated using the Raman scatter of water as a reference to ensure accurate wavelength measurement.

7.2 Synthetic Procedures

Compound 10

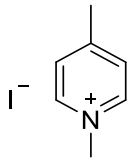

$C_7H_{10}N^+I^-$
235.07 g/mol

In a round bottom flask 2.09 mL 4-Methylpyridin (2.00 g, 21.4 mmol, 1.00 eq.) was dissolved in 7 mL acetone (V = 3,33 mL/10 mmol). 4.01 mL iodomethane (9.14 g, 64.4 mmol, 3.00 eq.) was added and the reaction mixture was stirred at 56 °C oil bath temperature for 2 hours. After cooling down the reaction to room temperature the precipitate was filtered off and washed three times with diethyl ether. The solid was dried overnight under reduced pressure. The product was obtained as a colorless solid with a yield of 4.10 g (17.4 mmol, 81 %).

^{1}H-NMR (400 MHz, DMSO-d_6): δ (ppm) = 8.83 (d, *J* = 6.6 Hz, 2H, arom.), 7.96 (d, *J* = 6.4 Hz, 2H, arom.), 4.28 (s, 3H, N-CH_3), 2.60 (s, 3H, C-CH_3).

HR-MS (ESI): m/z (calculated for $C_7H_{10}N^+$): 108.0808 $[M]^+$; found: 108.0809 $[M]^+$.

The spectroscopic data is in agreement with literature.[12]

Compound 11

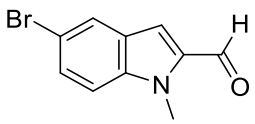

$C_{10}H_8BrNO$
238.08 g/mol

In a round bottom flask 3.00 g 5-Bromoindol-3-carbaldehyde (13.3 mmol, 1.00 eq.) and 2.04 g potassium carbonate (14.7 mmol, 1.10 eq.) were suspended in 19 mL DMF. 4.50 mL dimethyl carbonate (4.82 g, 53.5 mmol, 4.00 eq.) was added and the reaction mixture was stirred for 19 hours at 137 °C oil bath temperature. After letting the reaction cool down to room temperature, the reaction mixture was poured on 50 mL ice. The water phase was extracted three times with ethyl acetate. The combined organic phases were washed with water and brine solution. The organic layer was dried over sodium sulfate and the solvent was removed under reduced pressure. The product was obtained as a beige solid with a yield of 2.26 g (9.49 mmol, 71 %).

^{1}H-NMR (400 MHz, DMSO-d_6): δ (ppm) = 9.89 (s, 1H, R-CHO), 8.33 (s, 1H, arom.), 8.23 (d, *J* = 1.9 Hz, 1H, arom.), 7.58 (d, *J* = 8.7 Hz, 1H, arom.), 7.47 (dd, *J* = 8.7 Hz, 2.0 Hz, 1H, arom.), 3.89 (s, 3H, N-CH_3).

The spectroscopic data is in agreement with literature.[12]

Compound 4

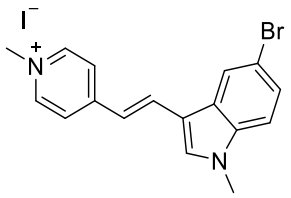

$C_{17}H_{16}BrN_2^+I^-$
455.14 g/mol

In a schlenk flask under argon atmosphere 0.700 g 1,4-dimethylpyridiniumiodid (**10**) (2.97 mmol, 1.00 eq.) was dissolved in 35 mL ethanol and stirred for 10 minutes. 1.06 g of the indole **11** (4.46 mmol, 1.50 eq.) and 1.76 mL piperidine (17.8 mmol, 6.00 eq.) were added to the reaction mixture. The reaction was stirred overnight at 85 °C oil bath temperature. After letting the reaction mixture cool down to room temperature, diethyl ether was added until no further precipitate was formed. The precipitate was filtered off and washed three times with diethyl ether and dried under reduced pressure. The product was obtained as an orange solid with a yield of 1.07 g (2.35 mmol, 79 %).

^{1}H-NMR (400 MHz, DMSO-d_6): δ (ppm) = 8.71 (d, *J* = 6.9 Hz, 2H, arom.), 8.36 (d, *J* = 1.7 Hz, 1H, arom.), 8.21 (d, *J* = 16.3 Hz, 1H, R-CH=CH-R), 8.16 (d, *J* = 6.9 Hz, 2H, arom.), 8.02 (s, 1H, arom.), 7.56 (d, *J* = 8.7 Hz, 1H, arom.), 7.44 (dd, *J* = 8.7, 1.8 Hz, 1H, arom.), 7.25 (d, *J* = 16.3 Hz, 1H, R-CH=CH-R), 4.18 (s, 3H, R-CH_3), 3.88 (s, 3H, R-CH_3).

HR-MS (ESI): m/z (calculated for $C_{17}H_{16}{}^{79}BrN_2^+$): 327.0491 $[M]^+$; found: 327.0485 $[M]^+$; m/z (calculated for $C_{17}H_{16}{}^{81}BrN_2^+$): 329.0471 $[M]^+$; found: 329.0461 $[M]^+$.

The spectroscopic data is in agreement with literature.[12]

Compound 35

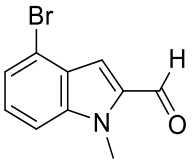

$C_{10}H_8BrNO$
238.08 g/mol

In a round bottom flask 2.01 g 4-Bromoindol-3-carbaldehyd (13.3 mmol, 1.00 eq.) and 2.04 g potassium carbonate (14.7 mmol, 1.10 eq.) were suspended in 19 mL DMF. 4.50 mL dimethylcarbonate (4.82 g, 53.5 mmol, 4.00 eq.) was added and the reaction mixture was stirred for 19 hours at 137 °C oil bath temperature. After letting the reaction cool down to room temperature, the reaction mixture was poured on 50 mL ice. The water phase was extracted three times with ethyl acetate. The combined organic phases were washed with water and brine solution. The organic layer was dried over sodium sulfate and the solvent was removed under reduced pressure. The product was obtained as a beige solid with a yield of 2.26 g (9.49 mmol, 86 %).

^{1}H-NMR (400 MHz, DMSO-d_6): δ (ppm) = 10.67 (s, 1H, R-CHO), 8.35 (s, 1H, arom.), 7.66 (d, *J* = 8.2 Hz, 1H, arom.), 7.52 (d, *J* = 7.7 Hz, 1H, arom.), 7.24 (t, *J* = 8.0 Hz, 1H, arom.), 3.91 (s, 3H, N-CH_3).

HR-MS (ESI): m/z (calculated for $C_{10}H_9{}^{79}BrNO^+$): 237.9862 $[M+H]^+$; found: 237.9859 $[M+H]^+$; m/z (calculated for $C_{10}H_9{}^{81}BrNO^+$): 239.9842$[M+H]^+$; found: 239.9835 $[M+H]^+$.

The spectroscopic data is in agreement with literature.[12]

Compound 36

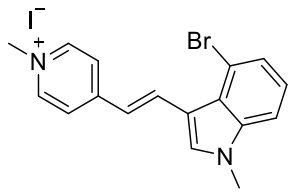

$C_{17}H_{16}BrN_2^+I^-$
455.14 g/mol

In a schlenk flask under argon atmosphere 0.500 g 1,4-dimethylpyridiniumiodid (**10**) (2.13 mmol, 1.00 eq.) was dissolved in 30 mL ethanol and stirred for 10 minutes. 0.760 g of the indole **35** (3.19 mmol, 1.50 eq.) and 1.05 mL piperidine (10.6 mmol, 5.00 eq.) were added to the reaction mixture. The reaction was stirred overnight at 85 °C oil bath temperature. After letting the reaction mixture cool down to room temperature, diethyl ether was added until no further precipitate was formed. The precipitate was filtered off and washed three times with diethyl ether and dried under reduced pressure. The product was obtained as an orange solid with a yield of 0.696 g (1.53 mmol, 72 %).

^{1}H-NMR (400 MHz, DMSO-d_6): δ (ppm) = 8.75 (d, *J* = 16.1 Hz, 1H, R-CH=CH-R), 8.68 (d, *J* = 6.8 Hz, 2H, arom.), 8.34 (s, 1H, arom.), 8.00 (d, *J* = 6.9 Hz, 2H, arom.), 7.62 (d, *J* = 7.8 Hz, 1H, arom.), 7.43 (d, *J* = 7.5 Hz, 1H, arom.), 7.22-7.18 (m, 1H, arom.), 7.17 (d, *J* = 3.4 Hz, 1H, R-CH=CH-R), 4.21 (s, 3H, R-CH_3), 3.91 (s, 3H, R-CH_3).

HR-MS (ESI): m/z (calculated for $C_{17}H_{16}{}^{79}BrN_2^+$): 327.0491 $[M]^+$; found: 327.0487 $[M]^+$; m/z (calculated for $C_{17}H_{16}{}^{81}BrN_2^+$): 329.0471 $[M]^+$; found: 329.0463 $[M]^+$.

The spectroscopic data is in agreement with literature.[12]

Compound 12

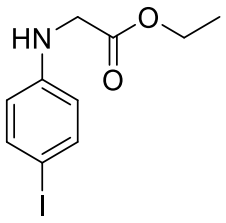

$C_{10}H_{12}INO_2$
305.12 g/mol

In a heated Schlenk flask under argon 10.0 g 4-iodoaniline (45.6 mmol, 1.00 eq.) was dissolved in 80 mL DMF. 7.57 g Potassium carbonate (54.7 mmol, 1.20 eq.) was added. 6.05 mL ethyl bromoacetate (9.15 g, 54.7 mmol, 1.20 eq.) was then added in portions for 10 minutes. The reaction mixture was allowed to stir overnight for 16 hours at room temperature. 9.92 mL diethylamine (7.01 g, 95.8 mmol, 2.10 eq.) was added in portions for 5 min and the reaction solution was allowed to stir for another hour. The solid was filtered off. The solvent of the filtrate was removed. The residue was purified by automated column chromatography (cyclohexane/ethylacetate 0-50 %). The product was obtained as a colorless solid with a yield of 11.0 g (36.0 mmol, 79 %).

^{1}H-NMR (400 MHz, DMSO-d_6): δ (ppm) = 7.34 (d, *J* = 8.8 Hz, 2H, arom.), 6.41 (d, *J* = 8.8 Hz, 2H, arom.), 6.22 (t, *J* = 6.4 Hz, 1H, R-NH-R), 4.10 (q, *J* = 7.1 Hz, 2H, R-CH_2), 3.87 (d, *J* = 6.4 Hz, 2H, R-CH_2), 1.19 (t, *J* = 7.1, 3H, R-CH_3).

^{13}C-NMR (126 MHz, DMSO-d_6): δ (ppm) = 171.0, 147.9, 137.1 (2C), 114.8 (2C), 76.9, 60.3, 44.4, 14.1.

HR-MS (ESI): m/z (calculated for $C_{10}H_{13}INO_2^+$): 305.9986 $[M+H]^+$; found: 305.9982 $[M+H]^+$.

The spectroscopic data is in agreement with literature.[13]

Compound 13

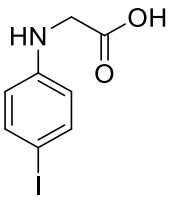

$C_8H_8INO_2$
277.06 g/mol

In a Schlenk flask under argon, 15.0 g **12** (49.1 mmol, 1.00 eq.) was placed and dissolved in 28 mL THF. The solution was cooled to 0 °C with an ice bath. Meanwhile, 2.35 g lithium hydroxide (98.3 mmol, 2.00 eq.) was dissolved in 35 mL water and then added to the reaction solution. The solution was allowed to stir at 0 °C for 30 minutes and then at room temperature for one hour. The THF was evaporated off. The remaining basic aqueous solution was washed once with ethyl acetate (discard the organic phase). A pH of 1 was then adjusted with HCl and the aqueous phase was washed three times with ethyl acetate. The combined organic phases were washed with Brine solution and then dried over sodium sulfate. The solvent was removed. The product was obtained as a light brown solid with a yield of 12.0 g (43.3 mmol, 88 %).

^{1}H-NMR (400 MHz, MeOD-*d_4*): δ (ppm) = 7.37 (d, *J* = 8.9 Hz, 2H, arom.), 6.43 (d, *J* = 8.9 Hz, 2H, arom.), 3.85 (s, 2H, R-CH_2).

^{13}C-NMR (101 MHz, MeOD-*d_4*): δ (ppm) = 174.7, 149.2, 138.7 (2C), 116.1 (2C), 78.3, 45.8.

HR-MS (ESI): m/z (calculated for $C_8H_9INO_2^+$): 277.9672 $[M+H]^+$; found: 277.9668 $[M+H]^+$.

The spectroscopic data is in agreement with literature.[13]

Compound 14

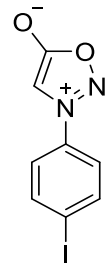

$C_8H_5IN_2O_2$
288.04 g/mol

In a heated Schlenk flask under argon, 5.61 g **13** (20.2 mmol, 1.00 eq.) was introduced and dissolved in 40 mL dry THF. Slowly 2.64 mL tert-butyl nitrite (2.30 g, 22.2 mmol, 1.10 eq.) was added to the reaction solution over 10 minutes. The reaction mixture was allowed to stir for 1 hour at room temperature. 3.10 mL Trifluoroacetic anhydride (4.68 g, 22.2 mmol, 1.10 eq.) was then added over 10 minutes and the reaction solution was allowed to stir at room temperature for another hour. Ethyl acetate was added and the solution is quenched with saturated sodium bicarbonate solution. The aqueous phase was extracted three times with ethyl acetate. The combined organic phases were dried over sodium sulfate and the solvent was removed. The crude product was purified by automated column chromatography (cyclohexane/ethyl acetate 10-70 %). The product was obtained as a brown solid with a yield of 4.90 g (17.0 mmol, 84 %).

^{1}H-NMR (400 MHz, DMSO-d_6): δ (ppm) = 8.08 (d, J = 8.8 Hz, 2H, arom.), 7.79 (s, 1H, sydnone core), 7.73 (d, J = 8.8 Hz, 2H, arom.).

HR-MS (ESI): m/z (calculated for $C_8H_6IN_2O_2^+$): 288.9468 $[M+H]^+$; found: 288.9464 $[M+H]^+$.

The spectroscopic data is in agreement with literature.[13]

Compound 5

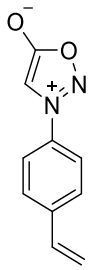

$C_{10}H_8N_2O_2$
188.19 g/mol

In a heated Schlenk flask under argon, 1.00 g **14** (3.47 mmol, 1.00 eq.) was introduced and dissolved in 70 mL DMF. To the reaction solution, 0.441 g lithium chloride (10.4 mmol, 3.00 eq.), 0.121 g $Pd(PPh_3)_2Cl_2$ (0.173 mmol, 0.05 eq.) and 0.866 g tetravinyltin (3.82 mmol, 1.10 eq.) were added. The reaction mixture was allowed to stir overnight at room temperature. The solvent was then removed. The residue was dissolved in DCM and 1M NaOH solution and allowed to stir for one hour. The aqueous phase was extracted with DCM three times. The combined organic phases were dried over sodium sulfate. The solvent was removed. The crude product was purified by automated column chromatography (cyclohexane/ ethyl acetate 15 – 80 %). The product was obtained as a light brown solid with a yield of 0.596 g (3.16 mmol, 91 %).

^{1}H-NMR (400 MHz, DMSO-d_6): δ (ppm) = 7.92 (d, *J* = 8.7 Hz, 2H, arom.), 7.79 (d, *J* = 8.6 Hz, 2H, arom.), 7.79 (s, 1H, sydnone core), 6.86 (dd, *J* = 17.7, 11.0 Hz, 1H, R-CH=CH_2), 6.06 (d, *J* = 17.7 Hz, 1H, R-CH=CH_2), 5.47 (d, *J* = 11.0 Hz, 1H, R-CH=CH_2).

HR-MS (ESI): m/z (calculated for $C_{10}H_9N_2O_2^+$): 189.0659 $[M+H]^+$; found: 189.0656 $[M+H]^+$.

The spectroscopic data is in agreement with literature.[13]

Compound 3

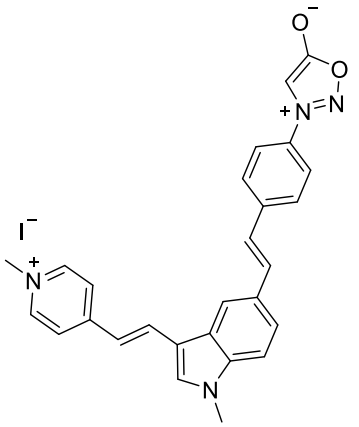

$C_{27}H_{23}N_4O_2^+I^-$
562.41 g/mol

In a heated 10 mL crimp vial under argon, 0.100 g **4** (0.220 mmol, 1.00 eq.), 0.010 g $Pd_2(dba)_3$ (0.010 mmol, 0.05 eq.), 0.031 g Qphos (0.040 mmol, 0.20 eq.) and 0.083 g **5** (0.440 mmol, 2.00 eq.) dried under high vacuum. The solids were then dissolved with 2.00 mL dry DMF and 0.15 mL triethylamine (0.111 g, 1.10 mmol, 5.00 eq.) was added. The reaction was stirred for 18 hours in a metal heating block at 80 °C. After the solution had cooled to room temperature diethyl ether was added until no further precipitate was formed. The suspension was transferred into reaction tubes. The solution was centrifuged and the supernatant was pipetted off and discarded. Subsequently, diethyl ether was added and the suspension was vortexed and centrifuged again in the next step and the supernatant discarded. This was carried out two more times. The residue was dried in high vacuum. The product was obtained as a brown solid with a yield of 0.062 g (0.110 mmol, 49 %).

^{1}H-NMR (400 MHz, DMSO-d_6): δ (ppm) = 8.72 (d, *J* = 6.4 Hz, 2H, arom.), 8.42 (s, 1H, arom.), 8.24 (d, *J* = 16.2 Hz, 1H, R-CH=CH-R), 8.17 (d, *J* = 6.5 Hz, 2H, arom.), 8.02 – 7.96 (m, 3H, arom., R-CH=CH-R), 7.93 (d, *J* = 8.6 Hz, 2H, arom.), 7.82 (s, 1H, arom.), 7.73 – 7.61 (m, 3H, arom.), 7.48 (d, *J* = 16.5 Hz, 1H, R-CH=CH-R), 7.35 (d, *J* = 16.2 Hz, 1H, R-CH=CH-R), 4.19 (s, 3H, R-CH_3), 3.91 (s, 3H, R-CH_3).

^{13}C-NMR (126 MHz, DMSO-d_6): δ (ppm) = 168.5, 154.0, 144.3, 141.7, 138.1, 136.1, 135.3, 132.8, 130.2, 127.4, 125.8, 124.8, 121.8, 119.8, 117.2, 113.0, 111.5, 94.5, 46.3, 33.3.

HR-MS (ESI): m/z (calculated for $C_{27}H_{23}N_4O_2^+$): 435.1816 $[M]^+$; found: 435.1811 $[M]^+$.

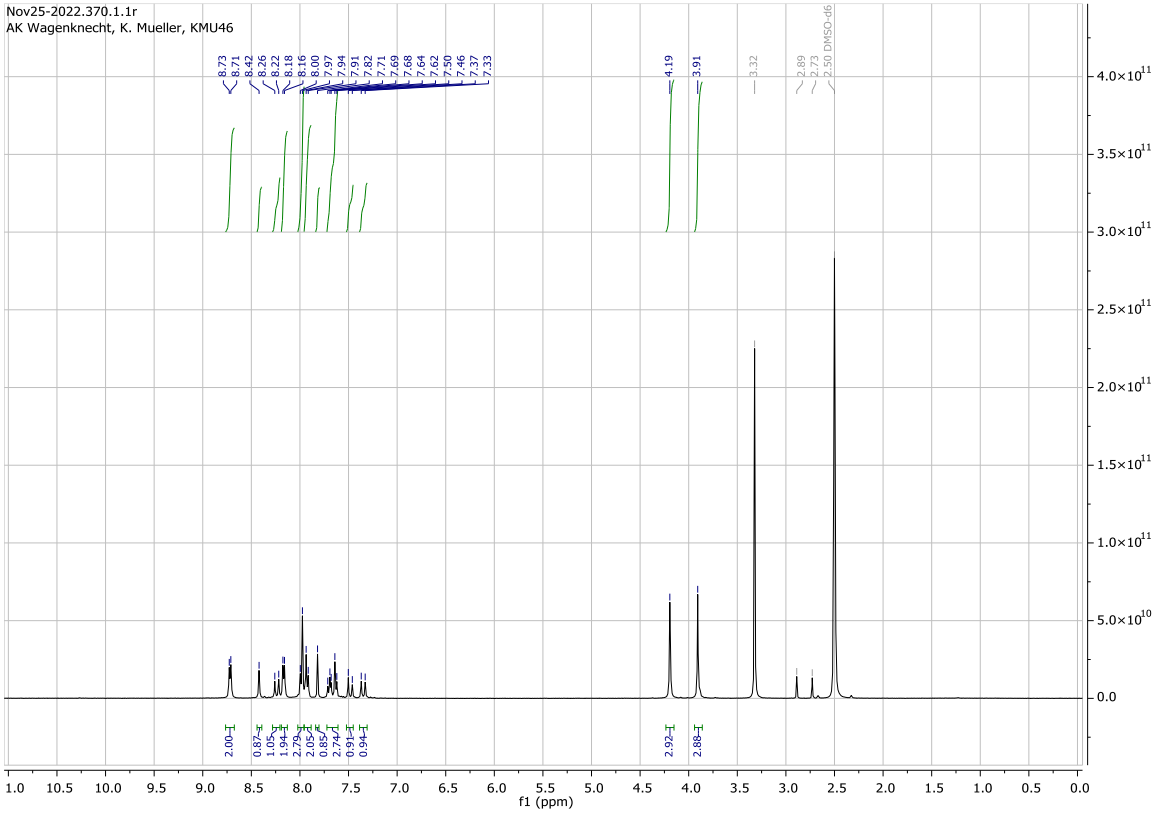

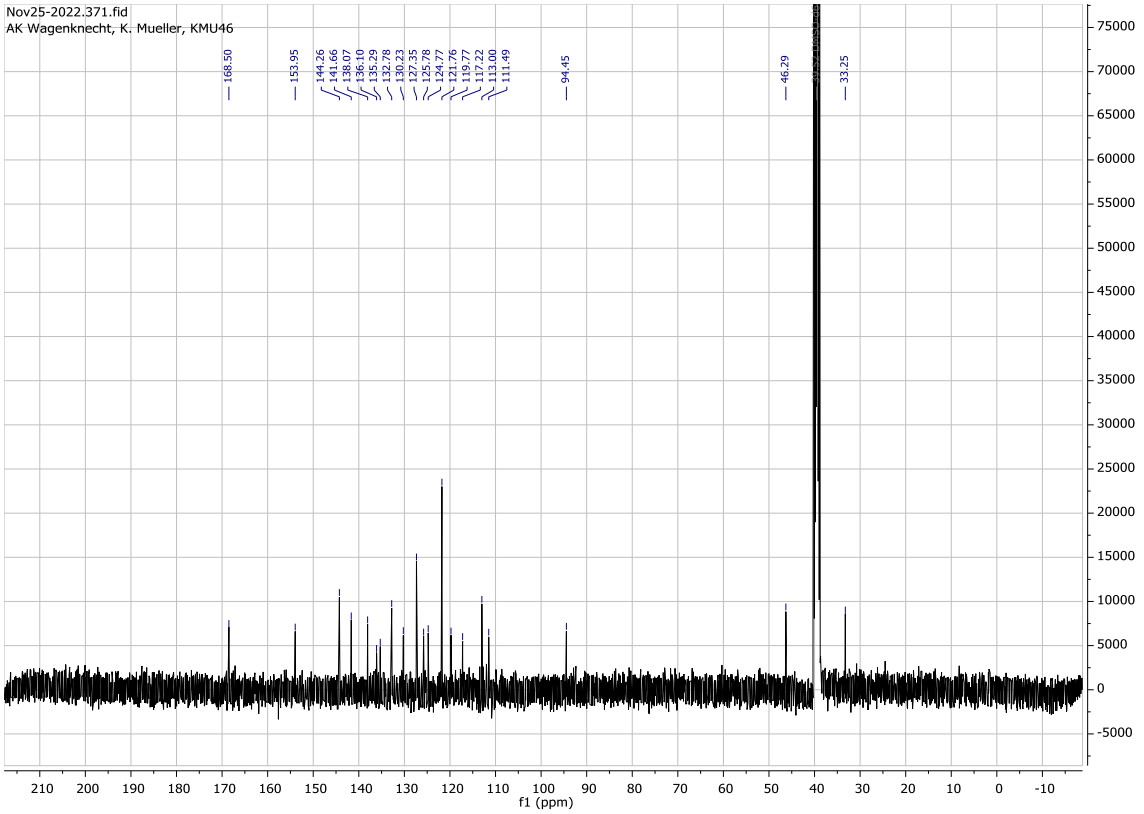
Nov25-2022.371.fid
AK Wagenknecht, K. Mueller, KMU46
168.50
153.95
144.26
141.66
138.07
136.10
135.29
132.78
130.23
127.35
125.78
124.77
121.76
119.77
117.22
113.00
111.49
94.45
46.29
33.25
f1 (ppm)

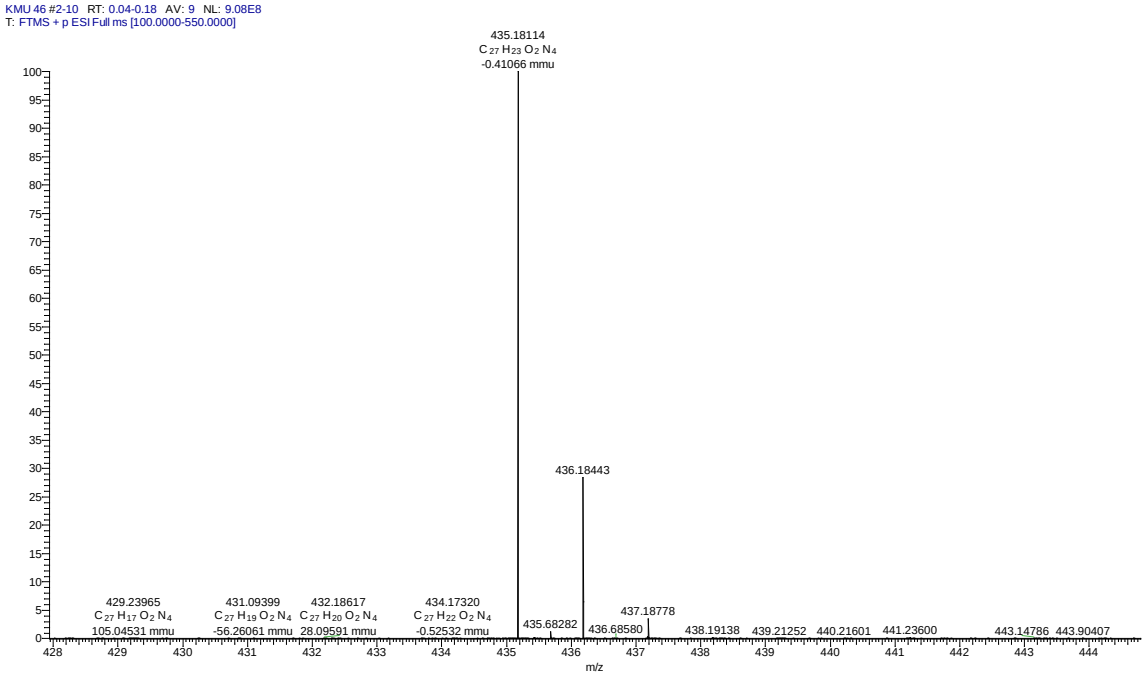
KMU 46 #2-10 RT: 0.04-0.18 AV: 9 NL: 9.08E8
T: FTMS + p ESI Full ms [100.0000-550.0000]
435.18114
C27 H23 O2 N4
-0.41066 mmu
436.18443
429.23965
C27 H17 O2 N4
105.04531 mmu
431.09399
C27 H19 O2 N4
-56.26061 mmu
432.18617
C27 H20 O2 N4
28.09591 mmu
434.17320
C27 H22 O2 N4
-0.52532 mmu
435.68282
436.68580
437.18778
438.19138
439.21252
440.21601
441.23600
443.14786
443.90407
m/z

Compound 33

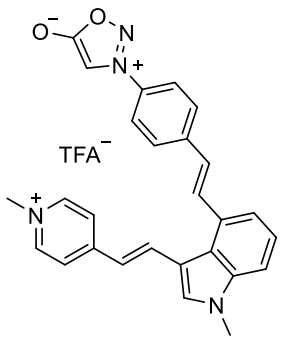

$C_{27}H_{23}N_4O_2^+C_2F_3O_2^-$
548.51 g/mol

In a heated 10 mL crimp vial under argon, 0.100 g **36** (0.220 mmol, 1.00 eq.), 0.010 g $Pd_2(dba)_3$ (0.010 mmol, 0.05 eq.), 0.031 g Qphos (0.040 mmol, 0.20 eq.) and 0.083 g **5** (0.440 mmol, 2.00 eq.) dried under high vacuum. The solids were then dissolved with 2.00 mL dry DMF and 0.15 mL triethylamine (0.111 g, 1.10 mmol, 5.00 eq.) was added. The reaction was stirred for 18 hours in a metal heating block at 80 °C. After the solution had cooled to room temperature diethyl ether was added until no further precipitate was formed. The suspension was transferred into reaction tubes. The solution was centrifuged and the supernatant was pipetted off and discarded. Subsequently, diethyl ether was added and the suspension was vortexed and centrifuged again in the next step and the supernatant discarded. This was carried out two more times. The residue was dried in high vacuum and purified via reversed-phase column chromatography. The product was obtained as a brown solid with a yield of 0.056 g (0.099 mmol, 45 %).

^{1}H-NMR (500 MHz, DMSO-d_6): δ (ppm) = 8.68 (d, *J* = 6.8 Hz, 2H, arom.), 8.41 (d, *J* = 15.8 Hz, 1H, R-CH=CH-R), 8.26 (d, *J* = 16.1 Hz, 1H, R-CH=CH-R), 8.21 (s, 1H, arom.), 8.04 (d, *J* = 8.7 Hz, 2H, arom.), 7.98 (t, *J* = 7.9 Hz, 4H, arom.), 7.82 (s, 1H, arom.), 7.57 (d, *J* = 8.1 Hz, 1H, arom.), 7.51 (d, *J* = 7.4 Hz, 1H, arom.), 7.33 (t, *J* = 7.8 Hz, 1H, arom.), 7.28 (d, *J* = 16.1 Hz, 1H, R-CH=CH-R), 7.14 – 7.09 (m, 1H, R-CH=CH-R), 4.17 (s, 3H, R-CH_3), 3.91 (s, 3H, R-CH_3).

^{13}C-NMR (126 MHz, DMSO-d_6): δ (ppm) = 168.6, 153.3, 144.5, 141.3, 138.0, 136.0, 133.2, 132.6, 130.8, 130.4, 129.1, 128.0, 123.9, 122.8, 121.8, 119.8, 118.6, 113.2, 111.2, 94.6, 46.5, 33.4.

HR-MS (ESI): m/z (calculated for $C_{27}H_{23}N_4O_2^+$): 435.1816 $[M]^+$; found: 435.1811 $[M]^+$

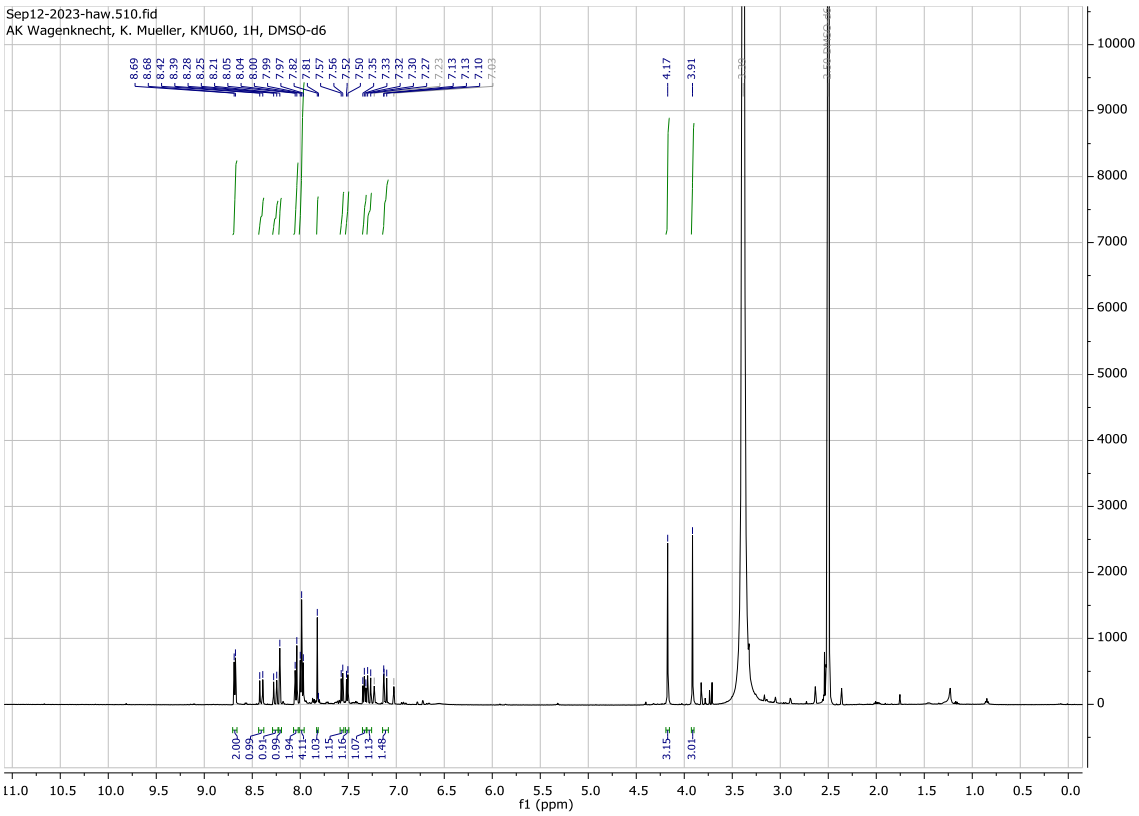

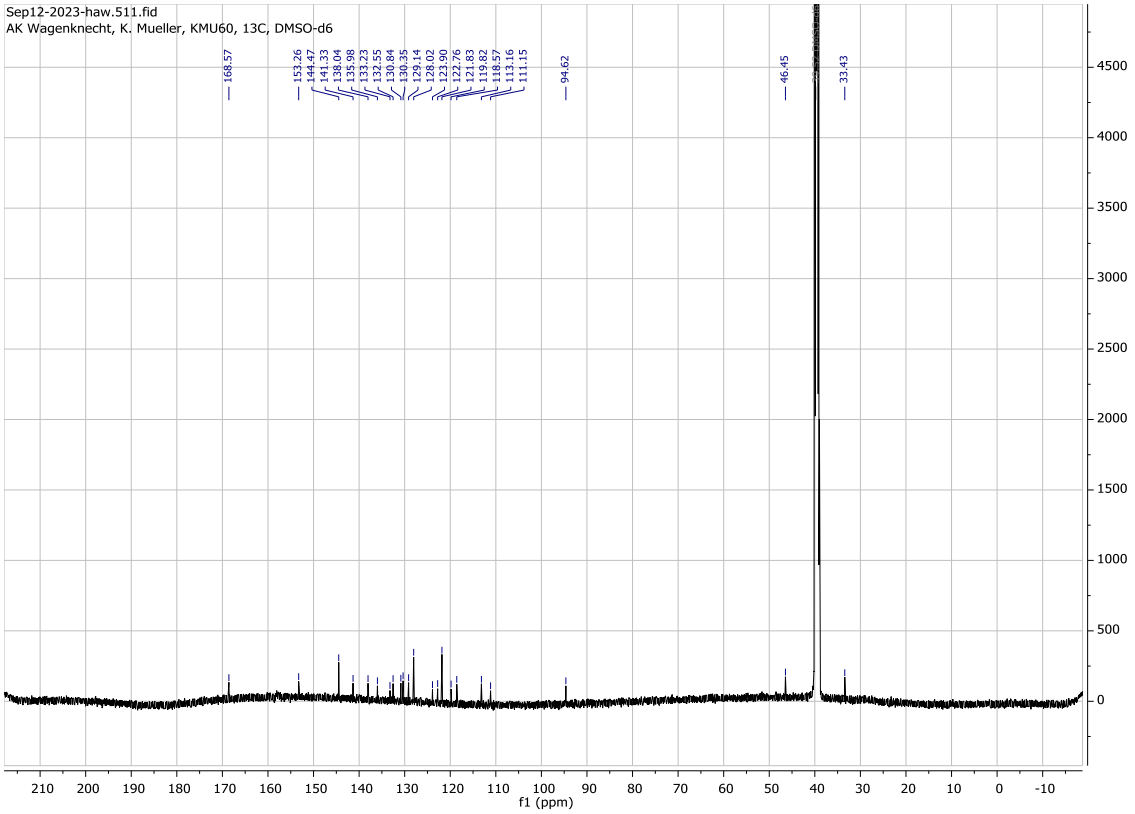
Sep12-2023-haw.511.fid
AK Wagenknecht, K. Mueller, KMU60, 13C, DMSO-d6
168.57
153.26
144.47
141.33
138.04
135.98
133.23
132.55
130.84
130.35
129.14
128.02
123.90
122.76
121.83
119.82
118.57
113.16
111.15
94.62
46.45
33.43
f1 (ppm)

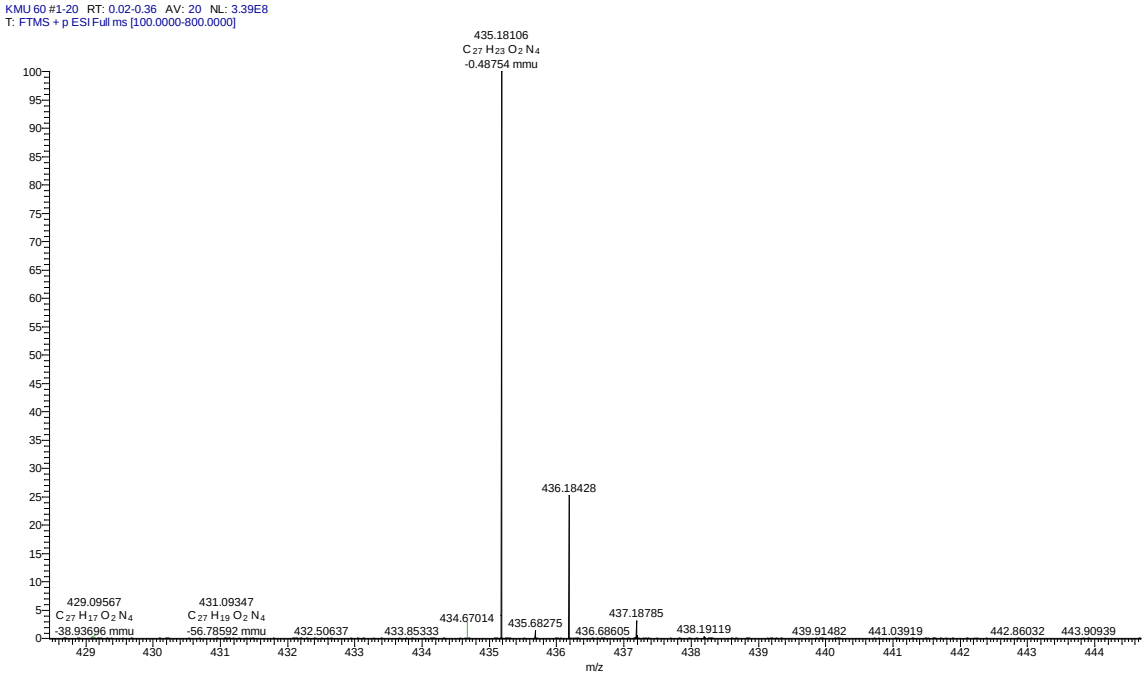
KMU 60 #1-20 RT: 0.02-0.36 AV: 20 NL: 3.39E8
T: FTMS + p ESI Full ms [100.0000-800.0000]
435.18106
C27 H23 O2 N4
-0.48754 mmu
436.18428
429.09567
C27 H17 O2 N4
-38.93696 mmu
431.09347
C27 H19 O2 N4
-56.78592 mmu
432.50637
433.85333
434.67014
435.68275
436.68605
437.18785
438.19119
439.91482
441.03919
442.86032
443.90939
m/z

Compound 39

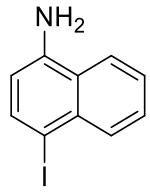

$C_{10}H_8IN$
269.09 g/mol

In a flask under air 5.23 g 1-Naphtylamine (36.5 mmol, 1.00 eq.) was solved in 314 mL DMSO and 8.22 g N-iodosuccinimide (36.5 mmol, 1.00 eq.) was added. The reaction mixture was stirred for 72 hours at room temperature. 5 g batch: divided reaction mixture into two 500 mL flask. The preparation of $NaHCO_3$ solution: amount of $NaHCO_3$ (4 eq.) solved in 600 mL water. (The reaction mixture gets warm when $NaHCO_3$ solution is added. Wait till the mixture is cooled down (product starts to participate).) The reaction mixture was extracted four times with 200 mL ethyl acetate. The combined organic phases were washed with a little amount of brine solution (200 mL - 300 mL) and dried over sodium sulfate. The solvent was removed under reduced pressure and the residue was purified via column chromatography (cyclohexane/ethyl acetate 0-20 %). The product was obtained as a violet-blue solid with a yield of 7.00 g (26.0 mmol, 71 %).

^{1}H-NMR (400 MHz, DMSO-d_6): δ (ppm) = 8.07 (d, *J* = 8.2 Hz, 1H, arom.), 7.83 (d, *J* = 8.0 Hz, 1H, arom.), 7.73 (d, *J* = 8.0 Hz, 1H, arom.), 7.54 (ddd, *J* = 8.3, 6.9, 1.0 Hz, 2H, arom.), 7.43 (ddd, *J* = 8.1, 6.9, 1.1 Hz, 2H, arom.), 6.52 (d, *J* = 8.1 Hz, 1H, arom.), 6.00 (s, 2H, R-NH_2).

The spectroscopic data is in agreement with literature.[169]

Compound 40

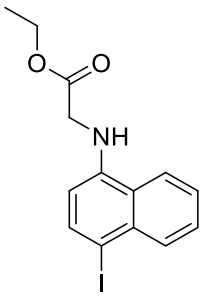

$C_{14}H_{14}INO_2$
355.18 g/mol

In a heated Schlenk flask under argon 6.50 g **39** (24.2 mmol, 1.00 eq.) was dissolved in 45 mL DMF. 4.01 g Potassium carbonate (28.9 mmol, 1.20 eq.) was added. 3.21 mL ethyl bromoacetate (4.84 g, 28.9 mmol, 1.20 eq.) was then added in portions for 10 minutes. The reaction mixture was allowed to stir overnight at room temperature. 5.25 mL diethylamine (3.71 g, 50.7 mmol, 2.10 eq.) was added in portions for 5 minutes and the reaction solution was allowed to stir for another hour. The solid was filtered off. The solvent of the filtrate was removed. The residue was purified by automated column chromatography (cyclohexane/ethyl acetate 0-40 %). The product was obtained as a red brown solid with a yield of 3.20 g (9.01 mmol, 37 %).

^{1}H-NMR (400 MHz, DMSO-d_6): δ (ppm) = 8.15 (d, *J* = 8.3 Hz, 1H, arom.), 7.89 (dd, *J* = 8.0, 1.3 Hz, 1H, arom.), 7.82 (d, *J* = 8.2 Hz, 1H, arom.), 7.60 (t, *J* = 7.2, 1H, arom.), 7.52 (t, *J* = 7.1 Hz, 1H, arom.), 6.94 (t, 1H, R-NH-R), 6.20 (d, *J* = 8.2 Hz, 1H, arom.), 4.13 (q, *J* = 7.1 Hz, 2H, R-C**H$_2$**-CH_3), 4.08 (d, *J* = 6.2 Hz, 2H, R-NH-CH_2-R), 1.20 (t, *J* = 7.1 Hz, 3H, R-CH_2-CH_3).

^{13}C-NMR (126 MHz, DMSO-d_6): δ (ppm) = 170.8, 144.6, 137.6, 133.7, 131.6, 127.8, 125.2, 124.1, 122.2, 105.3, 82.4, 60.4, 44.8, 14.1.

HR-MS (ESI): m/z (calculated for $C_{14}H_{15}INO_2^+$): 356.0142 $[M+H]^+$; found: 356.0140 $[M+H]^+$.

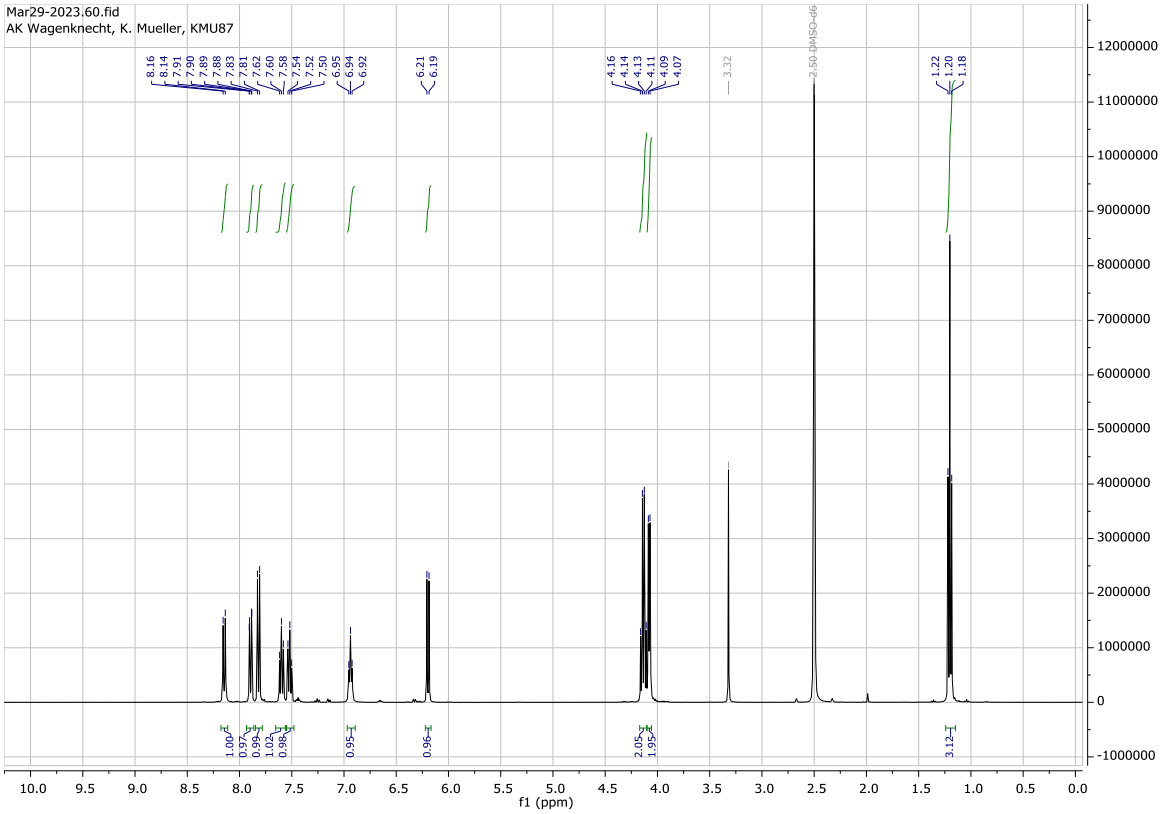
Mar29-2023.60.fid
AK Wagenknecht, K. Mueller, KMU87
8.16
8.14
7.91
7.90
7.89
7.88
7.83
7.81
7.62
7.60
7.58
7.54
7.52
7.50
6.95
6.94
6.92
6.21
6.19
4.16
4.14
4.13
4.11
4.09
4.07
3.32
2.50 DMSO-d6
1.22
1.20
1.18
1.00
0.97
0.99
1.02
0.98
0.95
0.96
2.05
1.95
3.12
f1 (ppm)

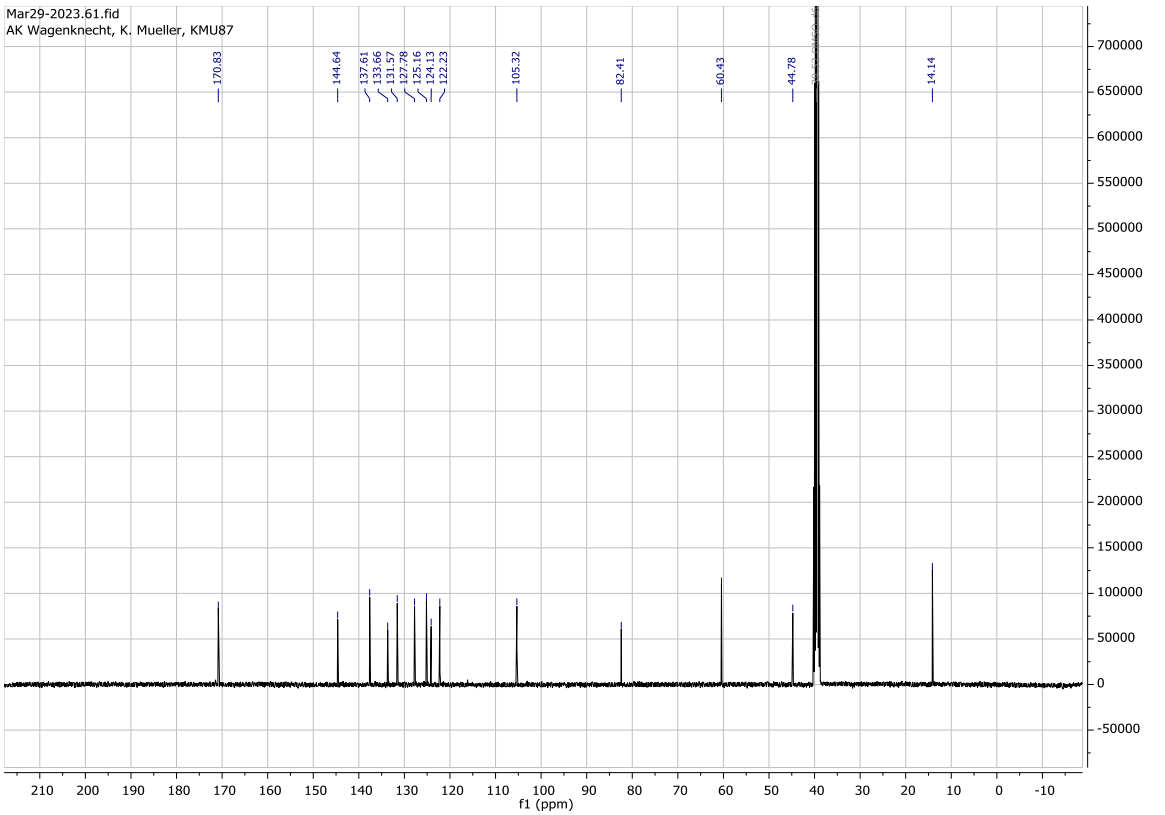
Mar29-2023.61.fid
AK Wagenknecht, K. Mueller, KMU87
170.83
144.64
137.61
133.66
131.57
127.78
125.16
124.13
122.23
105.32
82.41
60.43
44.78
39.50 DMSO-d6
14.14
f1 (ppm)

KMU87 #1-20 RT: 0.02-0.36 AV: 20 NL: 2.44E7
T: FTMS + p ESI Full ms [103.0000-500.0000]

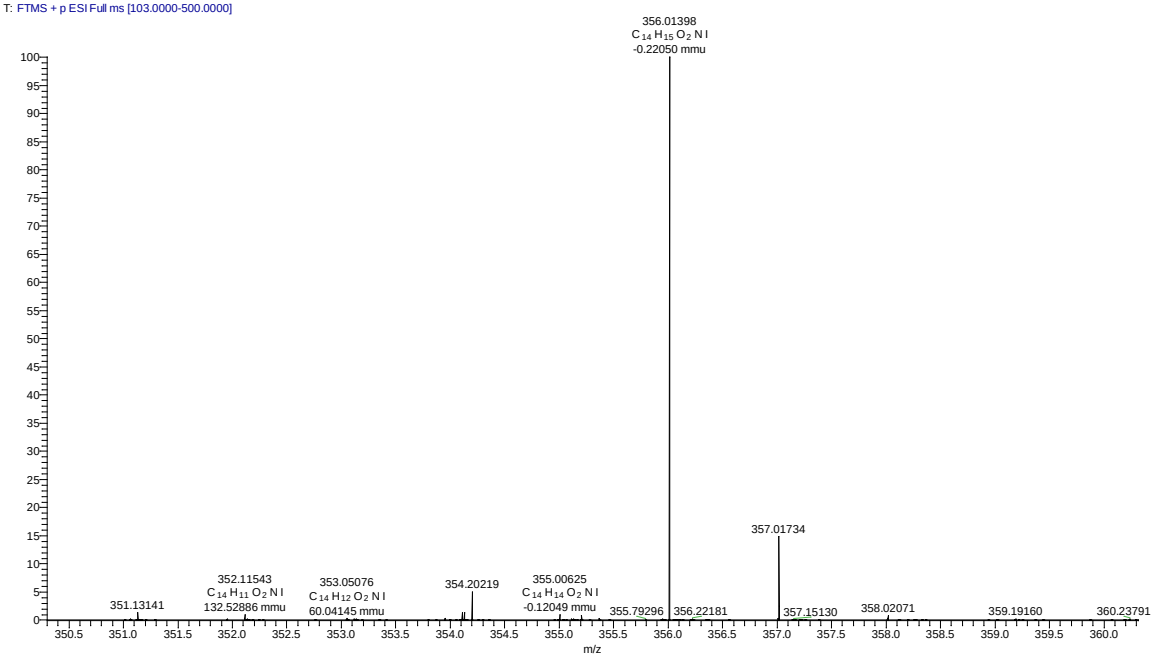

Compound 41

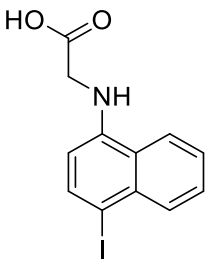

$C_{12}H_{10}INO_2$
327.12 g/mol

In a Schlenk flask under argon, 4.48 g **40** (12.6 mmol, 1.00 eq.) was placed and dissolved in 16 mL THF. The solution was cooled to 0 °C with an ice bath. Meanwhile, 0.604 g lithium hydroxide (25.2 mmol, 2.00 eq.) was dissolved in 16 mL water and then added to the reaction solution. The solution was allowed to stir at 0 °C for one hour and then at room temperature for one hour. The THF was evaporated off. A pH of 2 was then adjusted with HCl (2M) and the resulting precipitate was filtered off and washed with a small amount of water. The residue was dried under reduced pressure. The product was obtained as a light violet solid with a yield of 3.99 g (12.2 mmol, 97 %).

^{1}H-NMR (400 MHz, DMSO-d_6): δ (ppm) = 12.66 (s, 1H, R-COOH), 8.13 (d, *J* = 8.3 Hz, 1H, arom.), 7.89 (d, *J* = 8.3 Hz, 1H, arom.), 7.82 (d, *J* = 8.2 Hz, 1H, arom.), 7.59 (t, *J* = 7.3, 1H, arom.), 7.51 (t, *J* = 7.6 Hz, 1H, arom.), 6.83 (s, 1H, R-NH-R), 6.21 (d, *J* = 8.2 Hz, 1H, arom.), 3.98 (s, 2H, R-NH-CH_2-R).

^{13}C-NMR (126 MHz, DMSO-d_6): δ (ppm) = 172.2, 144.8, 137.7, 133.7, 131.5, 127.7, 125.1, 124.1, 122.2, 105.3, 82.1, 44.7.

HR-MS (ESI): m/z (calculated for $C_{12}H_{11}INO_2^+$): 327.9829 $[M+H]^+$; found: 327.9827 $[M+H]^+$.

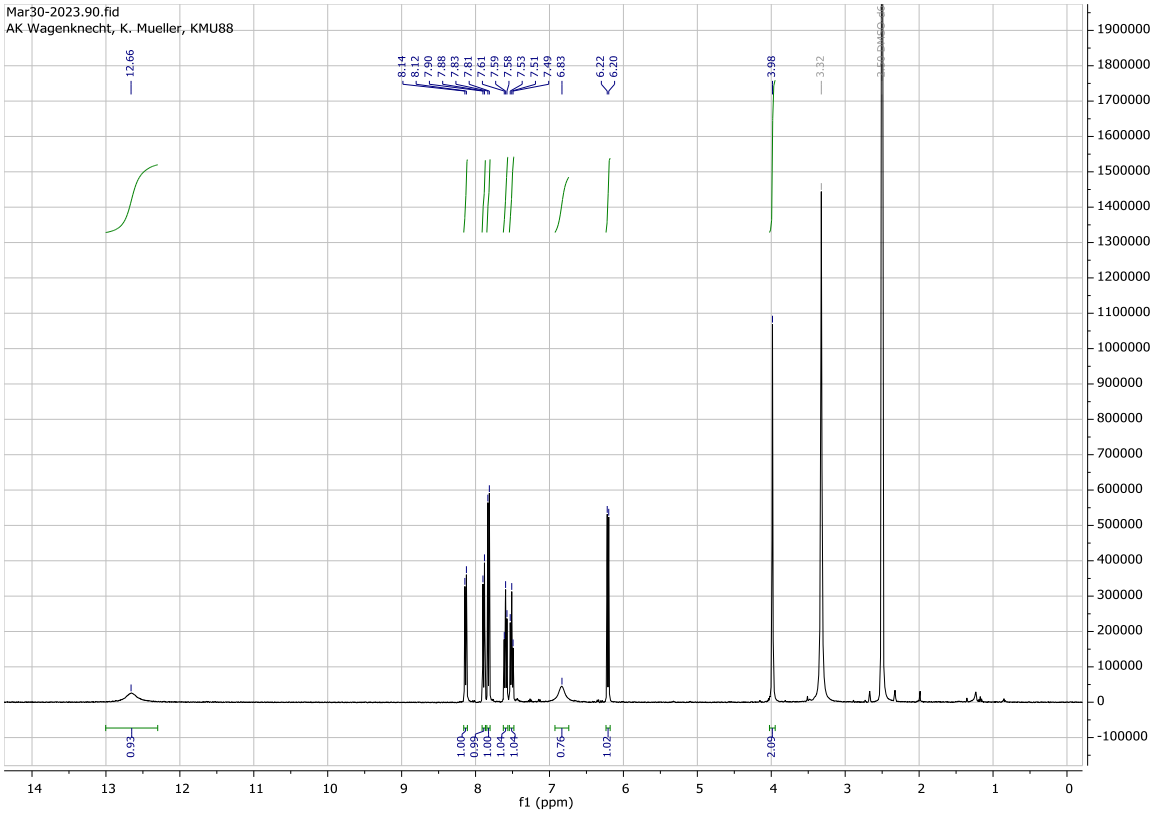
Mar30-2023.90.fid
AK Wagenknecht, K. Mueller, KMU88
12.66
8.14
8.12
7.90
7.88
7.83
7.81
7.61
7.59
7.58
7.53
7.51
7.49
6.83
6.22
6.20
3.98
3.32
2.50 DMSO
0.93
1.00
0.99
1.00
1.04
1.04
0.76
1.02
2.09
f1 (ppm)

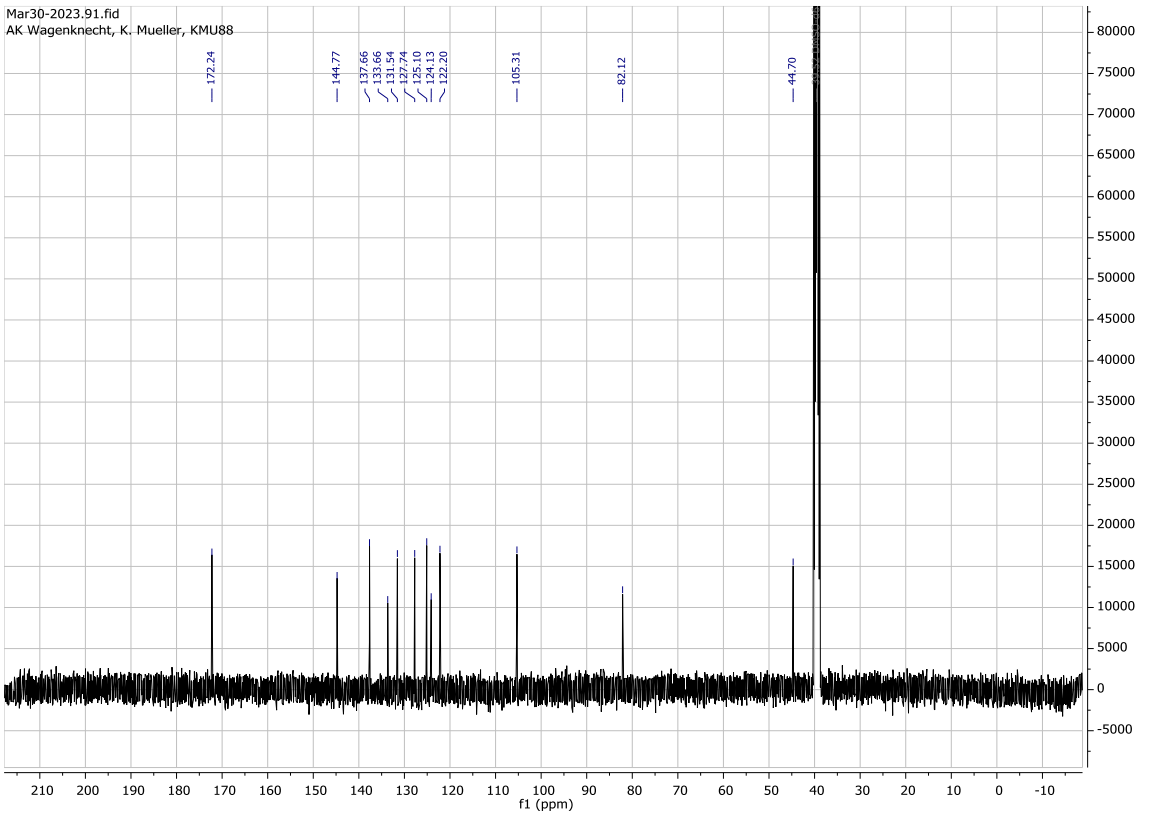
Mar30-2023.91.fid
AK Wagenknecht, K. Mueller, KMU88
172.24
144.77
137.66
133.66
131.54
127.74
125.10
124.13
122.20
105.31
82.12
44.70
39.52
f1 (ppm)

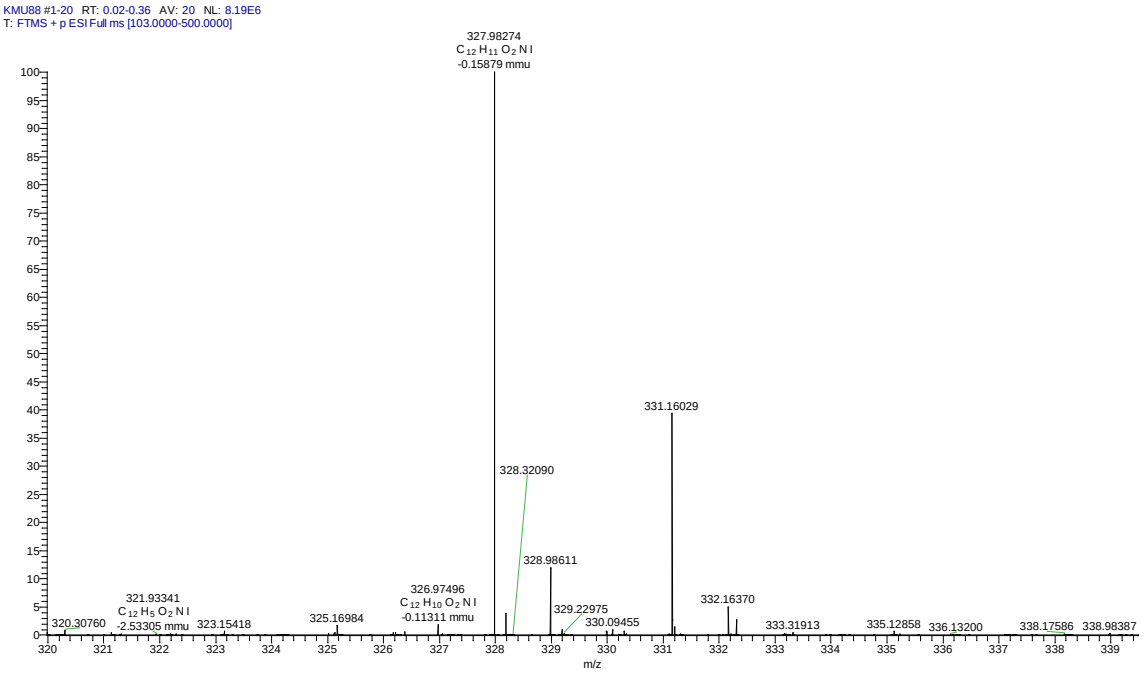
KMU88 #1-20 RT: 0.02-0.36 AV: 20 NL: 8.19E6
T: FTMS + p ESI Full ms [103.0000-500.0000]
327.98274
C12 H11 O2 N I
-0.15879 mmu
331.16029
328.32090
328.98611
321.93341
C12 H5 O2 N I
-2.53305 mmu
326.97496
C12 H10 O2 N I
-0.11311 mmu
329.22975
332.16370
320.30760
323.15418
325.16984
330.09455
333.31913
335.12858
336.13200
338.17586
338.98387
m/z

Compound 42

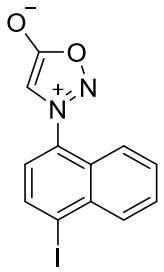

$C_{12}H_7IN_2O_2$
338.10 g/mol

In a heated Schlenk flask under argon, 3.99 g **41** (12.2 mmol, 1.00 eq.) was introduced and dissolved in 55 mL THF. Slowly 1.60 mL tert-butyl nitrite (1.38 g, 13.4 mmol, 1.10 eq.) was added to the reaction solution over 10 min. The reaction mixture was allowed to stir for 1 hour at room temperature. 1.87 mL Trifluoroacetic anhydride (2.82 g, 13.4 mmol, 1.10 eq.) was then added over 10 minutes and the reaction solution was allowed to stir at room temperature for another hour. Ethyl acetate was added and the solution was quenched with saturated sodium bicarbonate solution. The aqueous phase was extracted three times with EE. The combined organic phases were dried over sodium sulfate and the solvent was removed. The crude product was purified by automated column chromatography (DCM/MeOH 0-20 %). The product was obtained as a red-brown solid with a yield of 3.42 g (10.1 mmol, 83 %).

^{1}H-NMR (400 MHz, $CDCl_3$-*d_1*): δ (ppm) = 8.28 (d, *J* = 7.9 Hz, 2H, arom.), 7.81 – 7.66 (m, 3H, arom.), 7.42 (d, *J* = 7.8 Hz, 1H, arom.), 6.68 (s, 1H, sydnone core).

^{13}C-NMR (126 MHz, $CDCl_3$-*d_1*): δ (ppm) = 168.7, 136.5, 135.3, 133.5, 132.1, 130.1, 129.9, 127.3, 124.0, 105.5, 98.6, 77.4.

HR-MS (ESI): m/z (calculated for $C_{12}H_8IN_2O_2^+$): 338.9625 $[M+H]^+$; found: 338.9624 $[M+H]^+$.

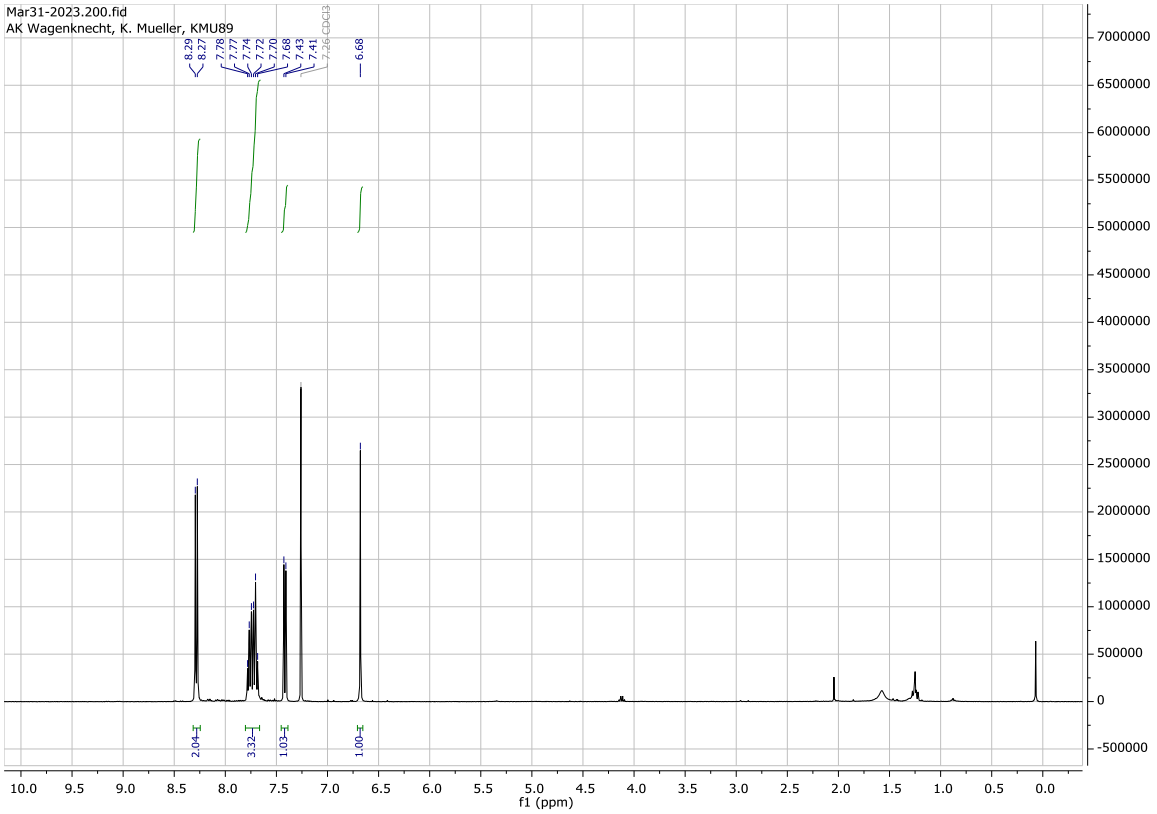
Mar31-2023.200.fid
AK Wagenknecht, K. Mueller, KMU89
8.29
8.27
7.78
7.77
7.74
7.72
7.70
7.68
7.43
7.41
7.26 CDCl3
6.68
2.04
3.32
1.03
1.00
f1 (ppm)

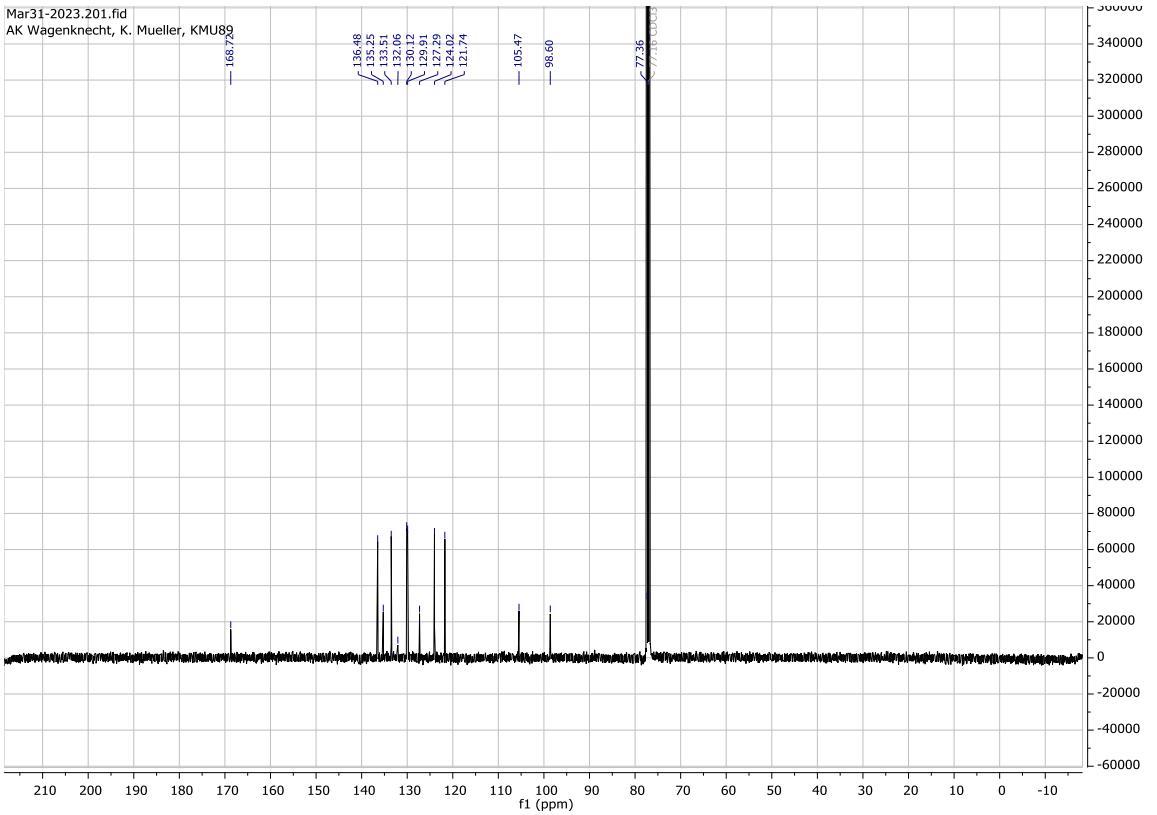
Mar31-2023.201.fid
AK Wagenknecht, K. Mueller, KMU89
168.729
136.48
135.25
133.51
132.06
130.12
129.91
127.29
124.02
121.74
105.47
98.60
77.36
77.16 CDCl3
f1 (ppm)

KMU89 #1-20 RT: 0.02-0.36 AV: 20 NL: 1.14E8
T: FTMS + p ESI Full ms [100.0000-500.0000]

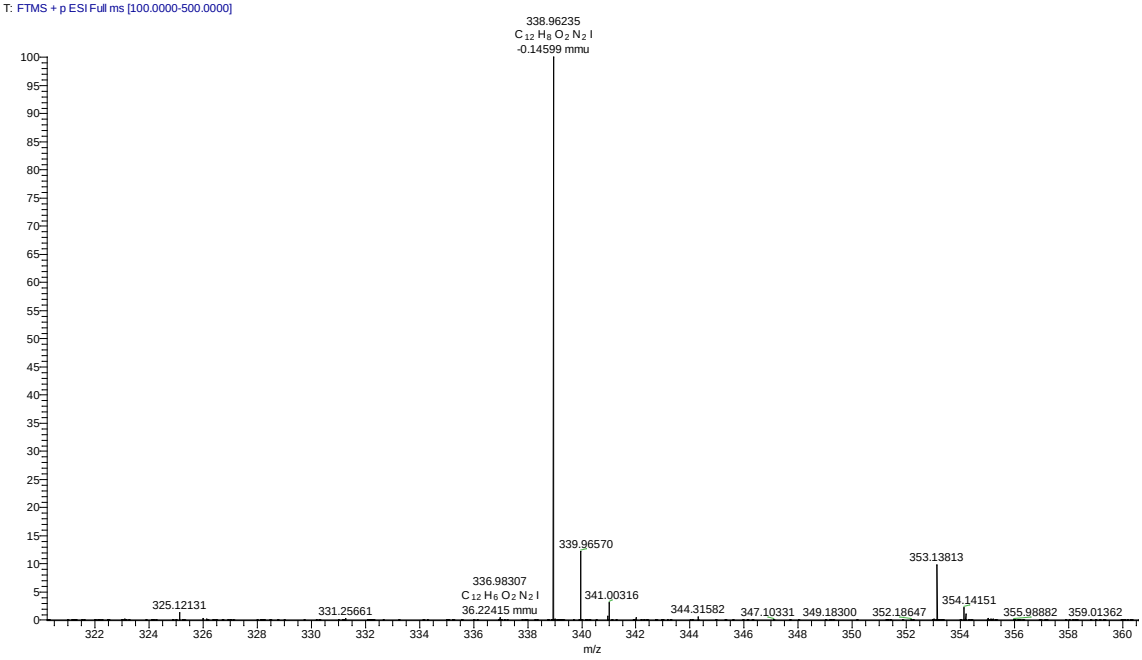

Compound 43

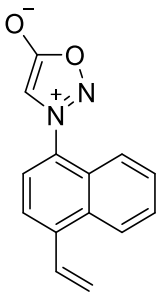

$C_{14}H_{10}N_2O_2$
238.25 g/mol

In a heated Schlenk flask under argon, 1.02 g **42** (3.00 mmol, 1.00 eq.) was introduced and dissolved in 70 mL DMF. To the reaction solution, 0.382 g LiCl (9.01 mmol, 3.00 eq.), 0.105 g $Pd(PPh_3)_2Cl_2$ (0.15 mmol, 0.05 eq.) and 0.60 mL tetravinyltin (0.750 g, 3.31 mmol, 1.10 eq.) were added. The reaction mixture was allowed to stir overnight at 65 °C. The solvent was then removed. The residue was dissolved in DCM and 1M NaOH solution and allowed to stir for 1 hour. The aqueous phase was extracted with DCM three times. The combined organic phases were dried over sodium sulfate. The solvent was removed. The crude product was purified by automated column chromatography (DCM/MeOH 0-10 %). The product was obtained as an orange solid with a yield of 0.715 g (3.00 mmol, 100 %).

^{1}H-NMR (400 MHz, $CDCl_3$-*d_1*): δ (ppm) = 8.29 – 8.21 (m, 1H, arom.), 7.78 – 7.73 (m, 1H, arom.), 7.72 (s, 1H, arom.), 7.69 (tt, *J* = 5.6, 3.0 Hz, 3H, arom.), 7.49 (dd, *J* = 17.3, 11.0 Hz, 1H, R-CH=CH_2), 7.47 (d, *J* = 11.0 Hz, 1H, arom.), 6.67 (s, 1H, sydnone core), 5.91 (dd, *J* = 17.3, 0.9 Hz, 1H, R-CH=CH_2), 5.69 (dd, *J* = 11.0, 0.9 Hz, 1H, R-CH=CH_2).

^{13}C-NMR (126 MHz, $CDCl_3$-*d_1*): δ (ppm) = 168.9, 141.0, 133.2, 131.8, 129.0, 128.1, 127.1, 125.0, 123.4, 122.7, 121.5, 120.7, 98.6, 77.4.

HR-MS (ESI): m/z (calculated for $C_{14}H_{11}N_2O_2^+$): 239.0815 $[M+H]^+$; found: 239.0825 $[M+H]^+$.

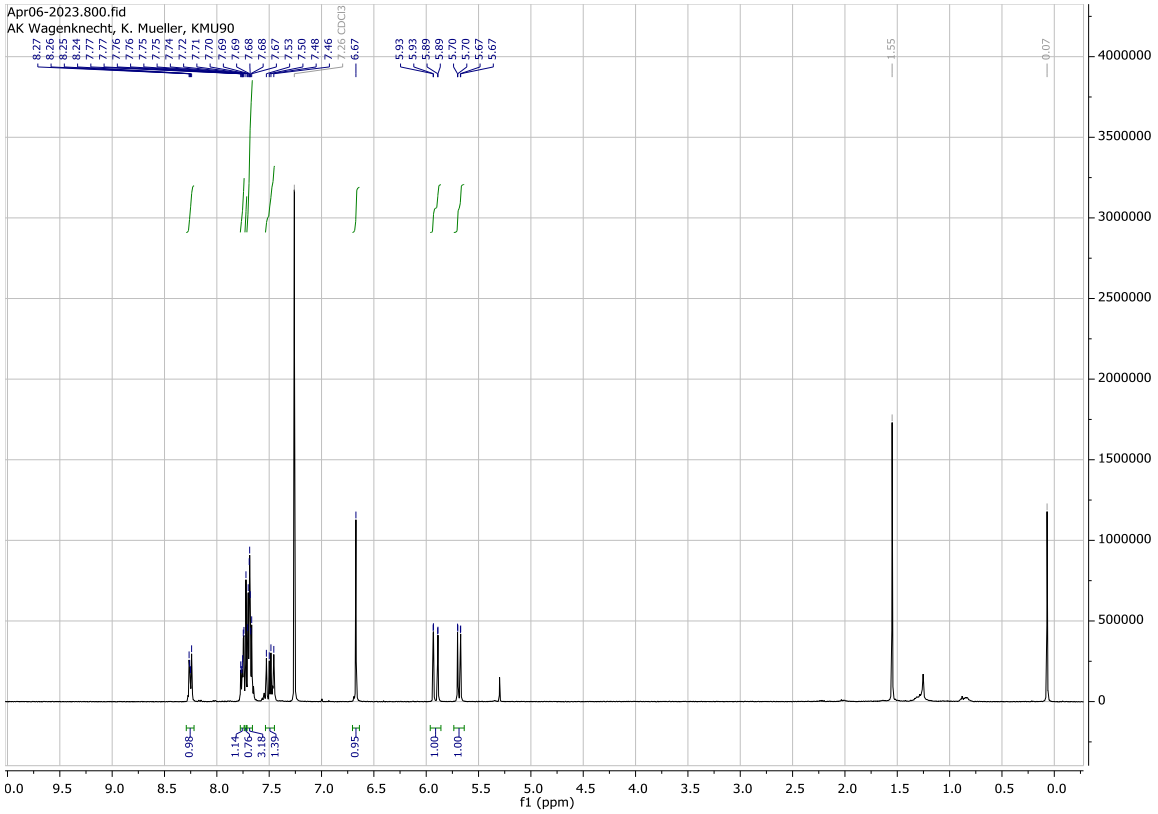
Apr06-2023.800.fid
AK Wagenknecht, K. Mueller, KMU90
f1 (ppm)

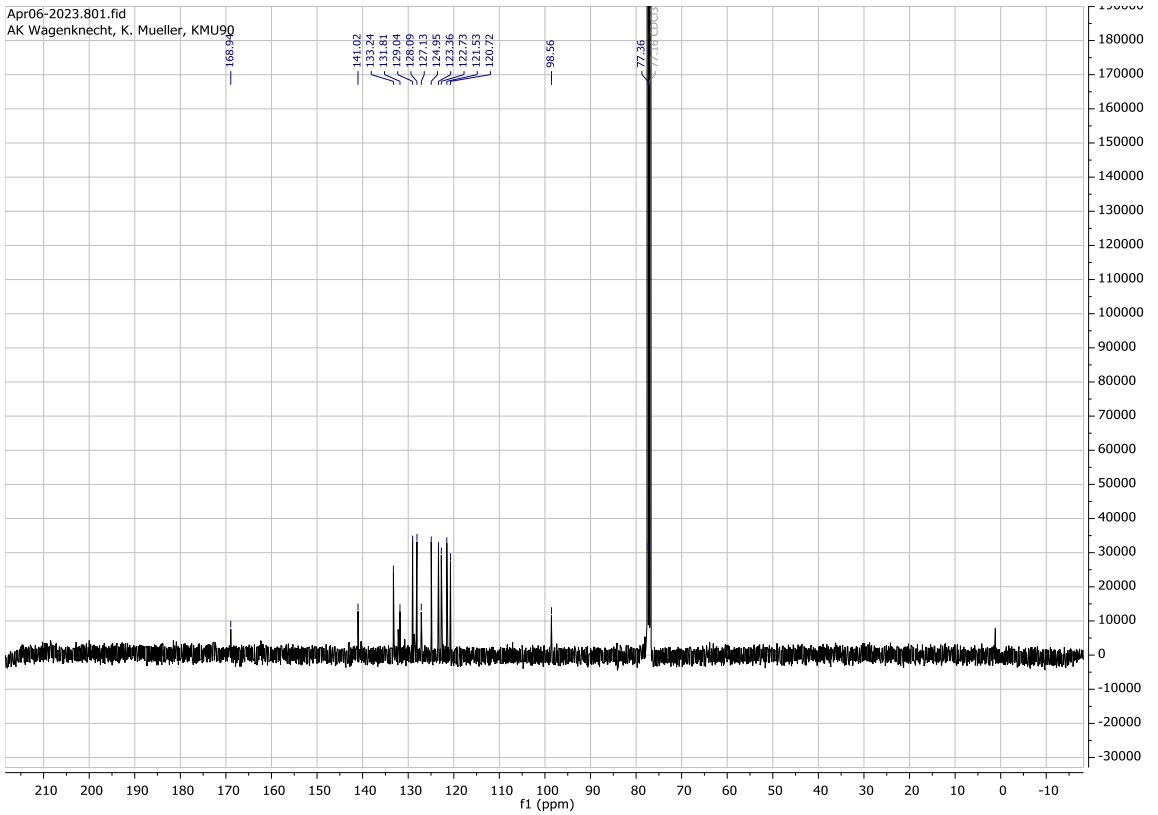
Apr06-2023.801.fid
AK Wagenknecht, K. Mueller, KMU90
f1 (ppm)

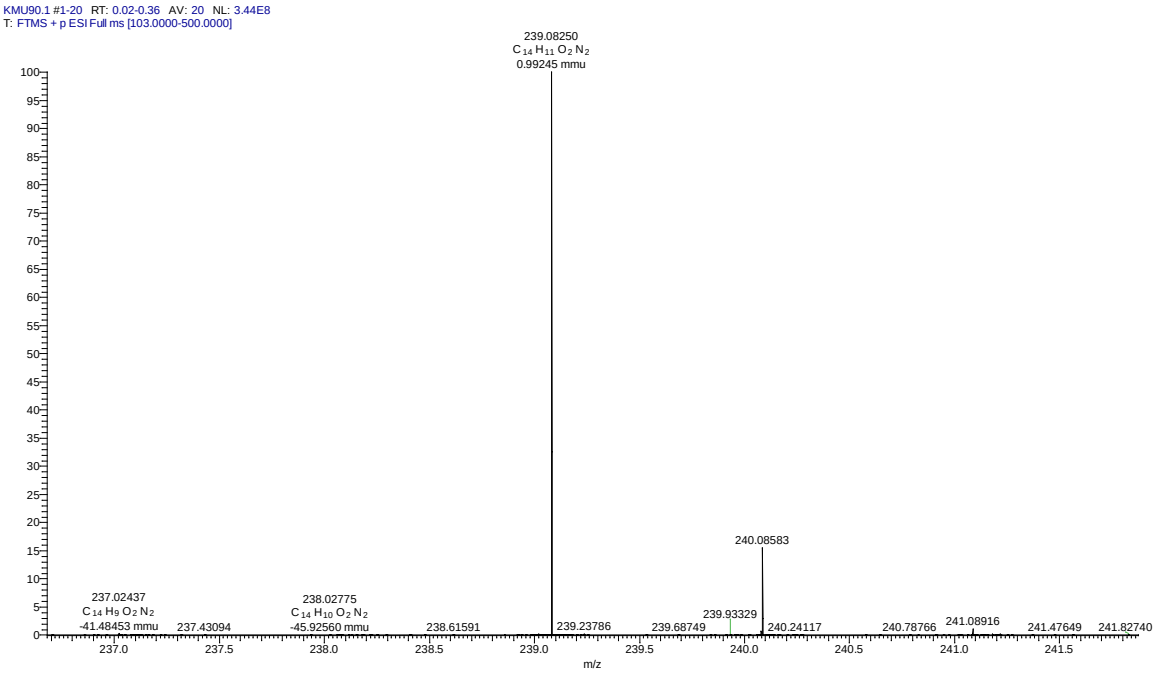
KMU90.1 #1-20 RT: 0.02-0.36 AV: 20 NL: 3.44E8
T: FTMS + p ESI Full ms [103.0000-500.0000]
239.08250
C 14 H 11 O 2 N 2
0.99245 mmu
240.08583
237.02437
C 14 H 9 O 2 N 2
-41.48453 mmu
238.02775
C 14 H 10 O 2 N 2
-45.92560 mmu
239.93329
241.08916
237.43094
238.61591
239.23786
239.68749
240.24117
240.78766
241.47649
241.82740
m/z

Compound 44

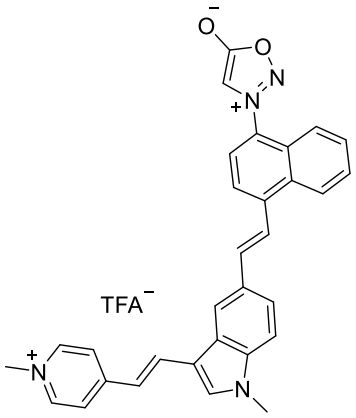

$C_{31}H_{25}N_4O_2^+C_2F_3O_2^-$
598.58 g/mol

In a heated 10 mL crimp vial under argon, 0.100 g **4** (0.220 mmol, 1.00 eq.), 0.010 g $Pd_2(dba)_3$ (0.010 mmol, 0.05 eq.), 0.031 g Qphos (0.040 mmol, 0.20 eq.) and 0.105 g **43** (0.440 mmol, 2.00 eq.) dried under high vacuum. The solids were then dissolved with 2.00 mL dry DMF and 0.15 mL triethylamine (0.111 g, 1.10 mmol, 5.00 eq.) was added. The reaction was stirred in a metal heating block at 80 °C for 18 hours. After the solution had cooled to room temperature, diethyl ether was added until no further precipitate was formed. The suspension was transferred into reaction tubes. The solution was centrifuged and the supernatant was pipetted off and discarded. Subsequently, diethyl ether was added and the suspension was vortexed and centrifuged again in the next step and the supernatant discarded. This was carried out two more times. The residue was dried in high vacuum and purified via reversed-phase column chromatography. The product was obtained as a brown solid with a yield of 0.079 g (0.132 mmol, 60 %).

^{1}H-NMR (500 MHz, DMSO-d_6): δ (ppm) = 8.76 – 8.70 (m, 3H, arom.), 8.50 (s, 1H, arom.), 8.24 (dd, *J* = 16.1, 12.6 Hz, 2H, R-CH=CH-R, arom.), 8.14 (dd, *J* = 14.5, 7.4 Hz, 3H, R-CH=CH-R, arom.), 8.06 (d, *J* = 7.8 Hz, 1H, arom.), 8.00 (s, 1H, arom.), 7.94 (d, *J* = 8.6 Hz, 1H, arom.), 7.82 (dtd, *J* = 16.0, 8.0, 3.8 Hz, 3H, R-CH=CH-R, arom.), 7.74 (s, 1H, arom.), 7.70 – 7.63 (m, 2H, arom.), 7.38 (d, *J* = 16.2 Hz, 1H, R-CH=CH-R), 4.19 (s, 3H, R-CH_3), 3.93 (s, 3H, R-CH_3).

^{13}C-NMR (126 MHz, DMSO-d_6): δ (ppm) = 168.4, 157.8, 157.6, 154.0, 144.3, 139.7, 138.1, 136.0, 135.6, 135.2, 131.0, 130.5, 129.7, 128.9, 127.8, 126.9, 125.8, 125.0, 124.2, 122.2, 121.8, 121.7, 117.3, 113.1, 111.5, 99.8, 46.3, 33.3.

HR-MS (ESI): m/z (calculated for $C_{31}H_{25}N_4O_2^+$): 485.1972 $[M]^+$; found: 485.1968 $[M]^+$

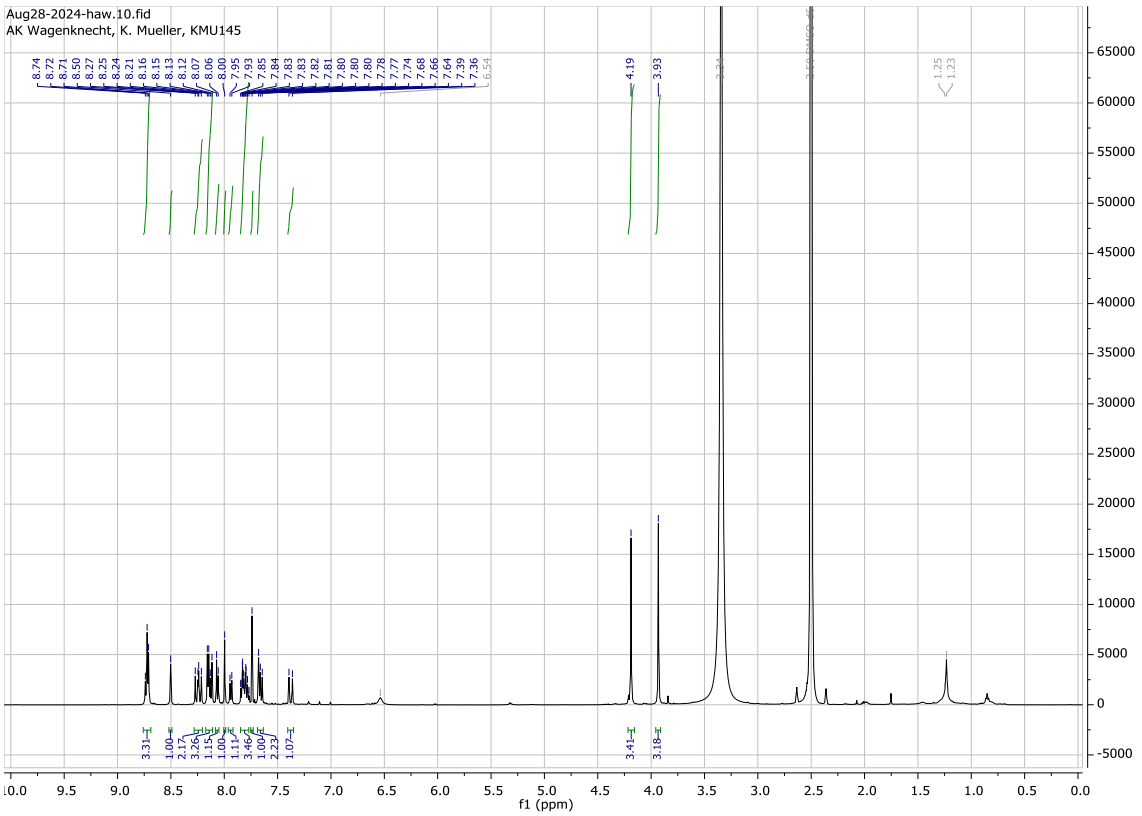

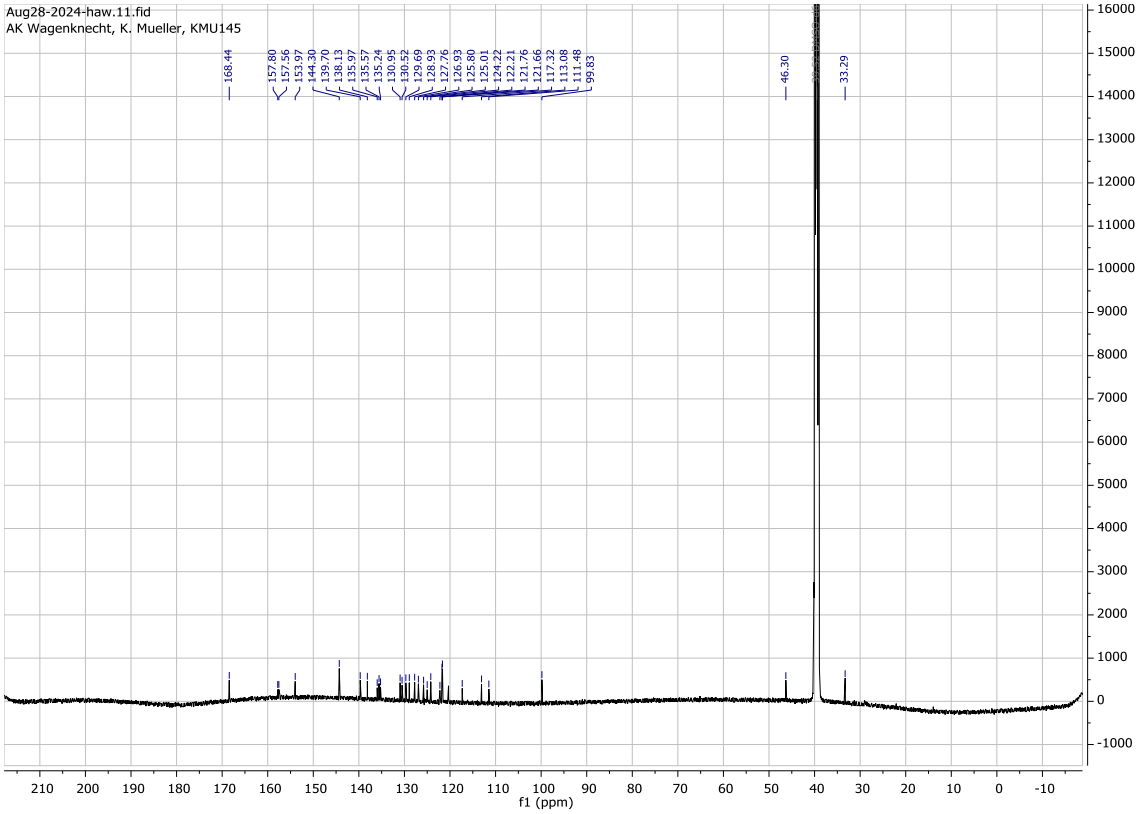
Aug28-2024-haw.11.fid
AK Wagenknecht, K. Mueller, KMU145
168.44
157.80
157.56
153.97
144.30
139.70
138.13
135.97
135.57
135.24
130.95
130.52
129.69
128.93
127.76
126.93
125.80
125.01
124.22
122.21
121.76
121.66
117.32
113.08
111.48
99.83
46.30
33.29
f1 (ppm)

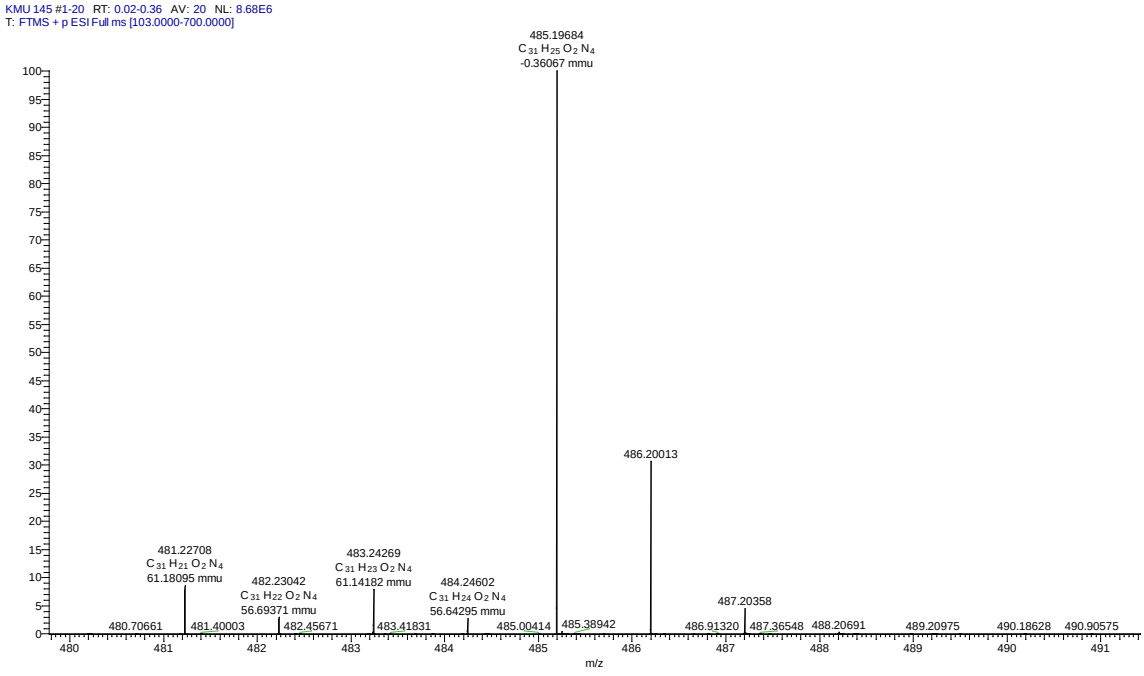
KMU 145 #1-20 RT: 0.02-0.36 AV: 20 NL: 8.68E6
T: FTMS + p ESI Full ms [103.0000-700.0000]
485.19684
C31 H25 O2 N4
-0.36067 mmu
486.20013
481.22708
C31 H21 O2 N4
61.18095 mmu
482.23042
C31 H22 O2 N4
56.69371 mmu
483.24269
C31 H23 O2 N4
61.14182 mmu
484.24602
C31 H24 O2 N4
56.64295 mmu
487.20358
480.70661
481.40003
482.45671
483.41831
485.00414
485.38942
486.91320
487.36548
488.20691
489.20975
490.18628
490.90575
m/z

Compound 45

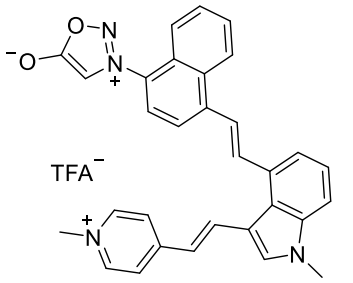

$C_{31}H_{25}N_4O_2^+C_2F_3O_2^-$
598.58 g/mol

In a heated 10 mL crimp vial under argon, 0.100 g **36** (0.220 mmol, 1.00 eq.), 0.010 g $Pd_2(dba)_3$ (0.010 mmol, 0.05 eq.), 0.031 g Qphos (0.040 mmol, 0.20 eq.) and 0.105 g **43** (0.440 mmol, 2.00 eq.) dried under high vacuum. The solids were then dissolved with 2.00 mL dry DMF and 0.15 mL triethylamine (0.111 g, 1.10 mmol, 5.00 eq.) was added. The reaction was stirred in a metal heating block at 80 °C for 18 hours. After the solution had cooled to room temperature, diethyl ether was added until no further precipitate was formed. The suspension was transferred into reaction tubes. The solution was centrifuged and the supernatant was pipetted off and discarded. Subsequently, diethyl ether was added and the suspension was vortexed and centrifuged again in the next step and the supernatant discarded. This was carried out two more times. The residue was dried in high vacuum and purified via reversed-phase column chromatography. The product was obtained as a brown solid with a yield of 0.059 g (0.099 mmol, 45 %).

^{1}H-NMR (500 MHz, DMSO-d_6): δ (ppm) = 8.70 – 8.63 (m, 3H, arom.), 8.48 (d, *J* = 15.9 Hz, 1H, R-CH=CH-R), 8.25 (dd, *J* = 22.0, 7.1 Hz, 3H, R-CH=CH-R, arom.), 8.12 – 8.05 (m, 2H, R-CH=CH-R, arom.), 8.02 (d, *J* = 6.9 Hz, 2H, arom.), 7.87 – 7.83 (m, 1H, arom.), 7.80 (d, *J* = 7.5 Hz, 1H, arom.), 7.79 – 7.74 (m, 3H, R-CH=CH-R, arom.), 7.60 (d, *J* = 8.2 Hz, 1H, arom.), 7.39 (t, *J* = 7.9 Hz, 1H, arom.), 7.13 (d, *J* = 15.9 Hz, 1H, R-CH=CH-R), 4.17 (s, 3H, R-CH_3), 3.94 (s, 3H, R-CH_3).

^{13}C-NMR (126 MHz, DMSO-d_6): δ (ppm) = 168.4, 157.7, 157.5, 153.2, 144.4, 139.3, 138.1, 136.0, 132.8, 132.6, 131.0, 130.8, 130.0, 129.0, 128.0, 126.9, 125.9, 124.8, 124.1, 123.9, 122.7, 122.5, 122.0, 121.7, 120.2, 118.8, 113.2, 111.2, 99.9, 46.4, 33.4.

HR-MS (ESI): m/z (calculated for $C_{31}H_{25}N_4O_2^+$): 485.1972 $[M]^+$; found: 485.1969 $[M]^+$

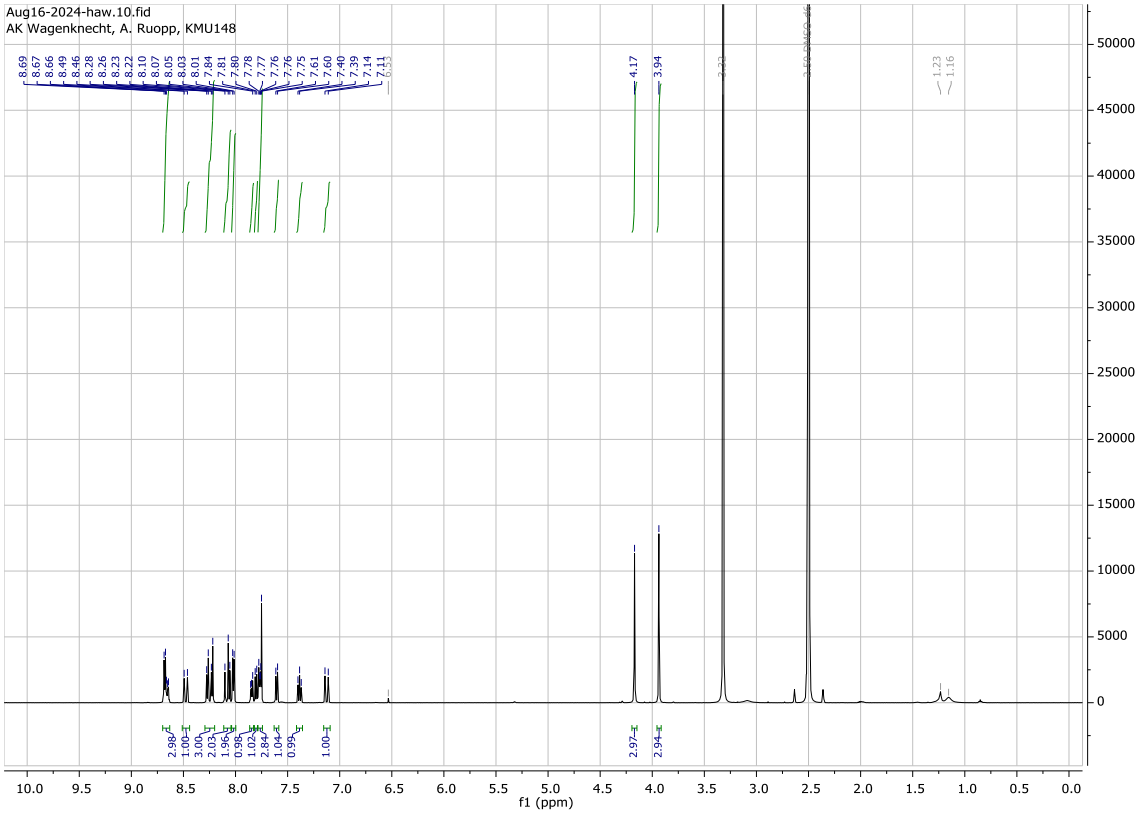

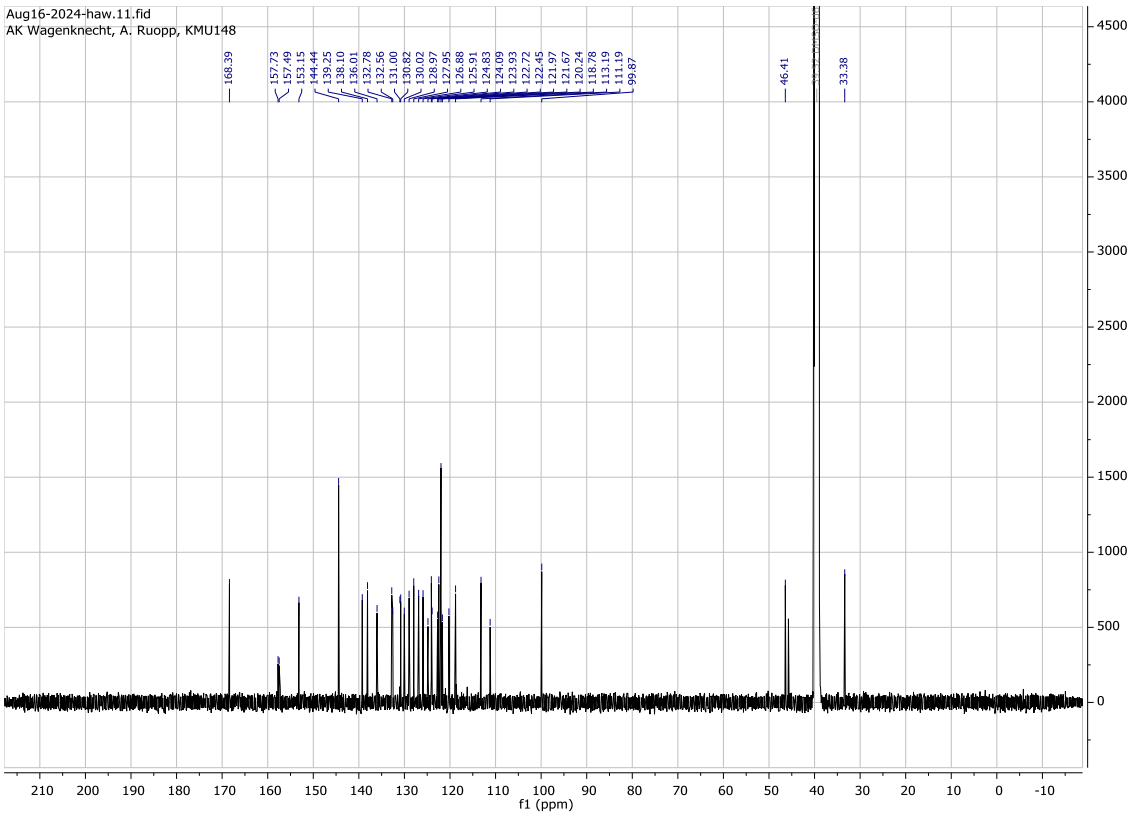
Aug16-2024-haw.11.fid
AK Wagenknecht, A. Ruopp, KMU148
168.39
157.73
157.49
153.15
144.44
139.25
138.10
136.01
132.78
132.56
131.00
130.82
130.02
128.97
127.95
126.88
125.91
124.83
124.09
123.93
122.72
122.45
121.97
121.67
120.24
118.78
113.19
111.19
99.87
46.41
33.38
f1 (ppm)

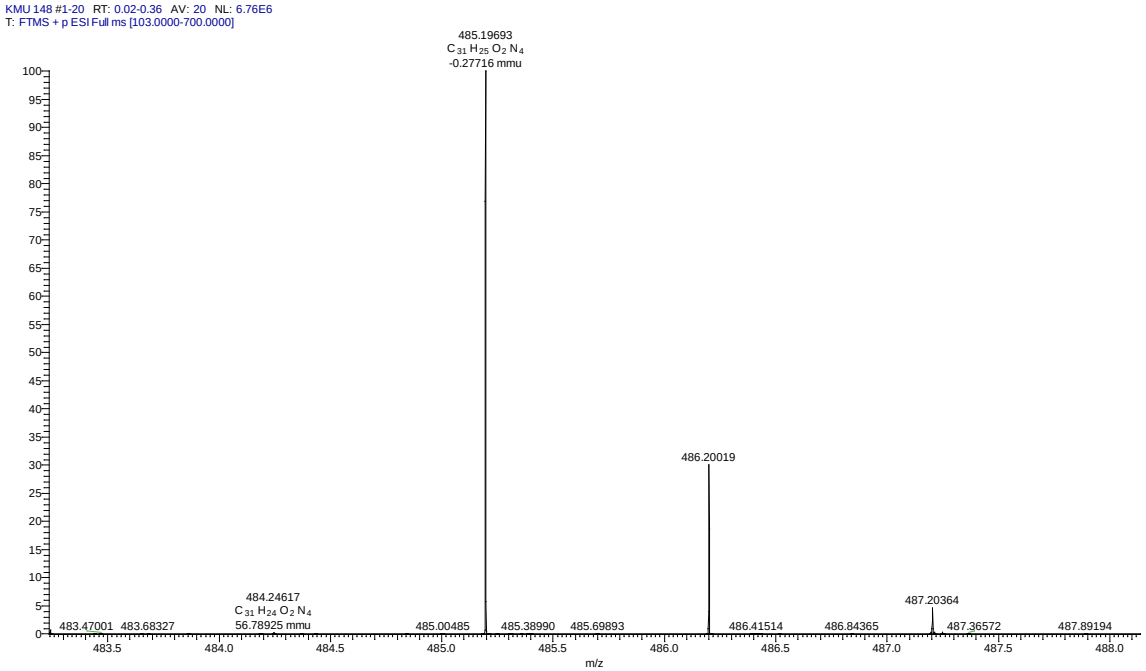
KMU 148 #1-20 RT: 0.02-0.36 AV: 20 NL: 6.76E6
T: FTMS + p ESI Full ms [103.0000-700.0000]
485.19693
C31 H25 O2 N4
-0.27716 mmu
486.20019
484.24617
C31 H24 O2 N4
56.78925 mmu
487.20364
483.47001
483.68327
485.00485
485.38990
485.69893
486.41514
486.84365
487.36572
487.89194
m/z

Compound 46

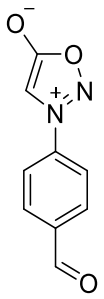

$C_9H_6N_2O_3$
190.16 g/mol

To a solution of 0.372 g **5** in a mixture acetone/water 3/1 (6 mL) was added 0.400 g NMO (2.96 mmol, 1.50 eq.) and OsO4 (2.5 wt% in tBuOH, 1.24 mL, 0.099 mL). The mixture was stirred at room temperature for 4 hours. A 25% solution of $Na_2S_2O_3$ was added and the aqueous layer was extracted six times with ethyl acetate. The organic layers were combined, dried over sodium sulfate and evaporated under reduced pressure. The residue was solubilized in a mixture of acetone/water 3/1 (6 mL) and 0.849 g $NaIO_4$ (3.95 mmol, 2.00 eq.) was added. The mixture was stirred at room temperature for 6 hours. The suspension was filtered through a plug of Celite and washed with ethyl acetate. The aqueous layer was extracted three times with ethyl acetate. The organic layers were combined, dried over sodium sulfate and evaporated under reduced pressure. The crude product was purified by flash chromatography (SiO_2, cyclohexane/ethyl acetate 20 – 50 %). The product was obtained as a light brown solid with a yield of 0.180 g (0.94 mmol, 48 %).

^{1}H-NMR (400 MHz, $CDCl_3$-*d_1*): δ (ppm) = 10.14 (s, 1H, R-COH), 8.16 (d, *J* = 8.6 Hz, 2H, arom.), 7.95 (d, *J* = 8.5 Hz, 2H, arom.), 6.86 (s, 1H, sydnone core).

HR-MS (ESI): m/z (calculated for $C_9H_7N_2O_3^+$): 191.0451 $[M+H]^+$; found: 191.0448 $[M+H]^+$.

The spectroscopic data is in agreement with literature.[13]

Compound 48

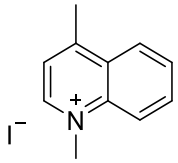

$C_{11}H_{12}N^{+}I^{-}$
285.13 g/mol

In a round bottom flask 9.26 mL 4-Methylchinolin (10.0 g, 69.8 mmol, 1.00 eq.) was dissolved in 21 mL acetone (V = 3,33 mL/10 mmol). 13.0 mL iodomethane (29.7 g, 209.5 mmol, 3.00 eq.) was added and the reaction mixture was stirred at 56 °C oil bath temperature for 2 hours. After cooling down the reaction to room temperature the precipitate was filtered off and washed three times with diethyl ether. The solid was dried overnight under reduced pressure. The product was obtained as a yellow solid with a yield of 19.2 g (67.3 mmol, 96 %).

^{1}H-NMR (400 MHz, DMSO-d_6): δ (ppm) = 9.39 – 9.31 (m, 1H, arom.), 8.58 – 8.46 (m, 2H, arom.), 8.27 (ddd, *J* = 8.7, 7.0, 1.3 Hz, 1H, arom.), 8.11 – 8.02 (m, 2H, arom), 4.58 (s, 3H, N-CH_3), 3.01 (s, 3H, C-CH_3).

The spectroscopic data is in agreement with literature.[155]

Compound 49

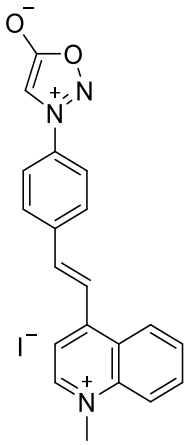

$C_{20}H_{16}N_3O_2^+I^-$
457.28 g/mol

In accordance with a literature prescription[13] to a solution of 0.088 g **48** (0.310 mmol, 1.00 eq.) and 0.065 g **46** (0.340 mmol, 1.10 eq.) in 8 mL MeOH was added three drops of piperidine. The mixture was stirred at 75 °C for 24 hours. Diethyl ether was added and the mixture was cooled to 0 °C and stirred for 1 hour, after which the precipitate was filtered. The precipitate was dried under reduced pressure. The product was obtained as a dark violet solid with a yield of 0.071 g (0.155 mmol, 50 %)

^{1}H-NMR (400 MHz, DMSO-d_6): δ (ppm) = 9.45 (d, *J* = 6.4 Hz, 1H, arom.), 9.09 (dd, *J* = 8.8, 1.3 Hz, 3H, arom.), 8.59 – 8.47 (m, 3H, arom.), 8.35 – 8.29 (m, 3H, arom.), 8.23 (d, *J* = 16.1 Hz, 1H, R-CH=CH-R), 8.16 – 8.09 (m, 3H, arom), 7.90 (s, 1H, sydnone core), 4.59 (s, 3H, N-CH_3).

^{13}C-NMR (101 MHz, DMSO-d_6): δ (ppm) = 168.5, 151.9, 148.6, 140.2, 139.2, 138.8, 135.2, 130.1 (2C), 129.6, 129.5, 126.60, 126.56, 123.1, 122.0 (2C), 119.5, 117.1, 94.9, 45.0.

HR-MS (ESI): m/z (calculated for $C_{20}H_{16}N_3O_2^+$): 330.1237 $[M]^+$; found: 330.1230 $[M]^+$

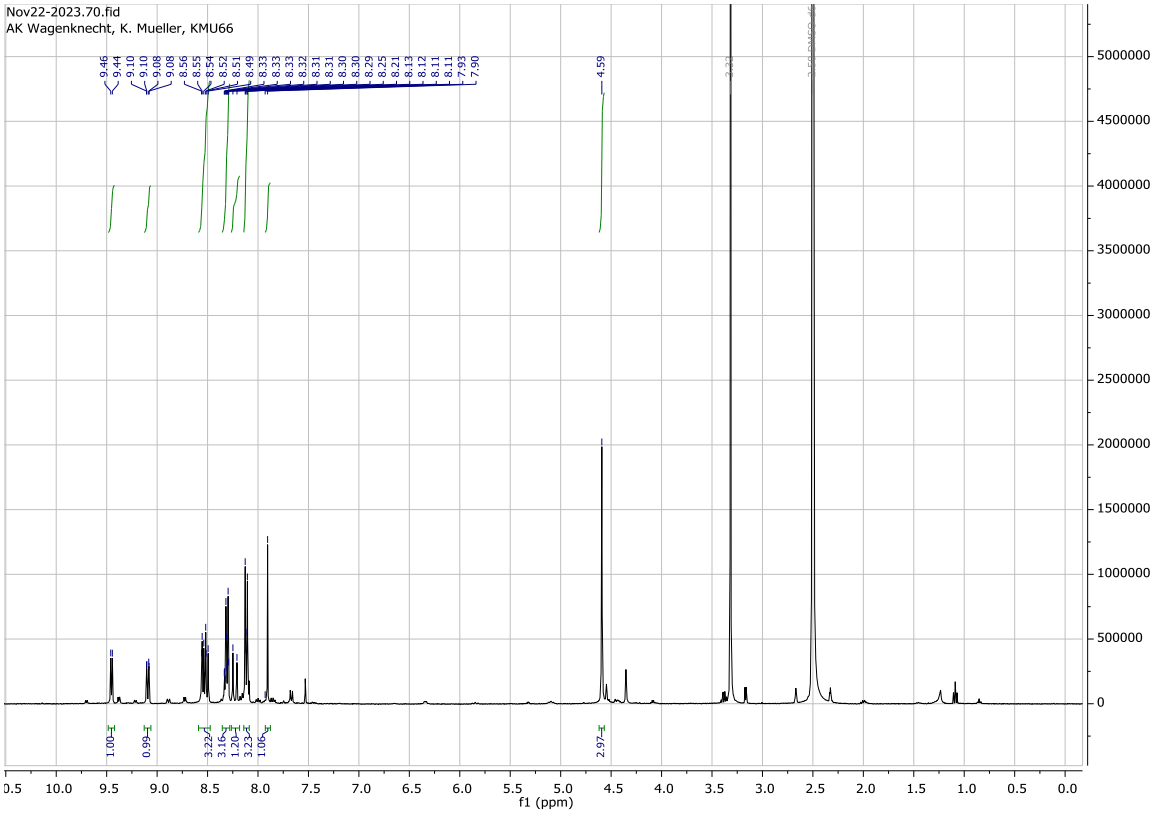
Nov22-2023.70.fid
AK Wagenknecht, K. Mueller, KMU66
9.46
9.44
9.10
9.10
9.08
9.08
8.55
8.55
8.54
8.52
8.51
8.49
8.33
8.33
8.33
8.32
8.31
8.31
8.30
8.30
8.29
8.25
8.21
8.13
8.12
8.11
8.11
7.93
7.90
4.59
3.22
1.00
0.99
3.22
3.16
1.20
3.23
1.06
2.97
f1 (ppm)

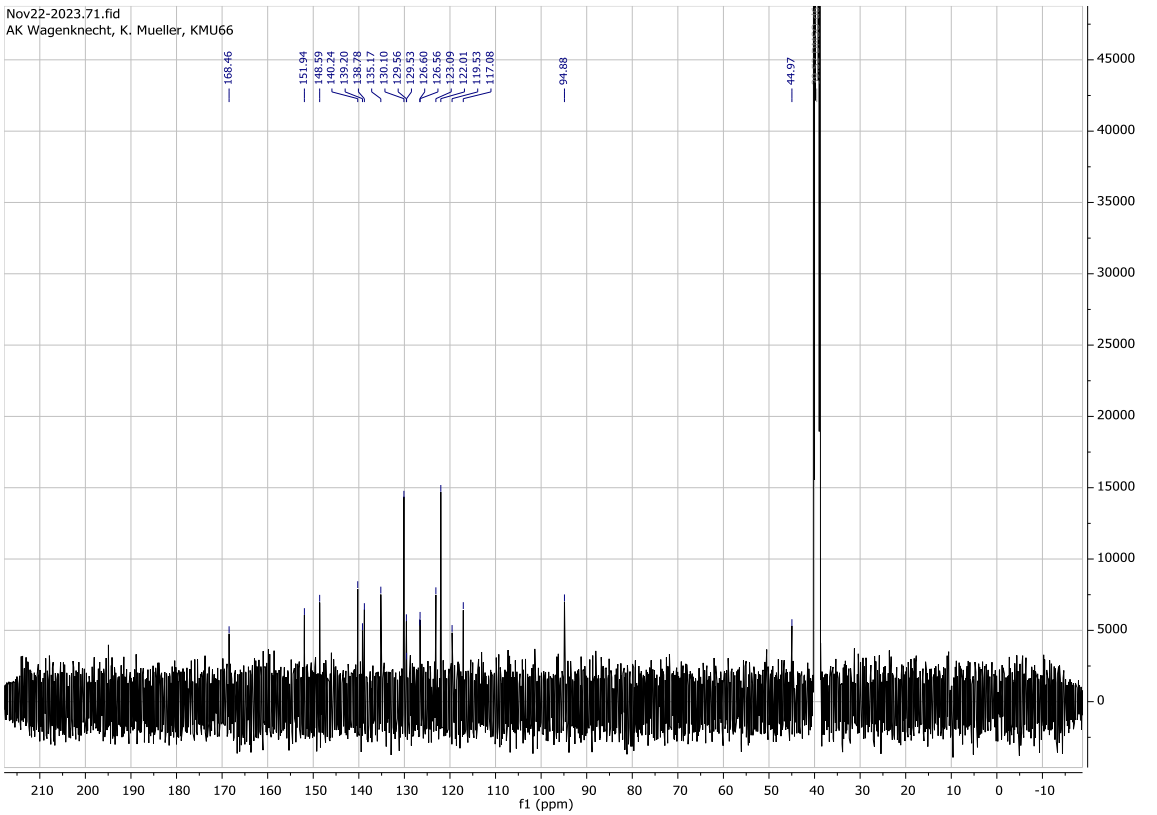
Nov22-2023.71.fid
AK Wagenknecht, K. Mueller, KMU66
168.46
151.94
148.59
140.24
139.20
138.78
135.17
130.10
129.56
129.53
126.60
126.56
123.09
122.01
119.53
117.08
94.88
44.97
f1 (ppm)

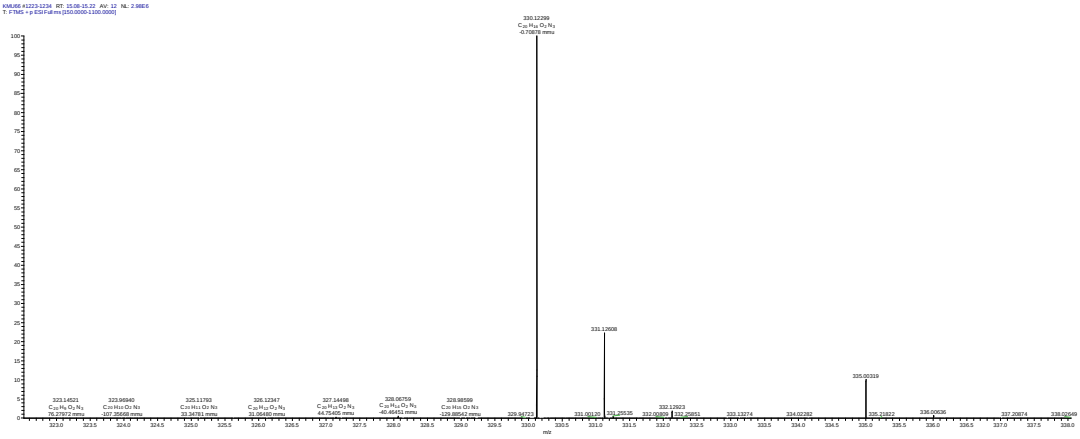
KMU6E-41223-1234 RT: 15.08-15.22 AV: 12 NL: 2.88E6
T: FTMS + p ESI Full ms [150.0000-1100.0000]
330.12299
C32 H18 O2 N3
-0.70878 mmu
331.12608
335.00319
323.14521
C20 H19 O3 N3
76.27972 mmu
323.96940
C16 H13 O7 N3
107.35668 mmu
325.11793
C16 H15 O7 N3
33.34781 mmu
326.12347
C20 H18 O3 N2
31.06480 mmu
327.14498
C20 H19 O3 N2
64.75405 mmu
328.06759
C24 H10 O2 N2
40.46451 mmu
328.98599
C16 H16 O7 N3
-129.88542 mmu
329.96723
331.00125
331.29236
332.12673
332.26851
333.13274
334.02282
335.21822
336.00636
337.20974
338.00649
m/z

Compound 18

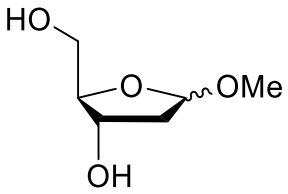

$C_6H_{12}O_4$
148,15800

5.00 g 2-desoxy-D-ribose (37.3 mmol, 1.00 eq.) was dissolved in 60 mL of dry methanol and degassed by introducing argon. For this purpose, 10 mL of a solution of 0.17 mL acetyl chloride in 10 mL dry methanol was added dropwise. The reaction mixture was stirred for 20 minutes at room temperature. Subsequently, $NaHCO_3$ was added, and the mixture was stirred for another 10 minutes at room temperature. The resulting solid was filtered off and washed with methanol. The filtrate was concentrated and dried in a high vacuum. The product was obtained as a brown oil in a quantitative yield.

^{1}H-NMR (400 MHz, $CDCl_3$-*d_1*)(alpha and beta isomer): δ (ppm) = 5.15 – 5.08 (m, 2H), 4.52 (br s, 1H), 4.17 – 4.10 (m, 2H), 4.09 – 4.04 (m, 1H), 3.75 – 3.58 (m, 4H), 3.46 (s, 1H), 3.37 (s, 6H), 2.87 – 2.80 (m, 1H), 2.69 (br s, 1H), 2.31 – 2.22 (m, 2H), 2.16 – 2.07 (m, 2H), 2.03 (s, 1H).

HR-MS (ESI): m/z (calculated for $C_6H_{12}O_4Na^+$): 171.0628 $[M+Na]^+$; found: 171.0625 $[M+Na]^+$.

The spectroscopic data is in agreement with literature.[156]

Compound 19

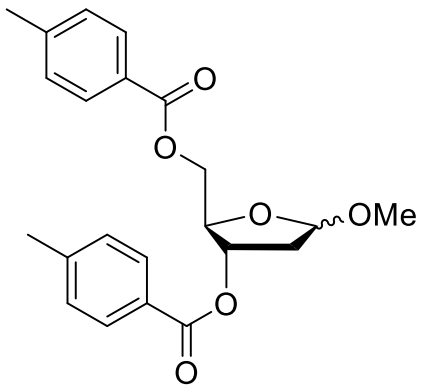

$C_{22}H_{24}O_6$
384.43 g/mol

5.91 g **18** (39.9 mmol, 1.00 eq.) was dissolved in 20 mL of acetone and 13.2 mL of p-toluoyl chloride (15.4 g, 99.7 mmol, 2.50 eq.) was added slowly. Subsequently, 13.9 mL triethylamine (10.1 g, 99.7 mmol, 2.50 eq.) was added and the solution was stirred overnight at room temperature. The precipitate was filtered off and washed with acetone. The solvent was removed under reduced pressure and the residue was purified by column chromatography (cyclohexane/ethyl acetate 0 – 15%). The product was obtained as a beige colored oil in a quantitative yield.

^{1}H-NMR (400 MHz, $CDCl_3$-*d_1*: δ (ppm) = 7.99 – 7.88 (m, 4H), 7.27 – 7.16 (m, 4H), 5.62 – 5.36 (m, 1 H), 5.24 – 5.14 (m, 1H), 4.64 – 4.40 (m, 3H), 3.41 (s, 1H), 3.34 (s, 2H), 2.58 – 2.48 (m, 1H), 2.42 – 2.35 (m, 7H).

HR-MS (ESI): m/z (calculated for $C_{22}H_{24}O_6^+$): 384.1573 $[M]^+$; found: 384.1520 $[M]^+$.

The spectroscopic data is in agreement with literature.[157]

Compound 20

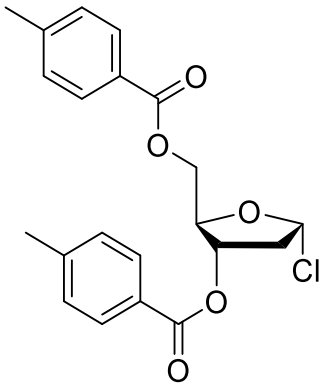

$C_{21}H_{21}ClO_5$
388.84 g/mol

In a round bottom flask 15.3 g **19** (39.9 mmol, 1.00 eq.) was dissolved in 90 mL acetic acid and then 101.6 mL 4M HCl in dioxan (398.6 mmol, 10.0 eq.) was added dropwise. The solution was cooled down to 0 °C and stirred for 2 hours. It was crystallized at -20 °C overnight and the precipitate was then filtered off and dried in a high vacuum. The product was obtained as a white solid with a yield of 8.00 g (20.6 mmol, 52 %).

^{1}H-NMR (400 MHz, $CDCl_3$-*d_1*: δ (ppm) = 7.99 (d, J = 8.0 Hz, 2H, arom.), 7.89 (d, J = 7.9 Hz, 2H, arom.), 7.24-7.21 (m, 4H, arom.), 6.46 (d, J = 5.0 Hz, 1H, 1‘-H), 5.56 (dd, J = 7.4, 2.9 Hz, 1H, 3‘-H), 4.85-4.84 (m, 1H, 4‘-H), 4.68 (dd, J = 12.1, 3.2 Hz, 1H, 5‘-H), 4.60 (dd, J = 12.1, 4.2 Hz, 1H, 5‘-H), 2.89-2.82 (m, 1H, 2‘-H), 2.75-2.71 (m, 1H, 2‘-H), 2.41 (s, 3H, C*H$_3$*), 2.40 (s, 3H, C*H$_3$*).

HR-MS (ESI): m/z (calculated for $C_{21}H_{21}O_5^+$): 353.1384 $[M\text{-}Cl]^+$; found: 353.1378 $[M\text{-}Cl]^+$.

The spectroscopic data is in agreement with literature.[159]

Compound 22

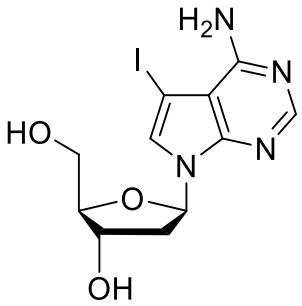

$C_{11}H_{13}IN_4O_3$
376.15 g/mol

In a round bottom flask 1.50 g 6-Chloro-7-iododeazapurine (5.37 mmol, 1.00 eq.) was dissolved in 55 mL acetonitrile and then 0.756 g KOH powder (13.5 mmol, 2.51 eq.) and 90 µL of TDA-I (0.087 g, 0.27 mmol, 0.05 eq.) were carefully added. The solution was stirred for 10 minutes at room temperature and then 2.30 g **20** (5.90 mmol, 1.10 eq.) was added. The solution was stirred for another hour, the solid was then filtered off and washed with hot acetone. The solvent was removed and the residue was dissolved in 50 mL NH_3 in methanol (7M) and stirred overnight at 120 °C. The solvent was removed and the crude product was purified by column chromatography (DCM/MeOH 0 – 10 %). The product was obtained as a white solid with a yield of 1.48 g (3.94 mmol, 73 %).

^{1}H-NMR (400 MHz, DMSO-d_6: δ (ppm) = 8.09 (s, 1H, H-2), 7.65 (s, 1H, H-8), 6.66 (br s, 2H, NH_2), 6.48 (dd, *J* = 8.3, 5.9 Hz, 1H, H-1'), 5.25 (d, *J* = 4.1 Hz, 1H, 3'-OH), 5.03 (t, *J* = 5.6 Hz, 1H, 5'-OH), 4.32 (dq, *J* = 5.6, 2.7 Hz, 1H, H-3'), 3.80 (td, *J* = 4.3, 2.3 Hz, 1H, H-4'), 3.60 – 3.45 (m, 2H, 2xH-5'), 2.44 (dd, *J* = 8.1, 5.3 Hz, 1H, H-2_a'), 2.15 (ddd, *J* = 13.1, 5.9, 2.8 Hz, 1H, H-2_b').

HR-MS (ESI): m/z (calculated for $C_{11}H_{14}IN_4O_3^+$): 377.0105 $[M+H]^+$; found: 377.0101 $[M+H]^+$.

The spectroscopic data is in agreement with literature.[160]

Compound 26

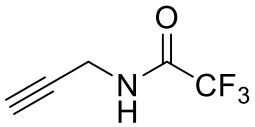

$C_5H_4F_3NO$
151.09 g/mol

In a round bottom flask under argon atmosphere, 10.4 mL of trifluoroacetic acid ethyl ester (12.4 g, 87.2 mmol, 1.20 eq.) was slowly added to an ice-cooled solution of 4.61 mL propargylamine (4.00 g, 72.6 mmol, 1.00 eq.) in 50 mL methanol. After 30 minutes, the ice bath was removed, and the reaction mixture was stirred at room temperature for 24 hours. The solvent was removed under reduced pressure and the residue was dissolved in 55 mL DCM. The organic phase was shaken with 100 mL saturated NaHCO3 and then the aqueous phase was washed with 35 mL DCM. The combined organic phases were washed with 50 mL water, which was washed with 25 mL DCM. The combined organic phases were dried over Na_2SO_4 and the solvent was removed under reduced pressure. The residue was purified by column chromatography (DCM 100 %). The product was obtained as a colorless liquid with a yield of 7.90 g (52.3 mmol, 72 %).

^{1}H-NMR (400 MHz, $CDCl_3$-*d_1*: δ (ppm) = 6.51 (br s, 1H, N*H*), 4.16 (dd, *J* = 5.4, 2.6 Hz, 2H, C*H_2*), 2.34 (t, *J* = 2.6 Hz, 1H, C*H*).

HR-MS (ESI): m/z (calculated for $C_5H_3F_3NO^+$): 150.0161 $[M-H]^+$; found: 150.0161 $[M-H]^+$.

The spectroscopic data is in agreement with literature.[162]

Compound 27

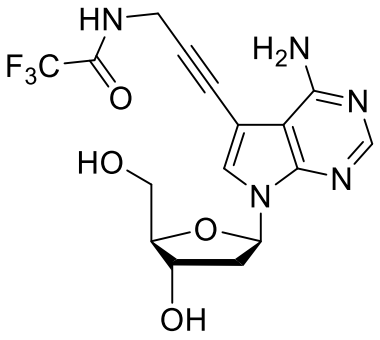

$C_{16}H_{16}F_3N_5O_4$
399.33 g/mol

In a heated round bottom flask under argon atmosphere, 1.48 g **23** (3.94 mmol, 1.00 eq.), 1.79 g **26** (11.8 mmol, 3.00 eq.), 0.165 g CuI (0.87 mmol, 0.22 eq.) and 1.10 mL triethylamine were dissolved in 24 mL dry DMF. The solution was degassed and then 0.456 g Pd(PPh3)4 (0.39 mmol, 0.10 eq.) was added. The reaction mixture was stirred at room temperature for 24 hours and the solvent was removed under reduced pressure. The residue was purified by column chromatography (DCM/MeOH 0 – 10 %). The product was obtained as a light brown solid with a yield of 1.32 g (3.30 mmol, 84 %).

^{1}H-NMR (400 MHz, DMSO-d_6: δ (ppm) = 10.1 (t, *J* = 5.5 Hz, 1H, N*H*), 8.11 (s, 1H, H-2), 7.75 (s, 1H, H-8), 6.47 (dd, *J* = 8.1, 5.9 Hz, 1H, H-1'), 5.26 (d, *J* = 4.0 Hz, 1H, 3'-OH), 5.06 (t, *J* = 5.6 Hz, 1H, 5'-OH), 4.34 (dd, *J* = 3.9, 3.0 Hz, 1H, H-3'), 4.31 (d, *J* = 5.1 Hz, 2H, CH_2), 3.81 (dd, *J* = 4.4, 2.4 Hz, 1H, H-4'), 3.60 – 3.50 (m, 2H, 2xH-5'), 2.44 (dd, *J* = 7.9, 5.5 Hz, 1H, H-2$_a$'), 2.17 (ddd, *J* = 13.1, 6.1, 2.8 Hz, 1H, H-2$_b$').

HR-MS (ESI): m/z (calculated for $C_{16}H_{17}F_3N_5O_4^+$): 400.1227 $[M+H]^+$; found: 400.1226 $[M+H]^+$.

The spectroscopic data is in agreement with literature.[166]

Compound 15

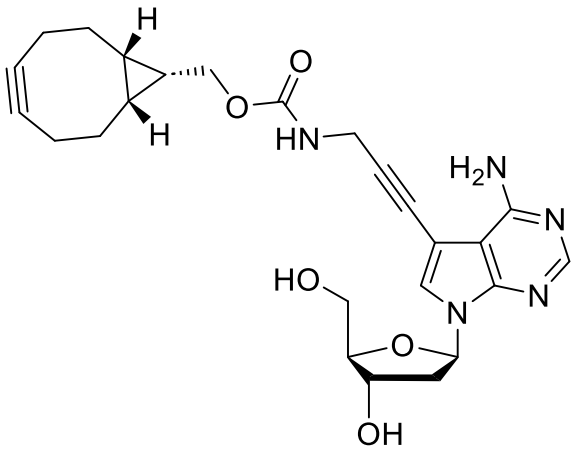

$C_{25}H_{29}N_5O_5$
479.54 g/mol

In a heated flask under argon atmosphere, 0.100 g **27** (0.25 mmol, 1.00 eq.) was dissolved in 5 mL of concentrate ammonium hydroxide solution and stirred overnight at room temperature. The solvent was removed under reduced pressure and the residue was dried in a high vacuum. The product was obtained as a brown solid with a quantitative yield.

In a heated round bottom flask under argon atmosphere, 0.038 g of the residue (0.13 mmol, 1.00 eq.), was dissolved in 5 mL dry DMF. Then 0.07 mL triethylamine (0.051 g, 0.50 mmol, 4.00 eq.) and 0.055 g BCN-NHS-ester (0.19 mmol, 1.50 eq.) were added, and the reaction mixture was stirred for 16 hours at room temperature. The solvent was then removed under reduced pressure. The residue was dissolved in 25 mL of methanol, approx. 50 mg of Amberlite IRA 402 bicarbonate was added and stirred for 30 min. The solid was filtered off and the solvent was removed under reduced pressure. The crude product was purified by column chromatography (SiO_2, DCM/MeOH 0 – 15 %). The product was obtained as a colorless solid with a yield of 0.061 g (0.12 mmol, 92 %).

1H-NMR (400 MHz, DMSO-d_6): δ = 8.09 (s, 1H, H-2), 7.71 (m, 2H, H-8, N*H*), 6.46 (dd, *J* = 7.9, 6.1 Hz, 1H, H-1'), 5.31 – 5.18 (m, 1H, 3'-OH), 5.06 (t, *J* = 5.5 Hz, 1H, 5'-OH), 4.41 – 4.26 (m, 1H, H-3'), 4.10 (d, *J* = 7.6 Hz, 2H, BCN), 4.02 (d, *J* = 5.4 Hz, 2H, CH_2), 3.84 – 3.78 (m, 1H, H-4'), 3.53 (dtd, *J* = 21.6, 11.5, 5.6 Hz, 2H, 2xH-5'), 2.47 – 2.39 (m, 2H, 2xH-2'), 2.23 – 2.11 (m,

6H, BCN), 1.55 (q, *J* = 10.8, 9.5 Hz, 2H, BCN), 1.36 – 1.22 (m, 1H, BCN), 0.87 (t, *J* = 8.1 Hz, 2H, BCN).

^{13}C-NMR (126 MHz, DMSO-d_6): δ (ppm) = 157.5, 156.5, 152.7, 149.2, 148.2, 125.9, 102.3, 99.0, 94.6, 89.3, 87.5, 83.6, 83.2, 75.2, 71.0, 62.0, 61.9, 48.6, 28.6, 20.8, 19.6, 17.6.

HR-MS (ESI): m/z (calculated for $C_{25}H_{30}N_5O_5^+$): 480.2242 $[M+H]^+$; found: 480.2245 $[M+H]^+$.

The spectroscopic data is in agreement with literature.[12]

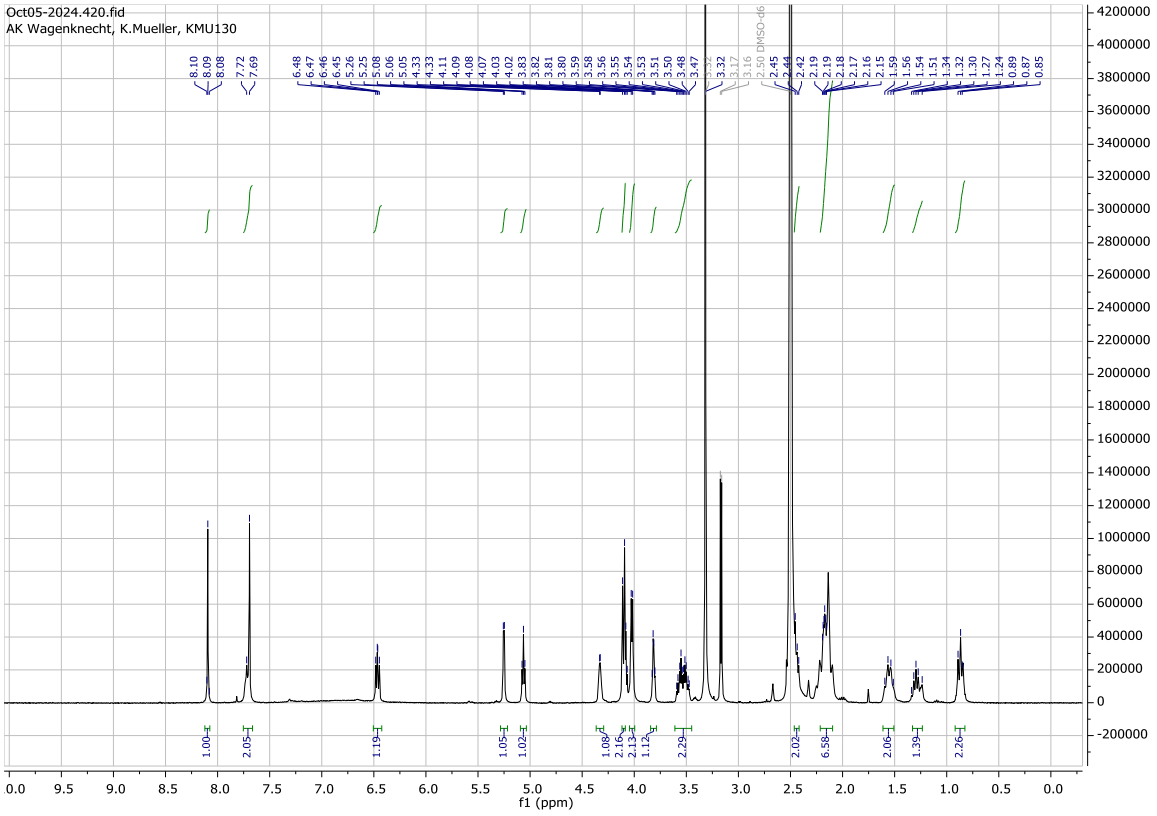

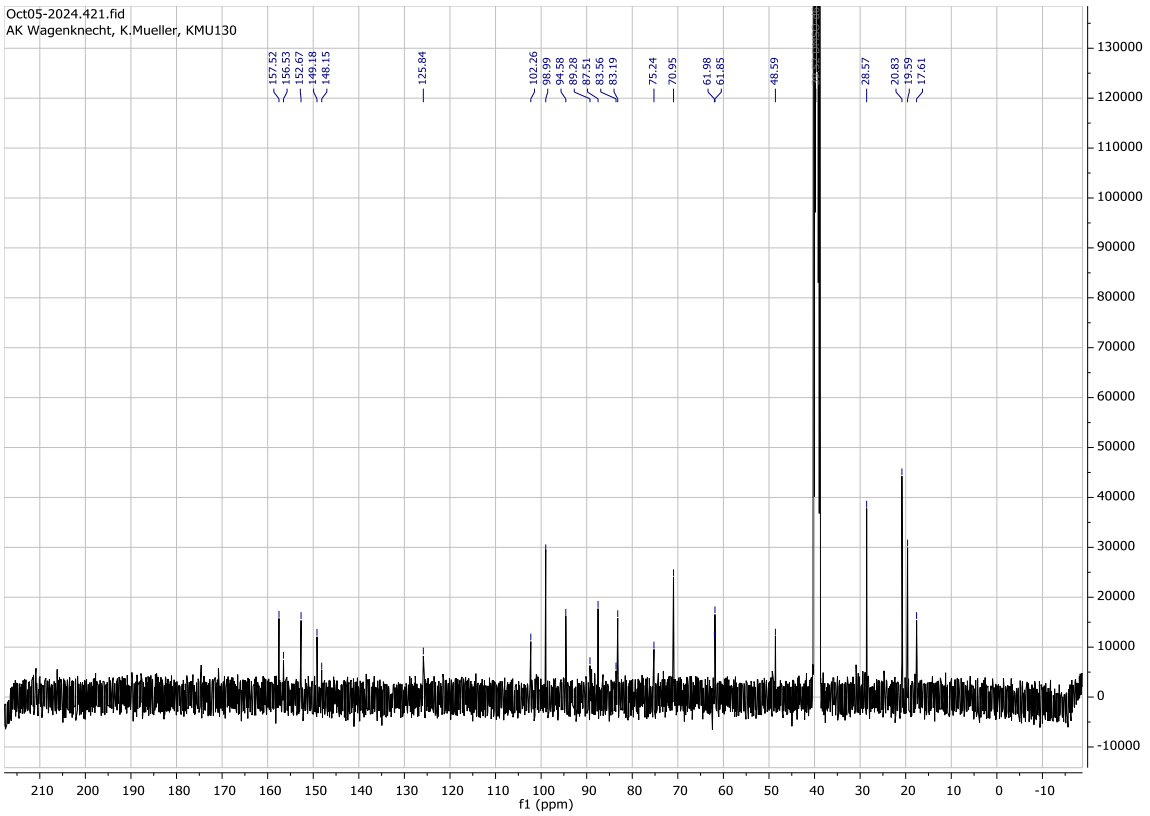
Oct05-2024.421.fid
AK Wagenknecht, K.Mueller, KMU130
157.52
156.53
152.67
149.18
148.15
125.84
102.26
98.99
94.58
89.28
87.51
83.56
83.19
75.24
70.95
61.98
61.85
48.59
28.57
20.83
19.59
17.61
f1 (ppm)

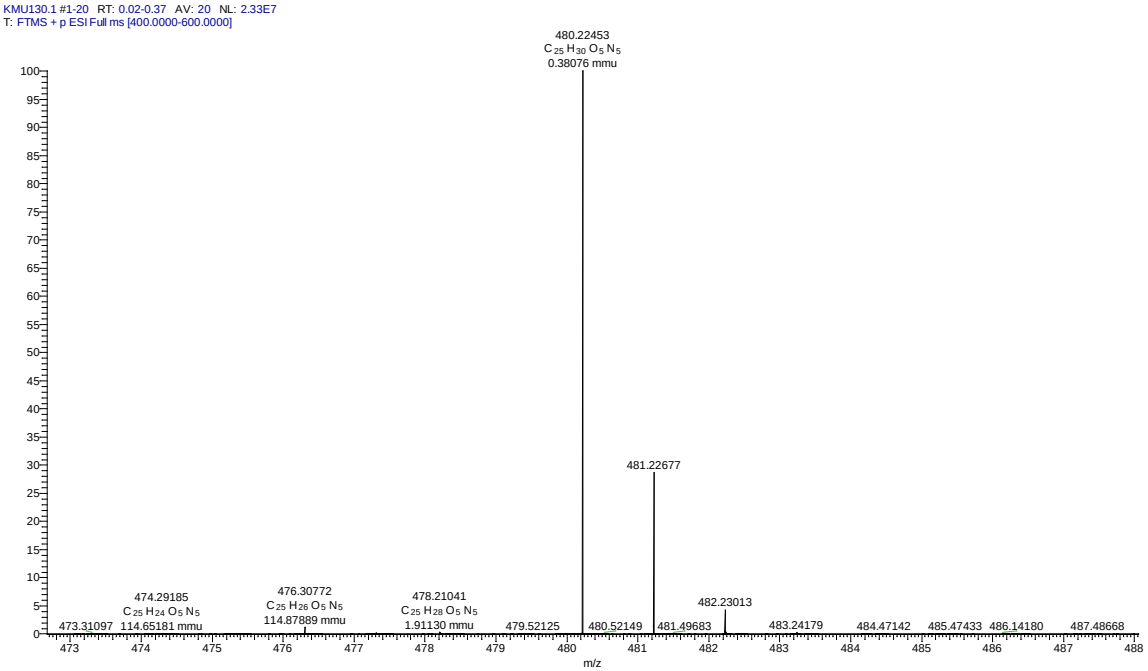
KMU130.1 #1-20 RT: 0.02-0.37 AV: 20 NL: 2.33E7
T: FTMS + p ESI Full ms [400.0000-600.0000]
480.22453
C25 H30 O5 N5
0.38076 mmu
481.22677
474.29185
C25 H24 O5 N5
114.65181 mmu
476.30772
C25 H26 O5 N5
114.87889 mmu
478.21041
C25 H28 O5 N5
1.91130 mmu
482.23013
m/z

Compound 58

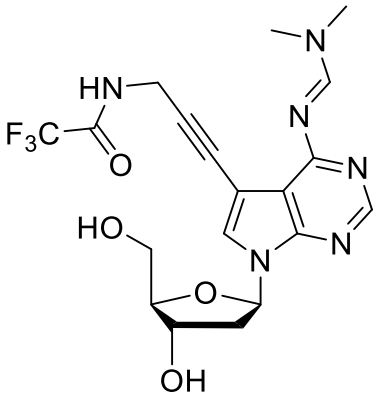

$C_{19}H_{21}F_3N_6O_4$
454.41 g/mol

In a heated round bottom flask under argon atmosphere, 0.500 g **27** (1.25 mmol, 1.00 eq.) was dissolved in 20 mL methanol. Then 2.84 mL DMF-DMA (2.54 g, 21.3 mmol, 17.0 eq.) was added and the reaction mixture was stirred for 3 hours at 40 °C. The solvent was then removed under reduced pressure. The crude product was purified by column chromatography (SiO_2, DCM/MeOH 0 – 15 %). The product was obtained as a colorless solid with a yield of 0.421 g (0.93 mmol, 74 %).

^{1}H-NMR (400 MHz, DMSO-*d_6*: δ (ppm) = 10.1 (s, 1H, N*H*), 8.80 (s, 1H, C*H*), 8.33 (s, 1H, H-2), 7.84 (s, 1H, H-8) 6.58 – 6.48 (m, 1H, H-1'), 5.27 (d, *J* = 4.0 Hz, 1H, 3'-OH), 5.05 (t, *J* = 5.5 Hz, 1H, 5'-OH), 4.38 – 4.32 (m, 1H, H-3'), 4.29 (s, 2H, C*H_2*), 3.86 – 3.80 (m, 1H, H-4'), 3.64 – 3.46 (m, 2H, 2xH-5'), 3.18 (s, 3H, NC*H_3*), 3.12 (s, 3H, NC*H_3*), 2.46 (m, 1H, H-2_a'), 2.19 (ddd, *J* = 13.0, 6.0, 2.8 Hz, 1H, H-2_b').

HR-MS (ESI): m/z (calculated for $C_{19}H_{22}F_3N_6O_4^+$): 455.1649 $[M+H]^+$; found: 455.1645 $[M+H]^+$.

The spectroscopic data is in agreement with literature.[155]

Compound 59

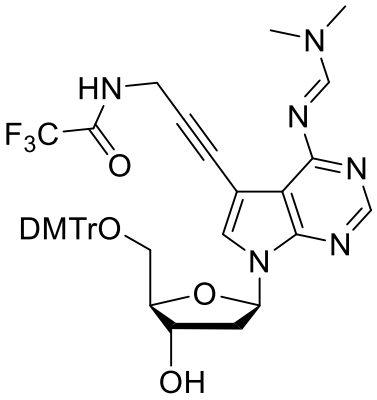

$C_{40}H_{39}F_3N_6O_6$
756.78 g/mol

In a heated round bottom flask under argon atmosphere, 0.420 g **58** (0.93 mmol, 1.00 eq.) was lyophilized and dissolved in 4 mL pyridine. Then 0.376 g DMT-Cl (1.11 mmol, 1.20 eq.) was added and the reaction mixture was stirred overnight at room temperature. On the following day, another portion DMT-Cl (0.45 eq.) was added and the reaction mixture stirred an additional hour. 5 mL methanol was added and the solvent was then removed under reduced pressure. The crude product was purified by column chromatography (SiO_2, DCM/MeOH 0 – 8 % + 0.1 % Et_3N). The product was obtained as a light beige foam with a yield of 0.560 g (0.74 mmol, 80 %).

1H-NMR (400 MHz, DMSO-d_6): δ = 10.04 (t, *J* = 5.5 Hz, 1H, N*H*), 8.79 (s, 1H, C*H*), 8.32 (s, 1H, H-2), 7.69 (s, 1H, H-8), 7.36 (d, *J* = 7.3 Hz, 2H, DMT), 7.29 – 7.16 (m, 7H, DMT), 6.82 (dd, *J* = 9.0, 2.5 Hz, 4H, DMT), 6.54 (t, *J* = 6.6 Hz, 1H, H-1'), 5.32 (d, *J* = 4.5 Hz, 1H, 3'-OH), 4.36 (dt, *J* = 9.3, 4.7 Hz, 1H, H-3'), 4.27 (d, *J* = 5.5 Hz, 2H, CH_2), 3.93 (dt, *J* = 5.8, 3.7 Hz, 1H, H-4'), 3.72 (s, 6H, 2xOCH_3), 3.21 – 3.07 (m, 8H, 2xNCH_3, 2xH-5'), 2.62 (dt, *J* = 13.3, 6.6 Hz, 1H, H-2_a'), 2.28 – 2.21 (m, 1H, H-2_b').

HR-MS (ESI): m/z (calculated for $C_{40}H_{40}F_3N_6O_6^+$): 757.2956 $[M+H]^+$; found: 757.2958 $[M+H]^+$.

The spectroscopic data is in agreement with literature.[155]

Compound 60

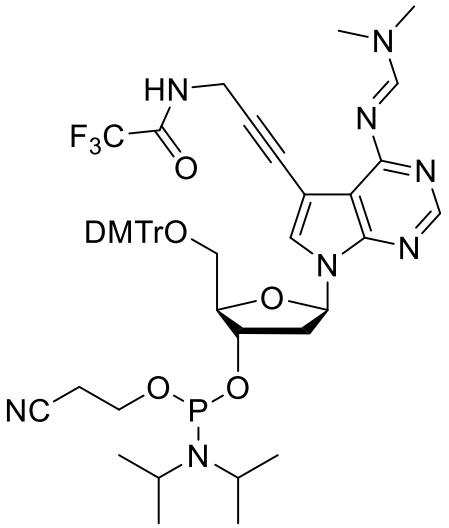

$C_{49}H_{56}F_3N_8O_7P$
957.01 g/mol

In a heated flask under argon atmosphere, 0.200 g **59** (0.26 mmol, 1.00 eq.) was lyophilized and dissolved in 5 mL dry DCM. Then 0.136 mL DIPEA (0.101 g, 0.78 mmol, 3.00 eq.) and 0.116 mL 2-cyanoethyl-N,N-diisopropylchlorophosphoramidite (0.123 g, 0.52 mmol, 2.00 eq.) were added and the reaction mixture was stirred for 3.5 hours at room temperature. The reaction mixture was then directly purified by column chromatography (SiO_2, DCM/MeOH 50 % +0.1 % Et_3N). The product was obtained as a light colorless foam with a yield of 0.249 g (0.26 mmol, 100 %).

^{31}P-NMR (162 MHz, DMSO-d_6): δ (ppm) = 147.8, 147.1.

HR-MS (ESI): m/z (calculated for $C_{49}H_{57}F_3N_8O_7P^+$): 957.4034 $[M+H]^+$; found: 957.4011 $[M+H]^+$.

The spectroscopic data is in agreement with literature.[155]

Compound 80

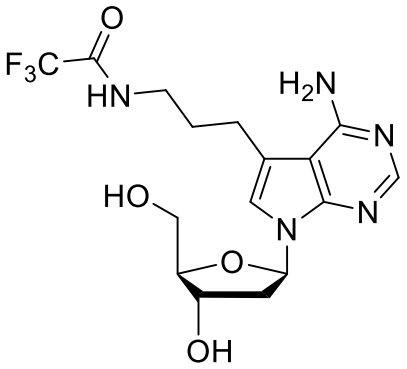

$C_{16}H_{20}F_3N_5O_4$
403.36 g/mol

In a heated flask under argon atmosphere, 0.200 g **27** (0.50 mmol, 1.00 eq.) and 0.040 g $Pd(OH)_2$ (on carbon, 20 w%) (0.05 mmol) were suspended in 10 mL in dry methanol and 0.80 mL triethylsilane (5.01 mmol, 10.0 eq.) was added. The reaction was stirred for 24 hours at room temperature. Subsequently, the solid was filtered off over a celite pad, eluted with methanol and the solvent was removed under reduced pressure. The crude product was purified by column chromatography (SiO_2, DCM/MeOH 0 – 12 %). The product was obtained as a light beige foam with a yield of 0.162 g (0.40 mmol, 80 %).

^{1}H-NMR (400 MHz, DMSO-d_6: δ (ppm) = 9.41 (t, *J* = 5.9 Hz, 1H, N*H*), 8.02 (s, 1H, H-2), 7.11 (s, 1H, H-8), 6.58 (s, 2H, R-NH_2), 6.46 (dd, *J* = 8.4, 5.9 Hz, 1H, H-1'), 5.22 (d, *J* = 4.0 Hz, 1H, 3'-OH), 5.04 (t, *J* = 5.7 Hz, 1H, 5'-OH), 4.31 (h, *J* = 2.6 Hz, 1H, H-3'), 3.82 – 3.75 (m, 1H, H-4'), 3.59 – 3.50 (m, 1H, H-5_a'), 3.48 – 3.45 (m, 1H, H-5_b'), 3.26 (q, *J* = 6.1 Hz, 2H, CH_2-NH), 2.84 – 2.76 (m, 2H, CH_2), 2.45 (dd, *J* = 8.3, 5.7 Hz, 1H, H-2_a'), 2.10 (ddd, *J* = 12.9, 5.9, 2.6 Hz, 1H, H-2_b'), 1.77 (p, *J* = 7.8 Hz, 2H, CH_2).

HR-MS (ESI): m/z (calculated for $C_{16}H_{21}F_3N_5O_4^+$): 404.1540 $[M+H]^+$; found: 404.1533 $[M+H]^+$.

The spectroscopic data is in agreement with literature.[166]

Compound 82

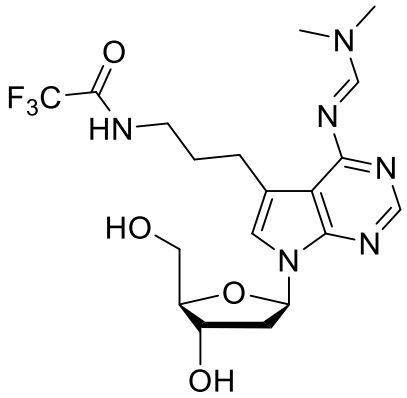

$C_{19}H_{25}F_3N_6O_4$
458.44 g/mol

In a heated round bottom flask under argon atmosphere, 0.249 g **80** (0.62 mmol, 1.00 eq.) was dissolved in 15 mL methanol. Then 1.40 mL DMF-DMA (1.25 g, 10.5 mmol, 17.0 eq.) was added and the reaction mixture was stirred for 3 hours at 40 °C. The solvent was then removed under reduced pressure. The crude product was purified by column chromatography (SiO_2, DCM/MeOH 0 – 15 %). The product was obtained as a colorless solid with a yield of 0.187 g (0.41 mmol, 66 %).

^{1}H-NMR (400 MHz, DMSO-*d_6*: δ (ppm) = 9.41 (t, *J* = 5.9 Hz, 1H, N*H*), 8.85 (s, 1H, C*H*), 8.26 (s, 1H, H-2), 7.24 (s, 1H, H-8), 6.51 (dd, *J* = 8.4, 5.9 Hz, 1H, H-1'), 5.24 (d, *J* = 4.1 Hz, 1H, 3'-OH), 5.04 (t, *J* = 5.6 Hz, 1H, 5'-OH), 4.33 (h, *J* = 2.7 Hz, 1H, H-3'), 3.80 (td, *J* = 4.7, 2.5 Hz, 1H, H-4'), 3.52 – 3.45 (m, 1H, H-5_a'), 3.44 – 3.36 (m, 1H, H-5_b'), 3.24 (q, *J* = 7.1 Hz, 2H, C*H_2*-NH), 3.17 (s, 3H, NC*H_3*), 3.09 (s, 3H, NC*H_3*), 2.83(h, *J* = 7.0 Hz, 2H, C*H_2*), 2.46 (m, 1H, H-2_a'), 2.13 (ddd, *J* = 13.0, 5.9, 2.6 Hz, 1H, H-2_b'), 1.89 (p, *J* = 7.5 Hz, 2H, C*H_2*).

HR-MS (ESI): m/z (calculated for $C_{19}H_{26}F_3N_6O_4^+$): 459.1962 $[M+H]^+$; found: 459.1953 $[M+H]^+$.

The spectroscopic data is in agreement with literature.[166]

Compound 83

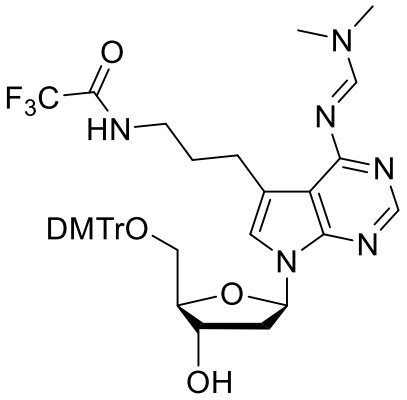

$C_{40}H_{43}F_3N_6O_6$
760.82 g/mol

In a heated round bottom flask under argon atmosphere, 0.187 g **81** (0.41 mmol, 1.00 eq.) was lyophilized and dissolved in 5 mL pyridine. Then 0.166 g DMT-Cl (0.49 mmol, 1.20 eq.) was added and the reaction mixture was stirred overnight at room temperature. On the following day, another portion DMT-Cl (0.45 eq.) was added and the reaction mixture stirred an additional hour. 5 mL methanol was added and the solvent was then removed under reduced pressure. The crude product was purified by column chromatography (SiO_2, DCM/MeOH 0 – 8 % + 0.1 % Et_3N). The product was obtained as a colorless solid with a yield of 0.204 g (0.27 mmol, 65 %).

^{1}H-NMR (400 MHz, DMSO-*d_6*: δ (ppm) = 9.36 (t, *J* = 5.9 Hz, 1H, N*H*), 8.85 (s, 1H, C*H*), 8.27 (s, 1H, H-2), 7.40 – 7.33 (m, 2H, DMT), 7.29 – 7.15 (m, 7H, DMT), 7.09 (s, 1H, H-8), 6.82 (dd, *J* = 8.9, 5.6 Hz 4H, DMT), 6.57 (t, *J* = 6.8 Hz, 1H, H-1'), 5.32 (d, *J* = 4.5 Hz, 1H, 3'-OH), 4.45 – 4.36 (m, 1H, H-3'), 3.92 (q, *J* = 4.0 Hz, 1H, H-4'), 3.71 (s, 6H, 2xOC*H_3*), 3.17 (s, 3H, NC*H_3*), 3.15 – 3.09 (m, 4H, NH-C*H_2*, H-5'), 3.09 (s, 3H, NC*H_3*), 2.73 (t, *J* = 7.4 Hz, 2H, C*H_2*), 2.59 – 2.53 (m, 1H, H-2$_a$'), 2.23 (ddd, *J* = 13.1, 6.3, 3.6 Hz, 1H, H-2$_b$'), 1.79 (p, *J* = 7.1 Hz, 2H, C*H_2*).

HR-MS (ESI): m/z (calculated for $C_{40}H_{44}F_3N_6O_6^+$): 761.3269 $[M+H]^+$; found: 761.3259 $[M+H]^+$.

The spectroscopic data is in agreement with literature.[166]

Compound 84

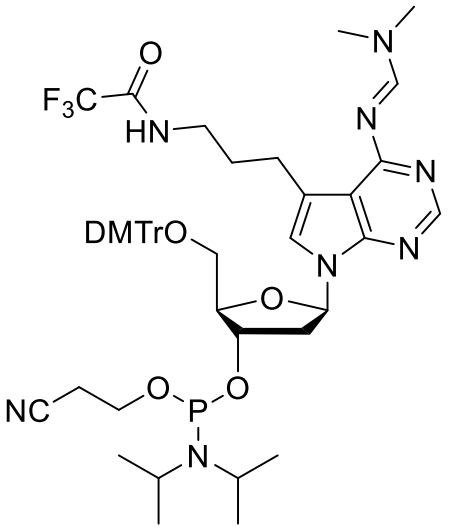

$C_{49}H_{60}F_3N_8O_7P$
961.04 g/mol

In a heated flask under argon atmosphere, 0.187 g **82** (0.41 mmol, 1.00 eq.) was lyophilized and dissolved in 5 mL dry DCM. Then 0.214 mL DIPEA (0.159 g, 0.78 mmol, 3.00 eq.) and 0.183 mL 2-cyanoethyl-N,N-diisopropylchlorophosphoramidite (0.194 g, 0.82 mmol, 2.00 eq.) were added and the reaction mixture was stirred for 3.5 hours at room temperature. The reaction mixture was then directly purified by column chromatography (SiO_2, DCM/MeOH 50 % +0.1 % Et_3N). The product was obtained as a light colorless foam with a yield of 0.204 g (0.27 mmol, 65 %).

^{31}P-NMR (162 MHz, DMSO-d_6): δ (ppm) = 147.5, 147.0.

HR-MS (ESI): m/z (calculated for $C_{49}H_{61}F_3N_8O_7P^+$): 961.4347 $[M+H]^+$; found: 961.4334 $[M+H]^+$.

The spectroscopic data is in agreement with literature.[166]

Compound 29

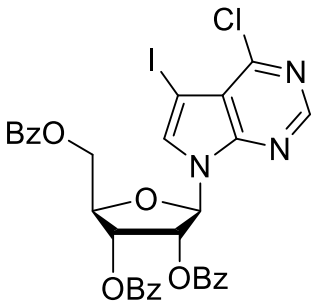

$C_{32}H_{23}ClIN_3O_7$
723.90 g/mol

In a heated flask under argon atmosphere, 5.00 g 6-Chloro-7-iodo-7-deazapurine (17.9 mmol, 1.00 eq.) was suspended in 90 mL dry MeCN. Then 1.33 mL BSA (1.10 g, 19.7 mmol, 1.10 eq.) was added and the suspension stirred for 20 minutes at room temperature. 9.93 g ß-D-Ribofuranose-1-acetate-2,3,5-tribenzoate (19.7 mmol, 1.10 eq.) and 3.40 mL TMSOTf (4.18 g, 18.8 mmol, 1.05 eq.) were added to the mixture and heated to 80 °C and stirred for 2.5 hours. Upon completion, sat. $NaHCO_3$ solution (80 mL) was added to the mixture, extracted three times with ethyl acetate (3x50 mL), and dried over Na_2SO_4. The solvent was removed under reduced pressure and the crude product was then purified by column chromatography (SiO_2, cyclohexane/ethyl acetate 0 – 50 %). The product was obtained as a light yellow foam with a yield of 7.75 g (10.7 mmol, 60 %).

^{1}H-NMR (400 MHz, $CDCl_3$-d_1: δ (ppm) = 8.57 (s, 1H, H-2), 8.14 – 8.10 (m, 2H, Bz), 8.01 – 7.97 (m, 2H, Bz), 7.94 – 7.90 (m, 2H, Bz), 7.64 – 7.47 (m, 7H, Bz, H-8), 7.43 – 7.32 (m, 3H, Bz), 6.67 (d, *J* = 5.5 Hz, 1H, H-1'), 6.16 (t, *J* = 5.6 Hz, 1H, H-3'), 6.11 (dd, *J* = 5.8, 4.4 Hz, 1H, H-4'), 4.90 (dd, *J* = 12.2, 3.1 Hz, 1H, H-5_a'), 4.82 – 4.78 (m, 1H, H-2'), 4.69 (dd, *J* = 12.3, 3.6 Hz, 1H, H-5_b').

HR-MS (ESI): m/z (calculated for $C_{32}H_{24}ClIN_3O_7^+$): 724.0342 $[M+H]^+$; found: 724.0341 $[M+H]^+$.

The spectroscopic data is in agreement with literature.[143]

Compound 30

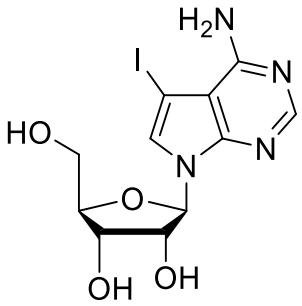

$C_{11}H_{13}IN_4O_4$
392.15 g/mol

In a pressure tube, 3.00 g **29** (4.14 mmol, 1.00 eq.) was suspended in 100 mL 7M NH_3 in methanol. The reaction mixture was heated to 120 °C and stirred for 24 hours. The solvent was removed under reduced pressure. The crude product was purified by column chromatography (SiO_2, DCM/MeOH 0 – 10 % + 1 % Et_3N). The product was obtained as a beige solid with a yield of 1.40 g (3.56 mmol, 86 %).

^{1}H-NMR (400 MHz, DMSO-d_6: δ (ppm) = 8.10 (s, 1H, H-2), 7.67 (s, 1H, H-8), 6.67 (br s, 2H, NH_2), 6.02 (dd, *J* = 6.3 Hz, 1H, H-1'), 5.30 (d, *J* = 6.4 Hz, 1H, 3'-OH), 5.15 (t, *J* = 5.6 Hz, 1H, 5'-OH), 5.10 (d, *J* = 4.8 Hz, 1H, 2'-OH), 4.35 (dd, *J* = 11.4, 6.5 Hz, 1H, H-3'), 4.07 (dd, *J* = 8.3, 3.3 Hz, 1H, H-4'), 3.88 (q, *J* = 3.8 Hz, 1H, H-2'), 3.64 – 3.57 (m, 1H, H-5_a'), 3.52 (ddd, *J* = 12.0, 6.1, 3.8 Hz, 1H, H-5_b').

HR-MS (ESI): m/z (calculated for $C_{11}H_{14}IN_4O_4^+$): 393.0054 $[M+H]^+$; found: 393.0049 $[M+H]^+$.

The spectroscopic data is in agreement with literature.[143]

Compound 31

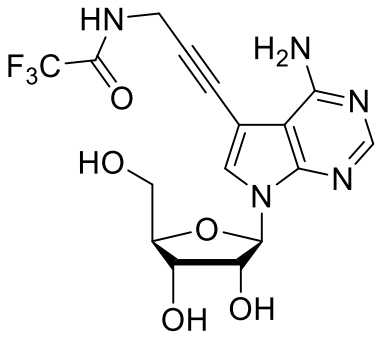

$C_{16}H_{16}F_3N_5O_5$
415.33 g/mol

In a heated round bottom flask under argon atmosphere, 1.88 g **30** (4.78 mmol, 1.00 eq.), 2.17 g **26** (14.3 mmol, 3.00 eq.), 0.200 g CuI (1.05 mmol, 0.22 eq.) and 1.33 mL triethylamine (0.968 g, 9.56 mmol, 2.00 eq.) were dissolved in 30 mL dry DMF. The solution was degassed and then 0.553 g $Pd(PPh_3)_4$ (0.48 mmol, 0.10 eq.) was added. The reaction mixture was stirred at room temperature for 24 hours and the solvent was removed under reduced pressure. The residue was purified by column chromatography (DCM/MeOH 10 – 50 %). The product was obtained as a light brown solid with a yield of 1.39 g (3.35 mmol, 70 %).

^{1}H-NMR (400 MHz, DMSO-*d_6*: δ (ppm) = 10.1 (t, *J* = 5.5 Hz, 1H, N*H*), 8.11 (s, 1H, H-2), 7.77 (s, 1H, H-8), 6.84 (br s, 2H, N*H_2*), 6.01 (d, *J* = 6.1 Hz, 1H, H-1'), 5.33 (d, *J* = 6.3 Hz, 1H, 3'-OH), 5.19 (t, *J* = 5.6 Hz, 1H, 5'-OH), 5.11 (d, *J* = 4.8 Hz, 1H, 2'-OH), 4.36 (q, *J* = 6.1 Hz, 1H, H-3'), 4.31 (d, *J* = 5.4 Hz, 2H, C*H_2*), 4.10 – 4.03 (m, 1H, H-4'), 3.89 (q, *J* = 3.6 Hz, 1H, H-2'), 3.66 – 3.58 (m, 1H, H-5_a'), 3.53 (ddd, *J* = 11.9, 6.1, 3.6 Hz, 1H, H-5_b').

^{13}C-NMR (126 MHz, DMSO-*d_6*): δ (ppm) = 157.5, 152.7, 149.6, 127.0, 112.2, 102.3, 94.1, 91.0, 87.3, 86.8, 85.2, 76.1, 74.0, 70.5, 61.5, 29.9.

HR-MS (ESI): m/z (calculated for $C_{16}H_{17}F_3N_5O_5^+$): 416.1176 $[M+H]^+$; found: 416.1172 $[M+H]^+$.

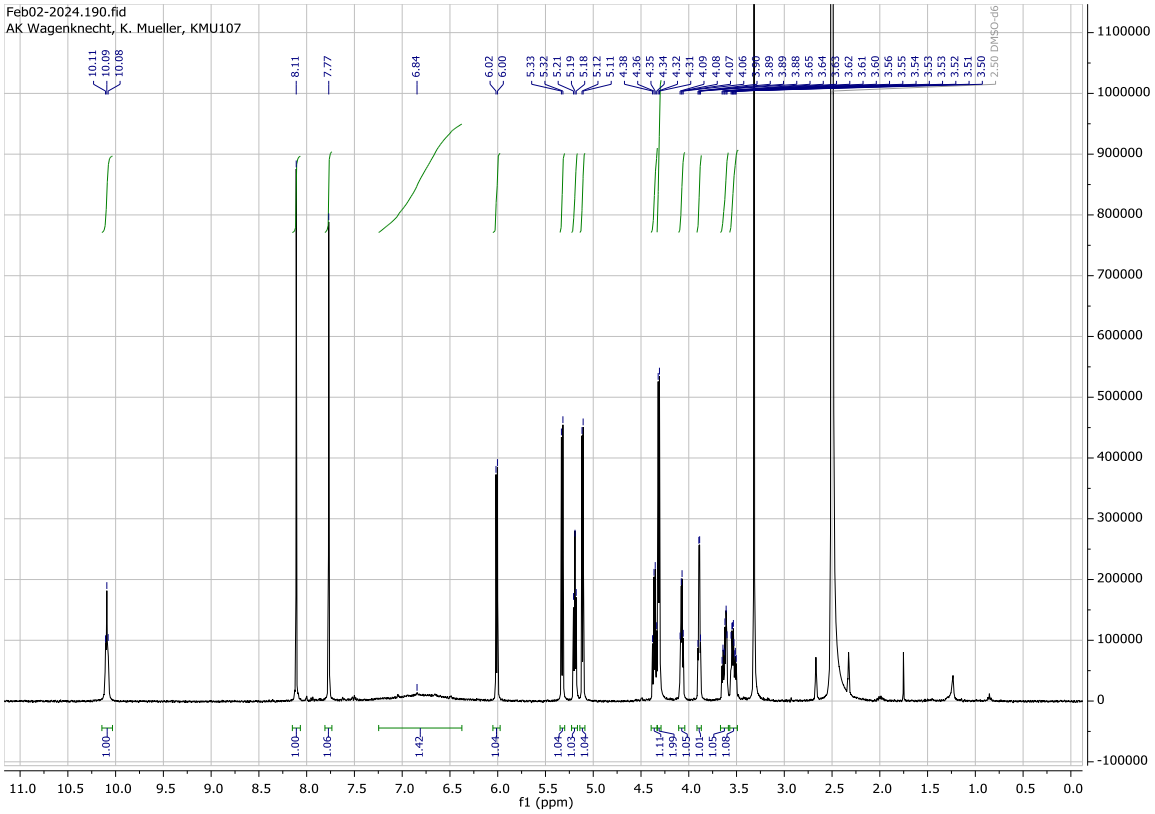
Feb02-2024.190.fid
AK Wagenknecht, K. Mueller, KMU107
10.11
10.09
10.08
8.11
7.77
6.84
6.02
6.00
5.33
5.32
5.21
5.19
5.18
5.12
5.11
4.38
4.36
4.35
4.34
4.32
4.31
4.09
4.08
4.07
4.06
3.90
3.89
3.89
3.88
3.65
3.64
3.63
3.62
3.61
3.60
3.56
3.55
3.54
3.53
3.53
3.52
3.51
3.50
2.50 DMSO-d6
1.00
1.00
1.06
1.42
1.04
1.04
1.03
1.04
1.14
1.99
1.05
1.01
1.05
1.08
f1 (ppm)

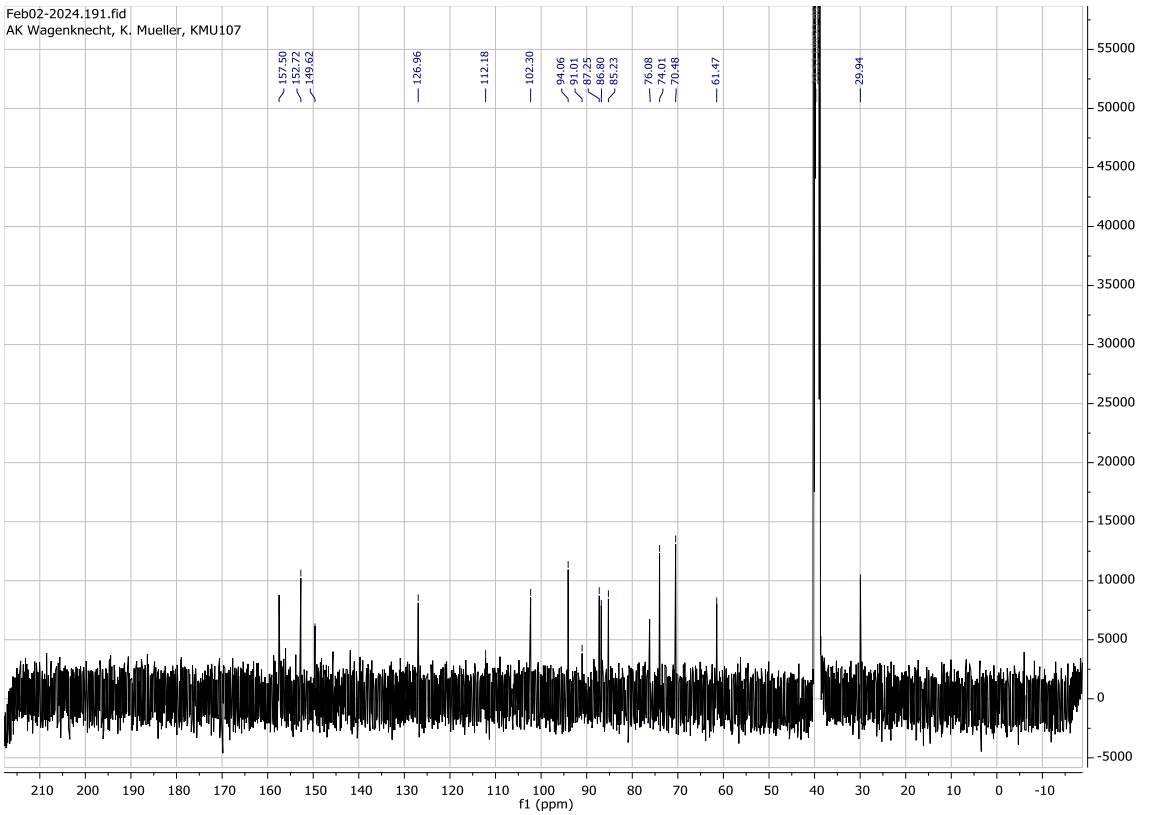
Feb02-2024.191.fid
AK Wagenknecht, K. Mueller, KMU107
157.50
152.72
149.62
126.96
112.18
102.30
94.06
91.01
87.25
86.80
85.23
76.08
74.01
70.48
61.47
29.94
f1 (ppm)

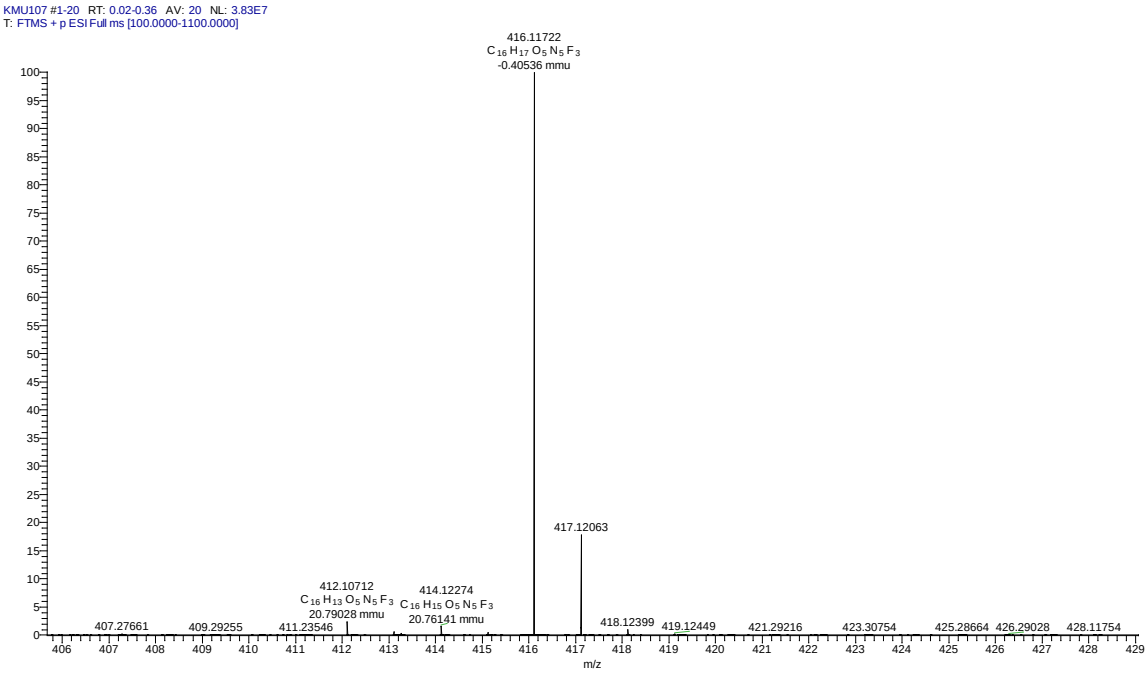
KMU107 #1-20 RT: 0.02-0.36 AV: 20 NL: 3.83E7
T: FTMS + p ESI Full ms [100.0000-1100.0000]
416.11722
C16 H17 O5 N5 F3
-0.40536 mmu
417.12063
412.10712
C16 H13 O5 N5 F3
20.79028 mmu
414.12274
C16 H15 O5 N5 F3
20.76141 mmu
407.27661
409.29255
411.23546
418.12399
419.12449
421.29216
423.30754
425.28664
426.29028
428.11754
m/z

Compound 16

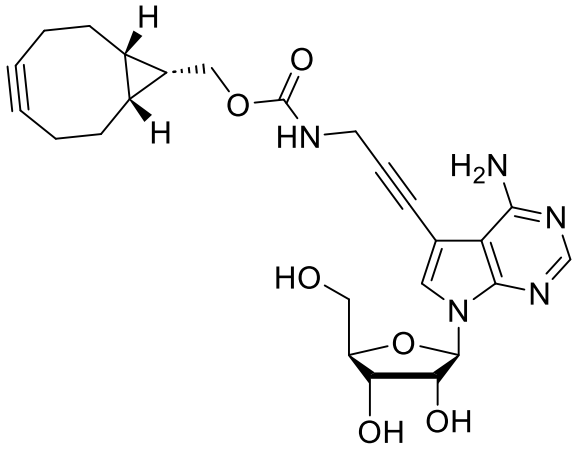

$C_{25}H_{29}N_5O_6$
495.54 g/mol

In a heated flask under argon atmosphere, 0.070 g **31** (0.25 mmol, 1.00 eq.) was dissolved in 3 mL of concentrate ammonium hydroxide solution and stirred overnight at room temperature. The solvent was removed under reduced pressure and the residue was dried in a high vacuum. The product was obtained as a brown solid with a quantitative yield.

In a heated round bottom flask under argon atmosphere, 0.046 g of the residue (0.14 mmol, 1.00 eq.), was dissolved in 5 mL dry DMF. Then 0.08 mL triethylamine (0.058 g, 0.58 mmol, 4.00 eq.) and 0.063 g BCN-NHS-ester (0.22 mmol, 1.50 eq.) were added, and the reaction mixture was stirred for 16 hours at room temperature. The solvent was then removed under reduced pressure. The residue was dissolved in 25 mL of methanol, approx. 50 mg of Amberlite IRA 402 bicarbonate was added and stirred for 30 min. The solid was filtered off and the solvent was removed under reduced pressure. The crude product was purified by column chromatography (SiO_2, DCM/MeOH 0 – 15 %). The product was obtained as a colorless solid with a yield of 0.056 g (0.11 mmol, 80 %).

1H-NMR (400 MHz, DMSO-d_6): δ = 8.10 (s, 1H, H-2), 7.71 (m, 2H, H-8, N*H*), 6.00 (d, *J* = 6.0 Hz, 1H, H-1'), 5.32 (d, *J* = 6.3 Hz, 1H, 3'-OH), 5.20 (t, *J* = 5.5 Hz, 1H, 5'-OH), 5.11 (d, *J* = 4.8 Hz, 1H, 2'-OH), 4.35 (q, *J* = 6.0 Hz, 1H, H-3'), 4.10 (d, *J* = 8.1 Hz, 2H, BCN), 4.09 – 4.05

(m, 1H, H-4'), 4.03 (d, *J* = 5.5 Hz, 2H, CH_2), 3.89 (q, *J* = 3.4 Hz, 1H, H-2'), 3.62 (dt, *J* = 11.7, 4.5 Hz, 1H, H-5_a'), 3.54 (dt, *J* = 5.7, 2.8 Hz, 1H, H-5_b')., 2.27 – 2.08 (m, 6H, BCN), 1.55 (q, *J* = 10.4, 9.5 Hz, 2H, BCN), 1.35 – 1.26 (m, 1H, BCN), 0.91 – 0.83 (m, 2H, BCN).

^{13}C-NMR (126 MHz, DMSO-d_6): δ (ppm) = 157.6, 152.7, 149.6, 126.3, 102.4, 99.0, 94.5, 89.3, 87.2, 85.2, 75.2, 74.0, 70.5, 61.5, 30.9, 28.6, 20.8, 19.6, 17.6.

HR-MS (ESI): m/z (calculated for $C_{25}H_{30}N_5O_6^+$): 496.2191 $[M+H]^+$; found: 496.2186 $[M+H]^+$.

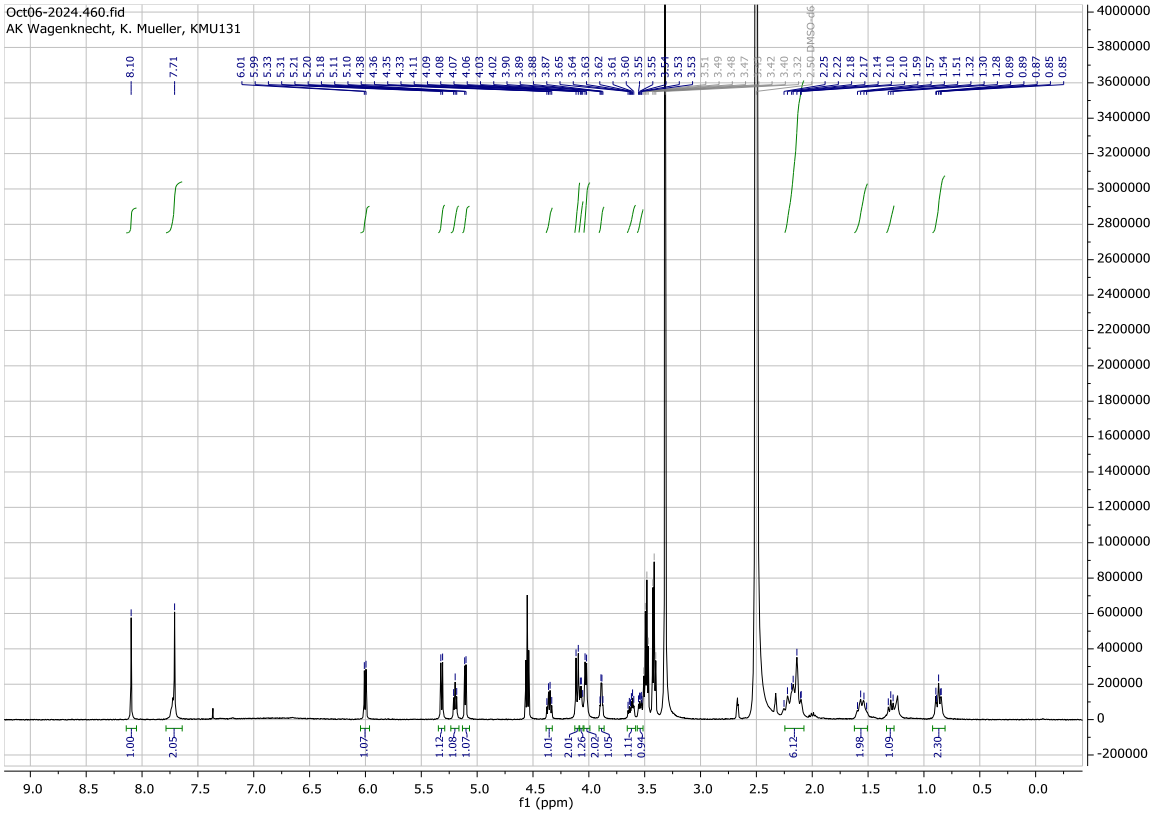

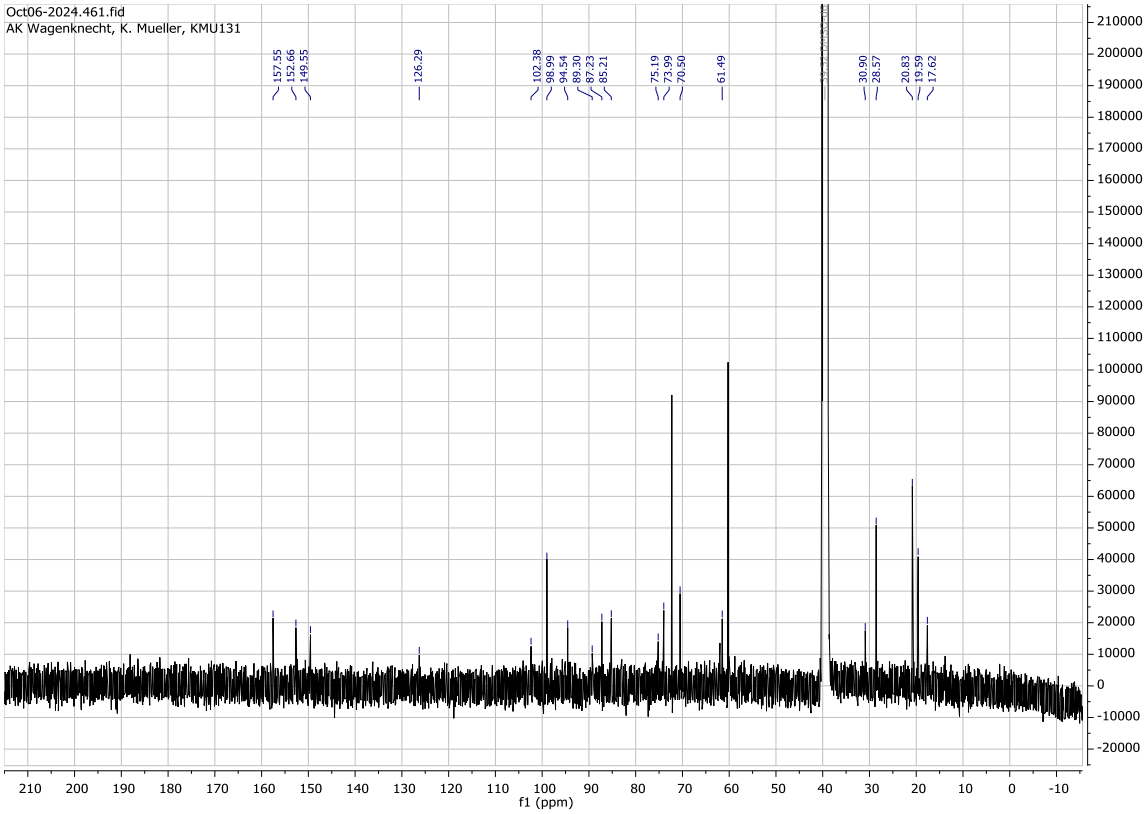
Oct06-2024.461.fid
AK Wagenknecht, K. Mueller, KMU131
157.55
152.66
149.55
126.29
102.38
98.99
94.54
89.30
87.23
85.21
75.19
73.99
70.90
61.49
30.90
28.57
20.83
19.59
17.62
f1 (ppm)

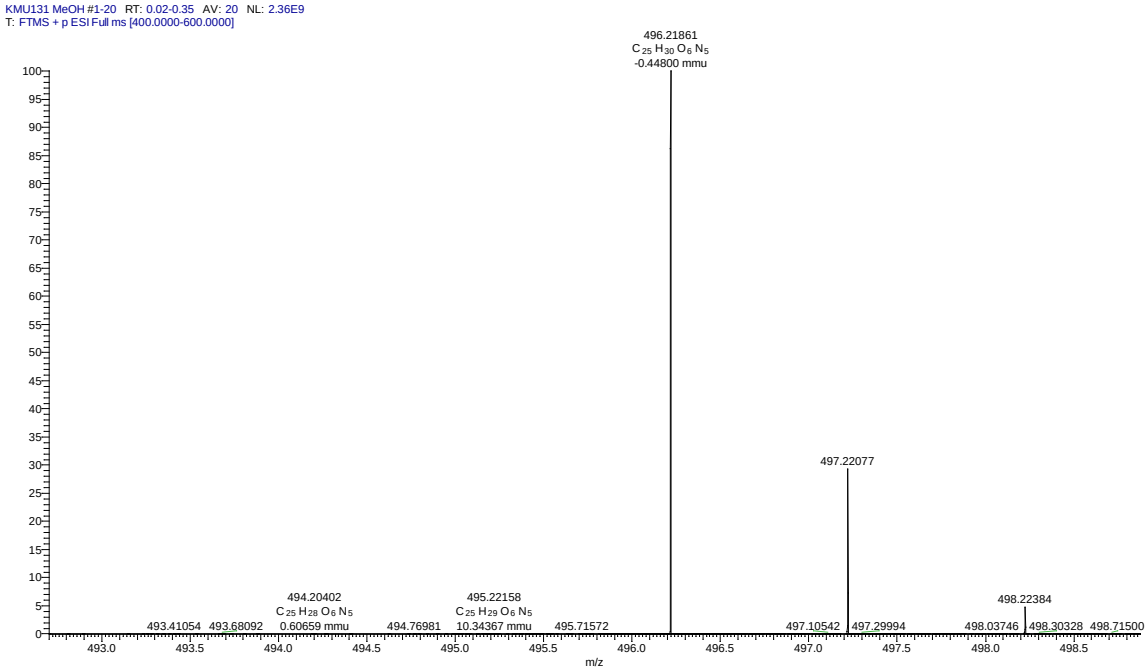
KMU131 MeOH #1-20 RT: 0.02-0.35 AV: 20 NL: 2.36E9
T: FTMS + p ESI Full ms [400.0000-600.0000]
496.21861
C25 H30 O6 N5
-0.44800 mmu
497.22077
494.20402
C25 H28 O6 N5
0.60659 mmu
495.22158
C25 H29 O6 N5
10.34367 mmu
498.22384
m/z

Compound 65

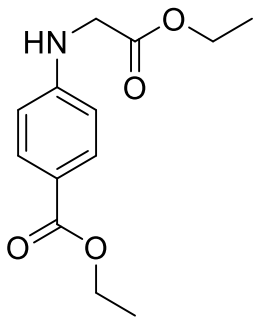

$C_{13}H_{17}NO_4$
251.28 g/mol

In a heated Schlenk flask under argon 3.00 g ethyl-4-aminobenzoate (18.2 mmol, 1.00 eq.) was dissolved in 27 mL DMF. 2.22 mL ethyl bromoacetate (3.34 g, 20.0 mmol, 1.10 eq.) and 3.48 mL N,N-diisopropylethylamine (2.58 g, 20.0 mmol, 1.10 eq.) were then added. The reaction mixture was allowed to stir overnight for 16 hours at 70 °C. The solvent was removed under reduced pressure. The residue was solved in diethylether and the solution was washed four times with brine solution. The organic phase was dried over sodium sulfate and the solvent was removed under reduced pressure. The residue was purified by automated column chromatography (cyclohexane/ethylacetate 0-50 %). The product was obtained as yellow crystals with a yield of 4.06 g (16.2 mmol, 89 %).

^{1}H-NMR (400 MHz, $CDCl_3$-*d_1*): δ (ppm) = 7.89 (d, *J* = 8.9 Hz, 2H, arom.), 6.56 (d, *J* = 8.9 Hz, 2H, arom.), 4.67 (s, 1H, R-N*H*-R), 4.29 (dq, *J* = 21.1, 7.1 Hz, 4H, 2xR-C*H_2*), 3.94 (s, 2H, R-NH-C*H_2*), 1.36 (t, *J* = 7.1, 3H, R-CH_3), 1.30 (t, *J* = 7.1 Hz, 3H, R-CH_3).

^{13}C-NMR (101 MHz, $CDCl_3$-*d_1*): δ (ppm) = 170.5, 166.9, 150.7, 131.7 (2C), 119.8 (2C), 111.9, 61.7, 60.4, 45.3, 14.6, 14.3.

HR-MS (ESI): m/z (calculated for $C_{13}H_{18}NO_4^+$): 252.1230 $[M+H]^+$; found: 252.1226 $[M+H]^+$.

The spectroscopic data is in agreement with literature.[165]

Compound 66

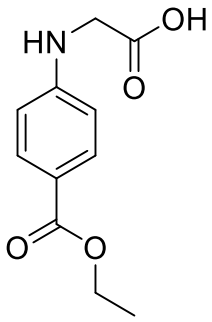

$C_{11}H_{13}NO_4$
223.23 g/mol

In a round bottom flask 3.00 g **65** (18.2 mmol, 1.00 eq.) was dissolved in 30 mL ethanol. 14 mL 1N NaOH (4 mL ~ 1 g) was added and the mixture was stirred for 3 hours at room temperature. The solvent was removed and the residue was dissolved in water and 14 mL 1N HCl was added. The formed white precipitate was collected by filtration, washed with water, and dried to give 2.08 g KMU157 (9.32 mmol, 76 %) as a white powder.

^{1}H-NMR (400 MHz, DMSO-d_6): δ (ppm) = 12.7 (s, 1H, R-COO*H*), 7.69 (d, *J* = 8.9 Hz, 2H, arom.), 6.73 (s, 1H, R-N*H*-R), 6.59 (d, *J* = 8.9 Hz, 2H, arom.), 4.21 (q, *J* = 7.1 Hz, 2H, R-CH_2), 3.88 (s, 2H, R-NH-CH_2), 1.27 (t, *J* = 7.1 Hz, 3H, R-CH_3).

^{13}C-NMR (126 MHz, DMSO-d_6): δ (ppm) = 172.0, 165.8, 152.3, 130.8 (2C), 116.8, 111.2 (2C), 59.6, 44.1, 14.4.

HR-MS (ESI): m/z (calculated for $C_{11}H_{12}NO_4^+$): 222.0761 $[M-H]^+$; found: 222.0767 $[M-H]^+$.

The spectroscopic data is in agreement with literature.[165]

Compound 67

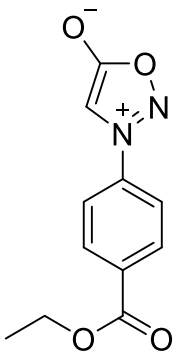

$C_{11}H_{10}N_2O_4$
234.21 g/mol

In a heated Schlenk flask under argon 2.08 g **66** (9.31 mmol, 1.00 eq.) was dissolved in 30 mL THF. 1.22 mL tBuONO (1.06 g, 10.2 mmol, 1.10 eq.) was added dropwise to the reaction mixture. The reaction was stirred for 1 hour, then 1.42 mL TFAA (2.15 g, 10.2 mmol, 1.10 eq.) was added dropwise. The reaction mixture was allowed to stir for 3 hours at room temperature. Ethyl acetate was added, and the reaction mixture was quenched with saturated $NaHCO_3$ solution. The mixture was extracted three times with ethyl acetate. The combined organic phases were dried over sodium sulfate and the solvent was removed under reduced pressure. The residue was dried under high vacuum. The product was obtained as an orange solid in a quantitative yield.

^{1}H-NMR (400 MHz, DMSO-d_6): δ (ppm) = 8.23 (d, *J* = 8.9 Hz, 2H, arom.), 8.10 (d, *J* = 8.8 Hz, 2H, arom.), 7.90 (s, 1H, sydnone core), 4.38 (q, *J* = 7.1 Hz, 2H, R-CH_2), 1.35 (t, *J* = 7.1 Hz, 3H, R-CH_3).

^{13}C-NMR (126 MHz, DMSO-d_6): δ (ppm) = 168.41, 164.40, 137.6, 133.2, 130.9 (2C), 122.0 (2C), 95.3, 61.5, 14.1.

HR-MS (ESI): m/z (calculated for $C_{11}H_{11}N_2O_4^+$): 235.0713 $[M+H]^+$; found: 235.0710 $[M+H]^+$.

The spectroscopic data is in agreement with literature.[83]

Compound 73

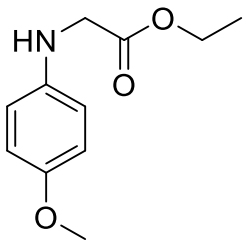

$C_{11}H_{15}NO_3$
209.25 g/mol

In a heated Schlenk flask under argon 3.00 g *p*-anisidine (24.4 mmol, 1.00 eq.) was dissolved in 4 mL ethanol. 2.69 mL ethyl bromoacetate (4.07 g, 24.4 mmol, 1.00 eq.) and 2.10 g sodium acetate (25.6 mmol, 1.05 eq.) were added and the reaction mixture was allowed to stir overnight for 16 hours at reflux. The solvent was removed under reduced pressure. The residue was solved in DCM/Brine. The water phase was extracted three times with DCM. The combined organic phase was dried over sodium sulfate and the solvent was removed under reduced pressure. The residue was purified by column chromatography (cyclohexane/ethylacetate 0-20 %). The product was obtained as yellow solid with a yield of 3.89 g (18.6 mmol, 76 %).

^{1}H-NMR (400 MHz, $CDCl_3$-d_1): δ (ppm) = 6.79 (d, *J* = 9.0 Hz, 2H, arom.), 6.59 (d, *J* = 8.9 Hz, 2H, arom.), 4.26 – 4.20 (m, 2H, R-CH_2), 4.10 (s, 1H, R-NH-R), 3.86 (s, 2H, R-NH-CH_2), 3.75 (s, 3H, R-O-CH_3) 1.29 (t, *J* = 7.1 Hz, 3H, R-CH_3).

The spectroscopic data is in agreement with literature.[130]

Compound 74

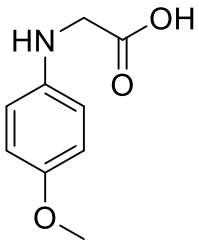

$C_9H_{11}NO_3$
181.19 g/mol

In a round bottom flask under argon 3.89 g **73** (18.6 mmol, 1.00 eq.) was dissolved in 54 mL ethanol/water (v/v, 1/1). 1.12 g NaOH (27.9 mmol, 1.50 eq.) was added and the mixture was stirred overnight at reflux. The reaction mixture was cooled to 0 °C and a pH value of 4 was adjusted with HCl. The formed precipitate was collected by filtration and dried under vacuum to give 2.63 g **74** (14.5 mmol, 78 %).

^{1}H-NMR (400 MHz, DMSO-d_6): δ (ppm) = 8.94 (s, 1H, R-COO*H*), 6.71 (d, *J* = 8.9 Hz, 2H, arom.), 6.50 (d, *J* = 9.0 Hz, 2H, arom.), 3.72 (s, 2H, R-NH-CH_2), 3.63 (s, 3H, R-O-CH_3).

^{13}C-NMR (126 MHz, DMSO-d_6): δ (ppm) = 172.9, 151.0, 142.4, 114.5 (2C), 113.1 (2C), 55.3, 45.5.

HR-MS (ESI): m/z (calculated for $C_9H_{12}NO_3^+$): 182.0812 $[M+H]^+$; found: 182.0809 $[M+H]^+$.

The spectroscopic data is in agreement with literature.[130]

Compound 75

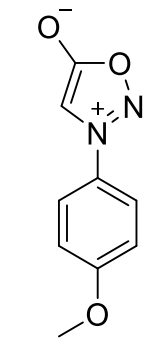

$C_9H_8N_2O_3$
192.17 g/mol

In a heated Schlenk flask under argon 2.63 g **74** (14.5 mmol, 1.00 eq.) was dissolved in 27 mL THF. 1.90 mL tBuONO (1.65 g, 16.0 mmol, 1.10 eq.) was added dropwise to the reaction mixture. The reaction was stirred for 1 hour, then 2.22 mL TFAA (3.36 g, 16.0 mmol, 1.10 eq.) was added dropwise. The reaction mixture was allowed to stir for 3 hours at room temperature. Ethyl acetate was added, and the reaction mixture was quenched with saturated $NaHCO_3$ solution. The mixture was extracted three times with ethyl acetate. The combined organic phases were dried over sodium sulfate and the solvent was removed under reduced pressure. The residue was dried under high vacuum. The product was obtained as light pink needle crystals with a yield of 1.26 g (6.56 mmol, 45 %).

^{1}H-NMR (400 MHz, $CDCl_3$-*d_1*): δ (ppm) = 7.68 – 7.60 (m, 2H, arom.), 7.12 – 7.03 (m, 2H, arom.), 6.63 (s, 1H, sydnone core), 3.90 (s, 3H, R-O-C*H_3*).

^{13}C-NMR (101 MHz, $CDCl_3$-*d_1*): δ (ppm) = 169.2, 162.7, 122.9 (2C), 115.4 (2C), 93.5, 56.0.

HR-MS (ESI): m/z (calculated for $C_9H_9N_2O_3^+$): 193.0608 $[M+H]^+$; found: 193.0605 $[M+H]^+$.

The spectroscopic data is in agreement with literature.[130]

Compound 77

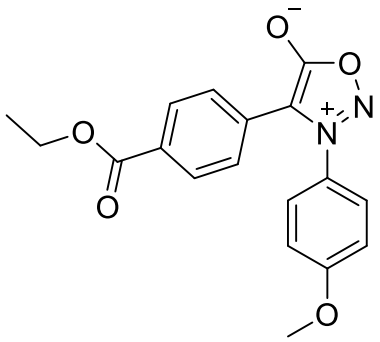

$C_{18}H_{16}N_2O_5$
340.34 g/mol

A mixture of 0.200 g **75** (1.04 mmol, 1.00 eq.), 0.27 mL aryl halide **76** (0.381 g, 1.67 mmol, 1.60 eq.), 0.012 g $Pd(OAc)_2$ (0.05 mmol, 0.05 eq.), 0.050 g XPhos (0.10 mmol, 0.10 eq.) and 0.360 g K_2CO_3 (2.60 mmol, 2.50 eq.) in 3.50 mL DMF was placed in a heated flask under argon. The flask equipped with a reflux condenser was heated at 100 °C for 19 h in the dark. After completion of the reaction (as monitored by TLC), the mixture was cooled to room temperature. Then, H_2O (30 mL~57 mg approach) was added and the mixture extracted with EtOAc (3 × 20 mL ~57 mg approach or 3 x 20 mL EE/PT 9/1). The combined organic layers were dried (Na_2SO_4), and concentrated under reduced pressure. The resulting residue was purified by flash column chromatography (Cyclohexane/EE 10 - 40 % or PT/EE 10 - 40 %). The product was obtained as yellow foam with a yield of 0.408 g (1.20 mmol, 58 %).

^{1}H-NMR (300 MHz, $CDCl_3$-*d_1*): δ (ppm) = 7.96 (d, *J* = 8.4 Hz, 2H, arom.), 7.40 (d, *J* = 7.7 Hz, 4H, arom.), 7.05 (d, *J* = 8.9 Hz, 2H, arom.), 4.35 (q, *J* = 7.1 Hz, 2H, R-CH_2), 1.37 (t, *J* = 7.1, 3H, R-CH_3).

^{13}C-NMR (75 MHz, $CDCl_3$-*d_1*): δ (ppm) = 166.9, 165.9, 162.5, 130.0, 129.9 (2C), 129.0, 127.2, 126.7 (2C), 126.3 (2C), 115.5 (2C), 106.8, 61.3, 55.9, 14.4.

HR-MS (ESI): m/z (calculated for $C_{18}H_{17}N_2O_5^+$): 341.1132 $[M+H]^+$; found: 341.1126 $[M+H]^+$.

The spectroscopic data is in agreement with literature.[130]

Compound 69

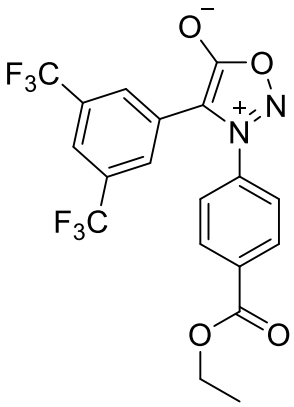

$C_{19}H_{12}F_6N_2O_4$
446.31 g/mol

A mixture of 0.200 g **67** (0.85 mmol, 1.00 eq.), 0.24 mL aryl halide **68** (0.400 g, 1.37 mmol, 1.60 eq.), 0.010 g $Pd(OAc)_2$ (0.04 mmol, 0.05 eq.), 0.041 g XPhos (0.09 mmol, 0.10 eq.) and 0.295 g K_2CO_3 (2.13 mmol, 2.50 eq.) in 3.50 mL DMF was placed in a heated flask under argon. The flask equipped with a reflux condenser was heated at 100 °C for 19 h in the dark. After completion of the reaction (as monitored by TLC), the mixture was cooled to room temperature. Then, H_2O (30 mL~57 mg approach) was added and the mixture extracted with EtOAc (3 × 20 mL ~57 mg approach or 3 x 20 mL EE/PT 9/1). The combined organic layers were dried (Na_2SO_4) and concentrated under reduced pressure. The resulting residue was purified by flash column chromatography (Cyclohexane/EE 10 - 40 % or PT/EE 10 - 40 %). The product was obtained as brown solid with a yield of 0.225 g (0.50 mmol, 59 %).

^{1}H-NMR (300 MHz, $CDCl_3$-*d_1*): δ (ppm) = 8.39 – 8.28 (m, 2H, arom.), 7.77 (s, 1H, arom.), 7.72 (s, 1H, arom.), 7.66 – 7.58 (m, 2H, arom.), 4.46 (q, *J* = 7.1 Hz, 2H, R-CH_2), 1.44 (t, *J* = 7.0 Hz, 3H, R-CH_3).

^{13}C-NMR (75 MHz, $CDCl_3$-*d_1*): δ (ppm) = 166.1, 164.4, 137.1, 135.0, 132.8, 132.3, 132.0 (2C), 126.6, 125.0 (2C), 124.6, 122.1, 121.0, 105.3, 62.3, 14.3.

HR-MS (ESI): m/z (calculated for $C_{19}H_{13}F_6N_2O_4^+$): 447.0774 $[M+H]^+$; found: 447.0765 $[M+H]^+$.

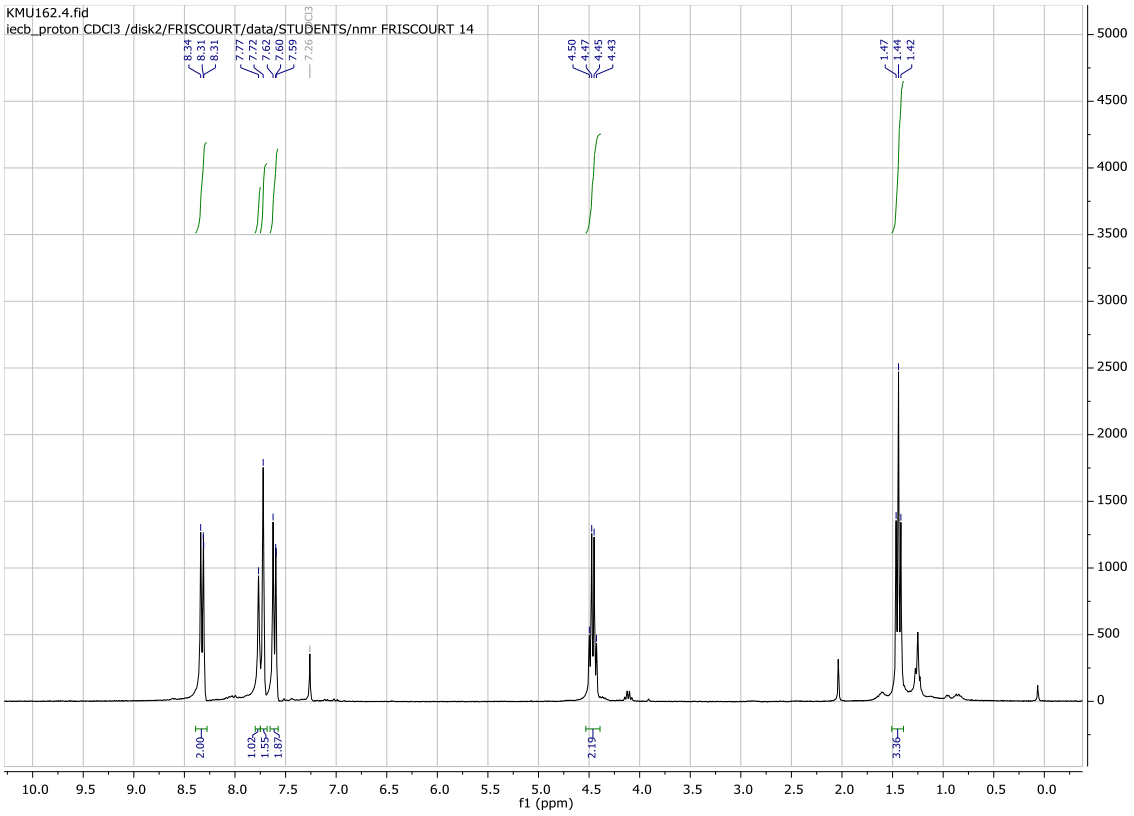

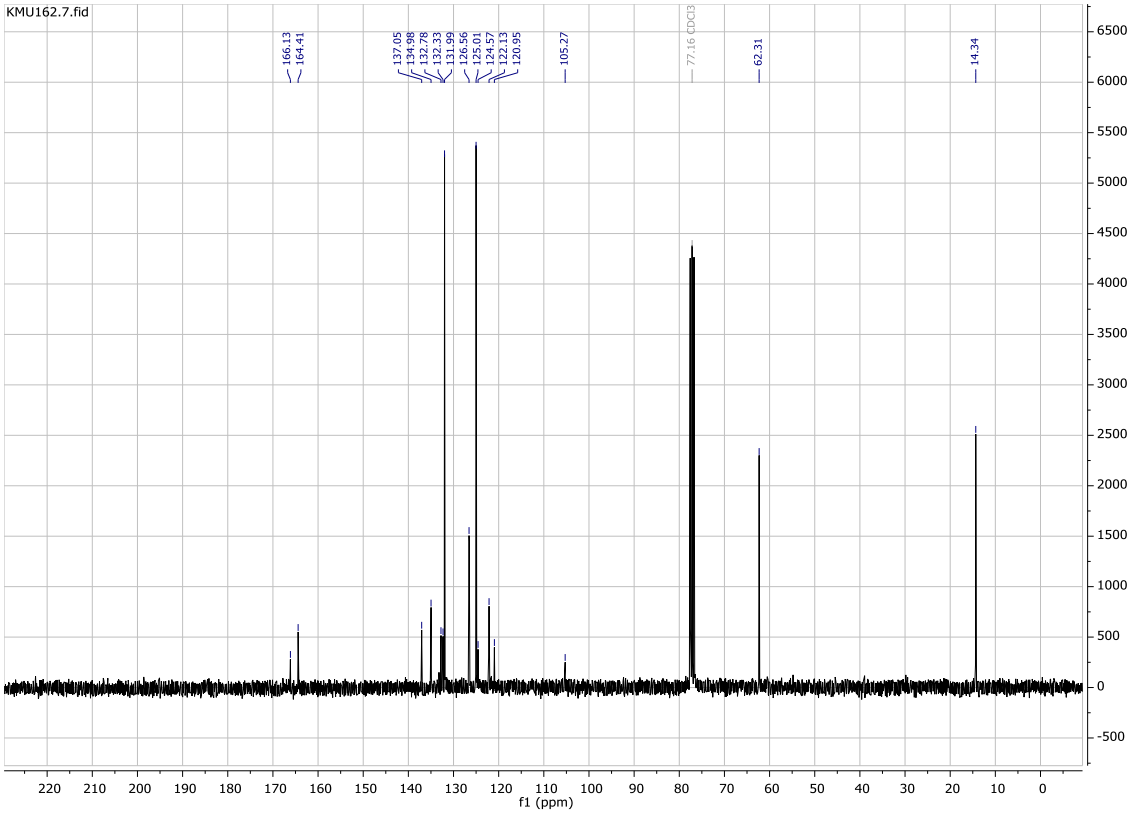
KMU162.7.fid
166.13
164.41
137.05
134.98
132.78
132.33
131.99
126.56
125.01
124.57
122.13
120.95
105.27
77.16 CDCl3
62.31
14.34
f1 (ppm)

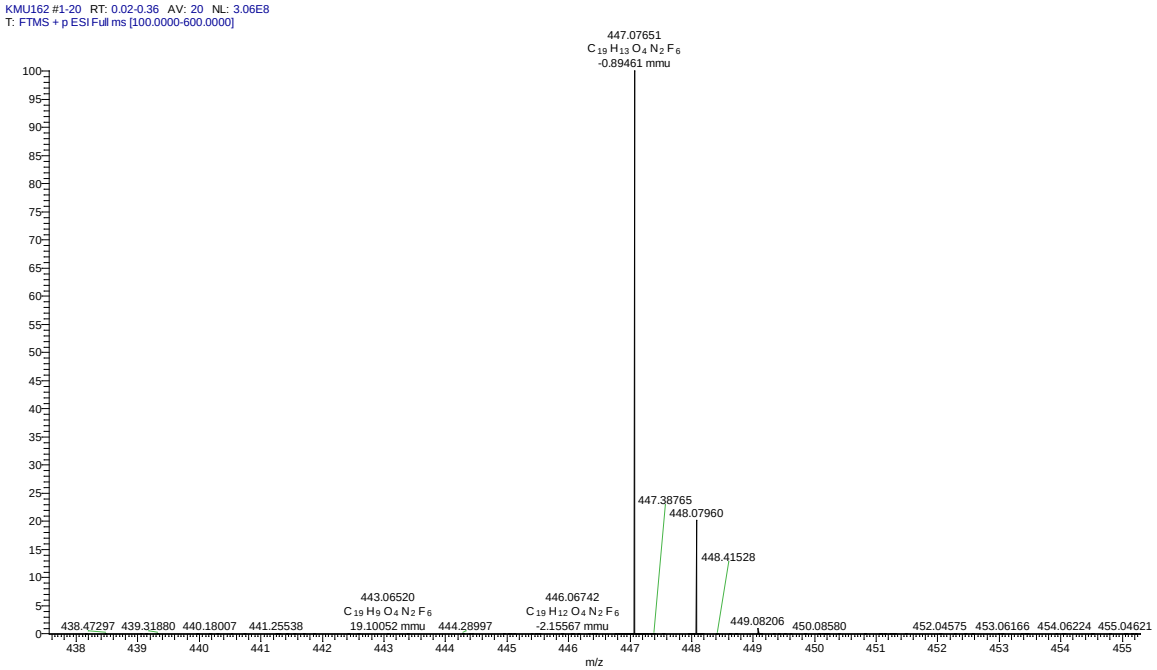
KMU162 #1-20 RT: 0.02-0.36 AV: 20 NL: 3.06E8
T: FTMS + p ESI Full ms [100.0000-600.0000]
447.07651
C19 H13 O4 N2 F6
-0.89461 mmu
447.38765
448.07960
448.41528
443.06520
C19 H9 O4 N2 F6
19.10052 mmu
446.06742
C19 H12 O4 N2 F6
-2.15567 mmu
438.47297
439.31880
440.18007
441.25538
444.28997
449.08206
450.08580
452.04575
453.06166
454.06224
455.04621
m/z

Compound 79

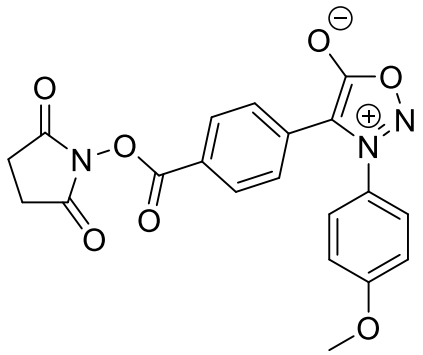

$C_{20}H_{15}N_3O_7$
409.35 g/mol

In a Schlenk flask under argon, 0.408 g **77** (1.20 mmol, 1.00 eq.) was placed and dissolved in 5 mL THF. The solution was cooled to 0 °C with an ice bath. Meanwhile, 0.072 g lithium hydroxide (3.00 mmol, 2.50 eq.) was dissolved in 5 mL water and then added to the reaction solution. The solution was allowed to stir at 0 °C for 30 minutes and then at room temperature for 4 hours. The THF was evaporated off. The remaining basic aqueous solution was adjusted with 1M HCl to a pH 3-4. The aqueous phase was extracted three times with DCM. The combined organic phases were washed with Brine solution and then dried over sodium sulfate. The solvent was removed. The combined organic layers were dried (Na_2SO_4) and concentrated under reduced pressure. The residue was used without further purification and was solved in 5 mL DMF in a heated flask under argon. 0.084 g NHS-ester (0.73 mmol, 1.50 eq.) and 0.141 g EDC were added, and the reaction mixture was stirred overnight at room temperature. 20 mL Ethyl acetate was added, and the organic phase was extracted three times with 60 mL water and once with 60 mL brine solution and then dried over sodium sulfate. The solvent was removed under reduced pressure and the residue was purified by column chromatography (SiO_2, DCM/MeOH 0 – 5 %). The product was obtained as a yellow foam with a yield of 0.130 g (0.32 mmol, 65 %).

^{1}H-NMR (400 MHz, $CDCl_3$-d_1): δ (ppm) = 8.04 (d, *J* = 8.7 Hz, 2H, arom.), 7.48 (d, *J* = 8.7 Hz, 2H, arom.), 7.41 (d, *J* = 8.7 Hz, 2H, arom.), 7.09 (d, *J* = 9.0 Hz, 2H, arom.), 3.93 (s, 3H, R-OCH_3), 2.90 (s, 4H, 2xCH_2)

^{13}C-NMR (101 MHz, $CDCl_3$-d_1): δ (ppm) = 169.3, 166.7, 162.7, 161.3, 131.3, 131.0 (2C), 127.1, 126.8 (2C), 126.3 (2C), 124.4, 115.7, 56.0 (2C), 29.8, 25.8 (2C).

HR-MS (ESI): m/z (calculated for $C_{20}H_{16}N_3O_7^+$): 410.0983 $[M+H]^+$; found: 410.0992 $[M+H]^+$.

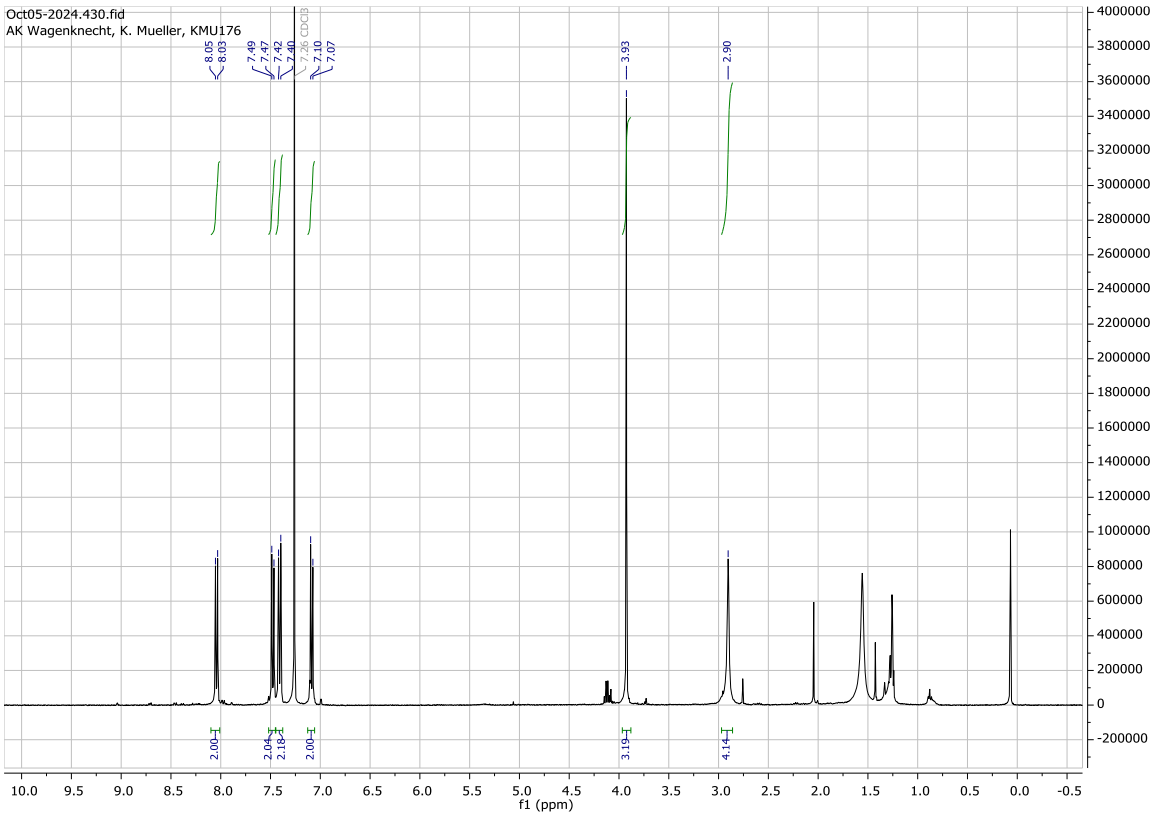

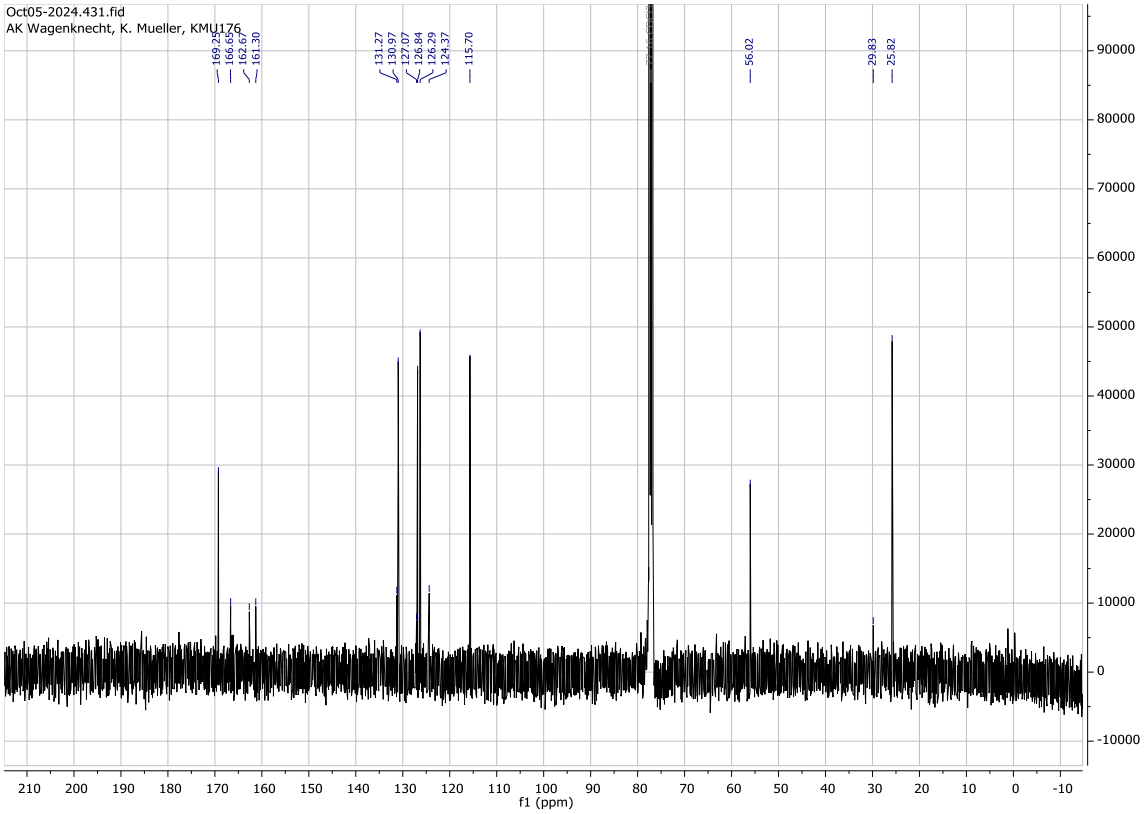
Oct05-2024.431.fid
AK Wagenknecht, K. Mueller, KMU176
169.25
166.65
162.67
161.30
131.27
130.97
127.07
126.84
126.29
124.37
115.70
56.02
29.83
25.82
f1 (ppm)

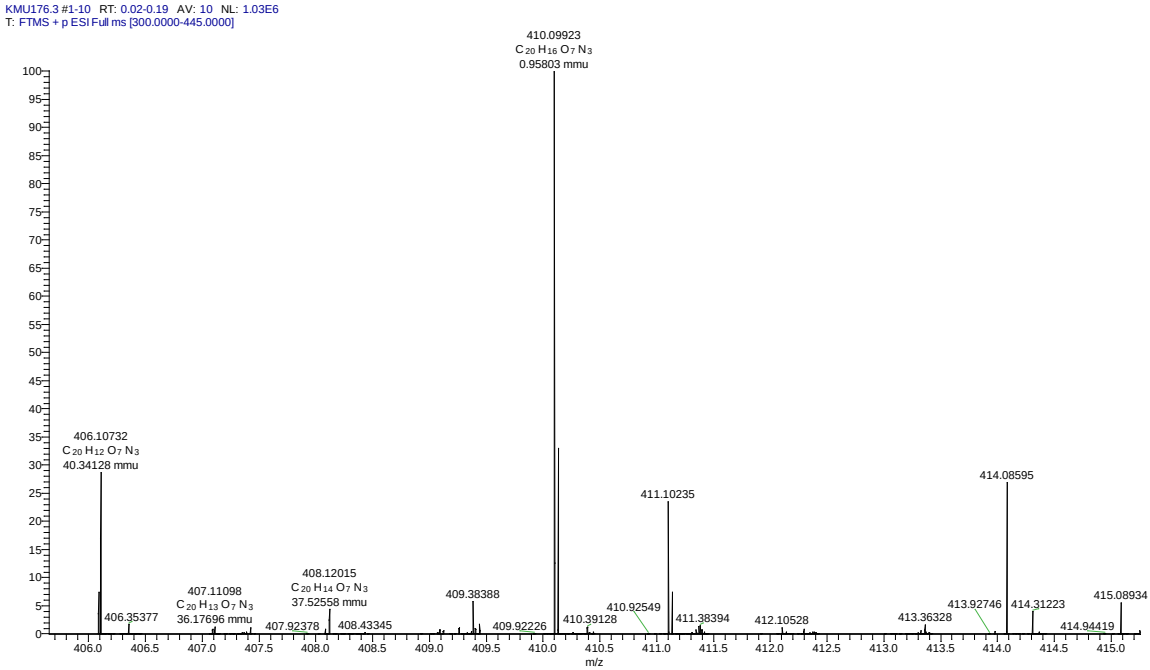
KMU176.3 #1-10 RT: 0.02-0.19 AV: 10 NL: 1.03E6
T: FTMS + p ESI Full ms [300.0000-445.0000]
410.09923
C20 H16 O7 N3
0.95803 mmu
406.10732
C20 H12 O7 N3
40.34128 mmu
406.35377
407.11098
C20 H13 O7 N3
36.17696 mmu
407.92378
408.12015
C20 H14 O7 N3
37.52558 mmu
408.43345
409.38388
409.92226
410.39128
410.92549
411.10235
411.38394
412.10528
413.36328
413.92746
414.08595
414.31223
414.94419
415.08934
m/z

Compound 71

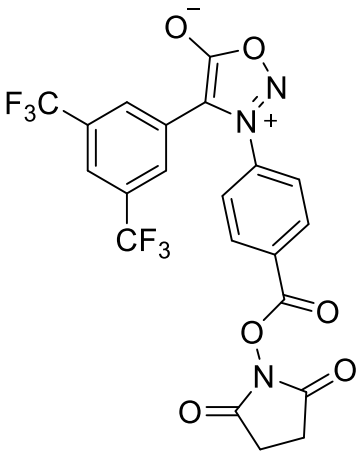

$C_{21}H_{11}F_6N_3O_6$
515.32 g/mol

In a Schlenk flask under argon, 0.172 g **69** (0.39 mmol, 1.00 eq.) was placed and dissolved in 3 mL THF. The solution was cooled to 0 °C with an ice bath. Meanwhile, 0.061 g lithium hydroxide monohydrate (1.45 mmol, 5.00 eq.) was dissolved in 3 mL water and then added to the reaction solution. The solution was allowed to stir at 0 °C for 30 minutes and then at room temperature for 4 hours. The THF was evaporated off. The remaining basic aqueous solution was adjusted with 1M HCl to a pH 3-4. The aqueous phase was extracted three times with DCM. The combined organic phases were washed with Brine solution and then dried over sodium sulfate. The solvent was removed. The combined organic layers were dried (Na_2SO_4) and concentrated under reduced pressure. The residue was used without further purification and was solved in 5 mL DMF in a heated flask under argon. 0.067 g NHS-ester (0.58 mmol, 1.50 eq.) and 0.111 g EDC (0.58 mmol, 1.50 eq.) were added, and the reaction mixture was stirred overnight at room temperature. 20 mL Ethyl acetate was added, and the organic phase was extracted three times with 60 mL water and once with 60 mL brine solution and then dried over sodium sulfate. The solvent was removed under reduced pressure and the residue was purified by column chromatography (SiO_2, DCM/MeOH 0 – 5 %). The product was obtained as a light brown solid with a yield of 0.100 g (0.19 mmol, 49 %).

^{1}H-NMR (300 MHz, $CDCl_3$-d_1): δ (ppm) = 8.44 – 8.40 (m, 2H, arom.), 7.82 (s, 1H, arom.), 7.77 – 7.74 (m, 2H, arom.), 7.73 – 7.70 (m, 2H, arom.), 2.95 (s, 4H, 2xCH_2).

^{13}C-NMR (75 MHz, $CDCl_3$-d_1): δ (ppm) = 168.8, 166.1, 160.2, 138.6, 132.9 (2C), 132.7, 129.9, 126.83, 126.80, 126.4, 125.5 (2C), 123.8, 122.5, 121.6, 105.3, 25.8 (2C).

HR-MS (ESI): m/z (calculated for $C_{21}H_{12}F_6N_3O_6^+$): 516.0625 $[M+H]^+$; found: 516.0632 $[M+H]^+$.

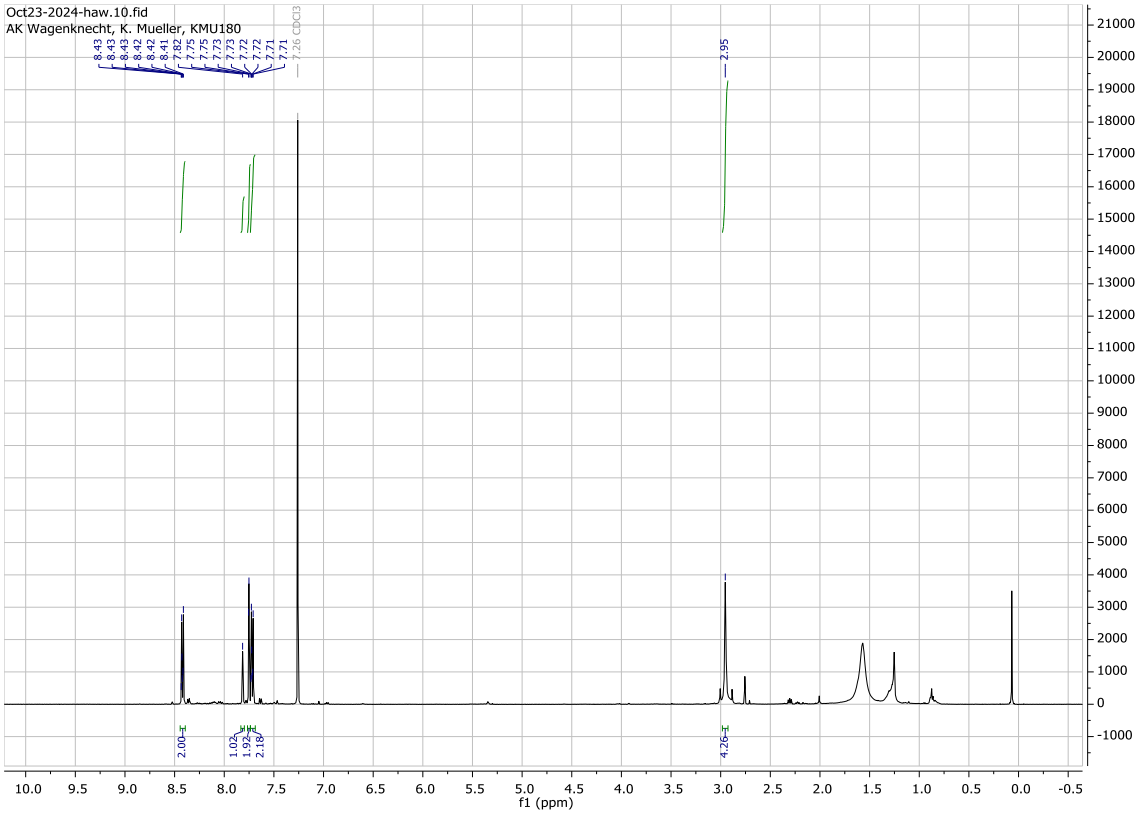

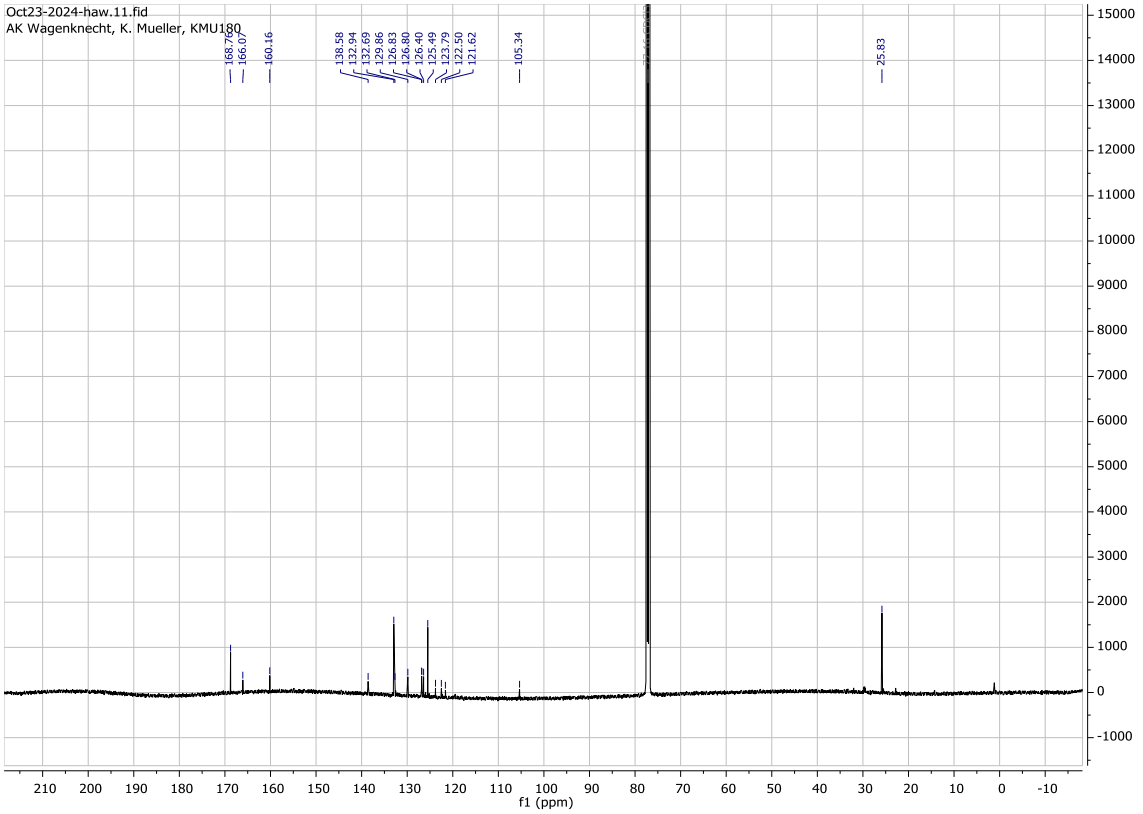
Oct23-2024-haw.11.fid
AK Wagenknecht, K. Mueller, KMU180
168.76
166.07
160.16
138.58
132.94
132.69
129.86
126.83
126.80
126.40
125.49
123.79
122.50
121.62
105.34
25.83
f1 (ppm)

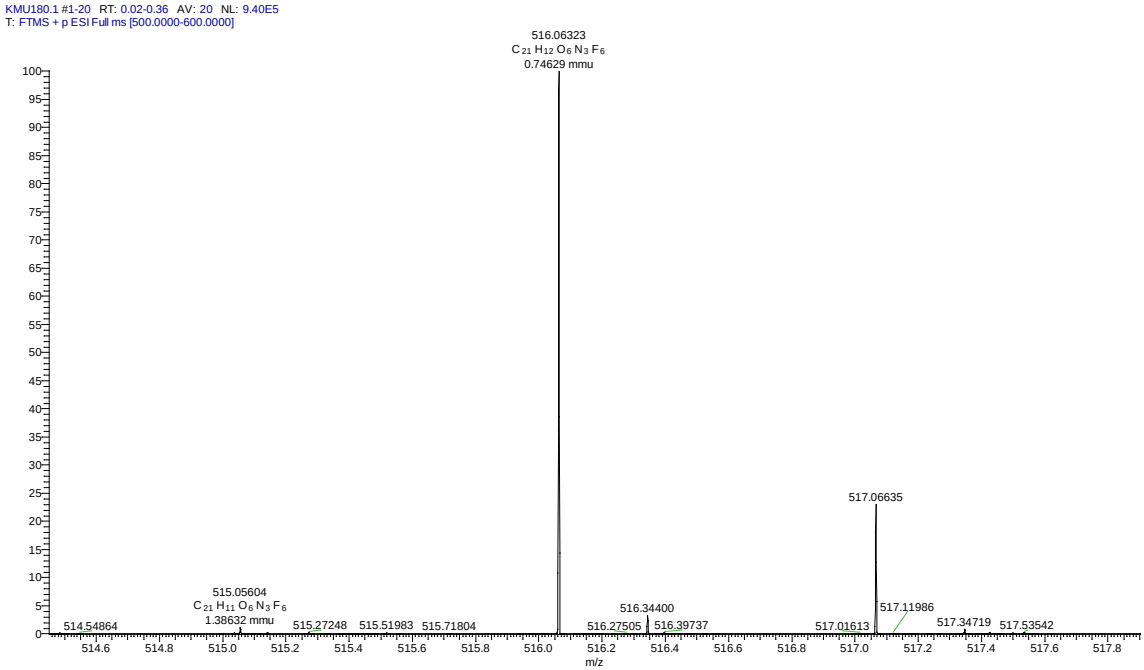
KMU180.1 #1-20 RT: 0.02-0.36 AV: 20 NL: 9.40E5
T: FTMS + p ESI Full ms [500.0000-600.0000]
516.06323
C21 H12 O6 N3 F6
0.74629 mmu
517.06635
515.05604
C21 H11 O6 N3 F6
1.38632 mmu
516.34400
517.11986
517.34719
517.53542
514.54864
515.27248
515.51983
515.71804
516.27505
516.39737
517.01613
m/z

Compound 81

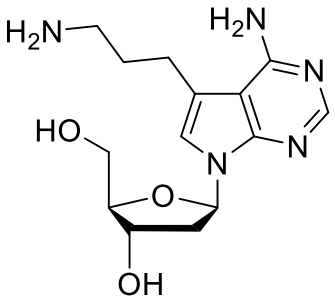

$C_{14}H_{21}N_5O_3$
307.35 g/mol

In a heated flask under argon atmosphere, 0.100 g **80** (0.25 mmol, 1.00 eq.) was dissolved in 5 mL of concentrated ammonium hydroxide solution and stirred overnight at room temperature. The solvent was removed under reduced pressure and the residue was dried in a high vacuum. The product was obtained as a brown solid with a quantitative yield.

The spectroscopic data is in agreement with literature.[166]

Compound 1

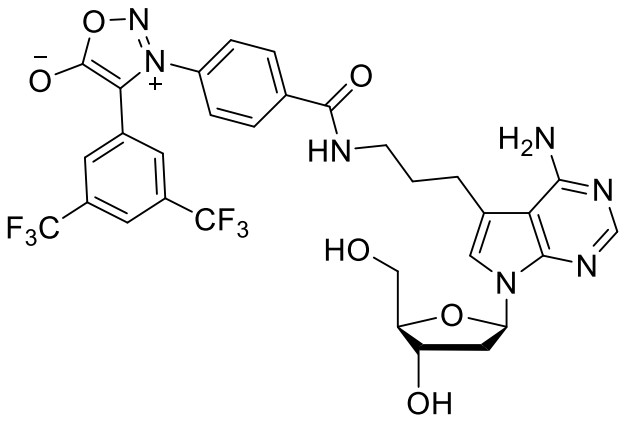

$C_{31}H_{27}F_6N_7O_6$
707.59 g/mol

In a Schlenk flask under argon, 0.050 g **81** (0.16 mmol, 1.00 eq.) was placed and dissolved in 5 mL DMF. 0.09 mL triethylamine (0.07 g, 0.65 mmol, 4.00 eq.) and 0.101 g **71** (0.20 mmol, 1.20 eq.) were added, and the reaction mixture was stirred over night at room temperature. The solvent was removed under reduced pressure and the crude product was redissolved in 10 mL methanol. The solution was treated with Amberlite IRA-402 bicarbonate form for 30 minutes. After filtration, the solvent was evaporated. The crude mixture was purified via column chromatography (SiO_2, DCM/MeOH 0 – 10 %). The product was obtained as a beige foam (0.06 g, 0.08 mmol, 49 %).

^{1}H-NMR (300 MHz, DMSO-d_6: δ (ppm) = 8.76 (t, *J* = 5.3 Hz, 1H, N*H*), 8.11 (d, *J* = 8.6 Hz, 3H, arom.), 8.02 (s, 1H, H-2), 7.86 (d, *J* = 8.6 Hz, 2H, arom.), 7.78 (s, 2H, arom.), 7.14 (s, 1H, H-8), 6.57 (s, 2H, R-NH_2), 6.47 (dd, *J* = 8.3, 6.0 Hz, 1H, H-1'), 5.24 (d, *J* = 4.1 Hz, 1H, 3'-OH), 5.07 (t, *J* = 5.6 Hz, 1H, 5'-OH), 4.38 – 4.25 (m, 1H, H-3'), 3.79 (q, *J* = 4.3 Hz, 1H, H-4'), 3.59 – 3.46 (m, 4H, 2xH-5', CH_2-NH), 2.86 – 2.77 (m, 2H, CH_2), 2.48 – 2.41 (m, 1H, H-2$_a$'), 2.11 (ddd, *J* = 12.8, 5.8, 2.3 Hz, 1H, H-2$_b$'), 1.84 (p, *J* = 7.5 Hz, 2H, CH_2).

^{13}C-NMR (75 MHz, DMSO-d_6): δ (ppm) = 166.0, 164.6, 157.6, 151.4, 150.5, 138.4, 135.4, 130.8, 130.3, 129.2 (2C), 127.3, 127.21, 127.17, 125.8 (2C), 118.8, 114.7, 106.3, 102.1, 87.2, 82.8, 71.2, 62.2, 54.9, 30.1, 23.4.

HR-MS (ESI): m/z (calculated for $C_{31}H_{28}F_6N_7O_6^+$): 708.2000 $[M+H]^+$; found: 708.2007 $[M+H]^+$.

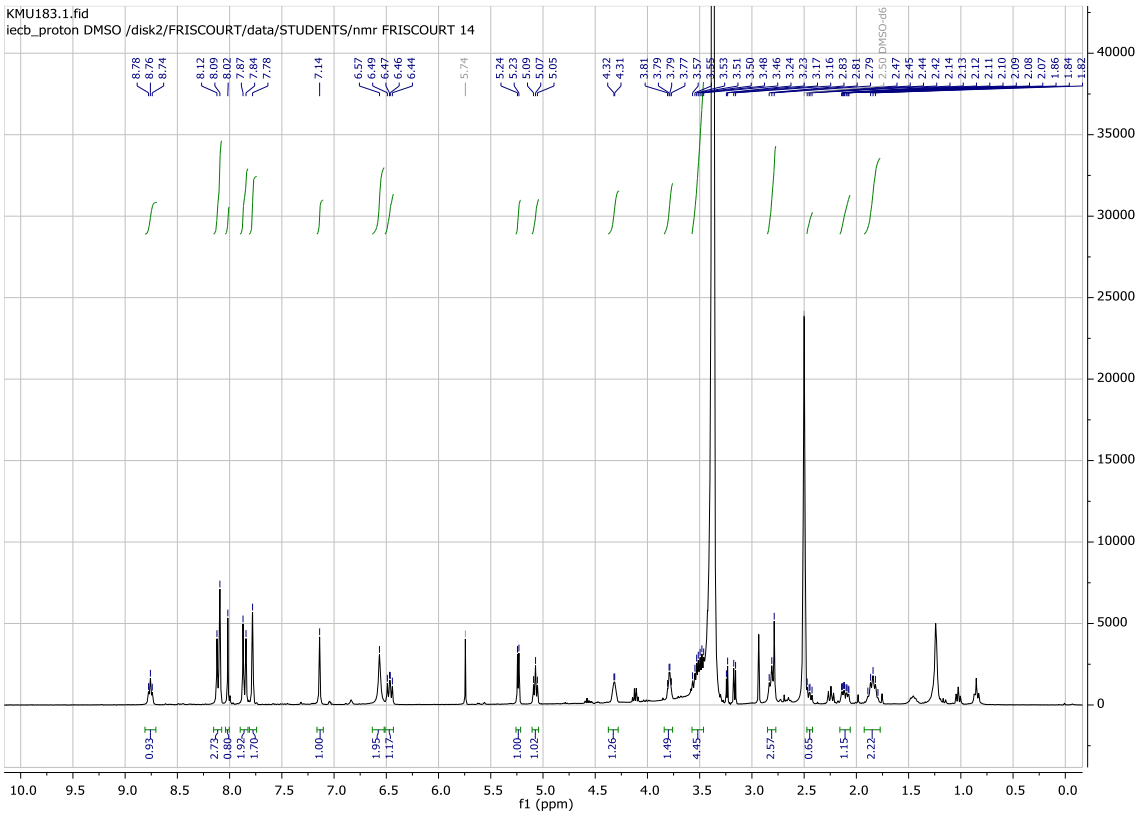

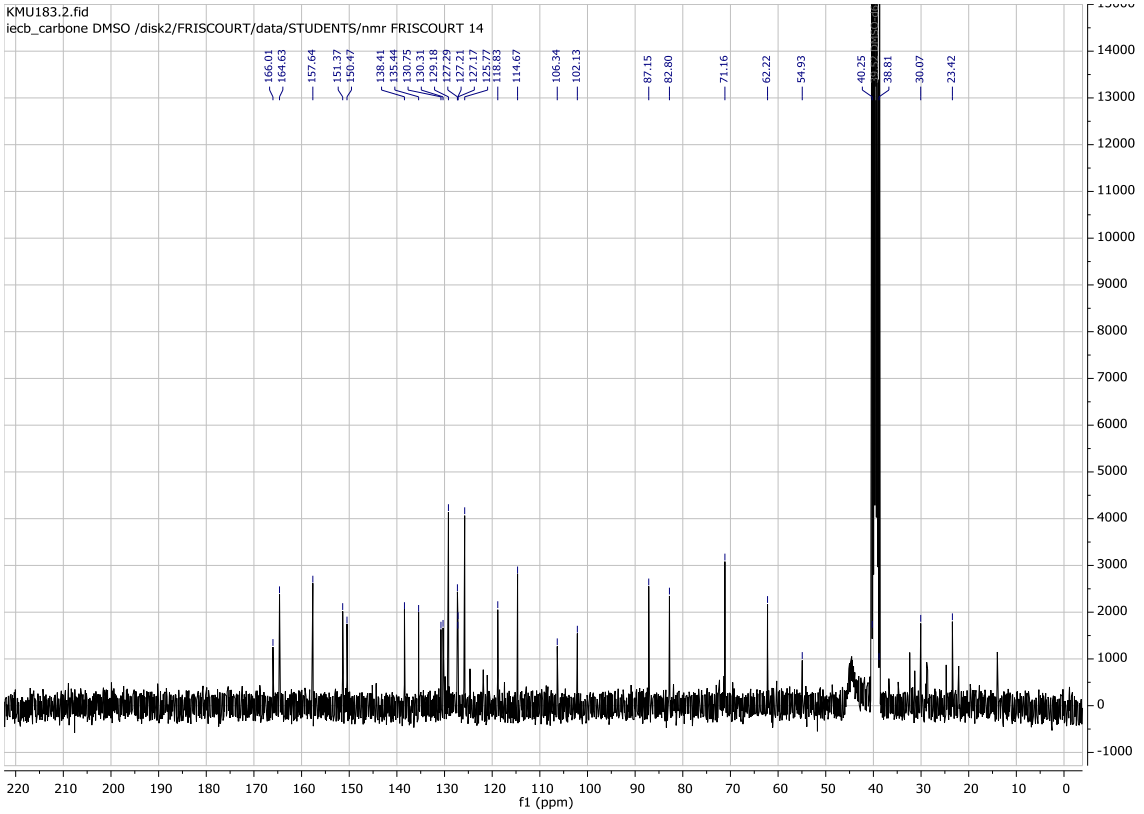
KMU183.2.fid
iecb_carbone DMSO /disk2/FRISCOURT/data/STUDENTS/nmr FRISCOURT 14
166.01
164.63
157.64
151.37
150.47
138.41
135.44
130.75
130.31
129.18
127.29
127.21
127.17
125.77
118.83
114.67
106.34
102.13
87.15
82.80
71.16
62.22
54.93
40.25
38.81
30.07
23.42
f1 (ppm)

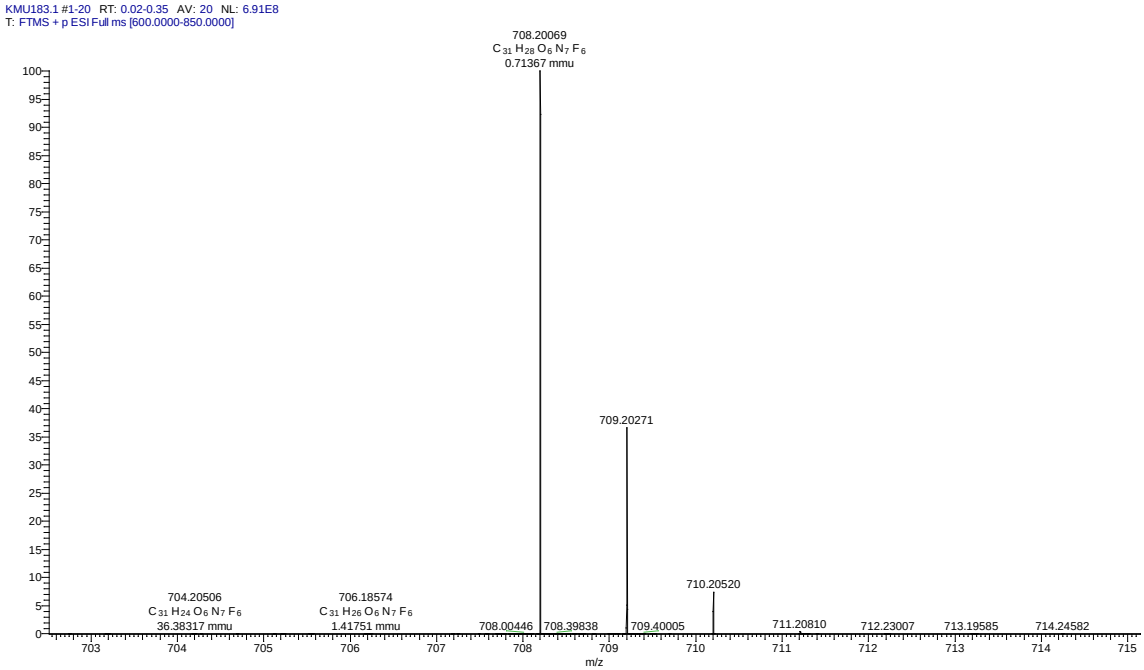
KMU183.1 #1-20 RT: 0.02-0.35 AV: 20 NL: 6.91E8
T: FTMS + p ESI Full ms [600.0000-850.0000]
708.20069
C31 H28 O6 N7 F6
0.71367 mmu
709.20271
710.20520
704.20506
C31 H24 O6 N7 F6
36.38317 mmu
706.18574
C31 H26 O6 N7 F6
1.41751 mmu
708.00446
708.39838
709.40005
711.20810
712.23007
713.19585
714.24582
m/z

Compound 2

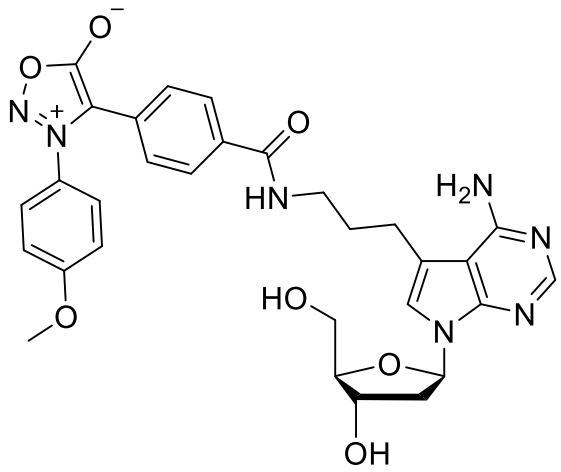

$C_{30}H_{31}N_7O_7$
601.62 g/mol

In a Schlenk flask under argon, 0.050 g **81** (0.16 mmol, 1.00 eq.) was placed and dissolved in 5 mL DMF. 0.09 mL triethylamine (0.07 g, 0.65 mmol, 4.00 eq.) and 0.080 g **79** (0.20 mmol, 1.20 eq.) were added, and the reaction mixture was stirred over night at room temperature. The solvent was removed under reduced pressure and the crude product was redissolved in 10 mL methanol. The solution was treated with Amberlite IRA-402 bicarbonate form for 30 minutes. After filtration, the solvent was evaporated. The crude mixture was purified via column chromatography (SiO_2, DCM/MeOH 0 – 10 %). The product was obtained as a white solid (0.011 g, 0.018 mmol, 11 %).

^{1}H-NMR (500 MHz, DMSO-d_6: δ (ppm) = 8.47 (t, *J* = 5.6 Hz, 1H, N*H*), 8.01 (s, 1H, H-2), 7.77 (d, *J* = 8.6 Hz, 2H, arom.), 7.65 (d, *J* = 9.0 Hz, 2H, arom.), 7.31 (d, *J* = 8.6 Hz, 2H, arom.), 7.19 (d, *J* = 9.0 Hz, 2H, arom.), 7.13 (s, 1H, H-8), 6.56 (s, 2H, R-NH_2), 6.46 (dd, *J* = 8.3, 5.9 Hz, 1H, H-1'), 5.22 (d, *J* = 4.0 Hz, 1H, 3'-OH), 5.05 (t, *J* = 5.6 Hz, 1H, 5'-OH), 4.35 – 4.26 (m, 1H, H-3'), 3.85 (s, 3H, OMe), 3.78 (td, *J* = 4.6, 2.4 Hz, 1H, H-4'), 3.56 – 3.51 (m, 1H, H-5$_a$'), 3.50 – 3.47 (m, 2H, CH_2-NH), 3.42 (d, *J* = 5.1 Hz, 1H, H-5$_b$'), 2.78 (t, *J* = 7.5 Hz, 2H, CH_2), 2.48 – 2.42 (m, 1H, H-2$_a$'), 2.09 (ddd, *J* = 13.0, 5.9, 2.4 Hz, 1H, H-2$_b$'), 1.84 (p, *J* = 7.5 Hz, 2H, CH_2).

^{13}C-NMR (126 MHz, DMSO-d_6): δ (ppm) = 166.2, 165.5, 161.7, 157.6, 151.3, 150.4, 134.1, 127.3 (2C), 127.1 (2C), 126.6 (2C), 115.3 (2C), 114.7, 107.5, 87.1, 82.7, 72.3, 71.1, 62.2, 60.3, 55.8, 40.1, 39.9, 39.8, 39.6, 39.4, 30.1.

HR-MS (ESI): m/z (calculated for $C_{30}H_{32}N_7O_7^+$): 602.2358 $[M+H]^+$; found: 602.2358 $[M+H]^+$.

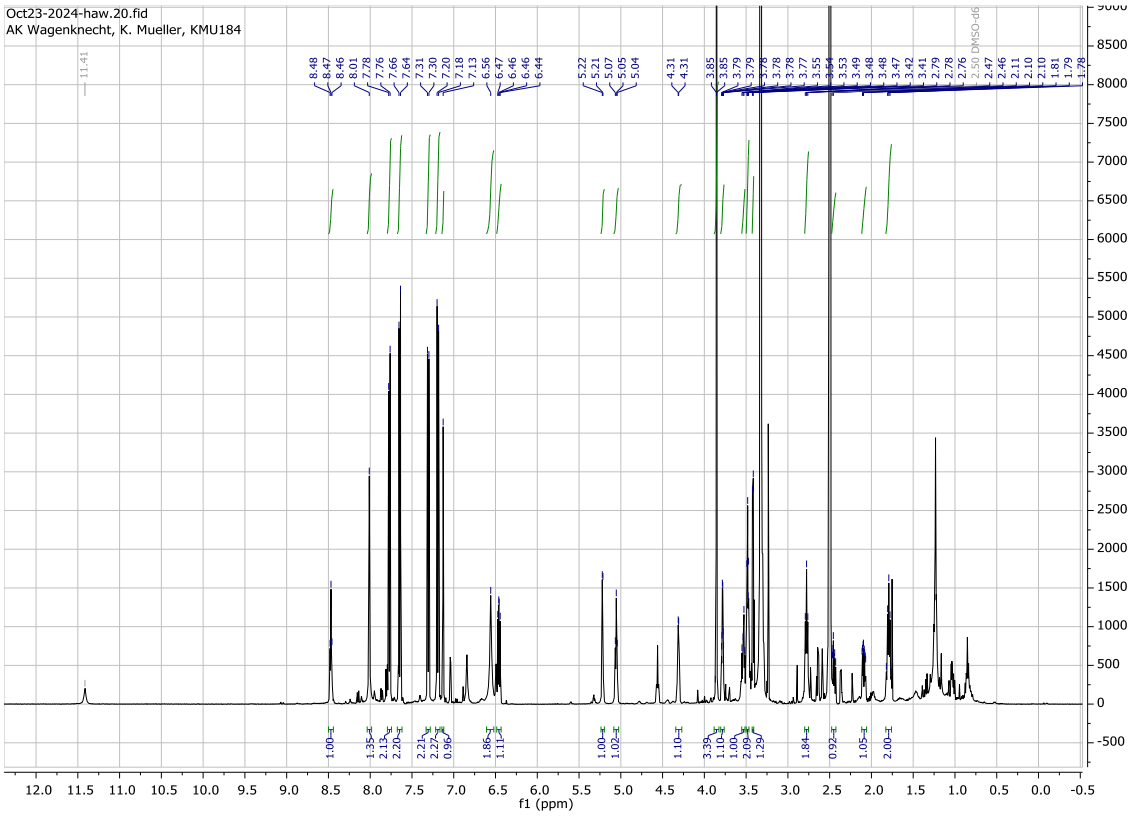

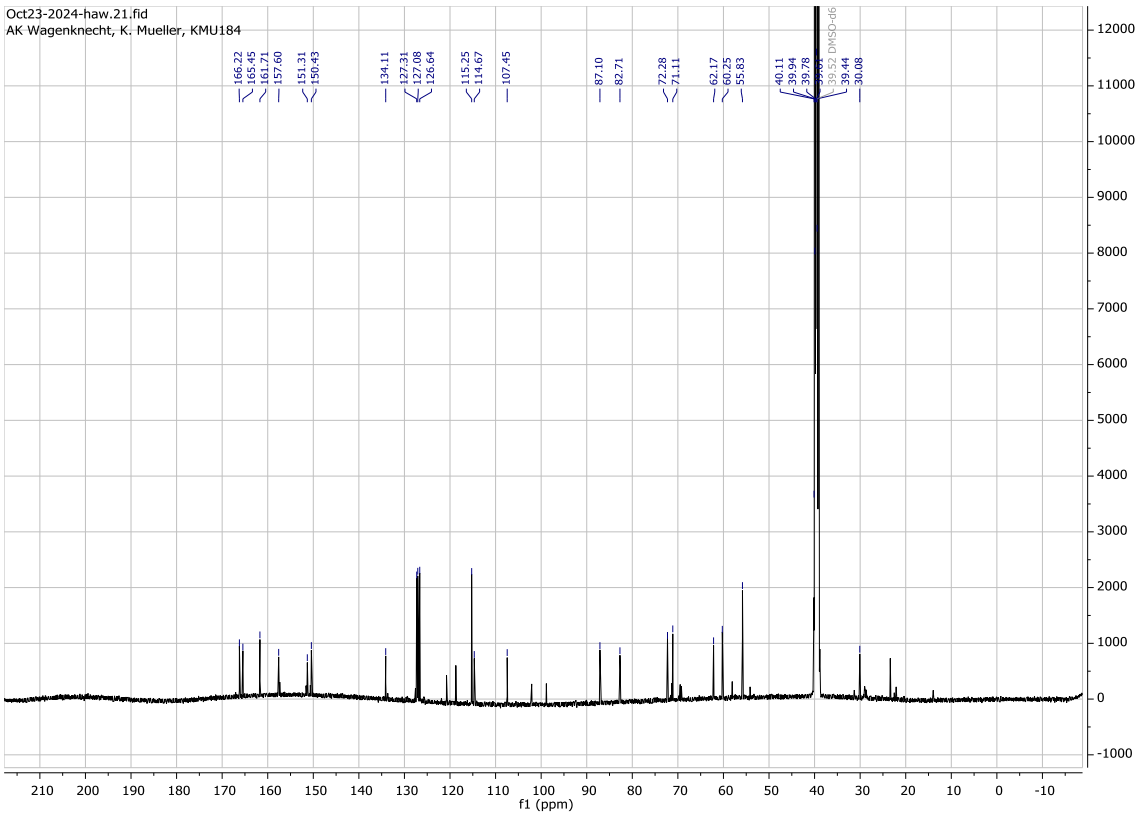
Oct23-2024-haw.21.fid
AK Wagenknecht, K. Mueller, KMU184
166.22
165.45
161.71
157.60
151.31
150.43
134.11
127.31
127.08
126.64
115.25
114.67
107.45
87.10
82.71
72.28
71.11
62.17
60.25
55.83
40.11
39.94
39.78
39.52 DMSO-d6
39.44
30.08
f1 (ppm)

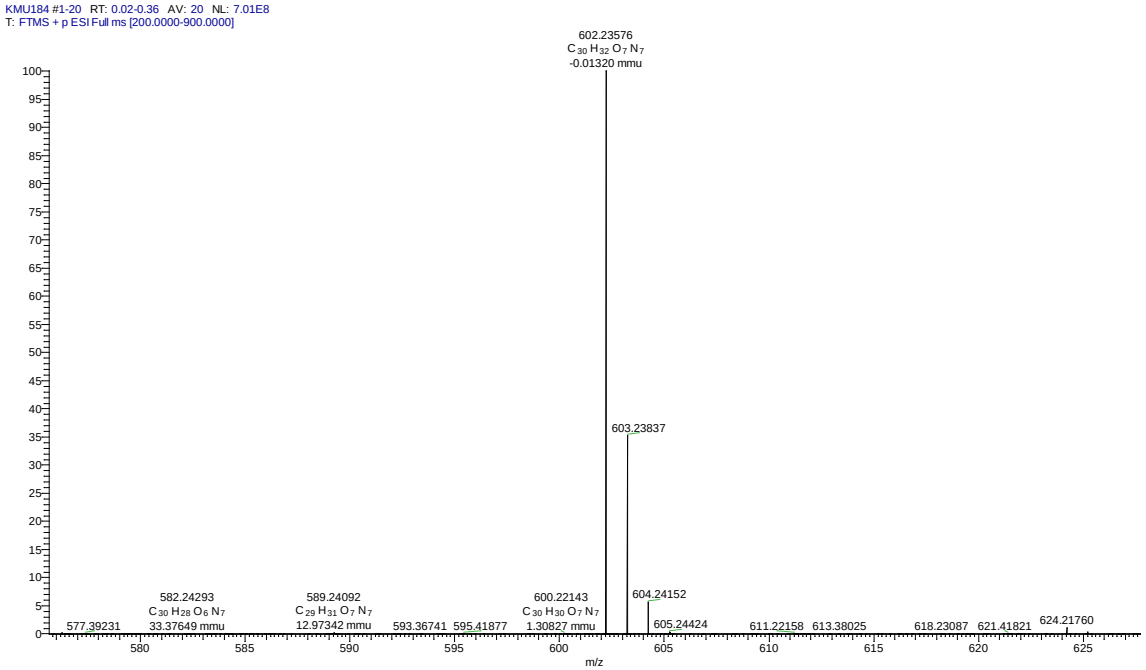
KMU184 #1-20 RT: 0.02-0.36 AV: 20 NL: 7.01E8
T: FTMS + p ESI Full ms [200.0000-900.0000]
602.23576
C30 H32 O7 N7
-0.01320 mmu
603.23837
604.24152
605.24424
582.24293
C30 H28 O6 N7
33.37649 mmu
589.24092
C29 H31 O7 N7
12.97342 mmu
600.22143
C30 H30 O7 N7
1.30827 mmu
577.39231
593.36741
595.41877
611.22158
613.38025
618.23087
621.41821
624.21760
m/z

7.3 DNA synthesis

Synthesis of the modified oligonucleotides

General information

The synthesis of the oligonucleotides were performed using the K&A H-6 DNA/RNA synthesizer and was done in the 3' to 5' direction. For the solid phase synthesis *Controlled Pore Glass* (CPG) with an occupancy of 1 µmol (500 Å) were employed. The CPG columns as well as the reagents required for the synthesis were bought commercially from GLENRESEARCH, CHEMGENES, PROLIGO and SIGMA ALDRICH. The synthesis of the oligonucleotides was carried out under argon as an inert gas. The synthesized and commercially bought phosphoramidites were inserted into the DNA using the standard phosphoramidite method. For this purpose, the natural and artificial phosphoramidites were dissolved in abs. acetonitrile. The artificial ones were used as 0.1 M solution and the natural phosphoramidites as 0.067 M solutions. A standard coupling protocol was used for the insertion of the natural building blocks. For the artificial building blocks, the standard synthesis protocol was modified to achieve longer coupling times, which should ensure more effective insertion of the artificial building blocks.

Synthesis protocol

The synthesis protocol enables to define the time sequence of the individual steps during the solid phase synthesis as well as the amount of reagent utilized during the individual partial steps of the synthesis. Table 4 shows the solvent mixtures of the reagents that were applied.

Table 4: Reagents used.

Function	Solvent mixture
Deblocker (TCA)	3 % Dichloroacetic acid in dichloromethane
Washing reagent (ACN)	Acetonitrile
Activator (TET)	0.45 M tetrazole in acetonitrile
Capping (CP_A)	Acetic anhydride in THF/pyridine
Capping (CP_B)	N-Methylimidazol in THF7pyridine
Oxidizer (OXI)	Iodine in water/THF/pyridine
Phosphoramidite (AMD)	Phosphoramidite in acetonitrile

Table 5 below shows the standard synthesis protocol and table 6 shows the synthesis protocols for the artificial building blocks 60 and 84.

Short table explanation:

- Time: Duration of the intermediary step, time unit 0.1 s (10 = 1 s).

- Source: Source from which the reagent is used.

- Mixed: Source of the second reagent, that is mixed with the first.

- Destin: Destination of the reagent.

- S. Col. Ptr.: (single column pointer) indicates the serial execution of the respective part of the subroutine.

- Delay: Time period during which nothing happens.

- Branch: The branch subroutine is called in this field.

Table 5: Standard synthesis protocol.

steps	time [0,1 s]	source	Destin.	S.Col.Ptr.	delay [s]	branch
			Deprotection			
1	4	TCA	COL			
2	30	TCA	TRM	ON		
3				ON		
4					15	
5	25	TCA	TRM	ON		
6				ON		
7					15	

8	25	TCA	TRM	ON		
9				ON		
10					15	
11	25	TCA	TRM	ON		
12				ON		
13					15	
14	25	TCA	TRM	ON		
15				ON		
16					15	
17	30	GAS	TRM			
18	10	ACN	M_W			
19	20	ACN	COL	ON		
20				ON		
21					4	
22	30	GAS	COL			
23	2	ACN	M_W			
24	20	ACN	COL	ON		
25				ON		
			coupling			
1	15	GAS	COL		2	
2	2	TET	COL	ON		
3				ON		
4					2	1
5	10	ACN	M_W		50	

6	10	ACN	COL	ON	
7				ON	
8	35	GAS	COL		
9	20	GAS	M_W		
			Branch		
1	4	TET	COL	ON	
2	8	AMD +TET	COL		
3				ON	
4					10
5	6	AMD + TET	COL	ON	
6				ON	
7					5
8	10	ACN	M_W		
9	10	GAS	M_W		
			Capping		
1	20	CP_A + CP_B	COL	ON	
2				ON	
3					15
4	10	CP_A + CP_B	COL	ON	
5				ON	
6					15
7	20	GAS	COL		
8	2	ACN	M_W		

9	12	ACN	COL	ON	
10				ON	
11	10	GAS	M_W		2
12	30	GAS	COL		
			Oxidation		
1	35	OXI	COL	ON	
2				ON	
3	10	ACN	M_W		9
4					9
5		WTH			150
6		WTH			150
7	30	GAS	COL		
8	2	ACN	M_W		
9	16	ACN	COL	ON	
10				ON	
11	20				
12	30	GAS	COL		
13	2	ACN	M_W		
14	15	ACN	COL	ON	
15				ON	
16	40				
17	15	ACN	COL	ON	
18				ON	
19	50				

20	10	GAS	M_W			
21	30	GAS	COL			

Table 6: Synthesis protocol for the insertion of **60** and **84**.

steps	time [0,1 s]	source	Destin.	S.Col.Ptr.	delay [s]	branch
			Branch			
1	4	TET	COL	ON		
2	4	AMD + TET	COL			
3				ON		
4					60	
5					60	
6					60	
7					60	
8	4	AMD+TET	COL	ON		
9				ON		
10					60	
11					60	
12					60	
13					60	
14	4	TET	COL	ON		
15				ON		
16	20	ACN	M_W			
17	20	GAS	M_W			

Using the reported synthesis protocols, the following oligonucleotides listed in **figure 60** were prepared.

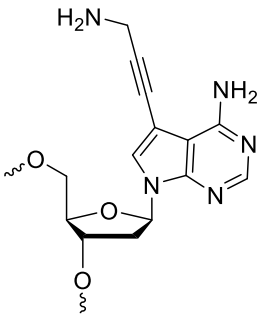

X

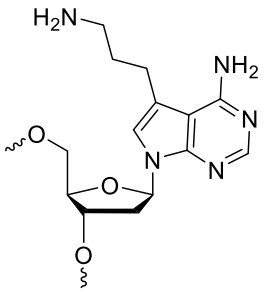

Z

DNA1 5'-G-C-A-G-T-C-**T-T-X-T-T**-C-A-C-T-G-A-3' **DNA3** 5'-G-C-A-G-T-C-**T-T-Z-T-T**-C-A-C-T-G-A-3'

Figure 60: Synthesized DNA strands.

Cleaving protocol

After the synthesis was completed, the CPG columns were dried under high vacuum for one hour. The CPG column was opened and the column material transferred to a microcentrifuge tube. 700 µl ammonium hydroxide solution (> 25 %, *trace select*, FLUKA) was added to cleave the synthesized strands from the solid phase and also to remove protective groups. The suspension was vortexed and was heated for 15 hours at 55 °C in a heating block. After cooling the suspension, the ammonia was removed using a vacuum concentrator (35 min, 35 °C, 100 mbar). The supernatant solution was pipetted off and the residue was washed three times with 200 µl HPLC water each time. The united centrifugates were lyophilized (25 °C, 0.1 mbar).

Purification of the modified oligonucleotides

The cleaved, modified oligonucleotides were purified using DMT affinity columns from GLEN RESEARCH (Glen-pak^{TM} DNA Purification Cartridges). The lyophilized crude DNA was dissolved in 1 mL dd-H2O. 1 mL NaCl-solution (100 mg/mL) was added to the solution to gain an end salt concentration of 50 mg/mL. The affinity column was first pretreated with 0.5 mL acetonitrile and 1 mL 2M Triethylammoniumacetat buffer (pH7). The oligonucleotide-salt solution was applied on to the column in 1 mL aliquots. After that, 1 mL of TFA solution (2 % in water) was added twice and the column was washed twice with 1 mL double distilled water. The oligonucleotide was eluted off the column with 1 ml 0.5 %

ammonium hydroxide in acetonitrile/water (1:1) and then evaporated to dryness under vacuum at 0.1 mbar and 25 °C overnight.

Postsynthetic modification of DNA1

Approximately 1 µmol of the oligonucleotide was dissolved in 300 µL dry DMSO. 2.00 mg BCN – NHS ester was dissolved in 300 µL dry DMSO and added to the oligonucleotide. The solution was then mixed with 5.00 µL triethylamine and shaken on a laboratory shaker at room temperature for 16 hours. The solvent was then removed overnight under vacuum at 0.1 mbar and 25 °C.

Postsynthetic modification of DNA3

Approximately 1 µmol of the oligonucleotide was dissolved in 300 µL dry DMSO. 2.00 mg of NHS ester **71** or **79** was dissolved in 300 µL dry DMSO and added to the oligonucleotide. The solution was then mixed with 5.00 µL DIPEA and shaken on a laboratory shaker at room temperature for 16 hours. The solvent was then removed overnight under vacuum at 0.1 mbar and 25 °C.

Purification of the modified oligonucleotides

A semi-preparative RP-HPLC was used to purify the postsynthetically produced oligonucleotides. The separation was carried out on a Dionex Ultimate3000 with autosampler, pump module, column oven, multi-diode array, RS fluorescence detector and fraction collector from THERMOFISHER SCIENTIFIC using Chromeleon 7 software. For semi-preparative separation, VDSphere OptiBio PUR 300 C18-SE column (250 x 10 mm, 5 µm) from VDS OPTILAB was used with a flow rate of 3.5 mL/min at a temperature of 40 °C. A gradient of 0 – 30 % acetonitrile and 0.1 M NH_4OAc over 30 minutes served as the mobile phase. The modified DNA was solved in 300 µL dd water and was injected via the autosampler with an injection volume of 300 µL. The oligonucleotide was detected at a wavelength of 260 nm and 280 nm and collected in fractions. The sequences obtained **DNA2**, **DNA4**, **DNA5** are shown in **figure 61**.

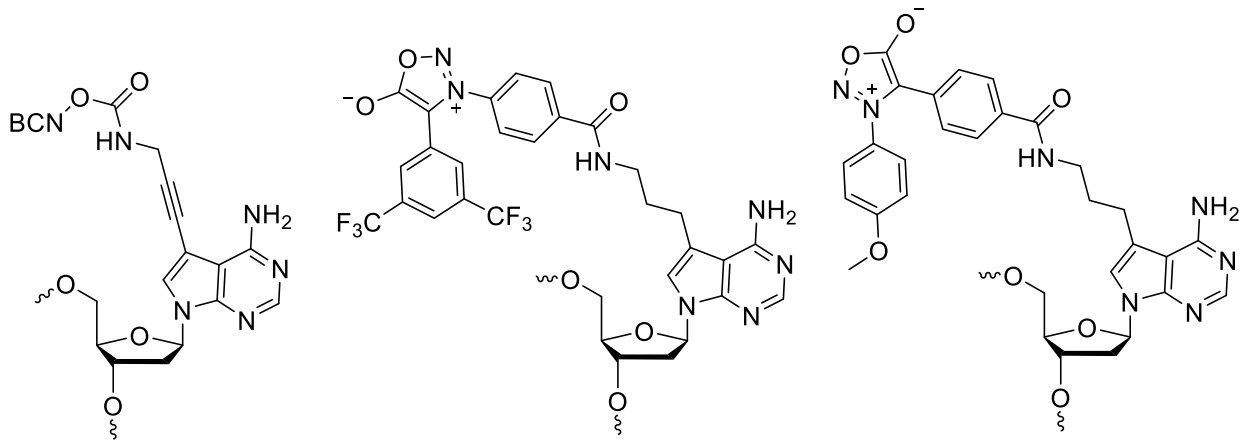

DNA2 5'-G-C-A-G-T-C-T-T- **Z**-T-T-C-A-C-T-G-A-3'

DNA4 5'-G-C-A-G-T-C-T-T- **Z**-T-T-C-A-C-T-G-A-3'

DNA5 5'-G-C-A-G-T-C-T-T- **Z**-T-T-C-A-C-T-G-A-3'

Figure 61: Postsynthetically modified DNA strands.

Determination of mass

The purity of the collected fractions was verified by MALDI-TOF mass spectrometry. The identified pure fractions were combined and lyophilised. **Table 7** shows the calculated and found masses.

Table 7: Calculated and measured masses.

DNA	Calculated mass [g/mol]	Measured mass [g/mol]
DNA2	5386 $[M]^+$	5389 $[M+H]^+$
DNA4	5508 $[M]^+$	5512 $[M+H]^+$
DNA5	5615 $[M]^+$	5615 $[M+H]^+$

Concentration measurement

The concentration of the DNA samples was calculated by using the *Lambert-Beer law*. For this purpose, the optical density at λ = 260 nm was measured on an *ND-1000 spectrophotometer* from NANODROP (in nucleic acid mode). The molar extinction coefficient ε_{260} of an oligonucleotide based only on natural bases at 260 nm in water is given by the following equation:

$$\varepsilon_{260} = (A \cdot \varepsilon_A + G \cdot \varepsilon_G + C \cdot \varepsilon_C + T \cdot \varepsilon_T) \cdot 0.9 + \varepsilon_{Chromophor/artificial\ nucleoside}$$

A,G,C,T: Number of natural bases

$\varepsilon_{A,G,C,T}$: molar extinction coefficient 260 nm

0.9: correction factor

For modified oligonucleotide strands, the molar extinction coefficients of the artificial building blocks were added. The molar extinction coefficients of the natural and artificial building blocks are shown in **table 8**. The extinction coefficient of **15** were taken from the literature.[155]

Table 8: Molar extinction coefficients.

Bases	Extinction coefficient ε_{260} [L M^{-1} cm^{-1}]
dA	15.400
dT	8.800
dC	7.300
dG	11.700
15	4.300
1	14.400
2	12.700

7.4 HPLC- and LC-MS methods

The methods used for the purification of the synthesized DNA and the LC-MS-analyses are shown in **table 9-12**.

Table 9: HPLC- and LC-MS analysis methods for the bioorthogonal SPSAC reaction on nucleosides.

Zeit [min]	% MeCN + 0.1 % TFA
0.00	0
15.00	40
30.00	40
40.00	60
45.00	80
50.00	90
55.000	90

55.001	0
65,000	0

Table 10: LC-MS analysis method for the bioorthogonal SPSAC reaction on oligonucleotides

Zeit [min]	% MeCN
0.00	0
30.00	20
40.00	20
40.001	80
50.000	80
50.001	0
60.000	0

Table 11: HPLC-MS method for the preparative purification of DNA2.

Zeit [min]	% MeCN
0.00	0
30.00	20
40.00	20
40.001	20
50.001	0
60.000	0

Table 12: HPLC-MS method for the preparative purification of DNA4 and DNA5.

Zeit [min]	% MeCN
0.00	0
30.00	30
40.00	30
40.001	30
50.001	0
60.000	0

LC-MS analysis and mass spectroscopic analysis (ESI):

Table 13 shows the measured masses of the LC-MS analysis and the measured ESI masses of the click reactions.

Table 13: measured masses of the LC-MS analysis and ESI masses. The calculated mass represents the product formed in the SPSAC or Photoclick reaction.

Product	Calculated mass [m/z]	measured mass [m/z]
32	870.4086	870.4080
50	886.4035	886.4007
37	870.4086	870.4057
51	886.4035	886.4007
52	920.4242	920.4204
53	936.4192	936.4161
54	920.4242	920.4214
55	936.4192	936.4161
56	765.3507	765.3477
57	781.3457	781.3426
61	1456.8 (z=4)	1456.05 (z=4)
62	1456.8 (z=4)	1456.05 (z=4)
63	1418.05 (z=4)	1417.28 (z=4)
85	775.2422	775.2423
86	669.2780	669.2773

7.5 In vitro ,,Click'' - Experiments

Spectroscopic investigation of the click and photoclick reaction via UV-Vis spectroscopy

The absorption spectra were measured on a Cary3500 spectrometer from AGILANT with a temperature controller. All spectra were baseline-corrected by using a blank. For the measurements, quartz cuvettes with a light path of 10 mm and a probe volume of 0.50 mL were used. All reactants were prepared as stock solutions with concentrations as shown in table 14. In each case, 2.5 µL were diluted with double-distilled water to a total volume of

0.5 mL, resulting in a solvent composition of H_2O/DMSO (99:1 V/V%) and a ratio between fluorophore/dienophile 1:5 and nucleoside **1** or **2**/NMM or BCN 1:10. Every diarylsydnone nucleoside was reacted with BCN-OH and NMM in the mentioned conditions and also the sydnone dyes were reacted with the BCN-nucleosides in the mentioned conditions. To monitor the progression of the reaction, the absorption was measured at regular time intervals. The determination of the second-order rate constant was based on the absorbance decrease of the sydnone band which correlates with the building of the click product. An overview of the batch records is provided in **table 15 and 16**.

Table 14: Stock solutions.

Stock solution	Concentration [µM]
3	4000
33	4000
44	4000
45	4000
49	4000
15	20000
16	20000
BCN-OH	50000
NMM	50000
1	5000
2	5000

Table 15: Overview of sample preparation for determining the reaction kinetics of the sydnone conjugates with the BCN-nucleosides **15** and **16**.

	$C_{flurophore}$ [µM]	$V_{SL\ fluorophore}$ [µL]	$C_{nucleoside}$ [µM]	$V_{SL\ nucleoside}$ [µL]	V_{Water} [µL]	V_{DMSO} [µL]
Blank	0	0	100	2.5	495	2.5
SPSAC	20	2.5	100	2.5	495	0

Table 16 Overview of sample preparation for determining the reaction kinetics of the diarylsydnone-nucleosides **1** and **2** with NMM and BCN-OH.

	$c_{diarylsydnone}$ [µM]	$V_{SL\ diarylsydnone}$ [µL]	$c_{BCN/NMM}$ [µM]	$V_{SL\ BCN/NMM}$ [µL]	V_{Water} [µL]	V_{DMSO} [µL]
Blank	0	0	250	2.5	495	2.5
Click	25	2.5	250	2.5	495	0

Spectroscopic investigation of the SPSAC and photoclick reaction via fluorescence spectroscopy

The fluorescence spectra were measured on a Fluoromax-4 spectrometer of the company HORIBA-SCIENTIFIC with a Peltier-element for temperature control. The measurements were corrected for Raman scattering of the respective solvent. Quartz cuvettes with a light path of 10 mm and a sample volume of 0.5 mL were used for the measurements. To monitor the increase in fluorescence intensity during the SPSAC or photoclick reaction by spectroscopy and to determine the reaction rate constants, stock solutions of all reactants were prepared in DMSO. The concentrations of the stock solutions are listed in **table 14**. Fluorescence spectra were recorded at defined time intervals to monitor the increase in fluorescence intensity during the SPSAC or photoclick reaction. For the SPSAC reactions between the sydnone dyes and the BCN nucleosides (**15**/**16**), 2.5 µL of the stock solutions were each adjusted to a final volume of 0.5 mL with double distilled water. This resulted in an end concentration of 100 µM nucleoside to 20 µM sydnone dye in H_2O/DMSO (99:1 V/V%) in the cuvette (see **table 15**). For measuring the SPSAC reaction between **DNA2** and the sydnone dyes, the concentrations were adjusted due to the smaller quantities available of **DNA2**. The stock solution of the oligonucleotide was prepared in water and the stock solutions of the sydnone dyes were diluted 1:10 with DMSO to obtain a concentration of 400 µM. This resulted in an end concentration of 2.0 µM sydnone dye and 10 µM oligonucleotide in water/DMSO 99:1 in the cuvette (**table 17**). The measured values were

also compared against two blank values: Blank H_2O/DMSO 99:1 and Blank SPSAC. Blank SPSAC was used to consider the excess of dienophile in the reaction solution. Blank H_2O/DMSO 99:1 was used to correct the starting fluorescence, in which only solvent was present in addition to the dye (t0). For the photoclick reaction 2.5 µL of the stock solutions were each adjusted to a final volume of 0.5 mL. This resulted in an end concentration of 25 µM diarylsydnone modified nucleoside (**1** or **2**) to 250 µM BCN-OH or NMM in H_2O/DMSO (99:1 V/V%) in the cuvette. A blank was used to consider the excess of BCN-OH or NMM. The dyes and diarylsydnone modified nucleosides were excited at their absorption maximum (see **table 18**). The emission spectra were measured with $\lambda_{exc.}$ + 15 nm - 800 nm to minimize the fluorescence of self-excitation.

Table 17: Overview of sample preparation for determining the reaction kinetics of the sydnone conjugates with **DNA2**.

	$c_{flurophore}$ [µM]	$V_{SL\ fluorophore}$ [µL]	$c_{nucleoside}$ [µM]	$V_{SL\ nucleoside}$ [µL]	V_{Water} [µL]	V_{DMSO} [µL]
Blank H_2O/DMSO (99:1 V/V%)	0	0	0	0	495	5
Blank SPSAC	0	0	10	10	485	5
t0	2	2.5	0	0	495	2.5
SPSAC	2	2.5	10	10	485	2.5

Table 18: Overview of excitation wavelengths used in H2O/DMSO (99:1 V/V%) for fluorescence spectroscopy and extinction coefficients of the fluorophores in DMSO.

Fluorophore	Excitation wavelength [nm]	Extinction coefficient ε [M^{-1} cm^{-1}]
3	437	33.000
33	424	10.300
44	448	33.000
45	424	17.000
49	372	16.200

To determine the reaction kinetics from the increase in fluorescence, the fluorescence was recorded over several time intervals. The emission spectra obtained were corrected, normalized and then integrated over the wavelengths $\lambda_{exc.}$ + 15 nm – 800 nm. A scatter plot was created from the obtained values and fitted using a monoexponential function (eq. **2**).

The rate constant k_2 can be calculated from the curvature k_{obs}. The rate constant is given in $M^{-1}s^{-1}$.

$$y = a + be^{-k_{obs}x} \qquad \text{(eq. 2)}$$

The turn-on was determined by forming ratios of the fluorescence intensity at the end of the reaction and at the start of the reaction.

$$\mathrm{F} = \frac{area(I_f)}{area(I_0)} \qquad \text{(eq. 1)}$$

F *Turn-on*

I_f integrated area below the obtained fluorescence spectra after time t

I_0 integrated area below the obtained fluorescence spectra at time t = 0

7.6 Cell culture

General information

All cell experiments were carried out under sterile conditions. The materials and equipment used, as well as protective gloves, were disinfected with an 80 % ethanol solution before use. Consumables that were not sterile-packaged were first autoclaved before use.

Cell cultivation

For transfection experiments, human cervical carcinoma cells (HeLa) from the company ATCC, were cultured under sterile conditions in Dulbecco's modified Eagle medium ([+] 4.5 g/L D-glucose, L-glutamine, [+] pyruvate, DMEM, Gibco™), supplemented with 10 % fetal calf serum (HI FBS, Gibco™) and 1 U/mL penicillin-streptomycin (Gibco™). The cells were incubated in a BINDER incubator at 37 °C, 5 % CO_2 and humidity of 90 %. The cells were passaged at a confluence of approximately 80 %. First the medium was removed and the cells washed with 5 mL Dulbecco's Phosphate Buffered Saline (DPBS, Gibco™). To detach the cells from the bottom of the cell culture flask, 1 mL of a 0.25 % trypsin/EDTA solution were put on the cells and the cells were incubated for 3 min at 37 °C. Then 9 mL DMEM was put on the cells to stop the trypsination and the cell suspension was transferred to a new cell culture flask in the appropriate dilution with fresh medium. For subsequent cell experiments, the cell number was determined using a Neubauer counting chamber. In a next step, the cells were diluted to the desired cell number and transferred to µ-slides 8-well (IBIDI).

Transfection of labeled oligonucleotides

For the transfection experiments $2 \cdot 10^4$ cells per well were seeded in a volume of 200 µL in an IBIDI (µ-slide 8 well ibiTreat, IBIDI) plate. Simultaneously, the oligonucleotide was transfected using Lipofectamine (Lipofectamine™ 2000, Invitrogen). For this purpose, 0.15 µL Lipofectamine™ stock solution was mixed with 4.85 µL Opti-MEM™ (serum-reduced medium, Gibco™) per well with 150 nM of the oligonucleotide or the in vitro clicked oligonucleotide-sydnone fluorophore (positive control) and incubated for 20 minutes at room temperature. The formed lipoplex was pipetted into the cell suspension in the IBIDI well and 2 µL Endoporter (GENE TOOL) per well was added, and the IBIDI was put on the laboratory shaker for 1 minute. After the cells were incubated for 24 hours the

cell culture medium was removed and the cells were washed with DPBS. 4.00 % paraformaldehyde solution was put on the cells and for 10 minutes incubated on the laboratory shaker. The fixation was stopped by adding 50.0 mM glycine and 50.0 mM NH_4Cl in DPBS for 5 minutes. After washing the cells two times with DPBS 150 nM (**44**), 300 nM (**45**) and 600 nM (**49**) (stock solution in DMSO, diluted in DMEM) was added. Two hours later the cells were washed twice with DPBS (2 x 15 min). Draq5 was added to stain the cell core and the cells were examined using a confocal fluorescence microscope (Leica DMI8, TCS SP8 inverted microscope) with a HC PL APO 63x/1.40 OIL CS2 objective. The fluorophore conjugates were excited with a 488 nm laser (10 % intensity) (**44** and **45**) and 405 nm (10 % intensity) (**49**) and the emission was measured in the range of 520 – 650 nm.

8. Additional spectra

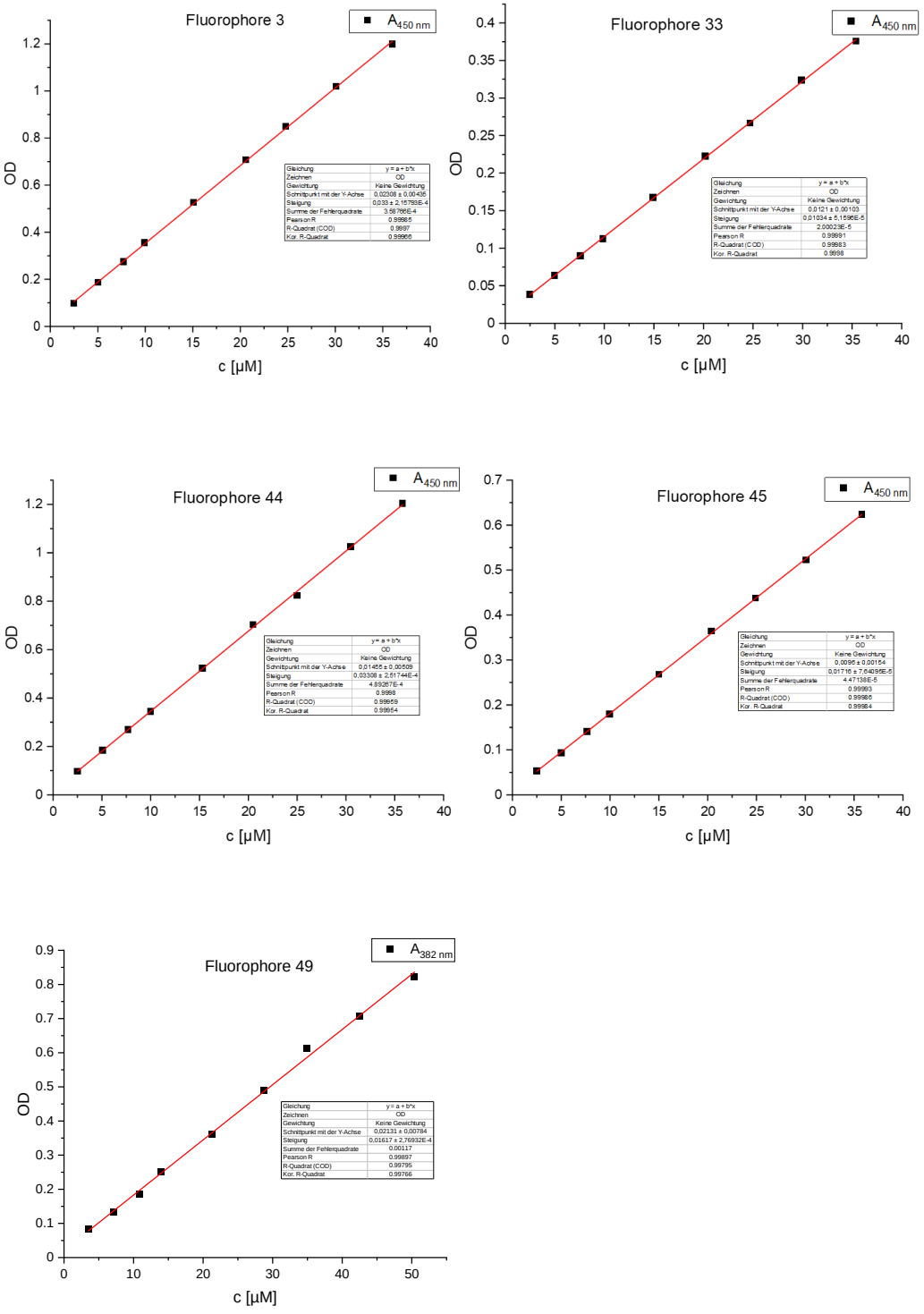

Figure 62: Determination of the molar extinction coefficient per decade of the sydnone dyes via linear regression.

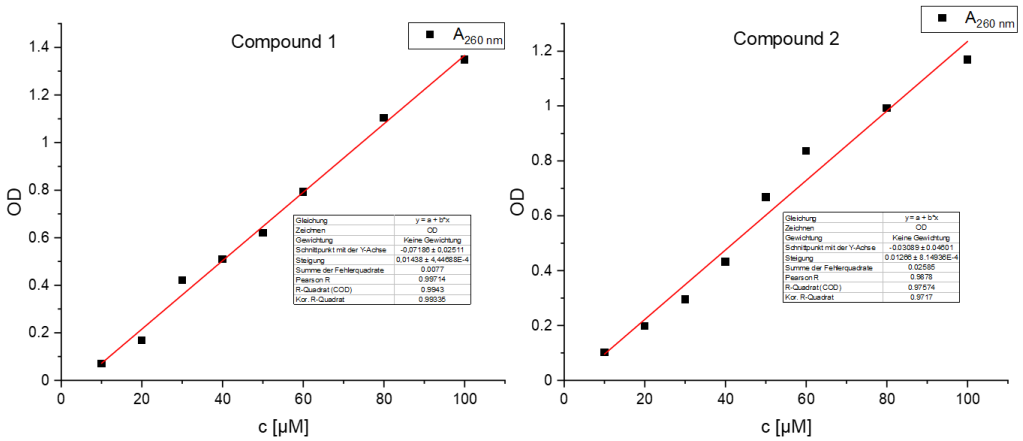

Figure 63: Determination of the molar extinction coefficient per decade of **1** and **2** via linear regression.

9. References

[1] A. Kammer, *Medizinnobelpreis für die Entdeckung der MicroRNA*, https://www.zeit.de/gesundheit/2024-10/nobelpreise-2024-medizin-nobelpreis-fuer-entdecker-der-microrna, aufgerufen am 11.10.2024.

[2] Tagesschau, *Zwei US-Genforscher erhalten Medizin-Nobelpreis*, https://www.tagesschau.de/wissen/forschung/nobelpreis-medizin-genforscher-100.html aufgerufen am 11.10.2024.

[3] T. Du, P. D. Zamore, *Cell Res* 2007, *17*, 661.

[4] E. M. Sletten, C. R. Bertozzi, *Angew Chem Int Ed* 2009, *48*, 6974.

[5] K. Lang, J. W. Chin, *ACS Chem. Biol.* 2014, *9*, 16.

[6] R. E. Bird, S. A. Lemmel, X. Yu, Q. A. Zhou, *Bioconjugate Chem.* 2021, *32*, 2457.

[7] J. C. Waters, in *Methods in Cell Biology*, Elsevier, 2007, pp. 115–140.

[8] C. Eggeling, A. Volkmer, C. A. M. Seidel, *ChemPhysChem* 2005, *6*, 791.

[9] L. G. Meimetis, J. C. T. Carlson, R. J. Giedt, R. H. Kohler, R. Weissleder, *Angewandte Chemie* 2014, *126*, 7661.

[10] G. Knorr, E. Kozma, J. M. Schaart, K. Németh, G. Török, P. Kele, *Bioconjugate Chem.* 2018, *29*, 1312.

[11] B. L. Oliveira, Z. Guo, G. J. L. Bernardes, *Chem. Soc. Rev.* 2017, *46*, 4895.

[12] P. Geng, E. List, F. Rönicke, H. Wagenknecht, *Chemistry A European J* 2023, *29*, e202203156.

[13] L. Plougastel, M. R. Pattanayak, M. Riomet, S. Bregant, A. Sallustrau, M. Nothisen, A. Wagner, D. Audisio, F. Taran, *Chem. Commun.* 2019, *55*, 4582.

[14] L. Rieger, B. Pfeuffer, H.-A. Wagenknecht, *RSC Chem. Biol.* 2023, *4*, 1037.

[15] L. Zhang, X. Zhang, Z. Yao, S. Jiang, J. Deng, B. Li, Z. Yu, *J. Am. Chem. Soc.* 2018, *140*, 7390.

[16] J. A. Prescher, C. R. Bertozzi, *Nat Chem Biol* 2005, *1*, 13.

[17] D. Dube, *Current Opinion in Chemical Biology* 2003, *7*, 616.

[18] M. Boyce, C. R. Bertozzi, *Nat Methods* 2011, *8*, 638.

[19] D. Ploschik, F. Rönicke, H. Beike, R. Strasser, H. Wagenknecht, *ChemBioChem* 2018, *19*, 1949.

[20] D. Ganz, P. Geng, H.-A. Wagenknecht, *ACS Chem. Biol.* 2023, *18*, 1054.

[21] Y. Tian, Q. Lin, *ACS Chem. Biol.* 2019, *14*, 2489.

[22] R. K. V. Lim, Q. Lin, *Chem. Commun.* 2010, *46*, 1589.

[23] G. Ben-Nissan, M. Sharon, *Chem. Soc. Rev.* 2011, *40*, 3627.

[24] J. C. Jewett, C. R. Bertozzi, *Chem. Soc. Rev.* 2010, *39*, 1272.

[25] Kenry, B. Liu, *Trends in Chemistry* 2019, *1*, 763.

[26] V. V. Rostovtsev, L. G. Green, V. V. Fokin, K. B. Sharpless, *Angew. Chem.* 2002, *114*, 2708.

[27] C. W. Tornøe, C. Christensen, M. Meldal, *J. Org. Chem.* 2002, *67*, 3057.

[28] D. C. Kennedy, C. S. McKay, M. C. B. Legault, D. C. Danielson, J. A. Blake, A. F. Pegoraro, A. Stolow, Z. Mester, J. P. Pezacki, *J. Am. Chem. Soc.* 2011, *133*, 17993.

[29] F. Wolbers, P. Ter Braak, S. Le Gac, R. Luttge, H. Andersson, I. Vermes, A. Van Den Berg, *Electrophoresis* 2006, *27*, 5073.

[30] V. Hong, N. F. Steinmetz, M. Manchester, M. G. Finn, *Bioconjugate Chem.* 2010, *21*, 1912.

[31] T. R. Chan, R. Hilgraf, K. B. Sharpless, V. V. Fokin, *Org. Lett.* 2004, *6*, 2853.

[32] Q. Wang, T. R. Chan, R. Hilgraf, V. V. Fokin, K. B. Sharpless, M. G. Finn, *J. Am. Chem. Soc.* 2003, *125*, 3192.

[33] S. I. Presolski, V. Hong, S.-H. Cho, M. G. Finn, *J. Am. Chem. Soc.* 2010, *132*, 14570.

[34] D. Soriano Del Amo, W. Wang, H. Jiang, C. Besanceney, A. C. Yan, M. Levy, Y. Liu, F. L. Marlow, P. Wu, *J. Am. Chem. Soc.* 2010, *132*, 16893.

[35] N. J. Agard, J. A. Prescher, C. R. Bertozzi, *J. Am. Chem. Soc.* 2005, *127*, 11196.

[36] L. Plougastel, O. Koniev, S. Specklin, E. Decuypere, C. Créminon, D.-A. Buisson, A. Wagner, S. Kolodych, F. Taran, *Chem. Commun.* 2014, *50*, 9376.

[37] O. Diels, K. Alder, *Justus Liebigs Ann. Chem.* 1928, *460*, 98.

[38] J. S. Clovis, A. Eckell, R. Huisgen, R. Sustmann, *Chem. Ber.* 1967, *100*, 60.

[39] W. Song, Y. Wang, J. Qu, M. M. Madden, Q. Lin, *Angew Chem Int Ed* 2008, *47*, 2832.

[40] N. J. Agard, J. A. Prescher, C. R. Bertozzi, *J. Am. Chem. Soc.* 2004, *126*, 15046.

[41] C. P. Ramil, Q. Lin, *Chem. Commun.* 2013, *49*, 11007.

[42] R. N. Butler, W. J. Cunningham, A. G. Coyne, L. A. Burke, *J. Am. Chem. Soc.* 2004, *126*, 11923.

[43] J. M. Baskin, J. A. Prescher, S. T. Laughlin, N. J. Agard, P. V. Chang, I. A. Miller, A. Lo, J. A. Codelli, C. R. Bertozzi, *Proc. Natl. Acad. Sci. U.S.A.* 2007, *104*, 16793.

[44] J. A. Codelli, J. M. Baskin, N. J. Agard, C. R. Bertozzi, *J. Am. Chem. Soc.* 2008, *130*, 11486.

[45] E. M. Sletten, H. Nakamura, J. C. Jewett, C. R. Bertozzi, *J. Am. Chem. Soc.* 2010, *132*, 11799.

[46] B. R. Varga, M. Kállay, K. Hegyi, S. Béni, P. Kele, *Chemistry A European J* 2012, *18*, 822.

[47] X. Ning, J. Guo, M. A. Wolfert, G. Boons, *Angew Chem Int Ed* 2008, *47*, 2253.

[48] M. F. Debets, S. S. Van Berkel, S. Schoffelen, F. P. J. T. Rutjes, J. C. M. Van Hest, F. L. Van Delft, *Chem. Commun.* 2010, *46*, 97.

[49] J. C. Jewett, E. M. Sletten, C. R. Bertozzi, *J. Am. Chem. Soc.* 2010, *132*, 3688.

[50] G. de Almeida, E. M. Sletten, H. Nakamura, K. K. Palaniappan, C. R. Bertozzi, *Angew Chem Int Ed* 2012, *51*, 2443.

[51] J. Dommerholt, F. P. J. T. Rutjes, F. L. Van Delft, in *Cycloadditions in Bioorthogonal Chemistry* (Eds.: M. Vrabel, T. Carell), Springer International Publishing, Cham, 2016, pp. 57–76.

[52] J. Dommerholt, S. Schmidt, R. Temming, L. J. A. Hendriks, F. P. J. T. Rutjes, J. C. M. van Hest, D. J. Lefeber, P. Friedl, F. L. van Delft, *Angew Chem Int Ed* 2010, *49*, 9422.

[53] I. Singh, C. Freeman, F. Heaney, *Eur J Org Chem* 2011, *2011*, 6739.

[54] I. Singh, C. Freeman, A. Madder, J. S. Vyle, F. Heaney, *Org. Biomol. Chem.* 2012, *10*, 6633.

[55] P. van Delft, E. van Schie, N. Meeuwenoord, H. Overkleeft, G. van der Marel, D. Filippov, *Synthesis* 2011, *2011*, 2724.

[56] F. Friscourt, C. J. Fahrni, G.-J. Boons, *J. Am. Chem. Soc.* 2012, *134*, 18809.

[57] F. Friscourt, C. J. Fahrni, G. Boons, *Chemistry A European J* 2015, *21*, 13996.

[58] X. Ren, M. Gerowska, A. H. El-Sagheer, T. Brown, *Bioorganic & Medicinal Chemistry* 2014, *22*, 4384.

[59] M. Shelbourne, T. Brown, A. H. El-Sagheer, T. Brown, *Chem. Commun.* 2012, *48*, 11184.

[60] Á. Eördögh, J. Steinmeyer, K. Peewasan, U. Schepers, H.-A. Wagenknecht, P. Kele, *Bioconjugate Chem.* 2016, *27*, 457.

[61] I. S. Marks, J. S. Kang, B. T. Jones, K. J. Landmark, A. J. Cleland, T. A. Taton, *Bioconjugate Chem.* 2011, *22*, 1259.

[62] M. F. Debets, J. C. M. Van Hest, F. P. J. T. Rutjes, *Org. Biomol. Chem.* 2013, *11*, 6439.

[63] M. Shelbourne, X. Chen, T. Brown, A. H. El-Sagheer, *Chem. Commun.* 2011, *47*, 6257.

[64] S. G. Zavgorodny, A. E. Pechenov, V. I. Shvets, A. I. Miroshnikov, *Nucleosides, Nucleotides and Nucleic Acids* 2000, *19*, 1977.

[65] V. A. Efimov, A. V. Aralov, S. V. Fedunin, V. N. Klykov, O. G. Chakhmakhcheva, *Russ J Bioorg Chem* 2009, *35*, 250.

[66] S. H. Weisbrod, A. Marx, *Chem. Commun.* 2007, 1828.

[67] K. Fauster, M. Hartl, T. Santner, M. Aigner, C. Kreutz, K. Bister, E. Ennifar, R. Micura, *ACS Chem. Biol.* 2012, *7*, 581.

[68] P. Kočalka, A. H. El-Sagheer, T. Brown, *ChemBioChem* 2008, *9*, 1280.

[69] C. Beyer, H.-A. Wagenknecht, *Chem. Commun.* 2010, *46*, 2230.

[70] M. A. Fomich, M. V. Kvach, M. J. Navakouski, C. Weise, A. V. Baranovsky, V. A. Korshun, V. V. Shmanai, *Org. Lett.* 2014, *16*, 4590.

[71] M. Aigner, M. Hartl, K. Fauster, J. Steger, K. Bister, R. Micura, *ChemBioChem* 2011, *12*, 47.

[72] J. M. Holstein, D. Schulz, A. Rentmeister, *Chem. Commun.* 2014, *50*, 4478.

[73] J. M. Holstein, F. Muttach, S. H. H. Schiefelbein, A. Rentmeister, *Chemistry A European J* 2017, *23*, 6165.

[74] J. M. Holstein, L. Anhäuser, A. Rentmeister, *Angew Chem Int Ed* 2016, *55*, 10899.

[75] L. Anhäuser, S. Hüwel, T. Zobel, A. Rentmeister, *Nucleic Acids Research* 2019, *47*, e42.

[76] A. B. Neef, N. W. Luedtke, *ChemBioChem* 2014, *15*, 789.

[77] J. C. Earl, A. W. Mackney, *J. Chem. Soc.* 1935, 899.

[78] D. L. Browne, J. P. A. Harrity, *Tetrahedron* 2010, *66*, 553.

[79] C. Favre, L. De Cremoux, J. Badaut, F. Friscourt, *J. Org. Chem.* 2018, *83*, 2058.

[80] S. Wallace, J. W. Chin, *Chem. Sci.* 2014, *5*, 1742.

[81] E. Decuypère, L. Plougastel, D. Audisio, F. Taran, *Chem. Commun.* 2017, *53*, 11515.

[82] M. K. Narayanam, Y. Liang, K. N. Houk, J. M. Murphy, *Chem. Sci.* 2016, *7*, 1257.

[83] H. Liu, D. Audisio, L. Plougastel, E. Decuypere, D. Buisson, O. Koniev, S. Kolodych, A. Wagner, M. Elhabiri, A. Krzyczmonik, S. Forsback, O. Solin, V. Gouverneur, F. Taran, *Angew Chem Int Ed* 2016, *55*, 12073.

[84] C. Favre, F. Friscourt, *Org. Lett.* 2018, *20*, 4213.

[85] Z. Zhou, C. J. Fahrni, *J. Am. Chem. Soc.* 2004, *126*, 8862.

[86] J. C. Jewett, C. R. Bertozzi, *Org. Lett.* 2011, *13*, 5937.

[87] K. Sivakumar, F. Xie, B. M. Cash, S. Long, H. N. Barnhill, Q. Wang, *Org. Lett.* 2004, *6*, 4603.

[88] K. Krell, B. Pfeuffer, F. Rönicke, Z. S. Chinoy, C. Favre, F. Friscourt, H. Wagenknecht, *Chemistry A European J* 2021, *27*, 16093.

[89] M. F. Hohmann-Marriott, R. E. Blankenship, *Annu. Rev. Plant Biol.* 2011, *62*, 515.

[90] J. E. Moses, A. D. Moorhouse, *Chem. Soc. Rev.* 2007, *36*, 1249.

[91] M. A. Tasdelen, Y. Yagci, *Angew Chem Int Ed* 2013, *52*, 5930.

[92] B. D. Fairbanks, L. J. Macdougall, S. Mavila, J. Sinha, B. E. Kirkpatrick, K. S. Anseth, C. N. Bowman, *Chem. Rev.* 2021, *121*, 6915.

[93] R. Huisgen, M. Seidel, J. Sauer, J. McFarland, G. Wallbillich, *J. Org. Chem.* 1959, *24*, 892.

[94] R. Huisgen, M. Seidel, G. Wallbillich, H. Knupfer, *Tetrahedron* 1962, *17*, 3.

[95] L. Garanti, A. Sala, G. Zecchi, *J. Org. Chem.* 1977, *42*, 1389.

[96] C. Wentrup, A. Damerius, W. Reichen, *J. Org. Chem.* 1978, *43*, 2037.

[97] Z. Yu, Y. Pan, Z. Wang, J. Wang, Q. Lin, *Angewandte Chemie* 2012, *124*, 10752.

[98] N. H. Toubro, A. Holm, *J. Am. Chem. Soc.* 1980, *102*, 2093.

[99] X. S. Wang, Y.-J. Lee, W. R. Liu, *Chem. Commun.* 2014, *50*, 3176.

[100] Y. Zhang, W. Liu, Z. Zhao, *Molecules* 2013, *19*, 306.

[101] W. Feng, L. Li, C. Yang, A. Welle, O. Trapp, P. A. Levkin, *Angewandte Chemie* 2015, *127*, 8856.

[102] S. Zhao, J. Dai, M. Hu, C. Liu, R. Meng, X. Liu, C. Wang, T. Luo, *Chem. Commun.* 2016, *52*, 4702.

[103] Z. Li, L. Qian, L. Li, J. C. Bernhammer, H. V. Huynh, J. Lee, S. Q. Yao, *Angew Chem Int Ed* 2016, *55*, 2002.

[104] P. An, T. M. Lewandowski, T. G. Erbay, P. Liu, Q. Lin, *J. Am. Chem. Soc.* 2018, *140*, 4860.

[105] S. Jiang, X. Wu, H. Liu, J. Deng, X. Zhang, Z. Yao, Y. Zheng, B. Li, Z. Yu, *ChemPhotoChem* 2020, *4*, 327.

[106] Y. Wang, C. I. Rivera Vera, Q. Lin, *Org. Lett.* 2007, *9*, 4155.

[107] C. P. Ramil, Q. Lin, *Current Opinion in Chemical Biology* 2014, *21*, 89.

[108] H. Zhang, M. Fang, Q. Lin, *Top Curr Chem (Z)* 2024, *382*, 1.

[109] A. N. Bashkatov, E. A. Genina, V. I. Kochubey, V. V. Tuchin, *J. Phys. D: Appl. Phys.* 2005, *38*, 2543.

[110] P. An, Z. Yu, Q. Lin, *Chem. Commun.* 2013, *49*, 9920.

[111] Z. Yu, L. Y. Ho, Z. Wang, Q. Lin, *Bioorganic & Medicinal Chemistry Letters* 2011, *21*, 5033.

[112] Z. Yu, T. Y. Ohulchanskyy, P. An, P. N. Prasad, Q. Lin, *J. Am. Chem. Soc.* 2013, *135*, 16766.

[113] P. Lederhose, K. N. R. Wüst, C. Barner-Kowollik, J. P. Blinco, *Chem. Commun.* 2016, *52*, 5928.

[114] P. W. Kamm, J. P. Blinco, A.-N. Unterreiner, C. Barner-Kowollik, *Chem. Commun.* 2021, *57*, 3991.

[115] B. Lehmann, H.-A. Wagenknecht, *Org. Biomol. Chem.* 2018, *16*, 7579.

[116] S. Arndt, H. Wagenknecht, *Angew Chem Int Ed* 2014, *53*, 14580.

[117] Y. Wu, G. Guo, J. Zheng, D. Xing, T. Zhang, *ACS Sens.* 2019, *4*, 44.

[118] J. M. Holstein, D. Stummer, A. Rentmeister, *Chem. Sci.* 2015, *6*, 1362.

[119] A. Poloukhtine, V. V. Popik, *J. Org. Chem.* 2003, *68*, 7833.

[120] A. A. Poloukhtine, N. E. Mbua, M. A. Wolfert, G.-J. Boons, V. V. Popik, *J. Am. Chem. Soc.* 2009, *131*, 15769.

[121] K. T. Potts, J. S. Baum, *Chem. Rev.* 1974, *74*, 189.

[122] C. D. McNitt, V. V. Popik, *Org. Biomol. Chem.* 2012, *10*, 8200.

[123] D. A. Sutton, V. V. Popik, *J. Org. Chem.* 2016, *81*, 8850.

[124] G. D. Almeida, L. C. Townsend, C. R. Bertozzi, *Org. Lett.* 2013, *15*, 3038.

[125] M. Martínek, L. Filipová, J. Galeta, L. Ludvíková, P. Klán, *Org. Lett.* 2016, *18*, 4892.

[126] S. Nainar, M. Kubota, C. McNitt, C. Tran, V. V. Popik, R. C. Spitale, *J. Am. Chem. Soc.* 2017, *139*, 8090.

[127] H. Gotthardt, F. Reiter, *Tetrahedron Letters* 1971, *12*, 2749.

[128] M. V. George, C. S. Angadiyavar, *J. Org. Chem.* 1971, *36*, 1589.

[129] K. Pfoertner, J. Foricher, *Helvetica Chimica Acta* 1980, *63*, 653.

[130] X. Zhang, X. Wu, S. Jiang, J. Gao, Z. Yao, J. Deng, L. Zhang, Z. Yu, *Chem. Commun.* 2019, *55*, 7187.

[131] F. M. K. Elekonawo, S. Lütje, G. M. Franssen, D. L. Bos, D. M. Goldenberg, O. C. Boerman, M. Rijpkema, *EJNMMI Res* 2019, *9*, 86.

[132] Y. Wang, J. Zhang, B. Han, L. Tan, W. Cai, Y. Li, Y. Su, Y. Yu, X. Wang, X. Duan, H. Wang, X. Shi, J. Wang, X. Yang, T. Liu, *Nat Commun* 2023, *14*, 974.

[133] D. M. Patterson, J. A. Prescher, *Current Opinion in Chemical Biology* 2015, *28*, 141.

[134] Y. Hu, J. M. Schomaker, *ChemBioChem* 2021, *22*, 3254.

[135] M. L. W. J. Smeenk, J. Agramunt, K. M. Bonger, *Current Opinion in Chemical Biology* 2021, *60*, 79.

[136] F. Peschke, A. Taladriz-Sender, M. J. Andrews, A. J. B. Watson, G. A. Burley, *Angewandte Chemie* 2023, *135*, e202313063.

[137] J. Schoch, M. Staudt, A. Samanta, M. Wiessler, A. Jäschke, *Bioconjugate Chem.* 2012, *23*, 1382.

[138] M. R. Karver, R. Weissleder, S. A. Hilderbrand, *Angew Chem Int Ed* 2012, *51*, 920.

[139] Z. Zawada, A. Tatar, P. Mocilac, M. Buděšínský, T. Kraus, *Angew Chem Int Ed* 2018, *57*, 9891.

[140] N. Seul, D. Lamade, P. Stoychev, M. Mijic, R. T. Michenfelder, L. Rieger, P. Geng, H. Wagenknecht, *Angew Chem Int Ed* 2024, *63*, e202403044.

[141] D. Ganz, D. Harijan, H.-A. Wagenknecht, *RSC Chem. Biol.* 2020, *1*, 86.

[142] S. Lutz, L. Liu, Y. Liu, *Chimia* 2009, *63*, 737.

[143] M. Kubota, S. Nainar, S. M. Parker, W. England, F. Furche, R. C. Spitale, *ACS Chem. Biol.* 2019, *14*, 1698.

[144] J. A. Prescher, C. R. Bertozzi, *Nat Chem Biol* 2005, *1*, 13.

[145] A. Salic, T. J. Mitchison, *Proc. Natl. Acad. Sci. U.S.A.* 2008, *105*, 2415.

[146] P. V. Danenberg, R. S. Bhatt, N. G. Kundu, K. Danenberg, C. Heidelberger, *J. Med. Chem.* 1981, *24*, 1537.

[147] F. Kohlmeier, A. Maya-Mendoza, D. A. Jackson, *Chromosome Res* 2013, *21*, 87.

[148] H. Zhao, H. D. Halicka, J. Li, E. Biela, K. Berniak, J. Dobrucki, Z. Darzynkiewicz, *Cytometry Pt A* 2013, *83*, 979.

[149] L. Guan, G. W. Van Der Heijden, A. Bortvin, M. M. Greenberg, *ChemBioChem* 2011, *12*, 2184.

[150] A. B. Neef, F. Samain, N. W. Luedtke, *ChemBioChem* 2012, *13*, 1750.

[151] S. Nainar, S. Beasley, M. Fazio, M. Kubota, N. Dai, I. R. Corrêa, R. C. Spitale, *ChemBioChem* 2016, *17*, 2149.

[152] J. T. George, S. G. Srivatsan, *Bioconjugate Chem.* 2017, *28*, 1529.

[153] P. R. Bohländer, H. Wagenknecht, *Eur J Org Chem* 2014, *2014*, 7547.

[154] P. Bohländer, Dissertation, Karlsruhe, Karlsruhe Institut für Technologie (KIT), Diss., 2015.

[155] P. Geng, Dissertation, Karlsruhe, Karlsruhe Institut für Technologie (KIT), Diss., 2023.

[156] M. Quintiliani, J. Balzarini, C. McGuigan, *Tetrahedron* 2013, *69*, 9111.

[157] I. Dhimitruka, J. SantaLucia Jr., *Synlett* 2004, 0335.

[158] T. Chin, L. Huang, L. Kan, *J Chinese Chemical Soc* 1997, *44*, 413.

[159] F. Seela, B. Westermann, U. Bindig, *J. Chem. Soc., Perkin Trans. 1* 1988, 697.

[160] F. Seela, M. Zulauf, *Synthesis* 1996, *1996*, 726.

[161] J. Steinmeyer, H.-A. Wagenknecht, *Bioconjugate Chem.* 2018, *29*, 431.

[162] A. S. K. Hashmi, T. Häffner, W. Yang, S. Pankajakshan, S. Schäfer, L. Schultes, F. Rominger, W. Frey, *Chemistry A European J* 2012, *18*, 10480.

[163] V. P. Tokar, M. Yu. Losytskyy, V. B. Kovalska, D. V. Kryvorotenko, A. O. Balanda, V. M. Prokopets, M. P. Galak, I. M. Dmytruk, V. M. Yashchuk, S. M. Yarmoluk, *J Fluoresc* 2006, *16*, 783.

[164] M. A. Ustimova, Y. V. Fedorov, V. B. Tsvetkov, S. D. Tokarev, N. A. Shepel, O. A. Fedorova, *Journal of Photochemistry and Photobiology A: Chemistry* 2021, *418*, 113378.

[165] Y. Kotake, T. Okauchi, A. Iijima, K. Yoshimatsu, H. Nomura, *Chem. Pharm. Bull.* 1995, *43*, 829.

[166] J. Steinmeyer, Dissertation, Karlsruhe, Karlsruhe Institut für Technologie (KIT), Diss., 2018.

[167] K. Krell, Dissertation, Karlsruhe, Karlsruhe Institut für Technologie (KIT), Diss., 2020.

[168] G. R. Fulmer, A. J. M. Miller, N. H. Sherden, H. E. Gottlieb, A. Nudelman, B. M. Stoltz, J. E. Bercaw, K. I. Goldberg, *Organometallics* 2010, *29*, 2176.

[169] H. Shen, K. Vollhardt, *Synlett* 2012, *2012*, 208.

Appendix

Publications

T. Simler, K. Möbius, K. Müller, T. J. Feuerstein, M. T. Gamer, S.Lebedkin, M. M. Kappes, P.W. Roesky, *Organometallics* 2019.

Conferences

09/2021 **Poster Presentation**

X. Nucleinsäurechemie-Treffen 2021, Bad Herrenalb

09/2023 **Poster Presentation**

XI. Nucleinsäurechemie-Treffen 2023, Würzburg

08/2024 **Poster Presentation**

International Round Table on nucleosides, nucleotides and nucleic acids (IRT3NA2024), Tokyo

Grants

Research Travel Grant from the Karlsruhe House of Young Scientist to support 3 months of research stay at University Bordeaux in Bordeaux, France.

Ehrenwörtliche Erklärung

Hiermit versichere ich, dass ich die vorliegende Arbeit selbst verfasst und keine anderen als die angegebenen Quellen und Hilfsmittel verwendet sowie die wörtlich oder inhaltlich übernommenen Stellen als solche kenntlich gemacht habe und die Satzung des Karlsruher Instituts für Technologie (KIT) zur Sicherung guter wissenschaftlicher Praxis in der jeweils gültigen Fassung beachtet habe. Weiterhin versichere ich, dass die elektronische Version der Arbeit mit der schriftlichen übereinstimmt und die Abgabe und Archivierung der Primärdaten gemäß Abs. A (6) der Regeln zur Sicherung guter wissenschaftlicher Praxis des KIT beim Institut gesichert ist.

_____

Karlsruhe, den 31.12.2024